An Investigation into the Bacterial Community Structure of an Electricity-Generating Microbial Fuel Cell

A thesis submitted to the University of Wales, Cardiff

by

Gwang Tae Kim

in candidature for the degree of

Philosophiae Doctor.

Cardiff School of Biosciences

University of Wales, Cardiff

April 2004

ProQuest LLC
789 East Eisenhower Parkway
P.O. Box 1346
Ann Arbor, MI 48106-1346

DECLARATION

This work has not previously been accepted in substance for any degree and is not being concurrently submitted in candidature for any degree.

Signed..... (candidate)

Date.....

STATEMENT 1

This thesis is the result of my own investigations, except where otherwise stated. Other sources are acknowledged by footnotes giving explicit references. A bibliography is appended.

Signed..... (candidate)

Date.....

STATEMENT 2

I hereby give consent for my thesis, if accepted, to be available for photocopying and for inter-library loan, and for the title and summary to be made available to outside organisations.

Signed..... (candidate)

Date.....

ACKNOWLEDGEMENTS

I would like to thank my PhD supervisors Prof. Julian W.T. Wimpenny and Dr Andrew J. Weightman for their help and supervision throughout the course of this project. I would also like to thank my MSc external supervisor Dr Byung Hong Kim for his endless guidance and support.

Grateful acknowledgement is extended to Prof. John Fry and Prof. David Lloyd as internal advisors.

I would also like to thank my colleagues Dr Gordon Webster, Dr Wendy Harrison, Dr Julian Marchesi, Dr Kevin Ashelford, Dr Barry Neish, Dr Louise O'Sullivan, Dr Rachel Dodds, Rhianedd James, Dr Natasha Banning and Dr S.B. Kim for their help and encouragement throughout this study. Many thanks must go to my Korea Institute of Science and Technology (KIST) colleagues Dr H.J. Kim, Dr H.S. Park, Dr M.S. Hyun, Dr I.S. Chang and M.A. Kim. I would also like to thank all Cardiff University technical staff for their help, in particular Mike Turner, Bill O'Neil and Gareth Lewis.

I would like to say a big thanks to all my friends for their kindness, in particular D.K. Kim, Jonathan Baker, KCC, Ana Elisabete Pires, Nevin Yagci, J.G. Hong, H. Cho and Flower. Finally, I would like to say a special thanks to my family grandmother, dad, mum, Ji-Min, Min-Seok, paternal aunt and Ji-Hyun for their encouragement and constant support.

This work was jointly funded by British Petroleum plc and Cardiff University.

SUMMARY

A microbial fuel cell is an electrochemical device that converts the chemical energy of fuel to electrical energy by the catalytic activities of microorganisms. Using this system, electrochemically-active bacteria were enriched from activated sewage sludge using an artificial wastewater supplemented with glucose and glutamate as electron donors. Within 4 weeks microbes enriched in the fuel cell removed organic contaminants in the wastewater and a current of 0.15–0.2 mA was generated over a resistance of 1 KΩ. Effects of operational conditions on fuel cell performance and metabolic inhibitor experiments demonstrated that current generation in the fuel cell involved a bacterial process. Electron microscopic observations showed that the electrode had a microbial biofilm attached to its surface along with loosely associated microbial clumps.

A 16S rRNA gene library was constructed and analysed from (i) the planktonic community, (ii) the membrane biofilm, (iii) bacterial clumps and (iv) the electrode biofilm. Results showed changes in bacterial diversity with time and due to sampling position within the microbial fuel cell. It was observed that γ-*Proteobacteria* sequences were present at higher numbers within clone libraries from the bacterial clump and electrode biofilm compared to other parts of the fuel cell. It was also observed that results of the 16S rRNA gene libraries were in excellent agreement with those of the *in situ* probing and denaturing gradient gel electrophoresis (DGGE) analysis. DGGE analysis also showed that the enriched bacterial populations were different from those found in the original activated sludge used to inoculate the microbial fuel cell at the start of the experiment.

Conventional microbiological methods revealed that members of the family *Enterobacteriaceae*, such as *Klebsiella* sp. and *Enterobacter* sp., and of the γ-*Proteobacteria* with Fe(III)-reduction and electrochemical activity had a significant potential for energy generation in this system. Based on these findings it is proposed that electrochemically-active bacteria are a common constituent of the bacterial community in the microbial fuel cell, and that their electrochemical activity is linked to a form of anaerobic respiration. Finally, this is the first study concerning the characterization of hitherto uncultivated microorganisms in a microbial fuel cell.

CONTENTS

LIST OF FIGURES

LIST OF TABLES

ABBREVIATIONS

AHL	acylated homoserine lactone
APS	ammonium persulphate
ATP	adenosine 5'-triphosphate
BOD	biological oxygen demand
bp	base pairs
BrdU	bromodeoxyuridine
C	coulomb
℃	degree Celsius
CFU	colony forming unit
CO_2	carbon dioxide
COD	chemical oxygen demand
CSLM	confocal scanning laser microscopy
CTAB	hexadecyltrimethyl ammonium bromide
CV	cyclic voltammogram
DCCD	dicyclohexylcarbodiimide
DGGE	denaturing gradient gel electrophoresis
DMA	dimethyl acetamide
DNA	deoxyribonucleic acid
DNP	2,4-dinitrophenol
DO	dissolved oxygen
EAM	electrochemically-active microorganism
EDTA	ethylenediaminetetraacetic acid
EPR	electron paramagnetic resonance
EPS	extracellular polymeric substances
Fe(O)OH	Amorphous ferric oxyhydroxide
FISH	fluorescent *in situ* hybridization
FITC	fluorescein isothiocyanate
h	hour
H_2	hydrogen
HCl	hydrochloric acid
HEPES	*N*-(2-Hydroxyethyl)piperazine-*N*'-(2-ethanesulfonic acid) (buffer)
HNQ	2-hydroxy-1,4-naphthoquinone
HQNO	2-heptyl-4-hydroxyquinolone-*N*-oxide
I	current
IPTG	isopropyl-β-D-thiogalactopyranoside
KCN	potassium cyanide
LB	luria-bertani medium

LVEM	low vacuum electron microcopy
M	molar
min	minute
mM	millimolar
MPP	1-methyl-4-phenyl-pyridinium
NaN_3	sodium azide
NTA	nitrilotriacetic acid
OD	optical density
p-CMPS	*p*-chloromercuriphenylsulphonate
PABA	*p*-aminobenzoic acid
PBBM	phosphate buffered basal medium
PCB	polychlorinated biphenyl
PCR	polymerase chain reaction
pmol	picomolar
PVC	polyvinyl chloride
R	resistance
RDP	ribosomal database project
RFLP	restriction fragments length polymorphism
s	second
S.D	standard deviation
SDS	sodium dodecyl sulphate
SEM	scanning electron microscopy
SIP	stable-isotope probing
SLP	substrate level phosphorylation
T-RFLP	terminal restriction fragment length polymorphism
t	time
TAE	tris-acetate-EDTA (buffer)
TEM	transmission electron microscopy
TEMED	*N,N,N',N'*-tetramethyl-ethylenediamine
TOC	total organic carbon
Tris	2-amino-2-(hydroxymethyl)-1,3-propandiol
TRITC	tetramethylrhodamine-5-isothiocyanate
UV	ultraviolet light (302 nm wavelength)
V	potential
VSS	volatile suspended solids
vvm	ratio of air feeding volume to working volume a minute
X-Gal	5-bromo-4-chloro-3-indolyl-β-D-galactopyranoside

CHAPTER I

General Introduction

1.1. Biological wastewater treatment system

With proper analysis and environmental control, almost all wastewaters containing biodegradable constituents can be treated biologically. Wastewater treatment and utilization therefore presents a specific challenge to biotechnologists and environmental engineers.

The major contaminants found in wastewater are biodegradable organics, volatile or recalcitrant organic compounds, toxic metals, suspended solids, nutrients (nitrogen and phosphorus), microbial pathogens and parasites (Metcalf and Eddy, 1991). Wastewater is highly variable as a function both of source and of time. Wastewater treatment processes are generally run in a non-aseptic environment and with mixed cultures of microorganisms. The challenge is to stabilize the systems and to design processes that will ensure the necessary degree of reliability and product specification.

The objectives of biological wastewater treatment processes are (i) to reduce the organic content of wastewater forming a biological floc or biofilm, (ii) to remove or reduce nutrients such as N- and P-compounds from for example, polluted surface waters and (iii) to remove or inactivate pathogenic microorganisms and parasites. Microorganisms are used to oxidize dissolved and particulate organic matter into simple end products, and to remove nitrogen and phosphorous in wastewater treatment processes. Specific bacteria are capable of oxidizing ammonia to nitrite and nitrate.

Wastewater treatment can be divided into two main categories: suspended growth and attached growth (or biofilm) processes. Table 1.1 shows some typical biological processes used for wastewater treatment as well as other methods of treatment.

There are five major treatment processes (i) aerobic; (ii) anoxic; (iii) anaerobic; (iv) combined aerobic, anoxic and anaerobic processes; and (v) lagoon (pond). These are further subdivided, depending on whether treatment is via suspended-growth systems,

Table 1.1 Major biological treatment processes used for wastewater treatment (Metcalf and Eddy, 1991).

Type	Common name	Use
Aerobic processes		
Suspended growth	Activated-sludge process	Carbonaceous BOD[a] removal, nitrification
	Aerobic lagoons	Carbonaceous BOD removal, nitrification
	Aerobic digestion	Stabilization, carbonaceous BOD removal
Attached growth	Trickling filters	Carbonaceous BOD removal, nitrification
	Rotating biological contactors	Carbonaceous BOD removal, nitrification
	Packed-bed reactors	Carbonaceous BOD removal, nitrification
Hybrid suspended and attached growth processes	Trickling filter / activated sludge	Carbonaceous BOD removal, nitrification
Anoxic processes		
Suspended growth	Suspended-growth denitrification	Denitrification
Attached growth	Attached-growth denitrification	Denitrification
Anaerobic processes		
Suspended growth	Anaerobic digestion	Stabilization, solids destruction, pathogen kill
	Anaerobic contact process	Carbonaceous BOD removal
Attached growth	Anaerobic packed and fluidized bed	Carbonaceous BOD removal, waste stabilization, denitrification
Sludge blanket	Upflow anaerobic sludge blanket	Carbonaceous BOD removal, especially high-strength wastes
Hybrid	Upflow sludge blanket / attached growth	Carbonaceous BOD removal
Combined aerobic, anoxic and anaerobic processes		
Suspended growth	Single or multi stage process, various proprietary processes	Carbonaceous BOD removal, Nitrification, denitrification and phosphorus removal
Hybrid	Single or multi-stage process with packing for attached growth	Carbonaceous BOD removal, Nitrification, denitrification and phosphorus removal
Lagoon processes		
Aerobic lagoon	Aerobic lagoon	Carbonaceous BOD removal
Maturation (tertiary) lagoon	Maturation (tertiary) lagoon	Carbonaceous BOD removal, nitrification
Facultative lagoon	Facultative lagoon	Carbonaceous BOD removal
Anaerobic lagoon	Anaerobic lagoon	Carbonaceous BOD removal

[a]BOD: biological oxygen demand

attached-growth systems, or combined processes. Suspended-growth processes are biological treatment systems in which the microorganisms responsible for the conversion of the organic or other matter to gases and biomass are retained in suspension within the liquid. On the other hand, biomass in the attached-growth processes is retained as an inert medium, such as rock, slag, or specially designed ceramic or plastic materials. These processes are also known as fixed-film processes.

1.1.1. Suspended growth processes

Here, the microorganisms responsible for treatment are maintained in liquid suspension by appropriate mixing methods. Suspended growth processes used in municipal and industrial wastewater treatment are operated in aerobically or anaerobically. Most commonly used is the activated sludge process shown on Figure 1.1(A).

This was developed in England in 1913 (Ardern and Lockett, 1914) and was so named because it involved the production of an activated mass of microorganisms capable of stabilizing a waste aerobically. Many versions of the original process are in use today, but are fundamentally very similar.

1.1.2. Attached growth processes

The microorganisms responsible for the conversion of organic material or nutrients are attached to an inert packing material. Organic material and nutrients are removed from the wastewater flowing past the attached a biofilm. Packing material used in this processes include rock, gravel, slag, sand, redwood and wide range of plastic and other synthetic materials. The most common aerobic attached growth process used is the trickling filter in which wastewater is distributed over the surface vessels containing non-submerged packing material [Figure 1.1(B)].

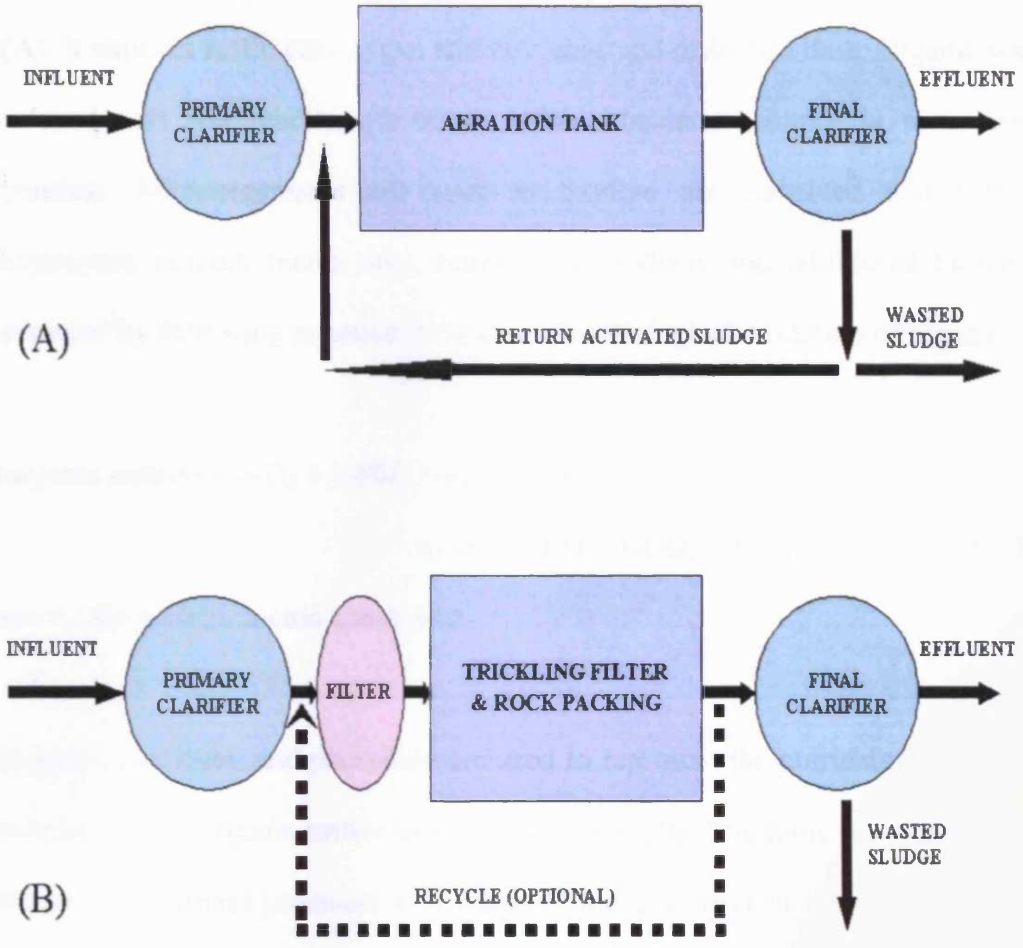

Figure 1.1 The simple schematic diagrams of (A) suspended and (B) attached growth biological treatment processes.

1.1.3. Aerobic biological oxidation

Most biological wastewater treatment applications involve the removal of organic constituents and compounds. Because a wide range of constituents and compounds exist in wastewater, the organic content is quantified in terms of biodegradable soluble chemical oxygen demand (COD) or biological oxygen demand (BOD).

1.1.3.1. The activated sludge process

The activated sludge process typically follows the flow diagram shown in Figure 1.1(A). It requires sufficient oxygen and nutrients, and residence time. Organic waste is introduced into the reactor where an aerobic bacterial culture is maintained in suspension. Microorganisms are used to oxidize the dissolved and particulate carbonaceous organic matter into simple end products and additional biomass, as represented by following equation for the aerobic biological oxidation of organic matter.

$$\nu_1 \text{ (organic matter)} + \nu_2 O_2 + \nu_3 NH_3 + \nu_4 PO_4^{3-} \rightarrow$$

$$\nu_5 \text{ (new cells)} + \nu_6 CO_2 + \nu_7 H_2O \qquad (1\text{-}1)$$

where ν_i = the stoichiometric coefficient.

Oxygen, ammonia, and phosphate are used to represent the nutrients needed for the conversion of the organic matter to simple end products. The term new cells is used to represent the biomass produced as a result of the oxidation of the organic matter. In general, the exact stoichiometry involved in the biological oxidation of a mixture of wastewater compounds is never known. However, for the purpose of illustration, assume organic matter can be represented as glucose and new cells can be represented as $C_5H_7NO_2$ (Hoover and Porges, 1952).

$$3C_6H_{12}O_6 + 8O_2 + 2NH_3 \rightarrow 2C_5H_7NO_2 + 8CO_2 + 14H_2O \qquad (1\text{-}2)$$

The quantity of oxygen utilized can be accounted for by considering i) the oxygen used for substrate oxidation to CO_2 and H_2O, ii) the COD of the biomass, and iii) the COD of any substrate not degraded. Based on the formula $C_5H_7NO_2$, the oxygen equivalent of the biomass is approximately 1.42 g O_2 g cells^{-1}.

$$C_5H_7NO_2 + 5O_2 \rightarrow 5CO_2 + 2H_2O + NH_3 + \text{Energy} \quad (1\text{-}3)$$

mw = 113 mw = 160; 160/113 = 1.42

Although this endogenous respiration reaction leads to relatively simple end products and energy, stable organic end products are also formed. From Eq. 1-3, it can be seen that, if all of the cells can be oxidized completely, the ultimate BOD or COD of the cells is equal to 1.42 times the concentration of cells. As the supply of available substrate is depleted, the microorganisms begin to consume their own protoplasm to obtain energy for cell maintenance reactions. So, finally biomass is oxidized aerobically to carbon dioxide, water and ammonia. The latter is subsequently oxidized to nitrate as digestion proceeds. This biochemical changes in an aerobic digester can be described by the following equations:

Biomass destruction:

$$C_5H_7NO_2 + 5O_2 \rightarrow 4CO_2 + H_2O + NH_4HCO_3 \quad (1\text{-}4)$$

Nitrification of released ammonia nitrogen:

$$NH_4^+ + 2O_2 \rightarrow NO_3 + 2H^+ + H_2O \quad (1\text{-}5)$$

Overall equation with complete nitrification:

$$C_5H_7NO_2 + 7O_2 \rightarrow 5CO_2 + 3H_2O + H^+ + NO_3 \quad (1\text{-}6)$$

Denitrification:

$$C_5H_7NO_2 + 4NO_3^- + H_2O \rightarrow NH_4^+ + 5HCO_3^- + 2N_2 \quad (1\text{-}7)$$

Complete nitrification and denitrification:

$$2C_5H_7NO_2 + 11.5O_2 \rightarrow 10CO_2 + 7H_2O + N_2 \quad (1\text{-}8)$$

The aerobic environment in the reactor is achieved by the use of diffused or

mechanical aeration, which also serves to maintain the liquor in a completely mixed regime. After a specified period of time, the mixture of new cells and old cells is passed into a settling tank, where the cells are separated from the treated wastewater. The biomass density in the reactor should be adjusted for the desired treatment efficiency and other considerations related to growth kinetics.

1.1.3.2. Process microbiology

A wide variety of microorganisms are found in aerobic treatment processes. The most important microorganisms in the activated sludge process are bacteria because they are responsible for the decomposition the organic waste. Aerobic and facultative bacteria use these substrates to obtain energy both for the biosynthesis of new cells and to catalyze nutrient transformations. They also produce polysaccharides and other polymeric materials that assist in the flocculation of microbial biomass.

Bacteria constitute the major component of activated sludge floc, and more than 300 strains thrive in it. The major genera identified are *Pseudomonas*, *Zoogloea*, *Achromobacter*, *Flavobacterium*, *Bacillus*, *Alcaligenes*, *Corynebacterium*, *Comamonas*, *Brevibacterium*, *Acinetobacter* (Hiraishi *et al.*, 1989) and the two nitrifying genera, *Nitrosomonas* and *Nitrobacter* (Wagner *et al.*, 1995). Additionally, filamentous species, such as *Sphaerotilus, Beggiatoa, Thiothrix* and *Lecicothrix* are also found. Whilst the bacteria are the microorganisms that actually degrade the organic waste in the influent, the metabolic activities of other microorganisms are also important in the activated sludge process. For example, protozoa act as effluent polishers by consuming free bacteria and colloidal particulates.

1.1.4. Anaerobic fermentation and oxidation

Anaerobic fermentation and oxidation processes are used primarily for the treatment

of waste sludge and high-strength organic wastes. Anaerobic digestion consists of a series of microbiological processes that convert organic compounds to methane and CO_2. Anaerobic fermentation processes are advantageous because of the lower biomass yields and because energy, in the form of methane, can be recovered from the biological conversion of organic substrates. While several types of microorganisms are implicated in aerobic oxidation, others drive the anaerobic processes.

Anaerobic digestion has long been used for the stabilization of wastewater sludge. In recent years, however, it has also been considered for the treatment of industrial wastewater. This was made possible through a better understanding of the microbiology of this process and through improved reactor designs. Anaerobic treatment is advantageous due to the lower sludge yield and the production of energy in the form of CH_4. There are also some disadvantages: It is a slower process than aerobic digestion, it is sensitive to toxicants and to high concentrations of primary substrates in the biodegradation of xenobiotic compounds (Rittmann *et al.*, 1988).

1.1.4.1. Single-stage high-rate digestion

Anaerobic digesters are large fermentation tanks provided with mechanical mixing, heating, gas collection, sludge addition and withdrawal ports and supernatant outlets [Figure 1.2(A)] (Metcalf and Eddy, 1991). Heating, auxiliary mixing, uniform feeding and thickening of the feed stream characterize the single-stage high-rate digestion process. Sludge digestion and settling occur simultaneously in the tank. Sludge stratifies and forms the following layers from the bottom to the top of the tank: digested sludge, actively digesting sludge, supernatant, a scum layer, and gas storage. Higher sludge loading rates are achieved in the high-rate version, in which sludge is continuously mixed and heated.

1.1.4.2. Two-stage digestion

Two-stage digestion, which was frequently used in the past, is seldom used in modern digester design mainly because of the expense of building a large tank that is fully utilized and because the second tank was of negligible benefit, operationally. This process consists of two digesters [Figure 1.2(B)] (Metcalf and Eddy, 1991). The first tank is continuously mixed and heated for sludge stabilization and the second is used for thickening and storage prior to sludge withdrawal and ultimate disposal. Although conventional high-rate and two-stage anaerobic digestion achieves comparable methane yields and COD stabilization efficiency, the latter process allows operation at much higher loading rates and shorter hydraulic retention times (Ghosh *et al.*, 1985).

1.1.4.3. Process microbiology

Three basic steps are involved in the overall anaerobic oxidation of a waste: (i) hydrolysis, (ii) fermentation (also known as acidogenesis) and (iii) methanogenesis (Figure 1.3).

Most bacteria are involved in the transformation of complex high-molecular weight organic compounds to methane and carbon dioxide. There are also synergistic interactions between the various groups of bacteria implicated in anaerobic digestion of wastes. The overall reaction is the following (Polprasert, 1989).

Carbon source (Organic compounds) $\rightarrow$

Products [Volatile fatty acids + CH_4 + CO_2 + H_2S + H_2O + N_2 + Fe(II)] (1-9)

Although some fungi and protozoa can be found in anaerobic digesters, bacteria are undoubtedly the dominant microorganisms. Large numbers of strict and facultative anaerobic bacteria (e.g., *Bacteroides, Bifidobacterium, Clostridium, Lactobacillus* and

Streptococcus) are involved in the hydrolysis and fermentation of organic compounds. These bacterial groups operate in a collaboration relationship (Archer and Kirsop, 1991; Sterritt and Lester, 1988).

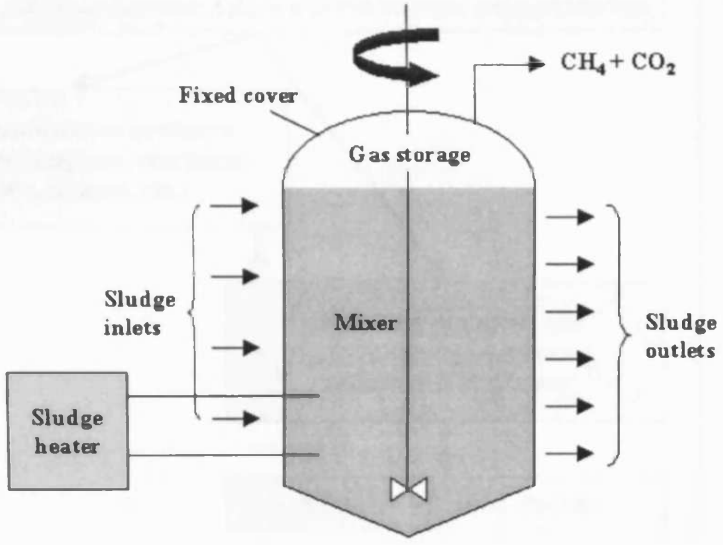

(A)

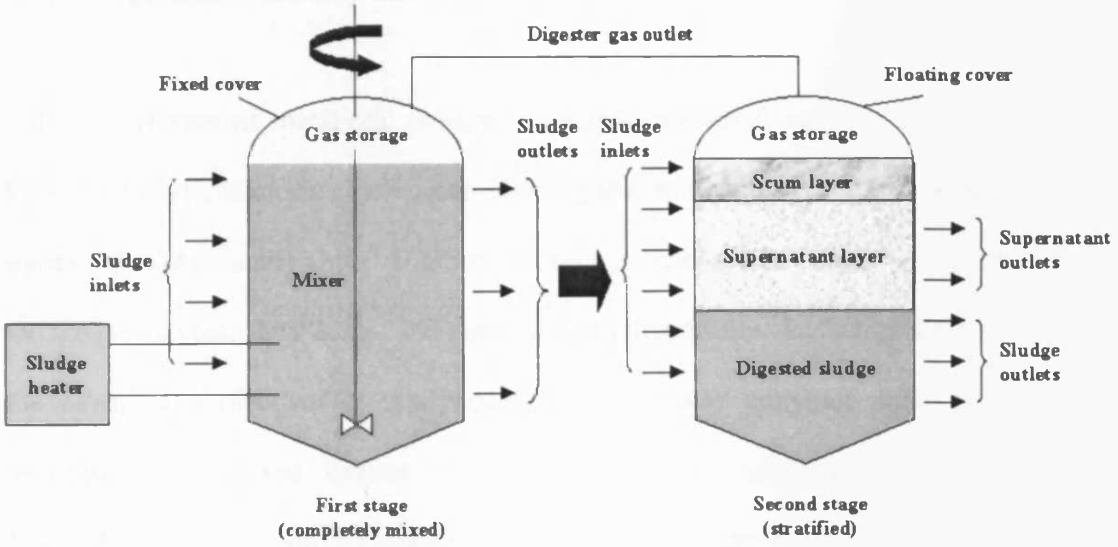

(B)

Figure 1.2 The simple schematic diagrams of typical anaerobic single-stage high-rate (A) and two-stage digesters (B) (Metcalf and Eddy, 1991).

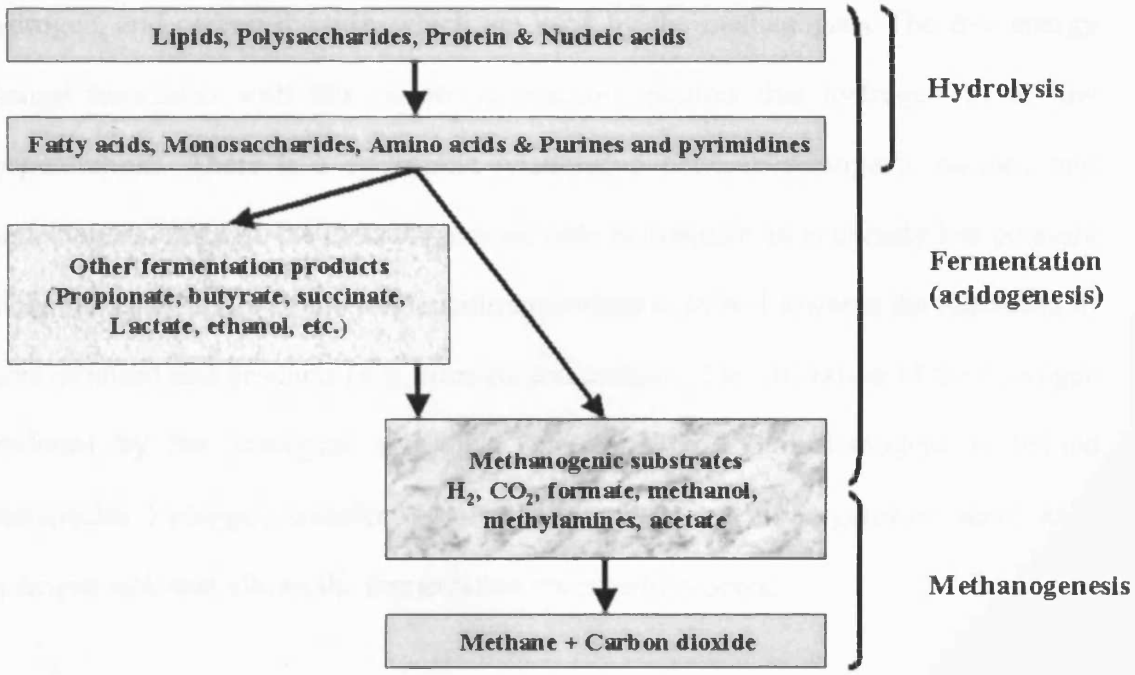

Figure 1.3 Anaerobic process schematic of hydrolysis, fermentation and methanogenesis (McCarty and Smith, 1986).

Four different of metabolic groups of bacteria are involved in anaerobic digestion. First, hydrolytic bacteria convert complex organic molecules (proteins, polysaccharides, lipids, nucleic acid) into soluble monomer molecules such as amino acids, monosaccharides, fatty acids, and purines and pyrimidines. In this group hydrolysis of the complex molecules is catalyzed by extracellular enzymes such as cellulases, proteases, urease and lipases. Second, fermentative acidogenic bacteria such as *Clostridium* species convert sugars, amino acids, and fatty acids to organic acids (e.g., acetate, propionate, formate, lactate, butyrate, succinate), alcohols and ketones (e.g., ethanol, methanol. glycerol, acetone), acetate, CO_2, and H_2. Acetate is the main product of carbohydrate fermentation. Third, acetogenic bacteria (acetate and H_2-producing

bacteria), such as *Syntrobacter wolinii* and *Syntrophomonas wolfei* (McInernay *et al.*, 1981), convert fatty acids (e.g., propionate, butyrate) and alcohols into acetate, hydrogen, and carbon dioxide, which are used by the methanogens. The free energy change associated with this metabolic reaction requires that hydrogen be at low concentrations. There is a syntrophic relationship between acetogenic bacteria and methanogens. Because the methanogens are able to maintain an extremely low pressure of H_2, the equilibrium of the fermentation reactions is shifted towards the formation of more oxidized end products (e.g., formate and acetate). The utilization of the hydrogen produced by the acetogens and other anaerobes by the methanogens is termed interspecies hydrogen transfer. In effect, the methanogenic organisms serve as a hydrogen sink that allows the fermentation reaction to proceed.

$$CH_3CH_2OH + H_2O \rightarrow CH_3COOH + H^+ + 2H_2 \quad (1\text{-}10)$$

$$CH_3CH_2COOH + 3H_2O \rightarrow CH_3COOH + HCO_3^- + H^+ + 3H_2 \quad (1\text{-}11)$$

$$CH_3CH_2CH_2COOH + H_2O \rightarrow 2CH_3COOH + H^+ + 2H_2 \quad (1\text{-}12)$$

Fourth, methanogenic microorganisms, which grow slowly in wastewater and are subdivided into two subcategories.

The hydrogenotrophic methanogenic group, termed hydrogen-utilizing chemolithotrophs, uses hydrogen as the electron donor and CO_2 as the electron acceptor to produce methane.

$$CO_2 + 4H_2 \rightarrow CH_4 + 2H_2O \quad (1\text{-}13)$$

The acetotrophic methanogens group, called acetoclastic methanogens or acetate-splitting bacteria, convert acetate into methane and CO_2.

$$CH_3COOH \rightarrow CH_4 + CO_2 \qquad (1\text{-}14)$$

The acetoclastic bacteria grow much more slowly than the acid-forming bacteria. This group comprises two main genera *Methanosarcina* (Smith and Mah, 1978) and *Methanothrix* (Huser *et al.*, 1982). About two thirds of methane is derived from acetate conversion by acetotrophic methanogens. The other third is the result of carbon dioxide reduction by hydrogen (Mackie and Bryant, 1981)

1.1.5. Sludge management and disposal

Wastewater treatment plants generate effluents and sludge that must be disposed of safely and economically. Sludge is defined as the solids separated from wastewater during treatment and concentrated for further treatment and disposal. As wastewater treatment standards have become stricter because of increasing environmental regulations, so the volume of sludge has increased. The further handling, treatment, and disposal of sludge from municipal treatment work as well as industrial wastewater treatment plants, has become a complex management, economic, regulatory and ecological burden. The cleaning process at the wastewater treatment plant is fairly straightforward. First, large solids are settled or screened out of the wastewater. Next, the smaller solids and dissolved materials are biologically removed from the wastewater using naturally occurring microorganisms, which feed on the contaminants in the wastewater. Finally, the excess microorganisms are called sewage sludge. Proper sludge management is an opportunity to reuse these materials to the benefit to the community.

The most common methods of sludge disposal today include the following i) Landfill; at the wastewater treatment plant water is removed from the sludge to concentrate it from 4% solids and 96% water to 25% solids and 75% water. This dewatered sludge is then brought to a landfill site.

ii) Land application; the sludge may at this time be mixed with wood chips and allowed to decompose. The decomposed mixture is called compost. The dewatered sludge or compost product may be used to fertilize croplands or trees and can also be used for land reclamation projects. These materials can be applied as ground cover, or they can be turned into the ground during application. The 25% solids sludge can also be dried to 95% solids and made into pellets. These pellets can be used as a soil conditioner in potting soils or on golf courses. Land application of sludge uses the nitrates and phosphate nutrients found in sewage sludge as fertilizer and soil conditioner.

iii) Incineration; the sludge is further dried to greater than 80% solids to ensure proper combustion in an incinerator. The materials are then burnt. These methods of sludge management have becoming increasingly scrutinized by regulators, legislators, and the public at large. Air pollution, odors, truck traffic, water pollution, ash by-products, aesthetics, and site availability are issues that greatly concern local comminutes. These concerns can be adequately controlled using modern techniques, but do increase the costs associated with sludge disposal.

Wastewater treatment and wastewater solids and disposal systems must be chosen to assure the most efficient use of resources such as money, materials, energy, and ultimately the most benefit to society and hence the environment. Sludge disposal systems must be technically practicable, reasonably cost effective and environmentally acceptable and implementable in the required time frame.

1.1.6. Dissimilatory Fe(III)-reducing bacteria in activated sludge

Activated sludge from many wastewater treatment plants contains high concentrations of iron, 70 to 90% of which is in the form of Fe(III) (Rasmussen and Nielsen, 1996). Fe(III) in activated sludge can come from influent wastewater or through the addition of $FeSO_4$ which is commonly used as an agent for phosphorus removal. The reduction of Fe(III) in activated sludge starts as soon as anaerobic conditions prevail (Rasmussen and Nielsen, 1996; Nielsen, 1996). Fe(III) reduction can occur in anaerobic process tanks with phosphorous removal, in clarifiers with long residence times, in anaerobic storage tanks prior to dewatering, or possibly within anaerobic microzones in sludge flocs during aerobic bulk processes (Rasmussen and Nielsen, 1996).

A wide variety of bacteria from diverse environments are capable of coupling organic matter oxidation to dissimilatory Fe(III) reduction (Lovley, 1995). Recent studies have implicated that microbial Fe(III) anaerobic respiration as a mechanism for the Fe(III) reduction seen in anaerobically stored activated sludge. In addition, several studies suggest that microbial Fe(III) may play an important role in the disintegration of sludge flocs during anaerobic sludge storage (Caccavo *et al.*, 1996b). The activity of Fe(III)-reducing bacteria may have a significant economic impact on wastewater treatment industry because deflocculation leads to a reduction in sludge dewaterability (Rasmussen *et al.*, 1994). If Fe(III) reduction in activated sludge is microbially mediated, the population density of Fe(III) reducer will be a very important factor in wastewater treatment systems. However, a little is known about Fe(III) reducers and the mechanism of Fe(III) reduction in activated sludge. Such information is a vital precursor to any attempts at controlling this activity.

1.2. Electricity generation by microorganisms

The electrical activity of microorganisms is a fascinating and instructive field of bioscience, although much work remains to be done at the research level to elucidate the chemistry, electrochemistry and biochemistry of such phenomena. Recently, studies of microbial fuel cells have greatly advanced our interest and understanding of microbial electricity generation (Bennetto, 1984; 1990).

1.2.1. Microbial fuel cell

Electricity can be generated in different types of power plant systems, batteries or microbial fuel cell (Higgins and Hill, 1985). A microbial fuel cell is a device that directly converts microbial metabolic into electricity by using electrochemical technology (Allen and Bennetto, 1993; Roller *et al.*, 1984). A fuel cell is an electrochemical device consisting of a non-consumable anode and cathode, an electrolyte, and suitable controls. Chemical energy can be converted to electric energy by coupling the biocatalytic oxidation of organic or inorganic compounds to the chemical reduction of an oxidant at the interface between the anode and cathode (Willner, 1998). The free energy of the reactants, which are stored outside the cell itself, is converted into electrical energy.

1.2.2. Microbial metabolism in a fuel cell

When living creatures and microorganisms metabolize substrate to provide them with energy, they are tapping the energy of oxidation of high energy (electron-rich) substances from carbohydrates, lipids and proteins for example, in reaction such as:

$$C_6H_{12}O_6 + 6O_2 \rightarrow 6CO_2 + 6H_2O \qquad (1\text{-}15)$$

In microorganisms this process is a complex reaction involving many enzyme-catalyzed reactions. It progresses through a series of intermediates (e.g., NADH, quinones etc.) produced by energy-rich substances involving successive oxidation-reduction changes. A substrate such as a carbohydrate is oxidized initially without the participation of oxygen when its electrons are released by enzymatic reactions. The electrons are stored as intermediates, which become reduced, and in this state they are used to fuel the reactions, which provide the living cell with energy for maintenance and growth via biosynthetic reactions in a microbial fuel cell. A simple representation of the charge separation involved in the oxidation of glucose by whole bacterial cell would be as follows:

$$C_6H_{12}O_6 + 6H_2O \rightarrow 6CO_2 + 24H^+ + 24e^- \qquad (1\text{-}16)$$

In general, the bacterial cell is electrochemically inactive as the cell wall structure mainly consists of non-conductive material such as lipids and peptidoglycans. Although the cell wall of Gram-negative bacteria has surface charge due to lipopolysaccharide (LPS) in outer membrane, the ability of permeation in electron transfer is still inefficient. So, direct electron transfer from the microorganisms to the anode in a fuel cell is very inefficient as a result of the selective permeability of the cell wall and membrane (Delaney *et al.*, 1984). Bacterial cells can be modified using hydrophobic conducting polymers to increase the electrochemical activity (e.g., methyl viologen, 2-hydroxy-1,4-naphthoquinone (HNQ), tetrazolium salt, thionine and resorufin). These substances, called mediators, couple rich sources of electrons within microorganisms to an electrode. They are usually known as oxidation-reduction or "redox" mediators. Some of redox reagents undergo a colour change on reduction,

when they accept electrons. This colour change can reveal the course of biochemical reactions between the microorganisms in the microbial fuel cell and its mediators. The rate of reduction gives an indication of the reducing power of the microorganism. This is a direct measure of the microorganism's ability to support an electric current in a microbial fuel cell. Mediators shuttle electrons between the bacterial cell and the electrode. In other word, electrons may be diverted from the respiratory chain by the redox mediator, as it enters the outer cell membrane, becomes reduced, and leaves again in the reduced state. The reduced mediator the shuttles the "stolen" electrons to the negative electrode and they appear as an electric current driven around an external circuit. From there, electrons pass through a circuit to the positive electrode in cathode compartment, where they combine with oxygen and hydrogen ions crossed through the ion-exchange membrane to form water. The main features of the cell are shown schematically in Figure 1.4.

The development of effective mediators or mediator system is important for improving the efficiency of this type of electrochemical fuel cell, and the requirements for a suitable mediator may be detailed as follows:

(1) The mediator should not be toxic to microorganisms. This requirement is not fulfilled by many of the redox materials employed so far, especially it used at higher concentrations.

(2) The reagent should be able to penetrate the cell wall of the microorganism to react with source of electrons.

(3) It should be electrochemically active at the electrode surface.

(4) The formal redox potential should be near to that of the redox couple providing the reducing action within microorganism, which is likely in many cases to be NAD^+/NADH

(5) For practical application over long periods of time, the reagent should be

chemically stable in solution.

(6) The mediator must be reasonably soluble in buffer solutions, which are usually near pH 7.0.

If these conditions are fulfilled, electrochemical mediators can play an important role in the high efficiency microbial fuel cell construction.

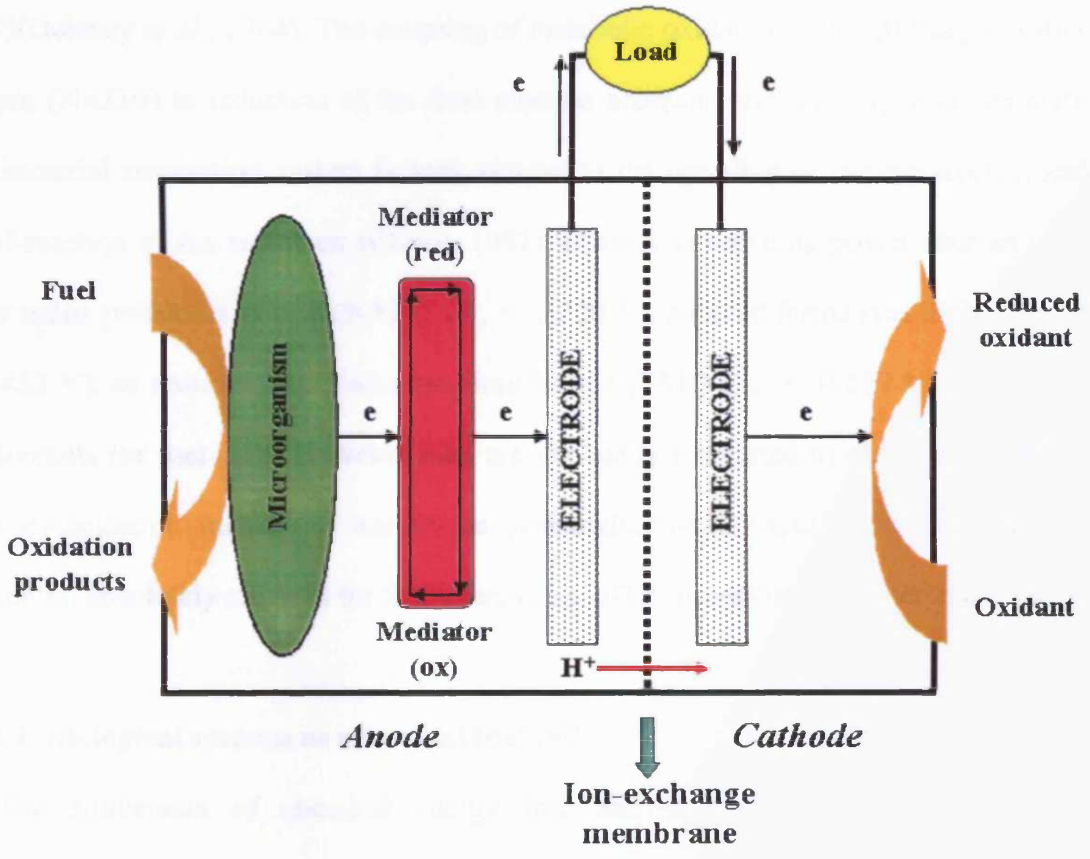

Figure 1.4 Schematic representation of a microbial fuel cell (Roller *et al.*, 1984).

1.2.3. Bioenergetics in a microbial fuel cell

In a microbial fuel cell, two redox couples are required, one for coupling reduction

of the electron mediator to bacterial oxidative metabolism and the other for coupling oxidation of the electron mediator to the reduction of the electron acceptor on the cathode surface (Ardeleanu *et al.*, 1983; Delaney *et al.*, 1984). The free energy produced by normal microbial metabolism or by microbial fuel cell systems is determined mainly by the potential difference (ΔE) between the electron donor and the acceptor according to following equation: $-\Delta G = nF\Delta E$, where ΔG is the variation in free energy, n is the number of electron moles, and F is the Faraday constant (96,487 J/V)(Delaney *et al.*, 1984). The coupling of metabolic oxidation of the primary electron donor (NADH) to reduction of the final electron acceptor such as oxygen or fumarate in bacterial respiration system is very similar to the coupling of the electrochemical half-reaction of the reductant (Chang, 1981). Biological reducing power sources with low redox potentials, such as NADH ($E_o' = -0.320$ V), reduced ferredoxin (FdH_2) ($E_o' = -0.432$ V), or reduced flavin adenine dinucleotide (FAD) ($E_o' = -0.219$ V), can act as reductants for fuel cells. However they are not easily converted to electricity because the cytoplasmic membrane has to be nonconductive to maintain the membrane potential absolutely required for free energy (i.e., ATP) production (Thauer *et al.*, 1977).

1.2.4. Biological systems as microbial fuel cell

The conversion of chemical energy into electrical energy via a thermal or combustion processes is inherently inefficient. The overall energy conversion is subject to the limitations of the Carnot cycle resulting in efficiencies much below 50%. The Carnot cycle (Turner *et al.*, 1982) can be thought of as the most efficient heat engine cycle allowed by physical laws. When the second law of thermodynamics states that not all the supplied heat in a heat engine can be used to do work, the Carnot efficiency sets the limiting value on the fraction of the heat which can be so used. Fuel cells are theoretically much more efficient devices because they are not restricted by the Carnot

cycle. A fuel cell functions by the oxidation of a suitable fuel at an anode with simultaneous transfer of electrons via an external circuit and protons to a complementary reduction reaction at a cathode. The power output of the cell is a function of the number and rate of transfer of electrons and the potential difference between the electrodes. In theory, energy conversion efficiency of well over 50% can be achieved. Fundamentally, any oxidation-reduction reaction may be a potential fuel cell. Perhaps, the most highly refined fuel cell system is the human body, mechanism that catalytically (enzymically) burns (oxidizes) food (fuel) in an electrolyte (blood), to produce energy, some of which is electrical energy.

In 1839, the first fuel cell was described in which electricity was generated by supplying hydrogen and oxygen to two separate electrodes immersed in sulphuric acid (Yue and Lowther, 1986). Since then many other fuels have been proposed for use in fuel cells, but they are either relatively expensive or may require operation of the cell at relatively high temperatures to achieve any worthwhile results. At present, the hydrogen-oxygen cell remains as the only fuel cell that is commercially attractive (Tofield, 1981). The key to the utilization of other economically realistic fuels lies in more research on innovative electrocatalysis.

Few options exist at present, which can exploit the conventional electrochemical fuel cell. Cells consume organic materials, food and oxygen. At the same time, it has been shown that a potential difference exists between one part of a cell and the other and that a corresponding ionic current flows through the surrounding biological fluid under the influence of this potential difference. It is therefore reasonable to regard a biological cell as an electrochemical energy converter, one end oxidizes food, the other reduces oxygen, ions pass through the solution, and there is electron transport in the cell.

The operation of a microbial fuel cell relies on the principles of bioelectrocatalysis, making use of materials derived from biological systems as catalysts for reactions

occurring in anodic/cathodic compartments of the cell. The efficient transfer of electrons released from the oxidation/reduction reactions to the electrodes is crucial to the performance of a fuel cell. Biological systems possess the essential quality of controlled electron transfer. However, the microbial fuel cells described in the 1960s were mostly of the "indirect" type. Bioelectrocatalysis was effected with micro-organisms or with enzymes within the anodic half cell. The indirect mode of operation required the catalytic production of electroactive substances, which were then used to fuel conventional chemical fuel cells. The indirect fuel cell has the advantage of being able to function on very crude mixtures of feed, including waste materials, and the benefit of partly utilizing known fuel cell technology. Unfortunately, all indirect fuel cells gave very disappointing results.

The 1970s witnessed a shift to research on "direct" microbial fuel cells, much of this due to the rapid advance of the science and technology of enzymes. This type of microbial fuel cell functions by the direct transfer of electrons between an organism or enzyme and the electrode, thus providing a truly biocatalytic system independent of conventional electrochemical processes. Several attempts have been made to develop direct microbial fuel cells, which can exploit the potential of enzymatic oxidation reactions (Plotkin *et al.*, 1981; Davis *et al.*, 1983). The key enzymes involved in the bioelectrochemical reactions are oxidoreductases, which in theory are ideal for effective electron transfer required for oxidation/reduction reactions accompanying fuel cell operations. In practice, fast shuttling of electrons to the electrodes is far from easy to achieve. The principle of using a solution mediator of low molecular weight to facilitate electron transfer is well known. Plotkin and Davis (Plotkin *et al.*, 1981; Davis *et al.*, 1983) have examined the application of a number of mediators used in conjunction with alcohol dehydrogenases. A variety ways to enhance electron transfer from a redox protein to an electrode exist. These have been elegantly presented by

Aston and Turner (1984) who have also discussed problems associated with the use of mediators. Much more research is needed on study the design of electrodes, the interaction of enzymes with the electrode and the practicality of mediated systems, if the potential of microbial fuel cells is to be realized. The polarity of the mediator in both the reduced and oxidized forms should be such that it is soluble in aqueous media but be capable of passing in and out of the cell membrane despite its hydrophobic nature. The mediator should be stable in both the oxidized and reduced forms, and not decomposed during long-term redox cycling.

1.2.5. Mediator-less microbial fuel cell

Microbial fuel cells can use biocatalysts, enzymes or whole organisms in two different ways. i) Biocatalysts can generate fuel substrates of the cell by biocatalytic transformations or metabolic processes. ii) The biocatalysts participate in the electron transfer chain between the fuel-substrates and the electrode surfaces, thereby enhance the cell current (Itamar *et al.*, 1998). Until recently, it was widely recognized that the use of an electrochemical or redox mediator and/or a modified electrode is almost essential for detection of microbial electrochemical activity. Because their redox proteins are separated from their outer environment by layers of membrane which consist of phospholipids and related amphipatic compounds, the peptidoglycan cell wall, and outer membrane. Mainly due to the hydrophobic regions of the lipids, biological membranes are electrically nonconductive. Though the direct transfer of electron from microorganism to electrodes has been demonstrated, this process is inefficient both in terms of the proportion of electrons transferred (the coulombic yield) and the rate of electron transfer (the current available) due of the selective permeability of the cell wall and membrane. The inclusion of redox mediators that can be both rapidly reduced by the microorganisms and rapidly reoxidized at the anode provided

one way of overcoming this problem (Roller *et al.*, 1984; Delaney *et al.*, 1984), however, most of mediators are expensive and toxic to apply commercially.

In a direct electron transport system of a microbial fuel cell, energy-transducing redox reaction processes involve enzymes, in particular, the Fe-containing electron carriers known as cytochromes. The transport of electrons from one center to another in biological materials may be described in terms of electron tunneling. These are then passed from one redox system to another until they assist at a site in which O_2 undergoes reduction (Figure 1.5). Several electrochemical techniques such as cyclic voltammetry and square wave voltammetry have been used to characterize redox proteins including cytochromes. Those studies are conducted by exploiting the redox reaction of the protein at the electrode that acts as a redox bridge between the protein and the electrode (Hill and Hunt, 1993) and show that large numbers of redox proteins including *c*-type cytochromes are electrochemically active (Lojou *et al.*, 1998).

Recently, researches have been shown that anaerobic cultures with Fe(III)-reducing activity, isolated from a microbial fuel cell (Park *et al.*, 2001; Pham *et al.*, 2003) and submerged soil (Kim *et al.*, 2004), produced a quasi-reversible cyclic voltammogram (CV) with a reductive peak and an oxidative peak against a reference electrode. It can be said that intact metal reducing bacteria are electrochemical active (i.e. developing an electrode potential and a current) when the intact metal reducing bacteria are used in a microbial fuel cell format without electrochemical mediators and/or modified electrodes (Figure 1.6). The electrochemical activity of several Fe(III)-reducing bacteria including *Desulfobulbus propionicus* (Holmes *et al.*, 2004), *Rhodoferax ferrireducens* (Chaudhuri and Lovley, 2003) isolated from marine sediments was also confirmed by microbial fuel cell experiments. Following the degradation (oxidation) of substrate via electron transport system, electrons trapped as reduced intracellular intermediates are transferred to membrane-bound cytochromes on outer membrane,

which become reduced. The reduced form of cytochrome then donates the electrons to an anode directly. This transfer is completely effected by an externally exposed outer membrane cytochrome that diverts electrons from the reduced intermediates and via the anode, to the external circuit, which is completed by a suitable cathode.

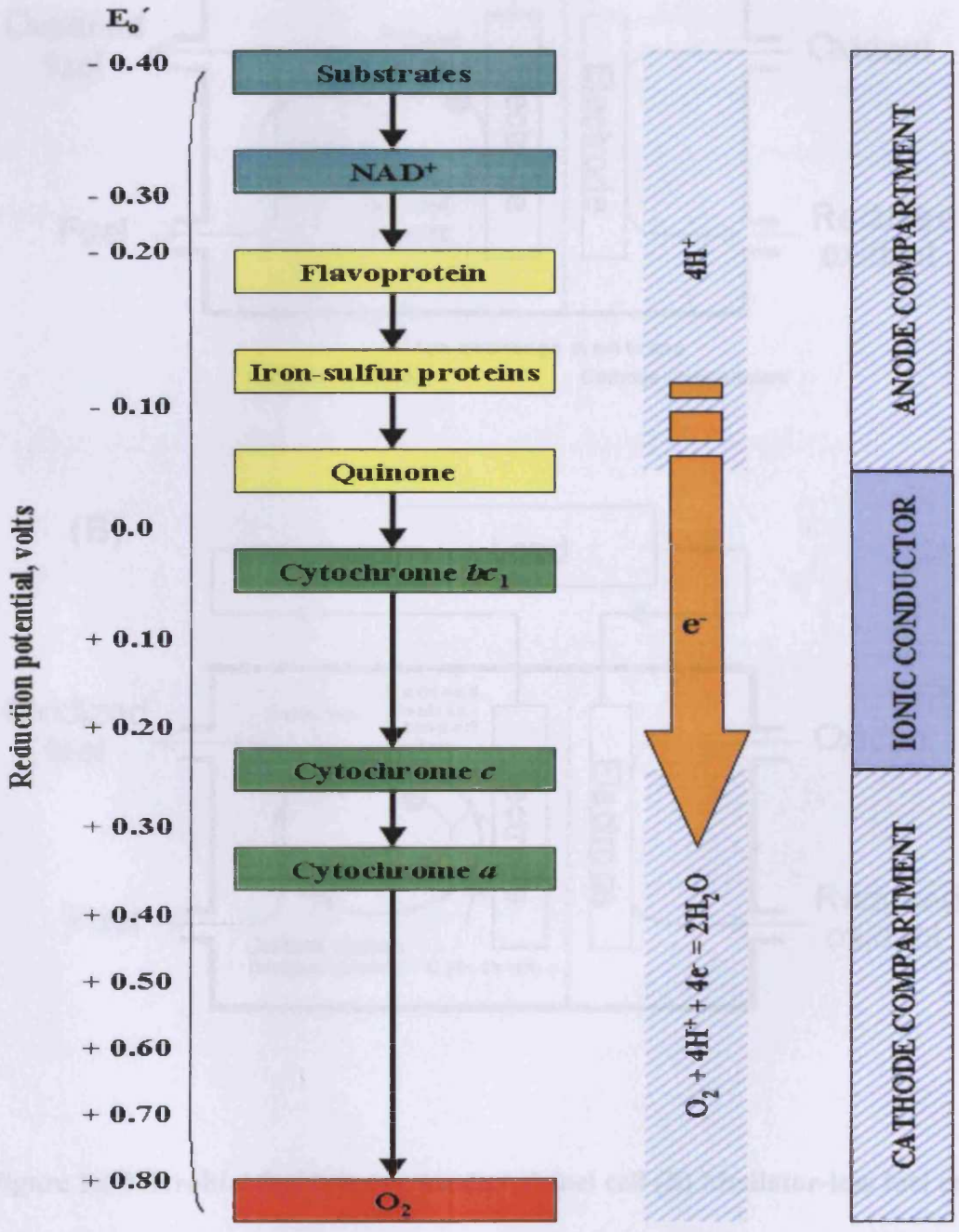

Figure 1.5 The electron transport system between redox enzyme and electrodes in a microbial fuel cell.

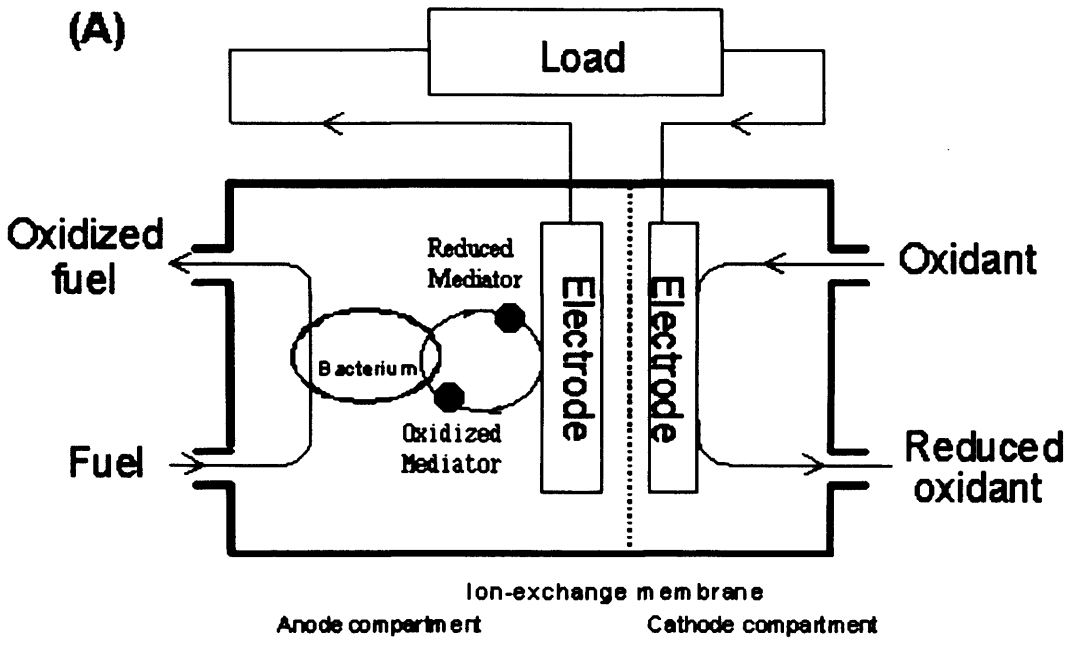

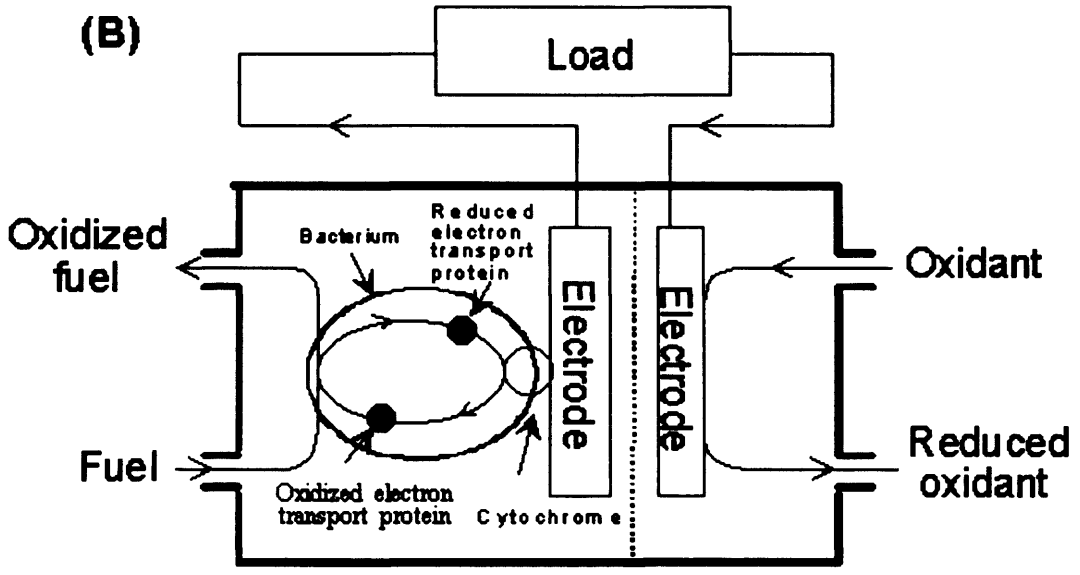

Figure 1.6 Microbial fuel cell. (A) Mediated fuel cell (B) Mediator-less fuel cell

Such mediator-less type microbial fuel cells have been developed using metal reducing bacteria (Kim *et al.*, 2002). Figure 1.7 shows electron transfer reactions between cytochrome located in the metal reducing bacteria outer membrane and the electrode in a mediator-less microbial fuel cell. Under anaerobic condition, the reduced form of outer membrane cytochromes transfer electrons to an anode as terminal electron acceptor. The microbial fuel cell will then generate electricity through the electric potential difference between the anode and the cathode. On the other hand, under aerobic conditions, electrons will be transferred to O_2 as terminal electron acceptor.

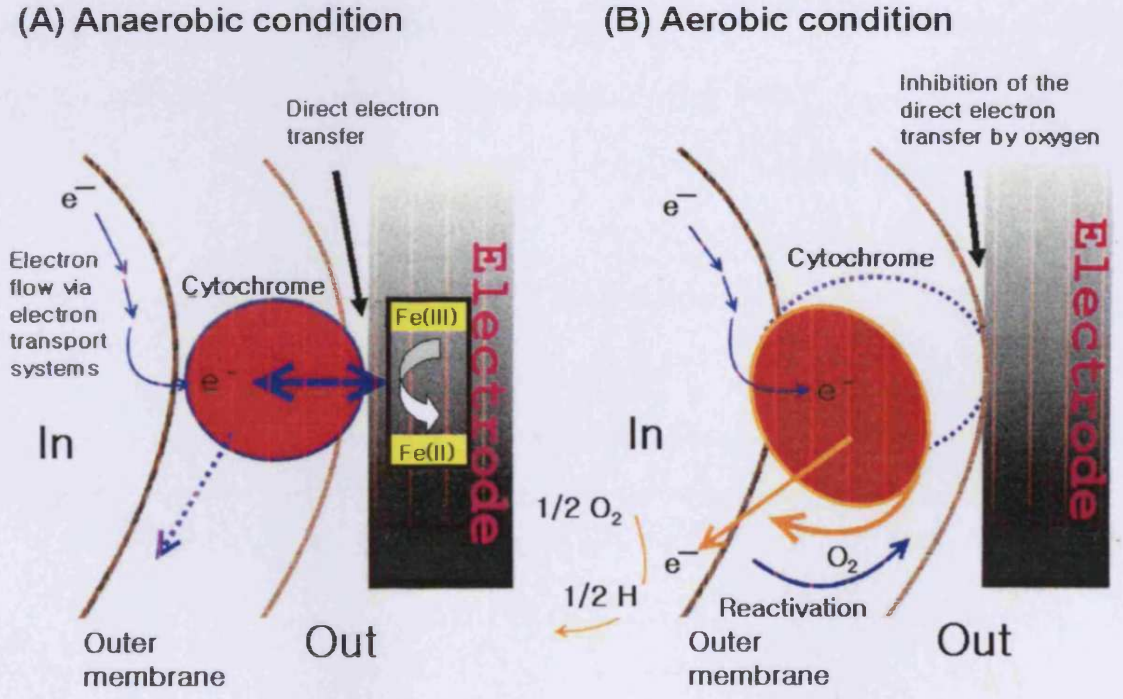

Figure 1.7 A proposed schematic diagram of electron transfer reaction between cytochrome located in metal reducing bacteria outer membrane and electrode in a mediator-less microbial fuel cell.

1.2.6. Applications of microbial fuel cells

Microbial fuel cells can be used for various purposes including bacterial activity monitoring, electricity generation, wastewater treatment process and biosensors. Mediator-less microbial fuel cells were tested as lactate sensors (Kim *et al.*, 1999). Microbial fuel cells were operated using wastewater collected from a starch processing plant as electron donor and activated sludge as a source of bacterial (Park *et al.*, 2001). The electricity generated from the microbial fuel cell was directly proportional to the concentration of the wastewater. This observation gave the possibility to use it as a BOD sensor (Kim *et al.*, 2003).

1.3. Metal reduction

The microbial oxidation of organic compounds with the reduction of metals is an important ecological process in a variety of sedimentary and subsurface environments. Microorganisms in anaerobic environments that use metals, nitrate and sulphate as terminal electron acceptors (Table 1.2), or reduce metals as a detoxification mechanism, have play an important role in the geochemistry of aquatic sediments, submerged soils, and the terrestrial subsurface. The fundamental activity of dissimilatory metal-reducing microorganisms that use Fe(III), Mn(IV), U(VI), Cr(VI) or Se(VI) as terminal electron acceptors can greatly influence the fate of these metals in aquatic sediments and groundwater. Microbial reduction of Fe(III) to Fe(II) has been studied not only because of its influence on iron geochemistry but also because Fe(III) is one of the most abundant potential electron acceptors for organic matter decomposition in many aquatic sediments and subsurface environments (Lovley, 1991).

Table 1.2 The generated free energy by NADH oxidation in biological respiration (Kim, 1995).

Reduction reaction			$\Delta G^{\circ\prime}$ (kJ/2e$^-$)
O_2	→	$2H_2O$	-219.1
$2NO_3^-$	→	N_2	-206.1
Fe(III)	→	Fe(II)	-209.5
Mn(IV)	→	Mn(II)	-134.5
HSO_4^-	→	HS^-	-20.2
CO_2	→	CH_4	-14.6

1.3.1. Dissimilatory Fe(III)-reducing bacteria

Within the last decade, investigation into about Fe(III)-reducing bacteria have indicated that there are many microorganisms which can couple oxidation of organic compounds or H_2 to the reduction of Fe(III) (Table 1.3). Until recently, much of the Fe(III) reduction seen in sedimentary environments was generally considered to be the result of abiotic processes, where changes in pH and/or redox potential promoted the conversion of Fe(III) to Fe(II) (Frenchel and Blackburn, 1979). However, it is now known that in the anaerobic, non-sulfidogenic environments in which Fe(III) reduction is most important, dissimilatory Fe(III) reducers enzymatically catalyze nearly all of the Fe(III) reduction (Lovley, 1997).

The first dissimilatory Fe(III)-reducing bacteria discovered were fermentative, and did not require Fe(III) for growth. They were capable of reducing Fe(III) while fermenting sugars or amino acids and generating acetate, alcohols, H_2 and other fermentation products. However, less than 5% of the reducing equivalents from the metabolized substrates was transferred to Fe(III) (Lovley, 1991).

The majority of Fe(III) reduction is due to the oxidation of fermentation end products such as acetate, lactate and pyruvate (Lovley, 1993). *Geobacter metallireducens* was the first pure culture shown to completely oxidize acetate with Fe(III) as the electron acceptor (Lovley *et al.*, 1993a). This microorganism is member of the δ subclass of *Proteobacteria,* a strict anaerobe isolated from freshwater sediments, capable of oxidizing several organic acids using Fe(III) as the electron acceptor. Other members of this genus such as *Geobacter hydrogenophilus*, *Geobacter chapellei* and *Geobacter grbiciae* (Coates *et al.*, 2001) have been identified, all capable of conserving energy through Fe(III) reduction. Members of the genera *Desulfuromonas* (Roden and Lovley, 1993), *Pelobacter* (Lovley *et al.*, 1995) and *Desulfuromusa* (Fredrickson and Gorby, 1996) were also Fe(III) reducers. As with

Geobacter, these genera also belong to the δ subdivision of *Proteobacteria*, suggesting that members of the *Geobacteraceae* family share a common Fe(III)-reducing ancestor (Lonergan *et al.*, 1996).

Although most of the known Fe(III)-reducing microorganisms isolated in many aquatic sediments and subsurface environments belong to the δ subdivision of *Proteobacteria*, the ability to reduce Fe(III) is not limited to *Geobacteraceae*.

Table 1.3 The metal reducers in a variety of sedimentary and subsurface environments (Lovley, 1995).

Reactant	Product	Strain
H_2 + 2Fe(III)	$2H^+$ + 2Fe(II)	*Pseudomonas* sp
H_2 + Mn (IV)	$2H^+$ + Mn(II)	*Shewanella putrefaciens*
Formate$^-$ + 2Fe(III) + H_2O	HCO_3^- + 2Fe(II) + $2H^+$	
Formate$^-$ + Mn(IV) + H_2O	HCO_3^- + Mn(II) + $2H^+$	
Lactate$^-$ + 4Fe(III) + $2H_2O$	Acetate$^-$ + HCO_3^- + 4Fe(II) + $5H^+$	
Lactate$^-$ + 2Mn(IV) + $2H_2O$	Acetate$^-$ + HCO_3^- + 2Mn(II) + $5H^+$	
Pyruvate$^-$ + 2Fe(III) + $2H_2O$	Acetate$^-$ + HCO_3^- + 2Fe(II) + $3H^+$	
Pyruvate$^-$ + Mn(IV) + $2H_2O$	Acetate$^-$ + HCO_3^- + Mn(II) + $3H^+$	
U(IV) + 2Fe(III)	U(VI) + 2Fe(II)	
Acetate$^-$ + 8Fe(III) + $4H_2O$	$2HCO_3^-$ + 8Fe(II) + $9H^+$	*Geobacter metallireducens*
Propionate$^-$ + 14Fe(III) + $7H_2O$	$3HCO_3^-$ + 14Fe(II) + $16H^+$	
Butyrate$^-$ + 20Fe(III) + $10H_2O$	$4HCO_3^-$ + 20Fe(II) + $23H^+$	
Ethanol + 12Fe(III) + $5H_2O$	$2HCO_3^-$ + 12Fe(II) + $14H^+$	
Benzoate$^-$ + 30Fe(III) + $19H_2O$	$7HCO_3^-$ + 30Fe(II) + $36H^+$	
Phenol + 28Fe(III) + $17H_2O$	$6HCO_3^-$ + 28Fe(II) + $34H^+$	
p-Cresol + 34Fe(III) + $20H_2O$	$7HCO_3^-$ + 34Fe(II) + $41H^+$	
Toluene + 36Fe(III) + $21H_2O$	$7HCO_3^-$ + 36Fe(II) + $43H^+$	
U(IV) + 2Fe(III)	U(VI) + 2Fe(II)	
S^o + 6Fe(III) + $4H_2O$	SO_4^{-2} + 6Fe(II) + $7H^+$	*Thiobacillus ferrooxidans*
S^o + $3MnO_2$ + 4H+	SO_4^{-2} + 3Mn(II) + $2H_2O$	

In the γ subdivision of *Proteobacteria*, microorganisms such as *Shewanella putrefaciens*, *Shewanella alga* and *Ferrimonas bacteria* can reduce Fe(III) with organic acid or H_2 as serving the electron donor (Lovley, 2000). Fe(III) reducers are also found outside the *Proteobacteria*. *Geovibrio ferrireducens* (Caccavo *et al.*, 1996a) and *Geothrix fermentans* (Coates *et al.*, 1999) are involved in Fe(III)-reduction, but are not closely related to each other or to any other previously described bacteria. The phylogenetic placement of these novel organisms suggest that the ability to reduce Fe(III) is spread throughout the domain bacteria (Lonergan *et al.*, 1996). The potential for Fe(III) reduction is also found in all hyperthermophiles described in the *Bacteria* and in the *Archaea* such as *Pyroaculum islandicum* and *Geothermobacterium ferrireducens* (Childers and Lovley, 2001; Kashefi *et al.*, 2002; Zhou *et al.*, 2001; Lovley *et al.*, 2000; Lovley, 2000).

1.3.2. Anaerobic respiration of Fe(III)-reducing bacteria

The oxidation of organic matter coupled to the reduction of Fe(III) requires the cooperative activity of several metabolic types of dissimilatory Fe(III) reducers in most sedimentary environments (Figure 1.8) (Lovley, 1991). A wide diversity of microorganisms that can metabolize sugars or amino acids with the reduction of Fe(III) have been described (Lovley, 1987; Fischer, 1988; Ghiorse, 1988). However, in all the cases examined, Fe(III) reduction is a trivial side reaction in the metabolism of these organisms (Lovley, 1991).

Primary products of the metabolism of fermentative Fe(III)-reducing microorganisms are typical fermentation acids such as acetate, formate, lactate and pyruvate as well as alcohols and H_2. Numerous attempts to isolate or enrich for such organisms have been unsuccessful (Lovley, 1992). Even if microorganisms that completely oxidize glucose to carbon dioxide with Fe(III) as the sole electron acceptor

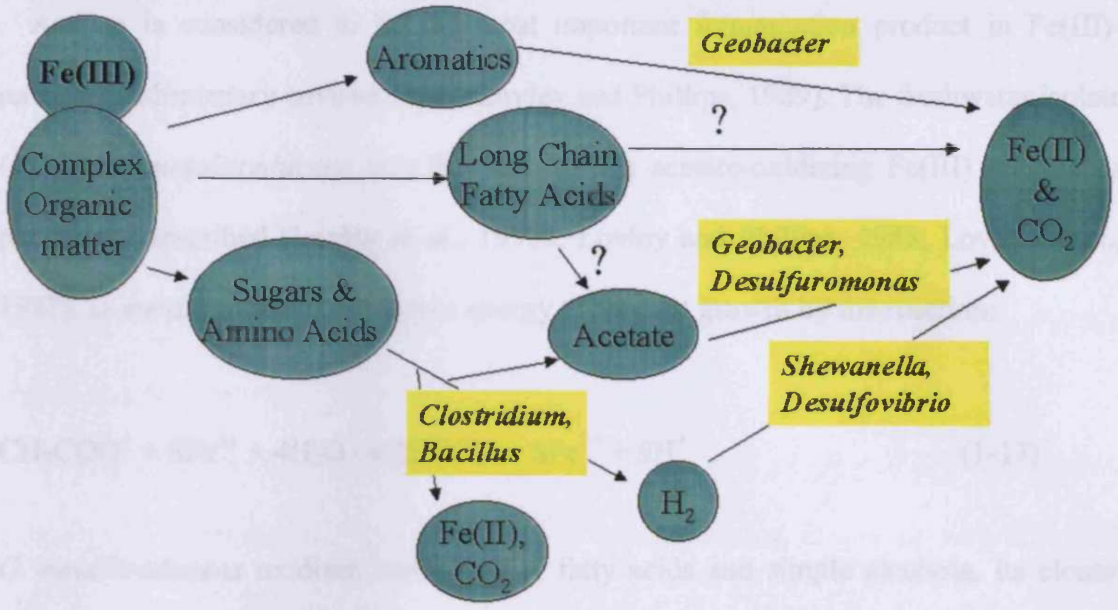

Figure 1.8 Model for microbial oxidation of organic matter in sediments coupled to dissimilatory Fe(III) reduction showing examples of the microorganisms in pure culture known to catalyze the various reactions (Lovley, 1991).

exist, their metabolism does not appear to be important in Fe(III)-reducing sediments since glucose is fermented to fatty acids rather oxidized directly to carbon dioxide (Lovley and Phillips, 1989). Thermodynamic considerations support this idea, suggesting that microorganism attempting to completely oxidize glucose to carbon dioxide with Fe(III) would be at a competitive disadvantage with microorganisms that convert glucose to fermentation products (Lovley and Phillips, 1989). This is because the amount of energy released per mole of electrons transferred is higher for fermentation than it is for glucose oxidation coupled to Fe(III) reduction. These findings have led to the hypothesis that, in Fe(III)-reducing environments, fermentative

microorganisms metabolize sugars and amino acids with relatively little Fe(III) reduction during this initial step.

Acetate is considered to be the most important fermentation product in Fe(III)-reducing sedimentary environments (Lovley and Phillips, 1989). The freshwater isolate, *Geobacter metallireducens* was the first known acetate-oxidizing Fe(III) reducer as previously described (Lovley *et al.*, 1993a; Lovley and Phillips, 1988; Lovley, *et al.*, 1987). *G. metallireducens* conserves energy to support growth by the reaction:

$$CH_3COO^- + 8Fe^{3+} + 4H_2O \rightarrow 2HCO_3^- + 8Fe^{2+} + 9H^+ \quad (1\text{-}17)$$

G. metallireducens oxidizes various other fatty acids and simple alcohols. Its closest known relative is *Desulfuromonas acetoxidans* in the phylogenetic placement. This organism was previously known primarily for its unique ability to couple the oxidation of acetate to the reduction of S^o. However, *D. acetoxidans* can also oxidize acetate with Fe(III) as the electron acceptor (Roden and Lovley, 1993). This finding show that some marine organisms can also effectively couple the oxidation of organic compounds to Fe(III) reduction.

Shewanella putrefaciens (formerly *Alteromonas putrefaciens*) can also conserve energy to support growth by coupling the oxidation of organic compounds to the reduction of Fe(III) (Lovley *et al.*, 1992; Lovley *et al.*, 1989b; Myers and Nealson, 1988). Formate is oxidized to carbon dioxide whereas lactate and pyruvate are incompletely oxidized to carbon dioxide and acetate:

$$HCOO^- + 2Fe^{3+} + H_2O \rightarrow HCO_3^- + 2Fe^{2+} + 2H^+ \quad (1\text{-}18)$$

$$CH_3CHOHCOO^- + 4Fe^{3+} + 2H_2O \rightarrow CH_3COO^- + HCO_3^- + 4Fe^{2+} + 5H^+ \quad (1\text{-}19)$$

$$CH_3COCOO^- + 2Fe^{3+} + 2H_2O \rightarrow CH_3COO^- + HCO_3^- + 2Fe^{2+} + 3H^+ \qquad (1\text{-}20)$$

Formate oxidation coupled to Fe(III) reduction is a potentially important process in sediments if formate replaces H_2 as an important fermentation product in Fe(III)-reducing environments. However, the metabolism of lactate and pyruvate by *S. putrefaciens* is expected to be a minor pathway for carbon and electron flow in Fe(III)-reducing environments.

The microorganism, *Shewanella alga* BrY (Caccavo *et al.*, 1992) and several *Desulfovibrio* species can also incompletely oxidize lactate to acetate and CO_2 with Fe(III) reduction (Lovley *et al.*, 1993b; Coleman *et al.*, 1993). Like *S. putrefaciens*, *S. alga* BrY conserves energy to support growth from Fe(III) reduction. Some *Desulfovibrio* species also oxidize H_2 with the reduction of Fe(III) at rates comparable to those observed with other Fe(III) reducers, but no net cell growth occurs. The minimum threshold for H_2 uptake in *D. desulfuricans* is lower with Fe(III) serving as the electron acceptor than with sulphate, suggesting that under conditions of limiting electron donor availability, *Desulfovibrio* species will preferentially reduce Fe(III).

A wide variety of monoaromatic compounds can be completely oxidized to carbon dioxide with Fe(III) serving as the sole electron acceptor (Lonergan and Lovley, 1991; Lovley *et al.*, 1991). *G. metallireducens*, *Geothrix fermentans* and *Ferroglobus placidus* are aromatic-oxidizing, Fe(III)-reducing microorganisms in pure culture (Lovley *et al.*, 1989a; Lovley and Lonergan, 1990; Coates *et al.*, 1999; Tor and Lovley, 2001). Aromatic compounds oxidized by those include prevalent contaminants such as toluene, *p*-cresol, benzoate, 4-hydroxybenzoate, benzaldehyde and phenol. The metabolism of *G. metallireducens* serve as a model for the oxidation of aromatic contaminants coupled to Fe(III) reduction frequently observed in polluted aquifers.

In acidic environments, elemental sulphur can serve as an electron donor for Fe(III) reduction. *Thiobacillus ferrooxidans*, *Thiobacillus thiooxidans*, and the thermophile, *Sulfolobus acidocaldarius*, reduce Fe(III) by the following reaction (Brock and Gustafson, 1976):

$$S^{o} + 6Fe^{3+} + 4H_2O \rightarrow HSO_4^{-} + 6Fe^{2+} + 7H^{+} \qquad (1\text{-}21)$$

It has been demonstrated that Fe(III) reduction provides energy to support amino acid transport and growth in *T. ferrooxidans* (Pronk *et al.*, 1991). Microorganisms that oxidize sulphur with the reduction of Fe(III) at circumneutral pH have not been reported. In addition, *S. acidocaldarius* provides evidence for the existence of thermophillic Fe(III) reducers. The recovery of large quantities of ultrafine-grained magnetite from depths as great as 6.7 km below the land surface may indicate the presence of Fe(III)-reducing life in such environments (Gold, 1992).

1.3.3. Mechanisms of enzymatic Fe(III) reduction

Studies into electron transport to Fe(III) in dissimilatory Fe(III) reducers are important not only for a better understanding of the mechanisms for enzymatic Fe(III) reduction but also because of the potential evolutionary significance of Fe(III) reduction. The geological evidence suggests that microbial Fe(III) reduction may have evolved before other respiratory processes, such as sulphate reduction, nitrate reduction, and oxygen reduction, which can also completely oxidize multicarbon organic compounds back to carbon dioxide (Lovley, 1991).

In many sedimentary environments, the majority of Fe(III) is present as insoluble Fe(III) oxides such as goethite [Fe(O)OH], FeS_2, $Fe_3(PO_4)_2$ and Fe_3O_4. The mechanisms of microbial electron transport to insoluble acceptors are poorly

understood. To respire using Fe(III), the Fe(III)-reducing bacteria must be able to either, (i) attach to the iron substrate and directly transfer electrons to it, or (ii) solubilize the iron and deliver it to the electron transport chain, or (iii) use available electron shuttling compounds or produce their own such as extracellular cytochromes, quinone, siderophores and Fe(III) chelators (Das and Caccavo, 2000; Myers and Myers, 1992; Newman and Kolter, 2000).

Until recently, studies on the relationship between direct cell to oxide adhesion or microbially secreted extracellular compounds and the rate of Fe(III) reduction amongst Fe(III)-reducing bacteria have suggested that direct cell-oxide contact was necessary (Arnold *et al.*, 1988; Nevin and Lovley, 2000; Das and Caccavo, 2000). Normal respiratory electron transport is associated with the bacterial cytoplasmic membrane, where soluble electron acceptors such as O_2 or nitrate enter the cell through passive diffusion. However, at neutral pH values, Fe(III) is insoluble and cannot enter into the cell. In Gram-negative bacteria, there are specific links between insoluble oxides and the electron transport system in the cytoplasmic membrane. In *Geobacter sulfurreducens* and *Shewanella putrefaciens* MR-1, the ferric reductase activity is located in the membrane fraction of anaerobically grown cells (Gaspard *et al.*, 1998; Myers and Myers, 1993). Growth under anaerobic conditions induces the placement of 80% of the membrane-bound *c*-type cytochromes in the outer membrane of *S. putrefaciens* MR-1 (Myers and Myers, 1992). It show that cytochromes can potentially make contact with Fe(III) oxides in the outer membrane. However, it has yet to be demonstrated whether the *c*-type cytochromes themselves or another electron carrier that accepts electrons from the *c*-type cytochrome actually donates electrons to the Fe(III) oxides. Magnuson *et al.* (2000) also show that ferric reductase complex contained a *c*-type cytochrome and required NADH as an electron donor in *Geobacter sulfurreducens*. A preliminary model for electron transport to insoluble Fe(III) has been

proposed (Figure 1.9) (Lovley, 2000).

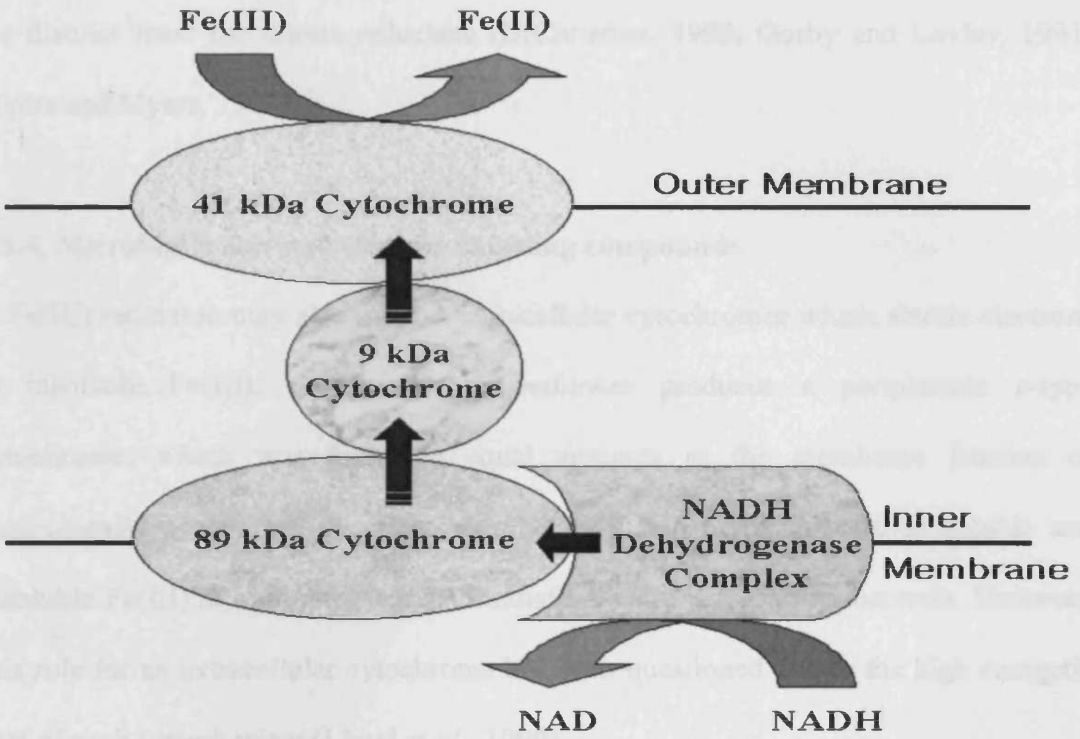

Figure 1.9 Proposed model for electron transport to extracellular Fe(III) in *Geobacter sulfurreducens* (Lovley, 2000).

The periplasmic cytochrome c_3 in *Desulfovibrio vulgaris* can function as a Fe(III) oxide reductase (Lovley *et al.*, 1993c). Whether this is the physiological Fe(III) reductase has yet to be demonstrated, electron transport via cytochrome c_3 may account for the ability of *D. vulgaris* and other *Desulfovibrio* species to reduce Fe(III) oxides. In addition, two Fe(III) reductases have been purified from *Thiobacillus ferrooxidans*. A purified periplasmic enzyme oxidizes sulfide to sulfite with Fe(III) as electron acceptor. Another membrane-bound Fe(III) reductase oxidizes sulfite to sulfate (Sugio

et al., 1988). No Fe(III) reductases have been purified from dissimilatory Fe(III) reducers that conserve energy to support growth from Fe(III) reduction at neutral pH. However, investigations have indicated that the Fe(III) reductases in such organisms are distinct from the nitrate reductase (DiChristina, 1992; Gorby and Lovley, 1991; Myers and Myers, 1993).

1.3.4. Microbially secreted electron shuttling compounds

Fe(III) reduction may also involve extracellular cytochromes which shuttle electrons to insoluble Fe(III). *Geobacter sulfurreducens* produces a periplasmic *c*-type cytochrome, which was found in equal amounts in the membrane fraction of anaerobically grown cell (Seeliger *et al.*, 1998). It can reduce various soluble and insoluble Fe(III) at high rates and also transfer electrons to partner bacteria. However, this role for an extracellular cytochrome has been questioned due to the high energetic cost of such a mechanism (Lloyd *et al.*, 1999).

Shewanella oneidensis MR-1 (formerly *Shewanella putrefaciens* MR-1) secretes a small, non-proteinaceous compound, which has the characteristics of an extracellular quinone and functions as an electron shuttle. It may also be involved in extracellular electron transfer to Fe(III) oxides (Newman and Kolter, 2000). Recently, Turick *et al.* (2002) reported that *Shewanella alga* BrY produced an extracellular melanin that contain quinoid compounds that could act as the sole terminal electron acceptor for growth. Bacterially secreted melanin can act as an electron shuttle between the cells and Fe(III) oxides.

The phylogenetic diversity throughout the *Bacteria* and *Archaea* domains of dissimilatory Fe(III)-reducing bacteria and the different environments they inhabit show that mechanisms of Fe(III) reduction, especially in electron transfer systems, vary among different groups of dissimilatory Fe(III)-reducing bacteria. *Shewanella* species

have at least two pathways for Fe(III) reduction involving either membrane-bound proteins such as heme-containing proteins and cytochromes, or microbially secreted electron shuttles such as extracellular quinoid compounds. In *Geobacter* species, studies show that membrane-bound ferric reductase activity with direct cell-oxide contact is necessary for Fe(III) reduction in the absence of exogenous electron shuttles.

In mediator-less microbial fuel cell operation, dissimilatory Fe(III)-reducing bacteria which are characterized by membrane-bound Fe(III) reduction with direct cell-oxide contact, can be used as new bacterial biocatalysts. This suggests that membrane-bound proteins and cytochromes in Fe(III)-reducing bacteria involve direct electron transfer to the electrode as terminal electron acceptor in anode compartment. As more dissimilatory Fe(III)-reducing bacteria are identified and applied to mediator-less microbial fuel cells, new mechanisms for accessing and reducing Fe(III) will emerge.

1.4. Microbial biofilms

1.4.1. Definition of biofilm

Bacterial cells attach firmly to almost any surface submerged in an aquatic environment. The immobilized cells grow, reproduce, and produce extracellular polymers which frequently extend from the cell forming a tangled matrix of fibers which provide structure to the assemblage which is termed a "biofilm" (Characklis and Marshall, 1990). The chemical and physical properties of biofilms are related to their main components, i.e., the microbial cells and the extracellular macromolecules, which are primarily polysaccharide. Common sugars such as glucose, galactose, mannose, rhamnose, N-acetylglucosamine, glucuronic acid, and galacturonic acid are typical constituents of polysaccharide. The extracellular polymeric substances (EPS) are organic polymers of biological origin which in biofilm systems are responsible for interactions with interfaces as well as a matrix for the location and transfer of dissolved and particulate compounds.

1.4.2. Biofilm systems

A biofilm system consists of the biofilm, the overlying gas and/ or liquid layer, and the substratum on which the biofilm is immobilized. It is generally composed of microorganisms immobilized in an organic polymer matrix. However, the biofilm may also contain degradable and/ or inert particles and sometimes macroorganisms as well.

As many as five compartments can be defined in a biofilm system (Figure 1.10): (i) the substratum, (ii) the base film, (iii) the surface film, (iv) the bulk liquid, and (v) the gas phase. Microbial communities at gas-solid, gas-liquid, and liquid-liquid interfaces also exist (Marshall, 1976). Bacteria, microeukaryotes (fungi, algae, and protozoans) and particulate (mineral, organic debris, phages, lysed cells and precipitates) attach to

surfaces to form biofilms. The substratum plays a major role in biofilm processes during the early stages of biofilm development and may influence both the rate of cell attachment as well as the initial cell population distribution.

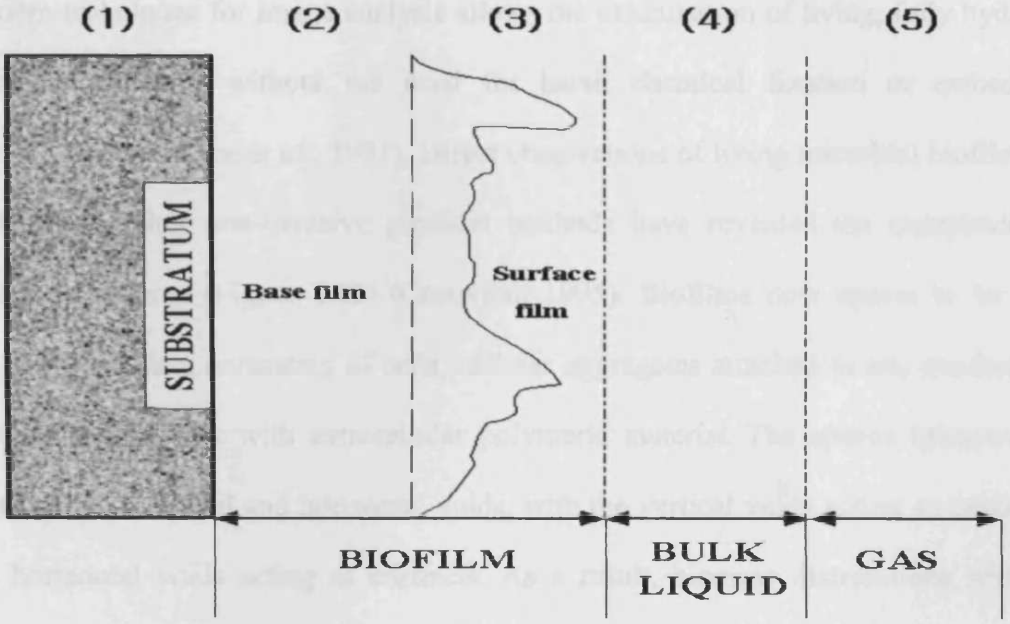

Figure 1.10 The biofilm system includes the following five compartments: (1) substratum, (2) base film, (3) surface film, (4) bulk liquid, and (5) gas. The base film and surface film constitute the biofilm (Characklis and Marshall, 1990).

The solid support may be natural material, such as rock in streams or old trickling filters, or it may be synthetic, such as the plastic packing in modern versions. The biofilm itself consists of two zones, the base film and the surface film. The base film consists of a structured accumulation of cells and other particulates, with well-defined boundaries. Transport in the base film is generally by diffusion. Surface films depend largely on the hydrodynamic characteristics of the system and the nature of the microorganisms in the biofilm. Gradients in biofilm properties in the direction away

from the substratum are most important in the surface film. Bulk liquid compartment processes affect biofilm system behavior as a result of the mixing or flow patterns.

1.4.3. Biofilm structure

The elegant confocal scanning laser microscope (CSLM) system coupled with modern techniques for image analysis allows the examination of living, fully hydrated microbial biofilms without the need for harsh chemical fixation or embedding techniques (Lawrence *et al.*, 1991). Direct observations of living microbial biofilms by optical and other non-invasive physical methods have revealed the complexity of biofilm structures (Figure 1.11) (Costerton, 1995). Biofilms now appear to be non-uniform structures consisting of cells, cellular aggregates attached to one another and to the solid support with extracellular polymeric material. The spaces between cell clusters form vertical and horizontal voids, with the vertical voids acting as pores and the horizontal voids acting as channels. As a result, biomass distributions within a biofilm are not uniform, nor are physical factors such as porosity and density. The cell clusters are microbial aggregates cemented with extracellular polymeric material, whereas the voids are open structures relatively free of it. The significance of the voids is that liquid can flow through them. This can have a profound effect on mass transfer in the biofilm.

1.4.4. Interaction between biofilm system compartments

The interaction between the various compartments (biofilm and bulk liquid) in a biofilm system occurs via internal transport as well as interfacial transfer processes (Figure 1.12). Both may occur in the bulk liquid compartment as well as in the biofilm. Bulk liquid compartment transport processes deliver substrate (electron donor and particulates) and microorganisms to the biofilm while carrying away cells and other

products of metabolism. Transport between surface biofilm and base film occurs primarily by molecular diffusion for dissolved components and by volumetric displacement for particulate components. These observations suggest that they obey the commonly accepted use of various transport parameters, such as an effective diffusion coefficient and thermal conductivity for describing the transport of substrate and electron acceptor.

Figure 1.11 Conceptual mode of the architecture of a single-species biofilm based on data collected by confocal scanning laser microscopy (CSLM) of living biofilms. Some microcolonies are simple conical structures, while others are mushroom shaped, convective fluid flow is seen in the water channels between and even below the microcolonies within these biofilm (Costerton, 1995).

The importance of competition for space in determining the ultimate distribution of competing species within a biofilm can be visualized by considering conceptualization of a base biofilm. A substrate and oxygen concentration gradient will exist through the biofilm as illustrated by Figure 1.13 because substrate can only move into the biofilm by diffusion. This means that bacteria near the liquid-biofilm interface are growing faster than those in the interior.

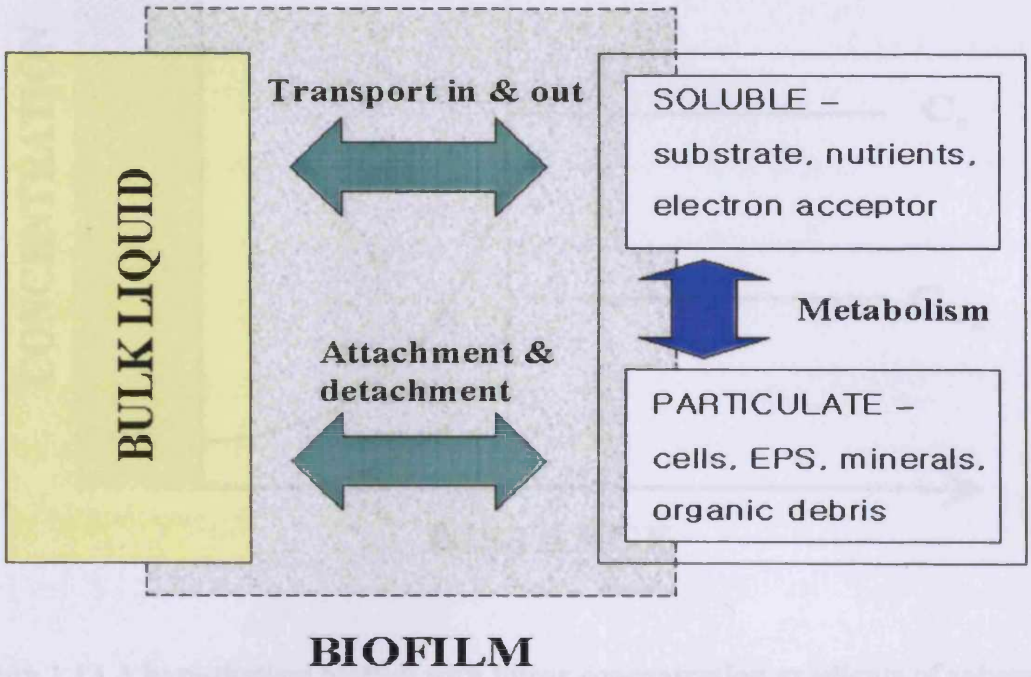

Figure 1.12 A hypothetical biofilm system, illustrating the interaction between the various compartments through transport processes (e.g., transport of soluble components in from the bulk liquid compartment to the biofilm) and interfacial transfer processes (e.g., attachment and detachment of particulate components to the biofilm) (Characklis and Marshall, 1990).

However, as bacteria in the interior grow, they occupy more space, pushing those that are closer to the liquid-biofilm interface further away from the solid support. In addition, all of the bacteria are subject to decay, regardless of their position in the biofilm, resulting in the accumulation of biomass debris. The effect of both processes is to cause a migration of particles from the base of biofilm to the surface and bulk compartment where allowing a biofilm of constant thickness to development. However, the distribution of active microorganisms will not be the same throughout the thickness, age and density of the biofilm.

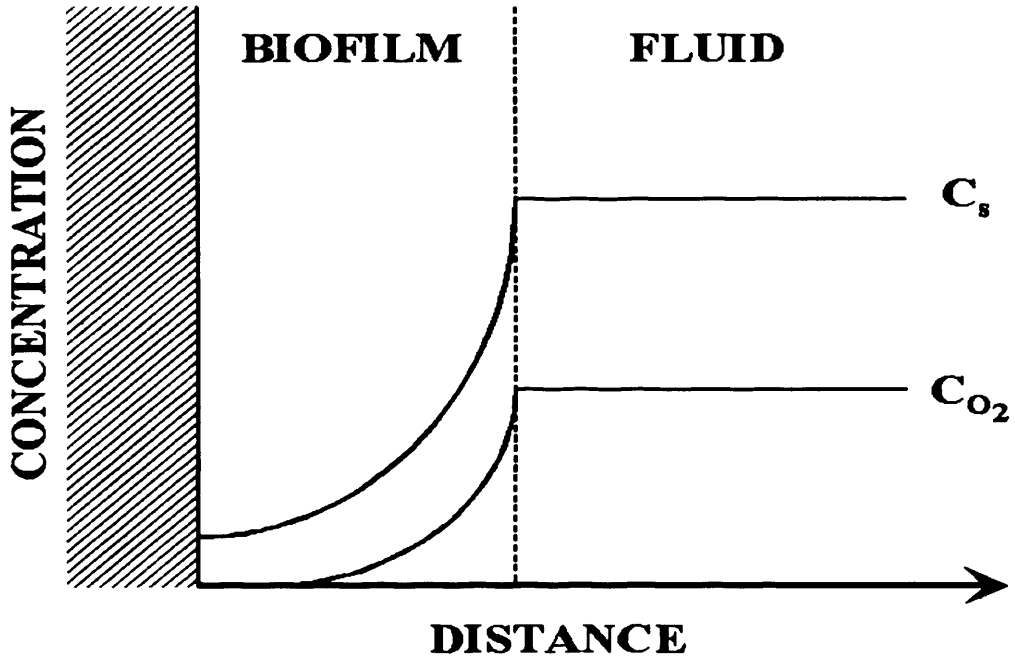

Figure 1.13 A hypothetical biofilm with linear concentration gradients of substrate (s) and oxygen (O_2) schematically indicated. This biofilm contains aerobic and anaerobic environments (Characklis and Marshall, 1990; Wimpenny *et al.*, 1993).

1.4.5. Biofilm formation

Between 1936 and 1943 Zobell (1943) studied the affinity of marine bacteria for surfaces and the more recent development of a battery of new methods for the direct study of living bacteria at interfaces, coupled with many refinements of image analysis, have made it possible to actually study the behavior of bacterial cells as they adhere to these surfaces. Some bacterial cells approach a surface, adhere rapidly to it, initiate glycocalyx (exopolysaccharide) production and form the discrete microcolonies that are the basic organizational units of biofilms. Other cells are seen by direct microscopic methods to adhere to surfaces and then to spread out by rolling or swarming maneuvers to produce an even lawn of glycocalyx-producing adherent cells before microcolony formation is initiated. These adherence behaviors are characteristic of cells of different species and are conditioned by the physiological state of the organisms concerned so

that must anticipate a very significant variety of adherence behavior as more species and more physiological states are examined.

In natural aquatic systems, the majority of bacteria are attached to surfaces. Indeed, surface area is a major limiting factor for microbial growth in nearly every freshwater and marine environment (Morita, 1985). The ratio of planktonic bacteria (free-floating) to biofilm bacteria is a function of several interrelated factors, including surface energetics, materials of construction (Vanhaecke *et al.*, 1990), topography hydraulic factors, and biofilm chemistry (Costerton and Lappin-Scott, 1989). First of all, physical forces (temperature, fluid shear stress, surface composition and hydraulic residence time) may be involved in the attraction or electrostatic repulsion of bacteria to or from surfaces, as both are charged or in a hydrophobic state. Second, the charged nature of surfaces attracts soluble extracellular polymeric substances to which bacteria are attracted. Bacteria become attached to these surface-bound nutrients via cellular appendages, such as flagella, pili, other surface proteins and exopolysaccharides. Third, bacteria may be simply transported by gravitational forces to form sediments on surfaces. Fourth, Brownian motion brings bacteria into contact with surfaces. Finally, various forms of chemical bonding, such as hydrogen bonding, attract and attach bacteria to surfaces.

The colonization of surfaces depends on the mixtures of bacterial species and the surface's physical and chemical properties present in the aqueous phase. Bacterial attachment and the formation of a biofilm appear to take place in a three-stage process (Figure 1.14). During the first stage, surfaces are rapidly coated with ions and organic molecules. This is called the "conditioning layer" because it alters the surface's physical and chemical properties (McEldowney and Fletcher, 1986; Heijnen *et al.*, 1992). In the second-stage, it is followed by the transportation of bacteria to the surface. Single bacterial cells are in contact with a uniform surface and adhesion introduces

some heterogeneity, as the cells may adhere to uncolonized areas of the surface or may join colonized areas. When more than one species of bacteria is present, colonization patterns differ, as each species may adhere, or one species may act as a primary colonizer and attract cells of the same or different species. Initially, bacterial adhesion sites are located randomly on a uniform surface, but once colonization commences, these sites begin to differ because of bacterial activity. Surface growth, replication, microcolony formation, and glycocalyx production all increase the heterogeneity of these attachment sites, and this further increase as a confluent biofilm forms. The composition and properties of the biofilm matrix depend on the bacterial inhabitants. For example, the exopolysaccharides produced by some species will bind metal ions and thus alter the chemical nature of the biofilm. Also, metabolic products such as organic acids can become trapped within the film, sometimes leading to marked differences in adjacent microcolonies. In this manner, a homogeneous surface is transformed by bacterial colonization into a profoundly heterogeneous surface. The mature, third-stage biofilm consists of the organic conditioning film, a succession of colonizing bacterial consortia with their associated EPS and various detrital particles and ionic species (Mittelman, 1998).

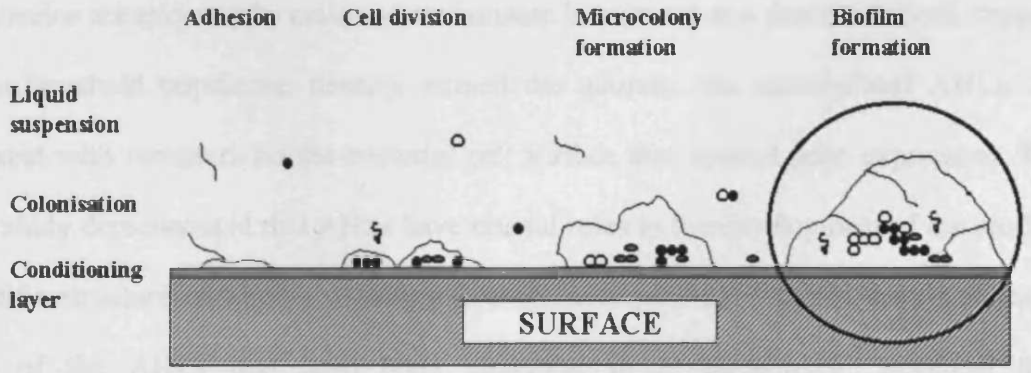

Figure 1.14 Biofilm formations on the surfaces (Heijnen *et al.*, 1992).

Recently, sets of well-characterized mutant strains have proved to be powerful tools in the investigation of the mechanisms by which bacteria initiate biofilm formation. In the case of *Escherichia coli*, mutants defective in biofilm formation on polyvinyl chloride (PVC) were obtained by transposon insertion mutagenesis (Pratt and Kolter, 1998). They were found either to lack the ability to produce type I pili or to be non-motile. The type I pili are mannose-sensitive adhesions and their role in biofilm initiation was confirmed in experiments in which a mannose analogue inhibited biofilm formation by the wild-type strain. Once the surface is reached, the type I pili are required to achieve stable cell-to-surface attachment. Surface attachment deficient (*sad*) mutants of *Pseudomonas fluorescens* were also isolated by transposon insertion (O'Toole and Kolter, 1998). Some of these mutants were found to be non-motile, whereas others were unable to produce a protein designated ClpP, which is normally exposed at the cell surface and forms part of a cytoplasmic protease system. It was suggested that *P. fluorescens* could adopt multiple strategies for initiating cell-to-surface interactions and that these strategies are dependent on environmental signals. In Gram-negative bacteria, cell communication can be achieved through the activity of acylated homoserine lactones (AHLs) (Fuqua *et al.*, 1996). These small signal molecules are excreted by cells and accumulate in cultures as a function of cell density. At a threshold population density, termed the quorum, the accumulated AHLs can interact with receptors on the bacterial cell surface that control gene expression. The key study demonstrated that AHLs have crucial roles in the development of the biofilm specific structure and cell physiology (Davies *et al.*, 1998). Mutants unable to make one of the AHLs that have been identified in *P. aeruginosa*, produced thin undifferentiated layers of cells on a glass surface. It was concluded that the accumulation of AHL in a developing biofilm causes the transformation of individual

cells from the planktonic to the biofilm phenotype and co-ordinates their behavior in some way so that they build the complex structures of the multicellular communities.

1.4.6. Adaptive advantages in environment of biofilm

Several adaptive advantages have been ascribed to life within a biofilm. It proposed that solid surfaces act not only to concentrate nutrients by adsorption but also to retard the diffusion of exoenzymes away from the cell, thus promoting the uptake of substrates that must be hydrolyzed extracellularly. Attachment appears to be an important adaptive mechanism in what Morita (1982) has termed the starvation-survival mechanism of bacteria in extreme environments. A decrease in the concentrations of bulk phase carbon sources promotes the attachment of marine and freshwater bacteria (Marshall, 1988).

Biofilm organisms are afforded a measure of protection from antagonistic agents that can be present in bulk-phase environments. Protection from lytic bacteria such as *Bdellovibrio* sp. (Venosa, 1975), the toxic effects of heavy metals (Mittelman and Geesey, 1985), and bactericidal agents, are important advantages afforded to microorganisms within biofilms (Mosteller and Bishop, 1993). This protective feature is a significant factor in many disease processes and biological fouling activities in industrial systems. Bacteria that are associated with biofilms are more resistant to antibiotic treatments that would otherwise prove effective against free-living populations (Hoyle and Costerton, 1990).

1.4.7. A microbial community analysis in biofilms

Despite advances in microbiological sampling and culture techniques, it is estimated that over 80% of the Earth's microbial species have not been cultured and are therefore uncharacterized (Wayne *et al.*, 1987). Recently, powerful molecular methods such as

PCR-clone library by restriction fragment length polymorphism (RFLP) profile, terminal restriction fragment length polymorphism (T-RFLP) and denaturing gradient gel electrophoresis (DGGE) have been developed for the investigation of microbial diversity from a wide variety of different habitats (Marsh, 1999; Muyzer *et al.*, 1993; Ward *et al.*, 1990). Studies have focused on the small subunit ribosomal RNA molecules (16S rRNA) and their associated genes. These genes are present in all organisms and contain both highly conserved and rapidly evolving variable sequences. Small subunit rRNA genes provide sufficient information for the determination of phylogenies and this has revolutionized bacterial classification (Hugenholtz *et al.*, 1998; Woese, 1987). Ribosomal database project II and NCBI BLAST service with more than 2000 small subunit molecules are now available and specifically developed computer programmes can be used in the phylogenetic analysis of new sequences (Dalevi *et al.*, 2001).

16S rRNA genes are retrieved from the biofilm samples by extraction of genomic DNA and amplification by the polymerase chain reaction (PCR). The heterogeneous population of amplified 16S rRNA genes is separated by cloning and clones from cultivable microorganisms recognized by digestion of the cloned DNA with restriction endonucleases to give a characteristic restriction fragment length polymorphism (RFLP) profile. Clones are then sequenced and identified by reference to a 16S rRNA database.

An understanding of biofilms is depending on knowledge regarding their microbial composition. The molecular method described has tremendous potential for elucidating the true microbial diversity of biofilms.

1.5. Aims of study

A microbial fuel cell is an electrochemical device that converts the chemical energy of organic fuel to electrical energy with the aid of the catalytic reactions of microorganisms. Until now, various microbial or biochemical fuel cells have been developed using *Desulfovibrio desulfuricans*, *Proteous vulgaris*, *Escherichia coli*, *Pseudomonas* species, *Bacillus* species and redox enzymes as biocatalysts. In a typical microbial fuel cell, an anodic electrode potential is generated when the electrons from the oxidation of the substrate by microorganisms are available to the electrode. Although the direct electron transfer from various microorganisms in a microbial cell to electrodes has been demonstrated, this process is inefficient both in terms of the proportion of electron transferred (i.e. the coulombic yield) and the rate of electron transfer (i.e. the current generation). A microbial fuel cell system can be used for various purposes including bacterial activity monitoring, electricity generation in local area, wastewater treatment processes and so on. Recently, anaerobically-grown cells of the iron-reducing bacterium, *Shewanella putrefaciens* IR-1, were shown to be electrochemically active using cyclic voltammetry and that the bacterium can be cultivated in an electrochemical cell without additions of any terminal electron acceptors such as oxygen or Fe(III) or electrochemical mediator. We describe the development of a mediator-less microbial fuel cell.

Activated sludge has been reported to contain a large population of Fe(III)-reducers and anaerobic reduction process of activated sludge-bound Fe(III) by Fe(III)-reducing bacteria can result in sludge deflocculation (Nielsen *et al.*, 1997; Caccavo *et al.*, 1996b). A wide variety of bacteria from diverse environments are capable of coupling the oxidation of organic matter to dissimilatory Fe(III) reduction. A fuel cell used to enrich electrochemically active microbes and a novel wastewater treatment using wastewater

as the electron donor with activated sludge as the bacterial source. This has led to novel wastewater treatments using microbial fuel cell in multi-purpose biosystems involving electricity energy generation and activated sludge removal. The effect of insoluble Fe(III) ion on growth and metabolite production has also been studied. The microbial population has obvious potential for pollution treatment since it can remove over 95% of the organic pollutants present. However, little is known about the microbes within the fuel cell or their responses to mixed organic and inorganic pollutants, e.g. metals, or the significance of the biofilm mode of growth and microbial diversity on the electrode.

The objectives of this project were therefore as follows:

(i) to characterize the microbes and their activities within the microbial fuel cell;

(ii) to determine the response of the bacterial community to different organic substrates and inhibitors in the fuel cell;

(iii) to investigate the significance of the biofilm on the electrode;

(iv) to analyse the bacterial community associated with fuel cell biofilm and its contribution to electrochemical activity; and

(v) to understand the biotechnological potential of the fuel cell for energy generation and wastewater pollution treatment.

CHAPTER II

Enrichment of Microbial Community Generating Electricity and Wastewater Treatment Using a Microbial Fuel Cell

The part of this work was undertaken in collaboration with Water Environment & Research Centre, Korea Institute of Science and Technology (KIST) and published as below. I was involved in all stages of the planning and execution of the work.

Kim, B.H., Park, H.S., Kim, H.J., Kim, G.T., Chang, I.S., Lee, J. & Phung, N.T. (2004) Enrichment of microbial community generating electricity using a fuel cell type electrochemical cell. *Applied Microbiology and Biotechnology* 63, pp. 672-681.

2.1. Introduction

Several electrochemical techniques can be used in various fields of biology, particularly biochemistry, to characterize redox proteins, including cytochromes, and in biotechnology to develop biosensors, bioelectrochemical synthetic processes and microbial fuel cells (Higgins and Hill, 1985). Though many of redox proteins are electrochemically active, the peptide chain adjoining the redox center of the protein hinders the direct electron transfer between the redox proteins and an electrode. Modification of the protein or the electrode surface can increase the rate of the electrochemical reaction (Uosaki and Hill, 1981). In most cases, intact microbial cells that contain active redox proteins are electrochemically inactive as their cell walls and other surface structures are electrically non-conductive. Mediators can be used to facilitate the transfer of electrons between microbial fuel cells and an electrode (Allen and Bennetto, 1993; Kim and Kim, 1988). The outer cell membrane in microorganisms must be permeated by both the oxidized and reduced forms of the mediator. Alternatively, the bacterial cells can be modified with hydrophobic conducting compounds to increase electrochemical activity (Park *et al.*, 1997; Park *et al.*, 1999).

A microbial fuel cell is a two-compartment structure divided by a cation specific ion exchange membrane. Electrons available through metabolism of the electron donors by microorganisms are transferred to the anode of the fuel cell, and then to the cathode through the circuit, where they reduce the oxidant, consuming protons available through the membrane from the anode (Allen and Bennetto, 1993). There are at least two types of microbial fuel cells. One involves the utilization of electrochemically active metabolites such as hydrogen sulfide produced by microbial metabolism (Haberman and Pommer, 1991), and the other involves the use of mediators as electron

carriers from a metabolic pathway of the microorganism or enzyme to electrodes (Allen and Bennetto, 1993; Park and Zeikus, 2000). Until recently, although a number of microbial or biochemical fuel cells have been developed using various microorganisms and redox enzymes as biocatalysts (Tayhas *et al.*, 1994), microbial fuel cells have not yet been commercialized due to costs in using mediators on a commercial scale (Bennetto *et al.*, 1987; Tayhas *et al.*, 1994). Studies of iron-reducing and electrochemically-active bacteria have suggested that the bacterium itself might have overcome problems associated with the use of mediators allowing to the construction of a mediator-less microbial fuel cell (Park *et al.*, 2001; Kim *et al.*, 2002).

A number of bacteria have been isolated with the ability to use Fe(III) as a terminal electron acceptor (Lovley, 1991; Nealson and Saffarini, 1994). Though there is some evidence that a soluble electron carrier is involved in the electron transfer to the water-insoluble electron acceptor (Turick *et al.*, 2002), direct electron contact between the bacterial cells and the electron acceptor is required for dissimilatory Fe(III) reduction (Nevin and Lovley, 2000). Among the Fe(III)-reducers *Shewanella putrefaciens* (Myers and Myers, 1992) and *Geobacter sulfurreducens* (Lloyd *et al.*, 2000) are known to localize the majority of their membrane-bound cytochromes on the outer membrane, and the *Shewanella putrefaciens* is electrochemically-active (Kim *et al.*, 1999a; Kim *et al.*, 1999b). *S. putrefaciens* grew on lactate in the absence of electron acceptors in an electrochemical fuel cell, but did not metabolize lactate when the anode was disconnected from the cathode (Kim *et al.*, 1999b). A mediator-less microbial fuel cell has been successfully operated using *S. putrefaciens* (Kim *et al.*, 2002). In addition, an electrochemically-active strain of *Clostridium butyricum* has been isolated from the mediator-less microbial fuel cell (Park *et al.*, 2001).

Iron (Fe) is present in large amounts in many activated sludge treatment plants, providing plenty of Fe(III) as substrate for the bacteria (Nielsen, 1996; Nielsen *et al.*, 1997). Fe is transported to the plant as part of the wastewater or added as Fe-salts, such as $FeSO_4$ chemically remove phosphate. About 50-60 mg Fe g^{-1} VSS have recently been reported in a wastewater treatment plant, all of which was accessible to microbial Fe(III) reduction under anaerobic conditions (Rasmussen and Nielsen, 1996). Microbial Fe(III) reduction in activated sludge has mainly been investigated in relation to processes taking place during the anaerobic storage of sludge. A wide variety of bacteria from diverse environments are capable of coupling organic matter oxidation to dissimilatory Fe(III) reduction (Lovley, 1995). Recent studies suggest that microbial Fe(III) may play an important role in the disintegration of sludge flocs during anaerobic storage. Cells of the dissimilatory metal-reducing bacterium *Shewanella alga* BrY coupled the oxidation of H_2 to the reduction of Fe(III) bound in autoclaved activated sludge flocs (Caccavo *et al.*, 1996b). Sludge disposal is an expensive process that is ameliorated by reducing the sludge volume through dewatering. The activity of Fe(III)-reducing bacteria may thus have a significant economic impact on the wastewater treatment industry, since deflocculation leads to decrease in sludge dewaterability (Mikkelsen *et al.*, 1996).

In the research reported in this Chapter II, a fuel cell-type electrochemical cell was used to enrich microbial consortia generating electricity using wastewater as fuel. We therefore describe the application of the mediator-less microbial fuel cell using activated sludge as source of bacteria and artificial wastewater as electron donor for the development of a novel energy producing wastewater treatment system.

2.2. Materials and methods

2.2.1. Wastewater and sludge

Artificial wastewater was adopted as a model wastewater in this study and aerobic activated sludge obtained from Ponthir sewage treatment works (Gwent, UK) was used a bacterial source. The chemical oxygen demand (COD) value of artificial wastewater was 500-1500 mg l^{-1}, depending on the operational conditions. The COD value was based on the oxygen requirement for organic substrates.

Table 2.1 The composition of modified artificial wastewater (De Lucas *et al.*, 2000).

Artificial wastewater (mg l^{-1})	
KH_2PO_4	15 as P
$(NH_4)_2SO_4$	30 as N
$MgSO_4 \cdot 7H_2O$	50
$CaCl_2$	3.75
$FeCl_3 \cdot 6H_2O$	0.25
$MnSO_4 \cdot H_2O$	5.0
$NaHCO_3$	105
Trace mineral solution	10 ml l^{-1}
Trace mineral solution (g l^{-1})	
Nitrilotriacetic acid (NTA: $C_6H_9NO_6$)	1.5
$FeSO_4 \cdot 7H_2O$	0.1
$MnCl_2 \cdot 4H_2O$	0.1
$CoCl_2 \cdot 6H_2O$	0.17
$CaCl_2 \cdot 2H_2O$	0.1
$ZnCl_2$	0.1
$CuCl_2 \cdot 2H_2O$	0.02
H_3BO_3	0.01
Na_2MoO_3	0.01
NaCl	1.0
Na_2SeO_3	0.017
$NiSO_4 \cdot 6H_2O$	0.026

* Glucose and glutamic acid were used as organic matters.

2.2.2. Electrodes used in the microbial fuel cell

Both anode and cathode were graphite felt (50×50×3 mm^3 in dimension, GF series, Electrosynthesis, E. Amherst, NY, U.S.A.). Platinum wire contacts (0.5×70 mm^2) were bonded to the electrodes with a conducting adhesive, ABLEBOND® 84-1LMIT1 (ABLESTIK, CA, U.S.A.) which was cured at 150℃ for 20 h. To aid initial wetting of the electrodes, they were soaked in pure ethanol then boiled in deionized water to remove the ethanol. Electrodes were cleaned and stored in HCl (0.1 M) and thoroughly rinsed in deionized water prior to use (Kim *et al.*, 2002).

2.2.3. The microbial fuel cell

The microbial fuel cell was constructed using transparent polyacrylic material and was similar to those used by other workers (Allen and Bennetto, 1993; Delaney *et al.*, 1984). The fuel cells had 20 ml capacity electrode compartments measuring 50×57×7 mm^3 (Figure 2.1). Each cell compartment had three ports at the top, for the electrode wire, the addition and sampling of solutions, and gassing. The two compartments of each cell were separated by a cation-permeable ion exchange membrane (model 55165, BDH Lab supplies, Dorset, UK) sealed between 2 mm thick silicon rubber gaskets. Contact between the electrodes and the ion-exchange membrane was prevented by inclusion of thin plastic bars (2×2×5 mm^3). The anode compartment was loaded with freshly prepared 20 ml artificial wastewater adjusted to pH 7.0 and aerobic activated sludge. The cathode compartment was then loaded with 50 mM Na-phosphate buffer (pH 7.0) containing 0.1 M NaCl (Kim *et al.*, 1999b). Nitrogen and air were continuously purged through anode and cathode compartments to maintain anaerobic or aerobic conditions, respectively (flow rate: 15 ml min^{-1}). The microbial fuel cell was immersed in a water bath to maintain temperature (30℃).

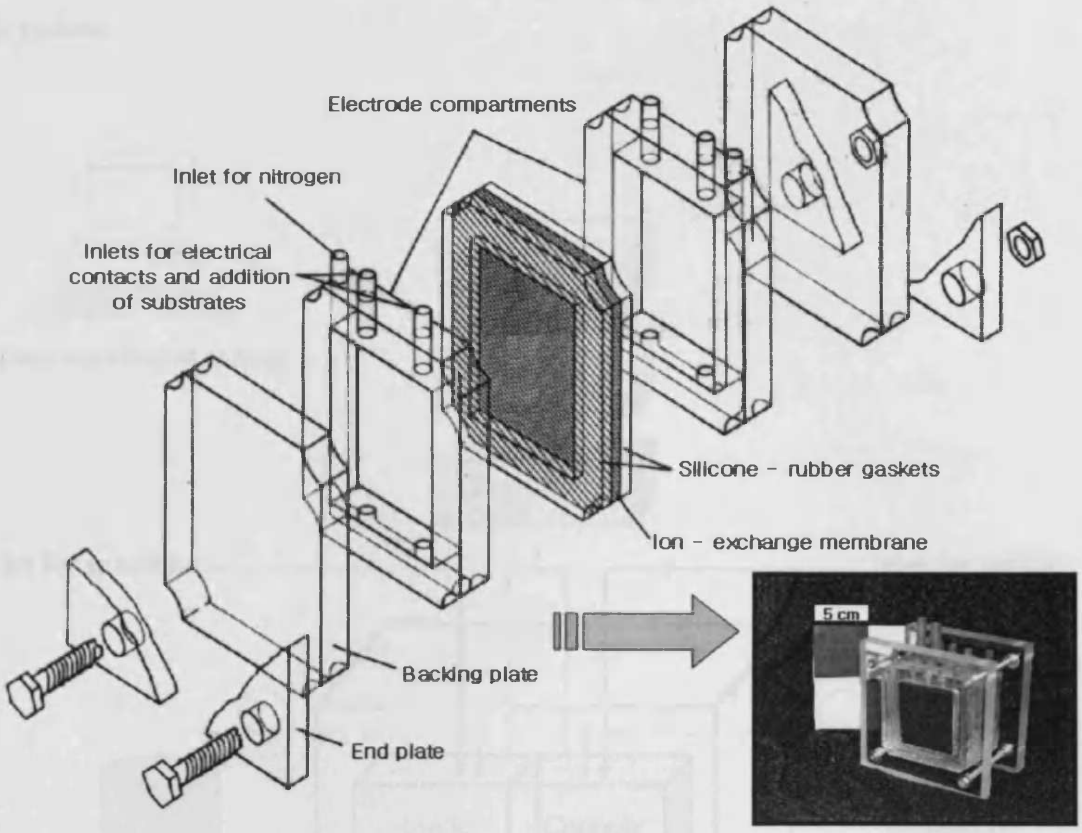

Figure 2.1 Construction of cell for microbial fuel cell experiments (Delaney *et al.*, 1984).

Each half-cell was provided with inlets for gas bubbling. The anode compartment of fuel cell was kept anoxic with oxygen free nitrogen (15 ml min^{-1}) whilst the cathode was saturated with air (15 ml min^{-1}). The circuit was connected by a 1 KΩ external resistance from anode to cathode to allow a current flow. Electrons are transferred to the cathode through the circuit. At start-up the microbial fuel cell was operated under open circuit (unlimited resistance) conditions for bacteria enrichment: the fuel cell was then discharged using a 1 KΩ resistance (closed circuit) for the enrichment of electrochemically-active bacteria after the maximum potential had been reached. Current and coulomb were compared to determine the optimum conditions for fuel cell operation. Figure 2.2 shows the schematic diagram of the mediator-less microbial fuel

cell system.

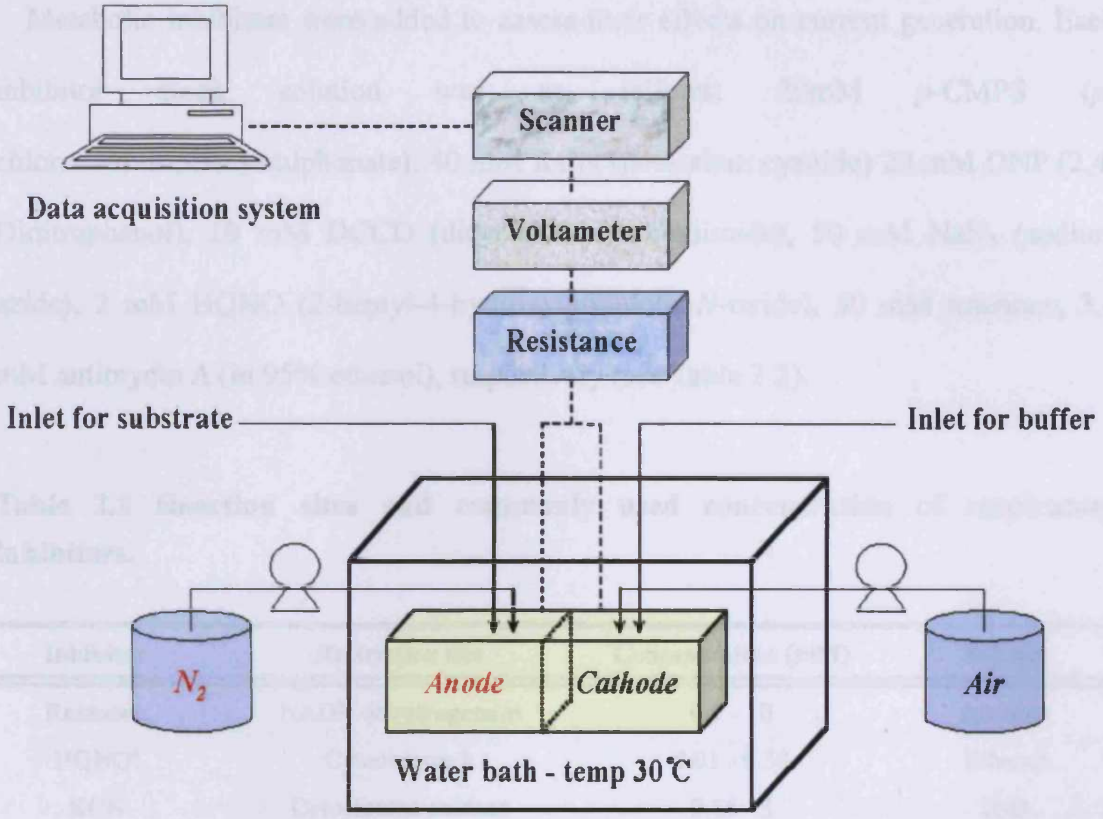

Figure 2.2 Schematic diagram of the mediator-less microbial fuel cell.

2.2.3.1. Optimization

The current and coulomb output were recorded to determine the optimum pH after the anode had been fed with wastewater adjusted to pH 5.0-9.0 Effects of temperature on microbial fuel cell were determined by changing the waterbath temperature from 20℃ to 45℃. The influence of resistance change was measured at 1 KΩ, 500 Ω, 200 Ω and 100 Ω, respectively. The effect of aeration rate to the cathode part of microbial fuel cell was analysed from 5 ml min^{-1} to 20 ml min^{-1}. Nitrogen feed rate to the anode compartment was from 5 ml min^{-1} to 20 ml min^{-1}. Areas of anode electrode and cation ion exchange membrane were from 5 cm^2 to 1.25 cm^2.

2.2.3.2. Operation with metabolic inhibitors

Metabolic inhibitors were added to assess their effects on current generation. Each inhibitor stock solution was as follows: 20mM *p*-CMPS (*p*-chloromercuriphenylsulphonate), 40 mM KCN (potassium cyanide) 20 mM DNP (2,4-Dinitrophenol), 10 mM DCCD (dicyclohexylcarbodiimide), 50 mM NaN_3 (sodium azide), 2 mM HQNO (2-heptyl-4-hydroxyquinolone-*N*-oxide), 50 mM rotenone, 3.4 mM antimycin A (in 95% ethanol), respectively (see Table 2.2).

Table 2.2 Reaction sites and commonly used concentration of respiratory inhibitors.

Inhibitor	Restriction site	Concentration (mM)	Solvent
Rotenone	NADH dehydrogenase	0.5 - 10	Acetone
HQNO[a]	Cytochrome *b*	0.01 - 0.38	Ethanol
KCN	Cytochrome oxidase	0.16 - 3	H_2O
NaN_3	Cytochrome oxidase	0.6 - 9	H_2O
DCCD[b]	F_o subunit of ATPase	0.03 - 1	Acetone
DNP[c]	Uncoupler	0.08 - 0.3	Acetone
p-CMPS[d]	Sulphydryl center (Fe-S protein)	0.01 - 0.4	H_2O
Antimycin A	Electron transport chain site II	0.002 – 0.68	Ethanol

[a] HQNO: 2-heptyl-4-hydroxyquinolone-*N*-oxide

[b] DCCD: Dicyclohexylcarbodiimide

[c] DNP: 2,4-dinitrophenol

[d] *p*-CMPS: *p*-chloromercuriphenylsulphonate

2.2.3.3. Operation in the presence of alternative electron donors and acceptors

Electron donors were used as followed; lactate (10 mM), pyruvate (5 mM), acetate (5 mM), glucose (10 mM), propionate (10 mM), iso-butyrate (5 mM) and citrate (5 mM), respectively. The effects of alternative electron acceptors were also tested. Sulphate was used from 10 μM to 3.6 mM. Nitrate and nitrite were added to anode part

from 10 μM to 640 μM, respectively. Air saturated (9.14-9.34 mg l^{-1}) wastewater was used to test the effects of air in the anode part as an alternative electron acceptor. Air saturated wastewater was mixed with anaerobic artificial wastewater.

The experiments in Chapter II were conducted using 5 microbial fuel cells. Two or three of these fuel cells were selected randomly for recording the results, which are presented are means and standard deviations in tables and bar graphs as an index of variability. Typical results are presented for monitoring current and means alone for COD results.

2.2.4. Analytical methods

2.2.4.1. Electrical potential and coulomb (C) measurements

Electrodes were connected to a voltmeter to measure the potential. Potential (V, volt) and current (I, ampere) of the fuel cells were measured using a voltmeter (Model 2000-20, Keithley, Cleveland, U.S.A.) linked to a multichannel scanner (Model 2000-SCAN, Keithley). Data were recorded digitally on an IBM compatible personal computer *via* IEEE488 input/output system (Model KPC-488.2AT, Keithley) and a cable (Model CTMGPIB-1, Keithley). The voltmeter and the scanner were regulated using control software (TestPoint®, Keithley). This software was used to calculate the current and coulombic yield [current (I) × time (t)] produced from the fuel cells.

When the fuel cell was initially set-up, the electrodes were connected to the voltmeter to start the measurement of the potential. When the potential from the fuel cell had stabilized, the cell was connected to its load resistance (Ω), and the resultant current (I) was measured as $I = V/R_{load}$, where V is the potential drop across R_{load}. A resistor (1 KΩ) was routinely used as the load resistor. The measured values were given

as an on-line graphic display which showed values made every 2 min.

Coulomb outputs of fuel cells were determined by graphical integration for the areas under current-time curves. The coulomb efficiency was defined as the percentage charge obtained compared to the theoretical charge obtainable from the complete oxidation of the consumed COD.

2.2.4.2. Chemical oxygen demand (COD)

COD of wastewater was analysed by colorimetric method (closed reflux method; Eaton *et al.*, 1995). Samples taken before and after fresh wastewater was added to the cell for analyses. Diluted samples of 2 ml were added to COD 1500-HC6153 monotest kit vials (HYDROCHECK, UK). Vials were mixed vigorously and heated with HYDROCHECK digester HC6040 at 148℃ for 2 h. COD values were read from HYDROCHECK photometer HC6502S22 using standard filter 585 nm and COD 1500 method card.

2.2.4.3. Energy conversion

The amounts of electricity produced were calculated on the basis of complete oxidation of the consumed COD to CO_2 and H_2O. Electrons available from 1 g COD are 4 × (1/32) mol = 0.125 mol. Current (amp·sec) is equivalent to mol electron by Faraday constant: 0.125 × 96,500 = 12,062 coulomb (C). The theoretical coulomb was calculated from mg COD consumed (12 C mg COD^{-1}).

2.3. Results

2.3.1. Enrichment of electrochemically-active microorganisms

Fuel cell-type electrochemical cells (shown in Figure 2.1) were used to enrich electrochemically-active microbes using artificial wastewater as the fuel and activated sludges collected from Ponthir sewage treatment works (Gwent, UK) as a microbial source. Sludges were collected from the aerobic treatment process. Current generation and COD removal from the fuel cells were shown in Figure 2.3 and Table 2.3.

At first, the fuel cell was operated with unlimited resistance (open circuit) for 22 h. The maximum open circuit potential of around 0.5 V was developed immediately after the addition of sludge. Similar results were obtained from all fuel cells to which activated sludge or anaerobic digester sludge had been added. The fuel cell containing only wastewater did not develop a significant potential. The size of the open circuit potential developed was dependent on the amount of sludge added. These results show that the sludge contains electrochemically active material. Using the Nernst equation, the expected voltage difference between the cathode and anode of microbial fuel cell can be predicted. In the present experiments, however, the values obtained (i.e. the open circuit potential of the microbial fuel cell) were not completely inline with their equation.

The fuel cell was discharged using a 1 KΩ resistance after current had reached a steady value. When the fuel cell was connected through a resistance of 1 KΩ, the potential dropped to 20 mV, which corresponds to a current of 20 μA. When a portion of the anode chamber content (10 ml) was replaced with fresh wastewater the current increased to 0.15 mA before falling to a background level of 20 μA with decrease in COD (Figure 2.3). Repeated wastewater replacements were coupled to current generation together with a stepwise fall in soluble COD from 1,120 mg l^{-1} to 110 mg l^{-1}.

Similar trends were observed in all fuel cells which had received activated sludge or anaerobic digester sludge. The fuel cells without the bacterial inoculums but containing wastewater showed similar results at slower rates. Soluble COD value of the anode content of the control fuel cell was reduced to around 110 mg l^{-1} in 4 weeks.

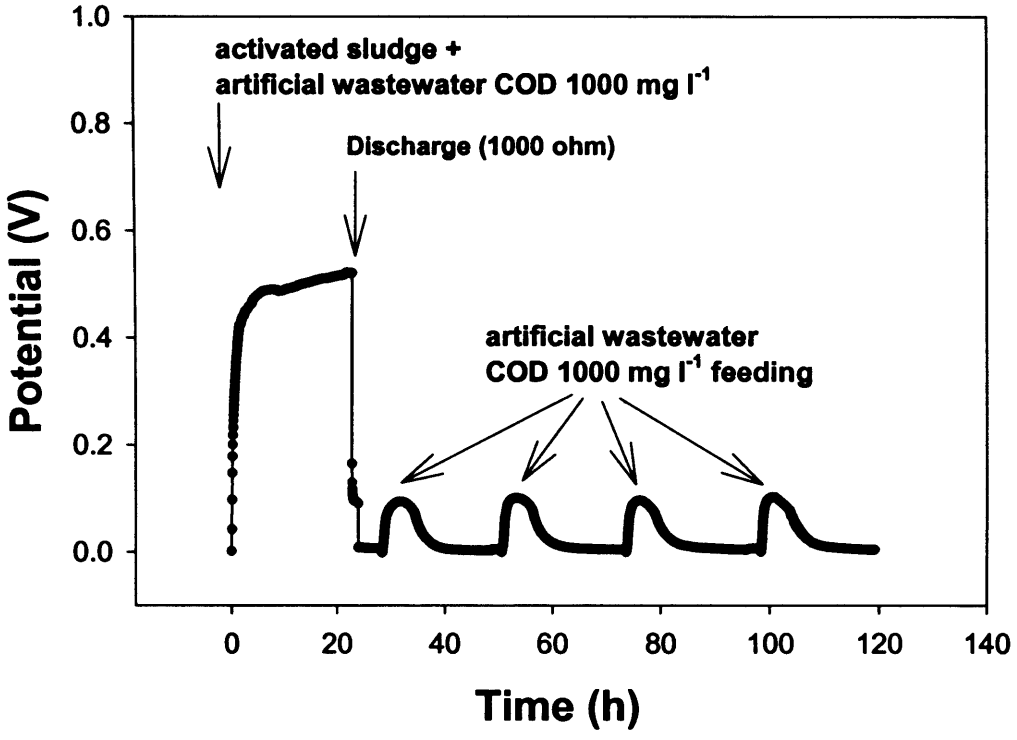

Figure 2.3 Start-up of a mediator-less microbial fuel cell through enrichment of electrochemically active microbes using artificial wastewater and sludge collected from an aerobic digester, as the inoculum.

Table 2.3 Wastewater treatment parameters and efficiency in a microbial fuel cell.

Parameters	Before treatment	After treatment	Removal rate (%)
pH	7.0 ± 0.21	6.9 ± 0.72	-
COD (mg l^{-1})	1120 ± 54.7	110 ± 13.1	90

*Data are presented as the mean ± S.D. (n=2)

The open-circuit control fuel cells were operated in a similar way as the others for 4 weeks before the anode was connected to the cathode through 1 KΩ resistance. These control fuel cells generated a much lower current than that from the closed-circuit microbial fuel cells (data not shown). This suggested that the electrochemically-active particles, probably bacteria in the sludge, propagated in the closed-circuit fuel cells but not in the open-circuit control. The current generation might have been the result of electrons transferred to the electrode by the electrochemically-active bacteria after they metabolized electron donor (s) in the wastewater in the absence of electron acceptors. The stepwise decrease in soluble COD showed that certain electron donor (s) in the wastewater were metabolized faster than others by the microorganisms present in the sludge at each given conditions, and that those electron donors consumed at a later stage were metabolized by the microorganisms enriched during operation of the fuel cell. The fuel cells generated current stably for over 2 years in semi-continuous mode. The pH of anode part did not fluctuate during the operation.

2.3.2. Effects of operational conditions on fuel cell performance

The microbial fuel cell enriched for over 6 months was used to test the effects of environmental parameters on the fuel cell performance.

2.3.2.1. Relationship between wastewater concentrations and current generation

The microbial fuel cell was fed with different concentration of fresh artificial wastewater to determine the relationship between the fuel consumption and current generation (Figure 2.4).

Table 2.4 The relationship between fuel consumption and electricity generation.

Concentration (mg l^{-1})	ΔCOD[a] (mg l^{-1})	Theoretical coulomb[b] (C)	Experimental coulomb[c] (C)	Coulombic yield (%)
50	26 ± 4.24	6.2	0.46 ± 0.05	7.41
250	180 ± 2.94	43.2	1.51 ± 0.02	3.49
500	399 ± 22.62	95.7	2.70 ± 0.56	2.82
1000	880 ± 7.07	211.2	4.51 ± 0.12	2.13
1500	1355 ± 14.04	325.2	7.75 ± 0.21	2.38

[a]ΔCOD: different COD between initial and final COD depend on feeding volume of wastewater

[b]Theoretical coulomb: ΔCOD (mg l^{-1}) × working volume (20 ml l^{-1}) = mg COD

[c]Data are presented as the mean ± S.D. (n=2) *1 mg COD = 12 coulomb

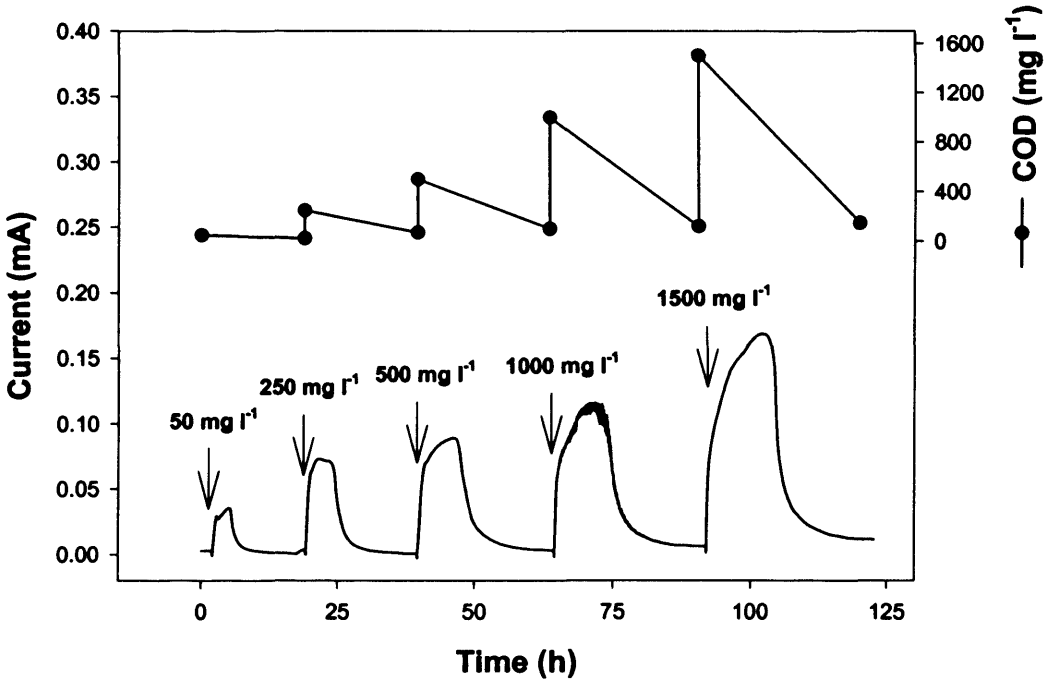

Figure 2.4 Current generation from the microbial fuel cell fed with different concentrations of wastewater as fuel.

The data were used to calculate coulombic yield. As the predicted, experimental coulomb output were increased in proportion to wastewater feeding concentration (Table 2.4). The highest coulombic yield was obtained when COD 1500 mg l^{-1} wastewater was added.

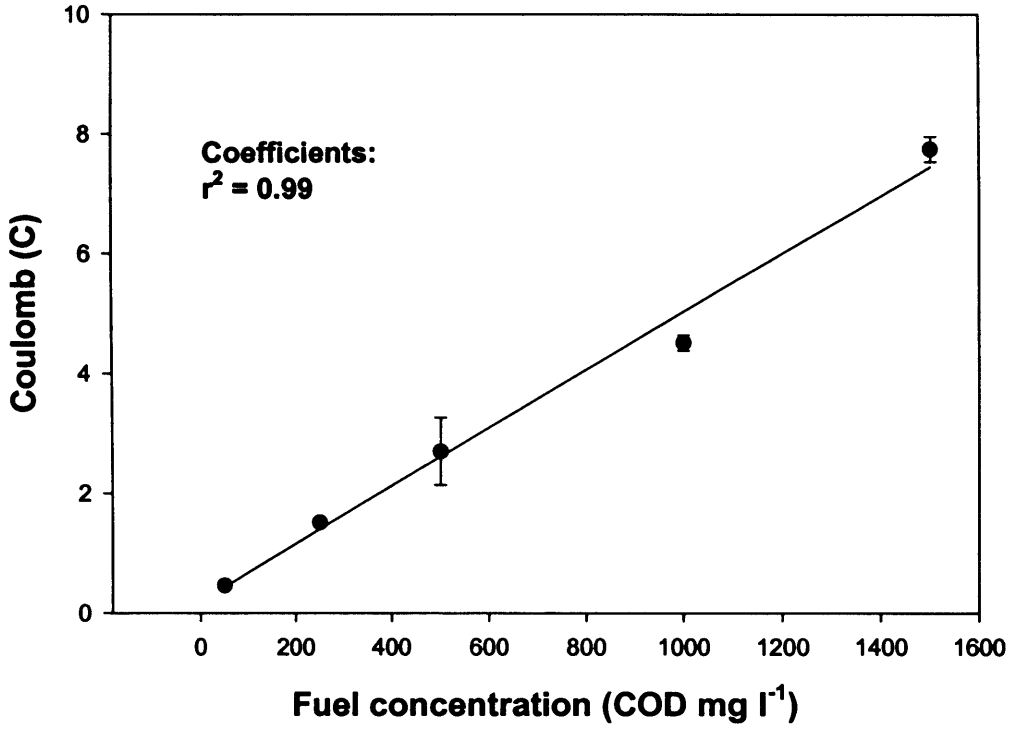

Figure 2.5 The relationship between coulomb and fuel concentration (COD). Data are presented as the mean ± S.D. (n=2)

2.3.2.2. Effects of pH

Current output was analysed when pH of the feed wastewater to the anode compartment was altered. The cathode pH was held at 7.0. Figure 2.6 shows that the current generation and COD change at different anode pH values. The highest current was generated at pH 8.0 followed by pH 7.0.

Table 2.5 The relationship between anode compartment pH and current generation in the fuel cell.

pH value	ΔCOD[a] (mg l^{-1})	Theoretical coulomb (C)	Experimental coulomb[b] (C)	Coulombic yield[c] (%)	Final pH
5.0	849 ± 7.64	203.7	6.11 ± 0.11	2.99	6.72
6.0	840 ± 5.14	201.6	8.70 ± 0.07	4.31	6.97
7.0	851 ± 21.77	204.2	11.93 ± 0.52	5.84	7.02
8.0	836 ± 29.24	200.6	13.89 ± 0.61	6.92	8.12
9.0	832 ± 34.14	199.6	8.89 ± 0.62	4.45	8.45

[a]The different COD between initial and final COD depend on pH

[b]Data are presented as the mean ± S.D. (n=2)

[c]Yield (%) = theoretical coulomb / experimental coulomb × 100

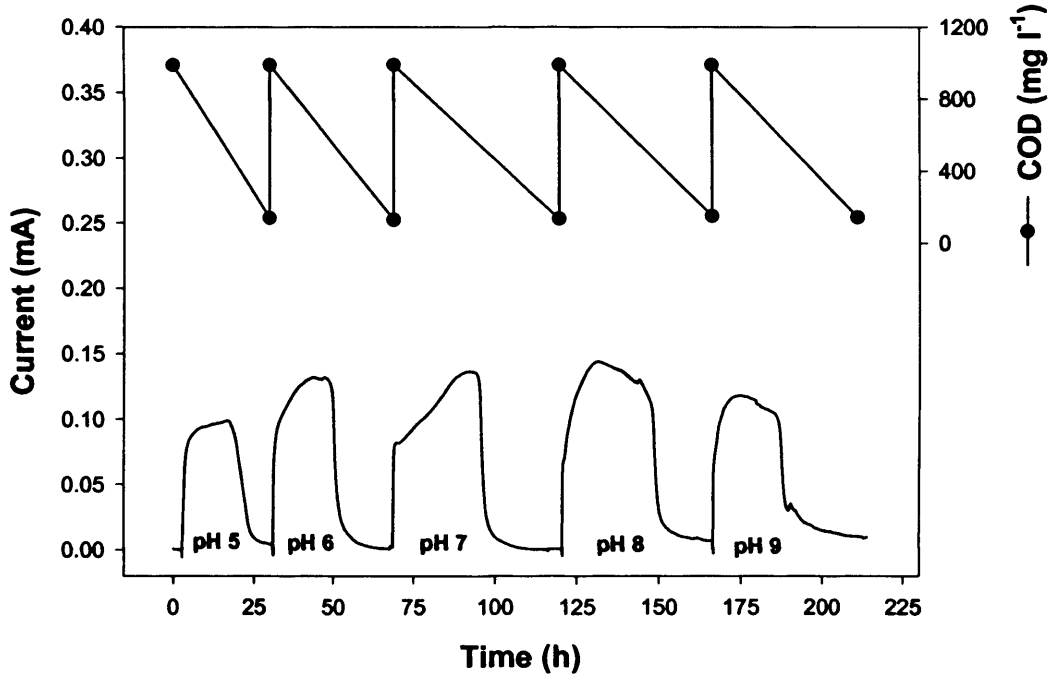

Figure 2.6 The effect of pH at the anode compartment on current and COD changes in the fuel cell.

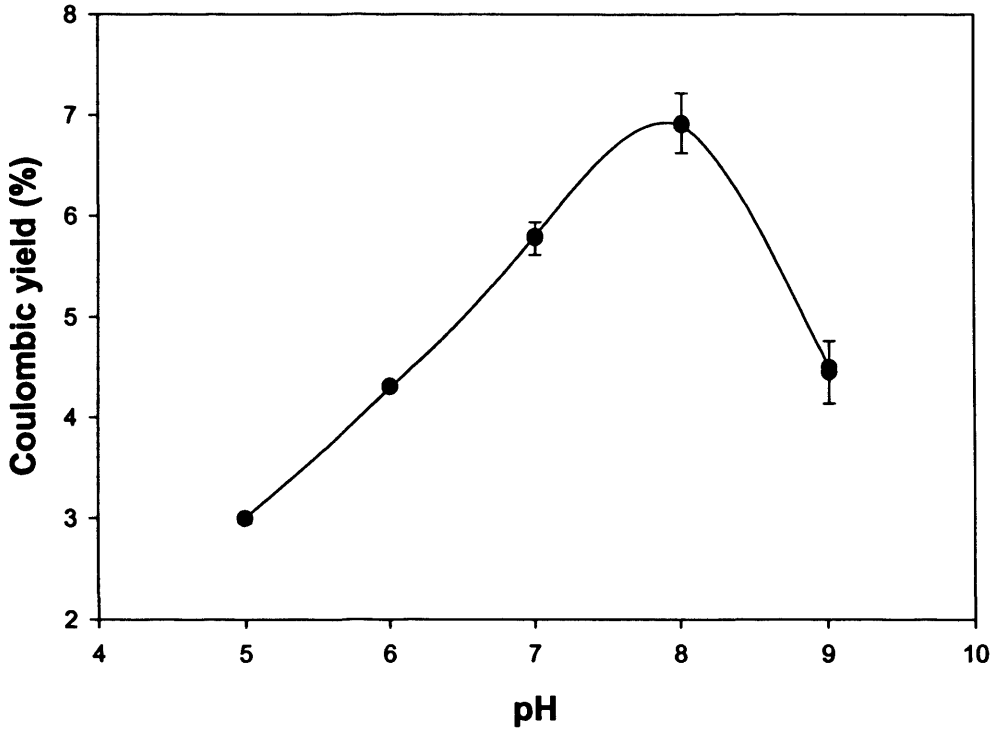

Figure 2.7 Coulombic yields in the fuel cell at different pH values. Data are presented as the mean ± S.D. (n=2)

The coulombic yield was highest at pH 8.0, whilst a value at pH 5.0 was less than half of this even though the differences in the organic contaminant consumption were less than 10% (Figure 2.7). These results showed that the microbial fuel cell functioned optimally at slightly alkaline pH values. The final pH in the anode compartment tended to return to neutral due to proton permeability characteristic of cation ion exchange membranes (Table 2.5). Therefore, different pH between the anode and cathode stabilized during the short time (with in 30 min, data not shown) and COD removal was similar at different pH values regardless of initial pH. Low coulombic yield at acidic and alkaline pH suggested that the electron donors were oxidized through unknown electron flow pathways diverting electron flow away from the

electrochemically active bacteria.

2.3.2.3. Effects of temperature

The anode content of the microbial fuel cell was replaced with fresh wastewater (10 ml) to measure current generation with a 1 KΩ resistance. The experiment was repeated at different temperature from 20℃ to 45℃ in a water bath (Figure 2.8).

Table 2.6 The relationship between temperature and current generation.

Temperature (℃)	ΔCOD[a] (mg l^{-1})	Theoretical coulomb (C)	Experimental coulomb[b] (C)	Coulombic yield (%)
20	849 ± 8.71	203.7	4.21 ± 0.10	2.06
25	858 ± 19.91	205.9	7.49 ± 0.29	3.63
30	856 ± 45.58	205.4	9.85 ± 0.69	4.79
37	835 ± 40.41	200.4	13.11 ± 0.66	6.54
45	845 ± 32.51	202.8	5.49 ± 0.42	2.71

[a]The different COD between initial and final COD depend on temperature change

[b]Data are presented as the mean ± S.D. (n=3)

Current generation was similar throughout the temperature tested, though slightly higher at 37℃ (Figure 2.9). COD removals were nearly the same regardless of temperature. However, the current output was a very low value at 45℃. Figure 2.8 and 2.9 and Table 2.6 show that current generation between bacterial growth and metabolic or electrochemical activity was affected by different temperatures. Additionally, the highest current and coulombic yield results at 37℃ show that fermentation product of microorganism at optimal temperature for bacterial growth can be easily used as substrate for the electrochemically active bacteria within biofilm on the electrode to generate electricity.

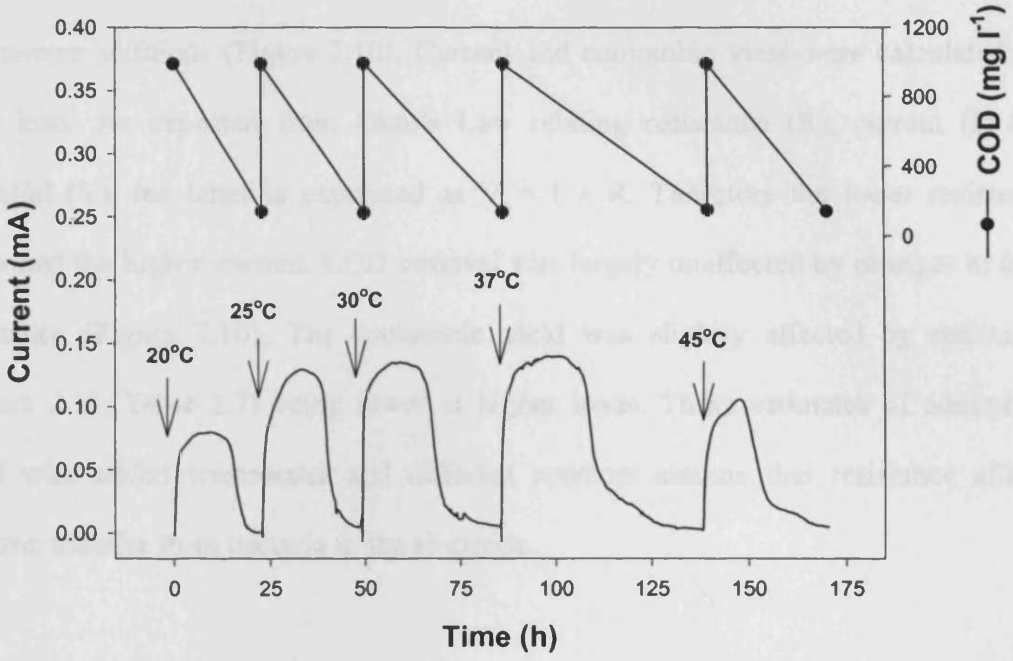

Figure 2.8 Current and COD change at different fuel cell temperatures.

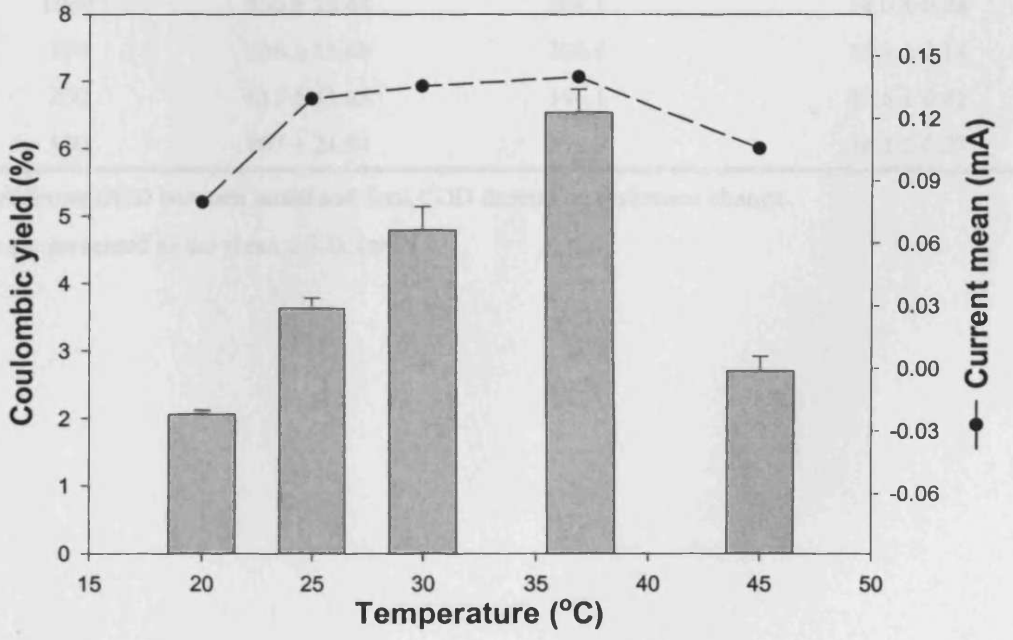

Figure 2.9 Coulombic yields and mean current generation in the fuel cell at different temperatures (℃). Data are presented as the mean ± S.D. (n=3)

2.3.2.4. Effects of resistance

The effects of different load (resistors) on the fuel cell were tested using 10 ml fresh wastewater additions (Figure 2.10). Current and coulombic yield were calculated for each load. As expected from Ohm's Law relating resistance (R), current (I) and potential (V), the latter is expressed as $V = I \times R$. Therefore the lower resistance generated the higher current. COD removal was largely unaffected by changes in load resistance (Figure 2.10). The coulombic yield was slightly affected by resistance (Figure 2.11; Table 2.7) being lower at higher loads. These estimates of coulombic yield with added wastewater and different resistors assume that resistance affects electron transfer from bacteria to the electrode.

Table 2.7 The relationship between electric load and coulomb output in the fuel cell.

Resistance (Ω)	ΔCOD[a] (mg l^{-1})	Theoretical coulomb (C)	Experimental coulomb[b] (C)
1000	850 ± 28.48	204.1	14.0 ± 0.28
500	836 ± 13.48	200.6	15.1 ± 0.14
200	817 ± 43.43	196.1	15.6 ± 0.42
100	807 ± 24.94	193.7	16.2 ± 0.27

[a]The different COD between initial and final COD depend on resistance change

[b]Data are presented as the mean ± S.D. (n=2)

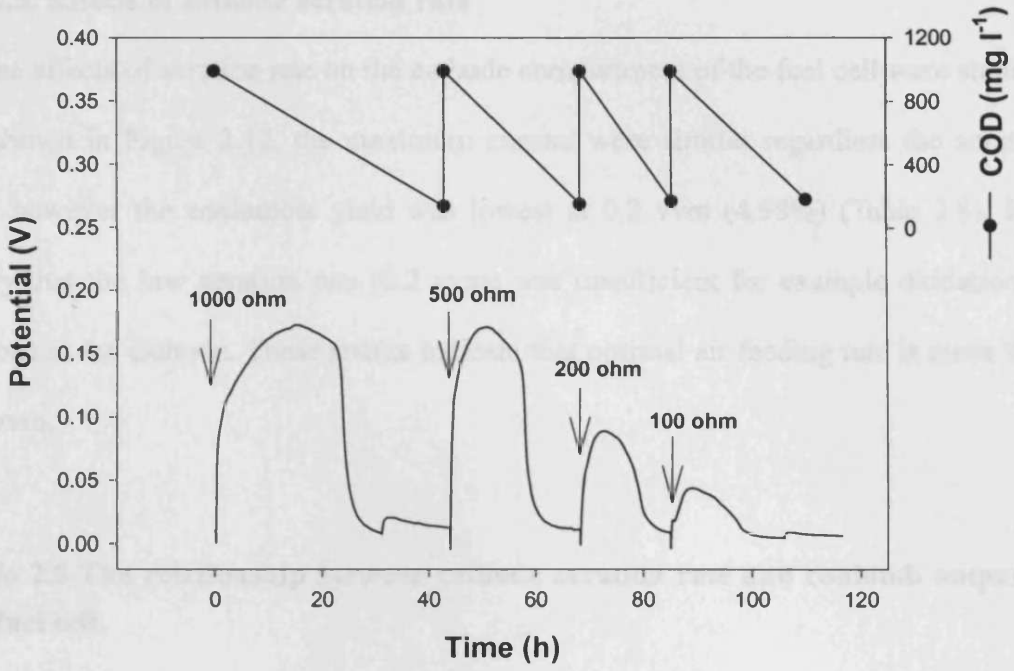

Figure 2.10 Performance of the fuel cell using different load resistances.

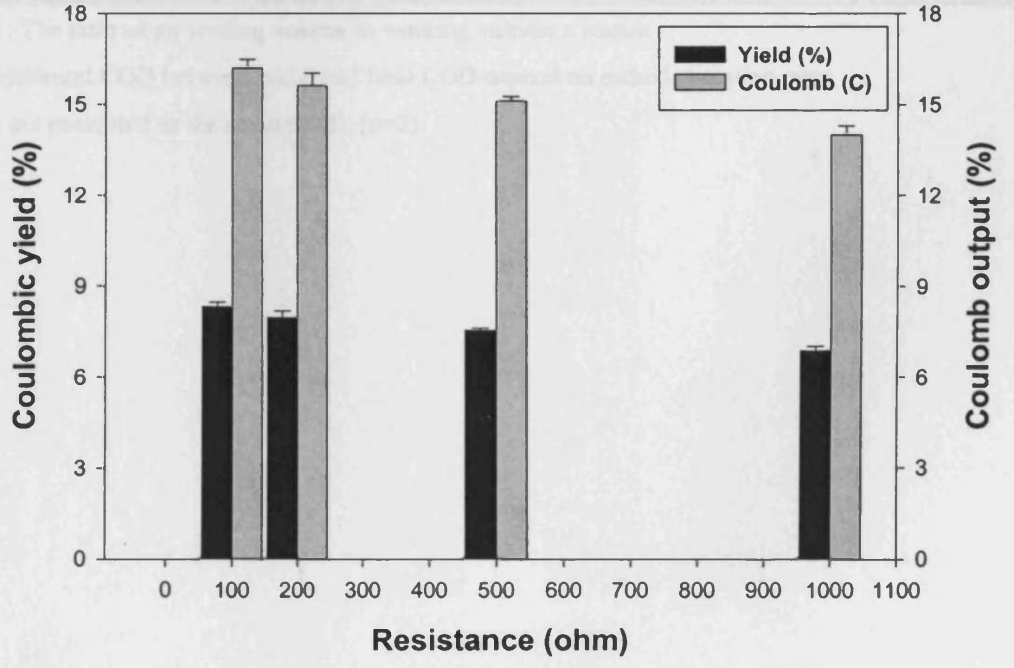

Figure 2.11 Coulomb output and yield with different load resistances. Data are presented as the mean ± S.D. (n=2)

2.3.2.5. Effects of cathode aeration rate

The effects of aeration rate on the cathode compartment of the fuel cell were studied. As shown in Figure 2.12, the maximum current were similar regardless the aeration rate, however the coulombic yield was lowest at 0.2 vvm (4.98%) (Table 2.8). It is likely that the low aeration rate (0.2 vvm) was insufficient for example oxidation of protons at the cathode. These results indicate that optimal air feeding rate is more than 0.4 vvm.

Table 2.8 The relationship between cathode aeration rate and coulomb output in the fuel cell.

Air[a] (ml min^{-1})	ΔCOD[b] (mg l^{-1})	Theoretical coulomb (C)	Experimental coulomb[c] (C)
5 (0.2 vvm)	870 ± 44.14	208.8	10.37 ± 0.71
10 (0.4 vvm)	860 ± 10.97	206.4	11.11 ± 0.15
15 (0.6 vvm)	830 ± 35.55	199.2	11.56 ± 0.62
20 (0.8 vvm)	810 ± 15.56	194.4	11.31 ± 0.34

[a]vvm : The ratio of air feeding volume to working volume a minute

[b]The different COD between initial and final COD depend on cathode aeration rates

[c]Data are presented as the mean ± S.D. (n=2)

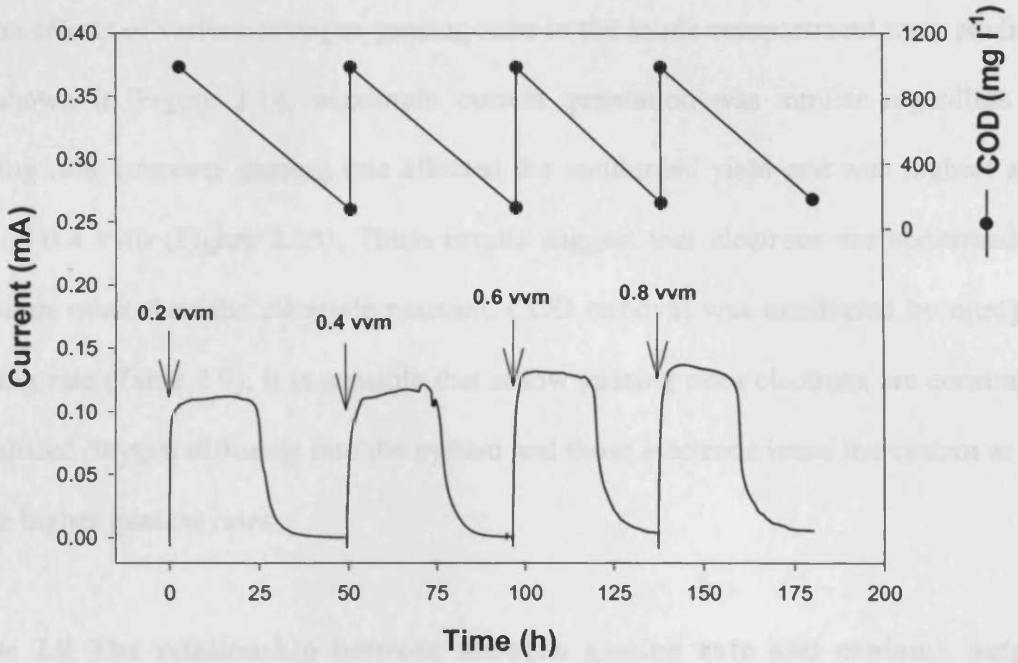

Figure 2.12 Current generation and COD change in the microbial fuel cell at different cathode aeration

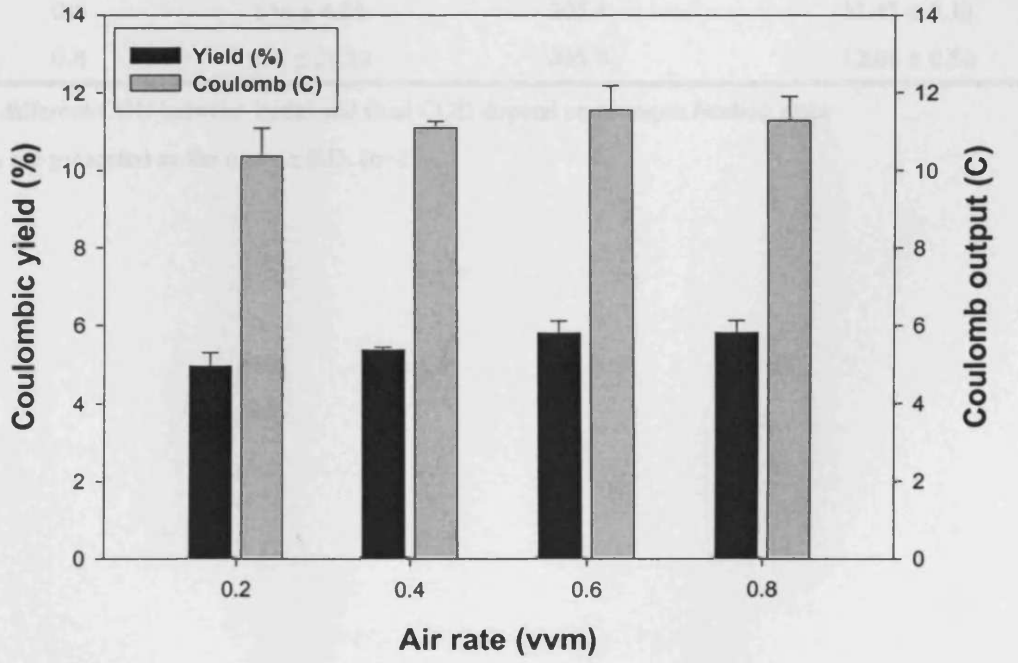

Figure 2.13 Coulomb output and yield at different cathode aeration rates. Data are presented as the mean ± S.D. (n=2)

2.3.2.6. Effects of nitrogen gassing to the anode of the fuel cell

The effects of various nitrogen-gassing rates in the anode compartment were studied. As shown in Figure 2.14, maximum current generation was similar regardless of gassing rate, however gassing rate affected the coulombic yield and was highest at a rate of 0.4 vvm (Figure 2.15). These results suggest that electrons are consumed in reactions other than the electrode reaction. COD removal was unaffected by nitrogen gassing rate (Table 2.9). It is possible that at low gassing rates electrons are consumed to reduced oxygen diffusing into the system and those electrons leave the system as H_2 at the higher gassing rates.

Table 2.9 The relationship between nitrogen gassing rate and coulomb output production in the fuel cell.

Gassing rate (vvm)	ΔCOD[a] (mg l^{-1})	Theoretical coulomb (C)	Experimental coulomb[b] (C)
0.2	854 ± 42.42	204.9	11.28 ± 0.85
0.4	844 ± 24.84	202.5	12.29 ± 0.41
0.6	856 ± 4.24	205.4	11.43 ± 0.13
0.8	858 ± 29.19	205.9	12.06 ± 0.56

[a]The different COD between initial and final COD depend on nitrogen feeding rates

[b]Data are presented as the mean ± S.D. (n=2)

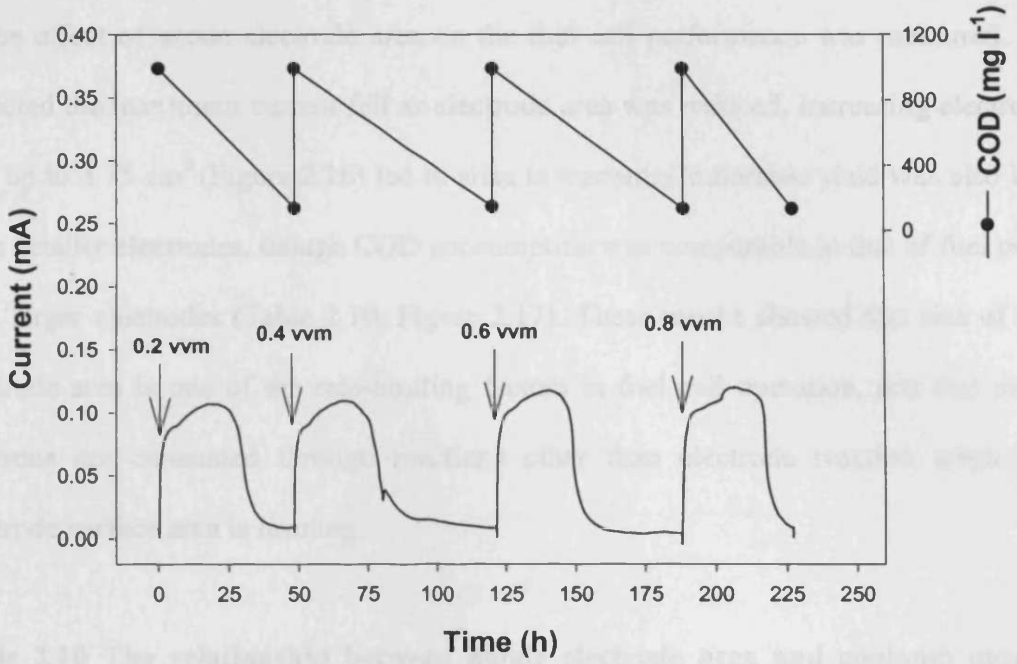

Figure 2.14 Current generation and COD change depends on nitrogen gassing rate in the anode compartment.

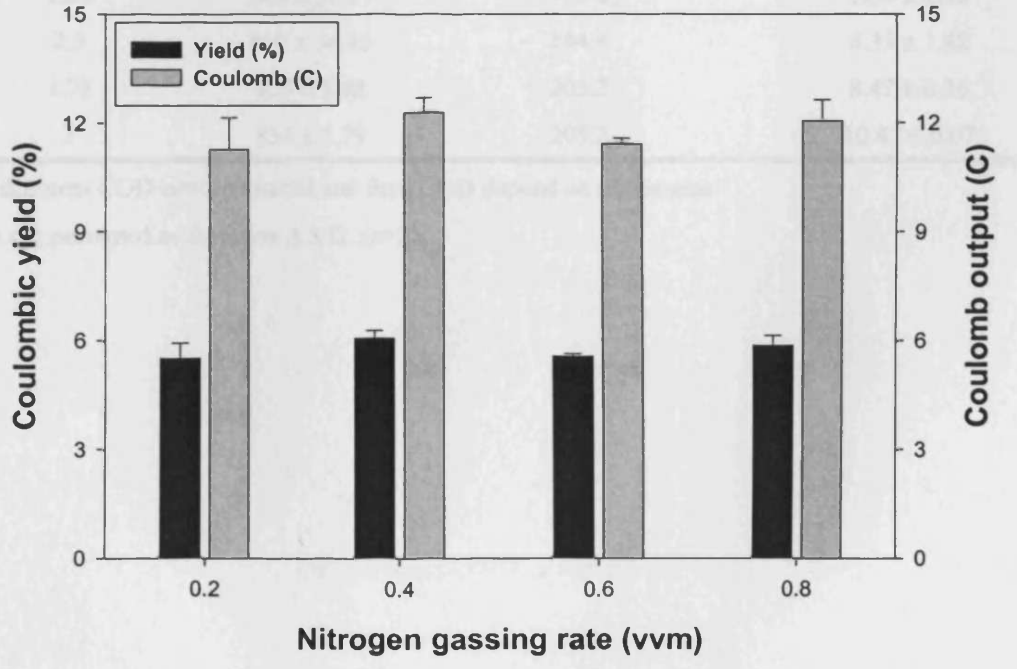

Figure 2.15 Coulomb output and yield at different nitrogen feeding rates to anode compartment of microbial fuel cell. Data are presented as the mean ± S.D. (n=2)

2.3.2.7. Anode electrode area

The effect of anode electrode area on the fuel cell performance was measured. As expected the maximum current fell as electrode area was reduced. Increasing electrode area up to 3.75 cm^2 (Figure 2.16) led to arise in current. Coulombic yield was also low from smaller electrodes, though COD consumption was comparable to that of fuel cells with larger electrodes (Table 2.10; Figure 2.17). These results showed that size of the electrode area is one of the rate-limiting factors in fuel cell operation, and that more electrons are consumed through reactions other than electrode reaction when the electrode surface area is limiting.

Table 2.10 The relationship between anode electrode area and coulomb output production in the fuel cell.

Area of anode electrode (cm^2)	ΔCOD[a] ($mg\ l^{-1}$)	Theoretical coulomb (C)	Experimental coulomb[b] (C)
1.25	640 ± 50.91	153.6	5.09 ± 1.13
2.5	810 ± 56.35	194.4	6.33 ± 1.42
3.75	855 ± 8.48	205.2	8.47 ± 0.26
5	854 ± 5.79	205.2	10.43 ± 0.07

[a]The different COD between initial and final COD depend on anode area

[b]Data are presented as the mean ± S.D. (n=2)

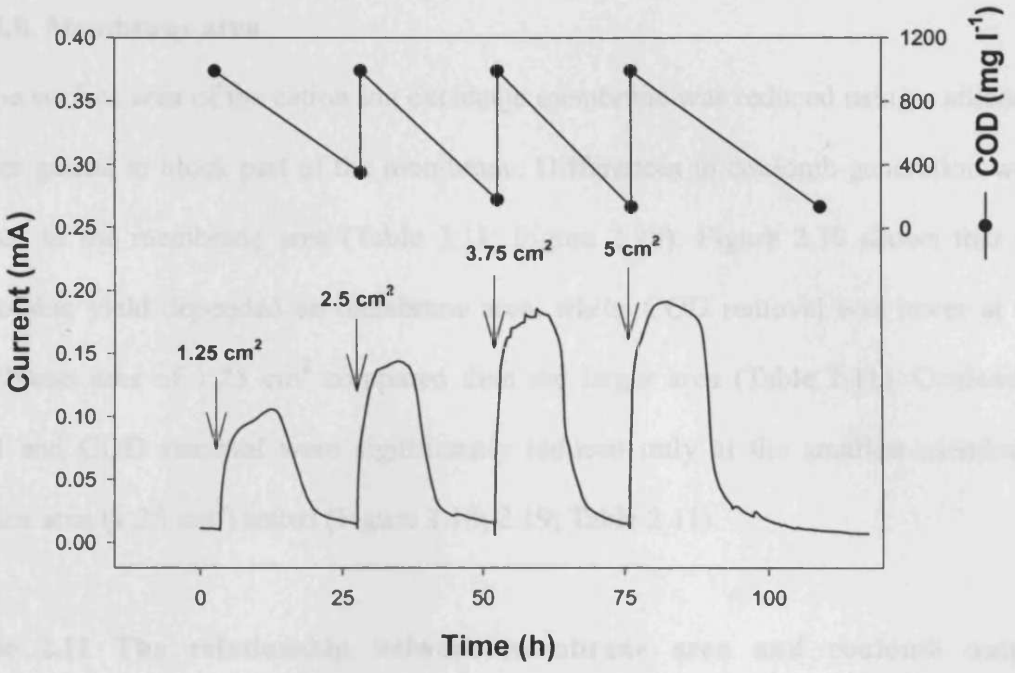

Figure 2.16 Current and COD change as function of anode electrode area.

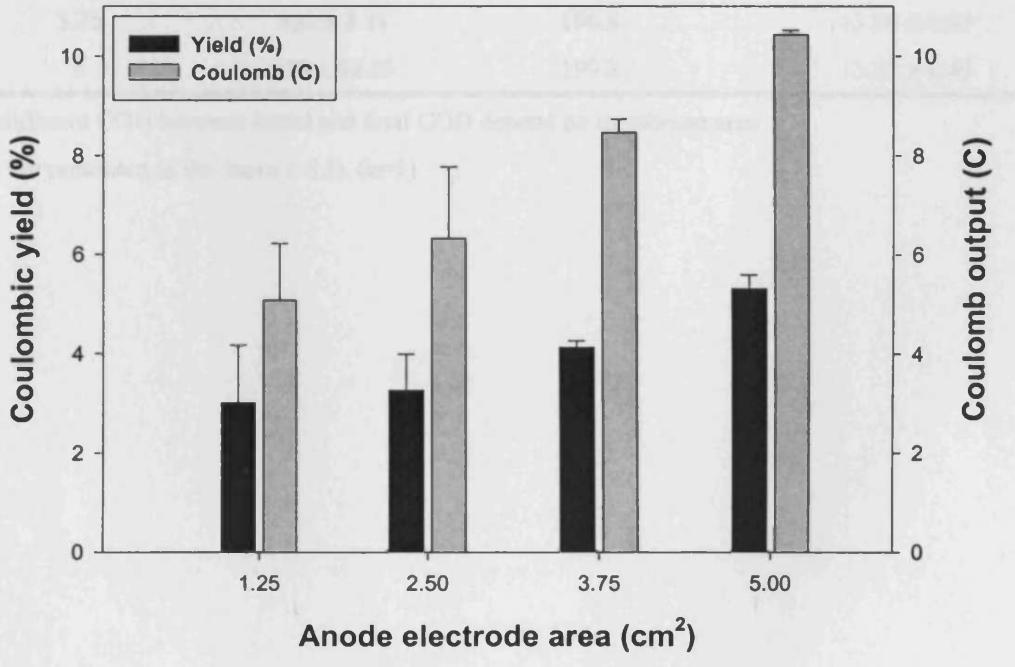

Figure 2.17 Coulomb output and yield as function of anode electrode area. Data are presented as the mean ± S.D. (n=2)

2.3.2.8. Membrane area

The surface area of the cation ion exchange membrane was reduced using a silicone-rubber gasket to block part of the membrane. Differences in coulomb generation were related to the membrane area (Table 2.11; Figure 2.18). Figure 2.19 shows that the coulombic yield depended on membrane area, whilst COD removal was lower at the membrane area of 1.25 cm^2 compared than the larger area (Table 2.11). Coulombic yield and COD removal were significantly reduced only at the smallest membrane surface area (1.25 cm^2) tested (Figure 2.18; 2.19; Table 2.11).

Table 2.11 The relationship between membrane area and coulomb output production in the fuel cell.

Area of membrane (cm^2)	ΔCOD[a] ($mg\ l^{-1}$)	Theoretical coulomb (C)	Experimental coulomb[b] (C)
1.25	690 ± 56.56	165.6	8.28 ± 0.42
2.5	860 ± 14.21	206.4	12.31 ± 0.13
3.75	820 ± 8.14	196.8	13.89 ± 0.07
5	830 ± 58.29	199.2	13.27 ± 0.49

[a]The different COD between initial and final COD depend on membrane area

[b]Data are presented as the mean ± S.D. (n=2)

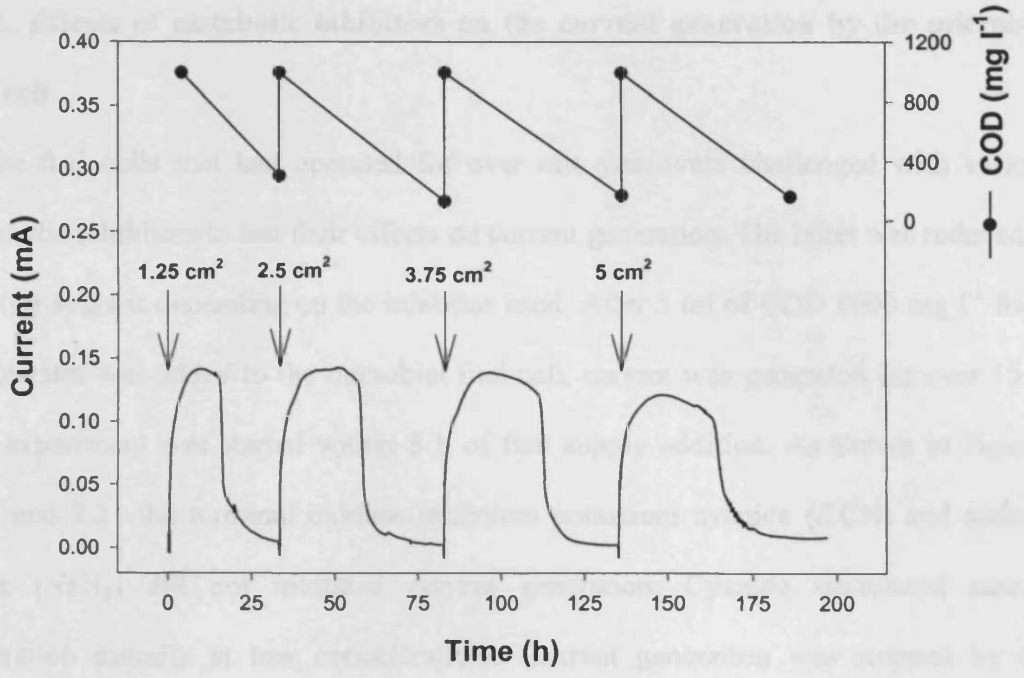

Figure 2.18 The effect of membrane area on current output and COD removal.

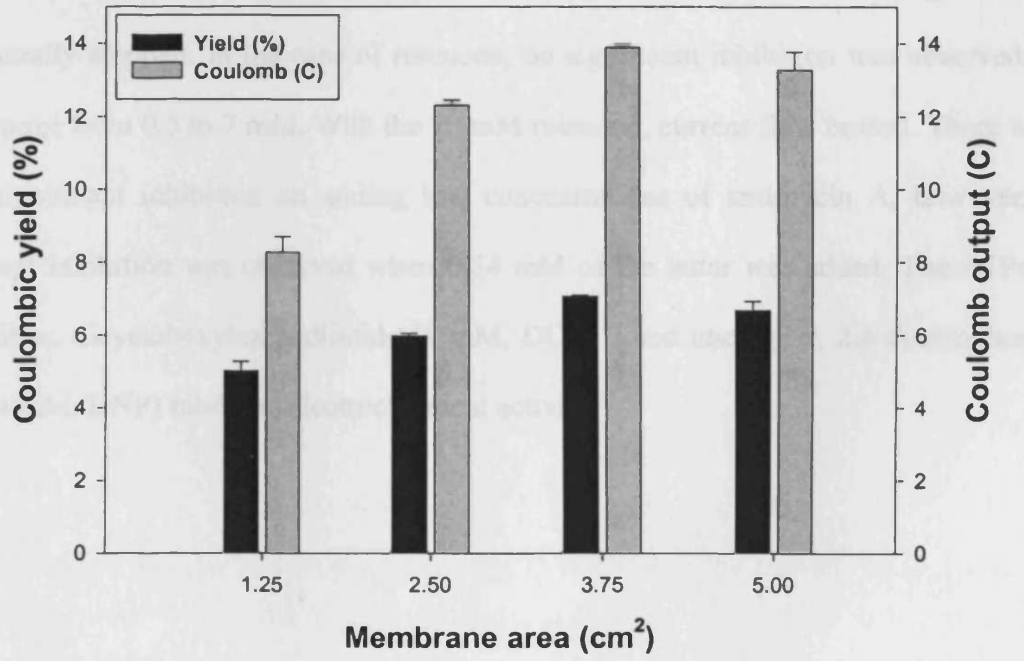

Figure 2.19 Coulomb output and yield as function of membrane area. Data are presented as the mean ± S.D. (n=2)

2.3.3. Effects of metabolic inhibitors on the current generation by the microbial fuel cell

The fuel cells that had operated for over one year were challenged with various metabolic inhibitors to test their effects on current generation. The latter was reduced to varying degrees depending on the inhibitor used. After 5 ml of COD 1000 mg l^{-1} fresh wastewater was added to the microbial fuel cell, current was generated for over 15 h. The experiment was started within 5 h of fuel supply addition. As shown in Figures 2.20 and 2.21 the terminal oxidase inhibitors potassium cyanide (KCN) and sodium azide (NaN_3) did not inhibited current generation. Cyanide stimulated current generation initially at low concentrations. Current generation was stopped by the addition of the iron-sulfur protein inhibitor, *p*-chloromercuriphenylsulphonate (0.32 mM, *p*-CMPS). The addition of NADH reductase inhibitors, 2-heptyl-4-hydroxyquinoline-*N*-oxide (HQNO) inhibited from about 24 μM and the current gradually fell. When 384 μM of HQNO was added to the cell, the current generation eventually stopped. In the case of rotenone, no significant inhibition was observed in the range from 0.5 to 7 mM. With the 10 mM rotenone, current flow ceased. There was no significant inhibition on adding low concentrations of antimycin A, however, a prompt inhibition was observed when 0.34 mM of the latter was added. The ATPase inhibitor, dicyclohexylcarbodiimide (1 mM, DCCD) and uncoupler, 2,4-dinitrophenol (0.24 mM, DNP) inhibited electrochemical activity.

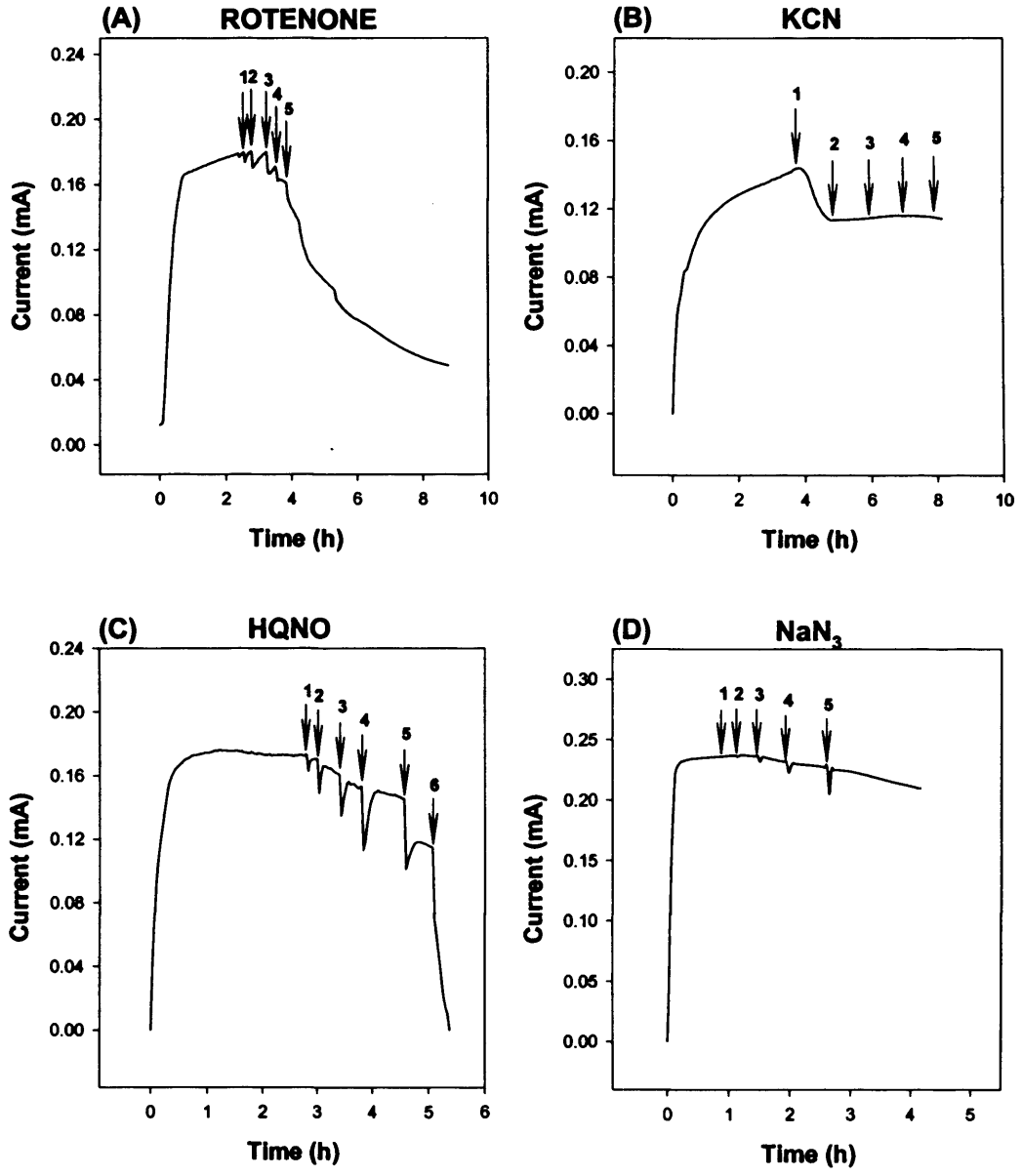

Figure 2.20 Current generation from the fuel cell fed with artificial wastewater and challenged with respiratory inhibitors. Inhibitors were added to the anode in increasing amounts at the points marked with arrows; (A) Rotenone (1-0.5, 2-1, 3-3.5, 4-7, 5-10 mM); (B) KCN (1-0.16, 2-0.32, 3-0.96, 4-1.5, 5-3 mM); (C) HQNO (1-12, 2-24, 3-48, 4-96, 5-192, 6-384 μM); (D) sodium azide (1-0.6, 2-1.2, 3-2.4, 4-4.8, 5-9 mM).

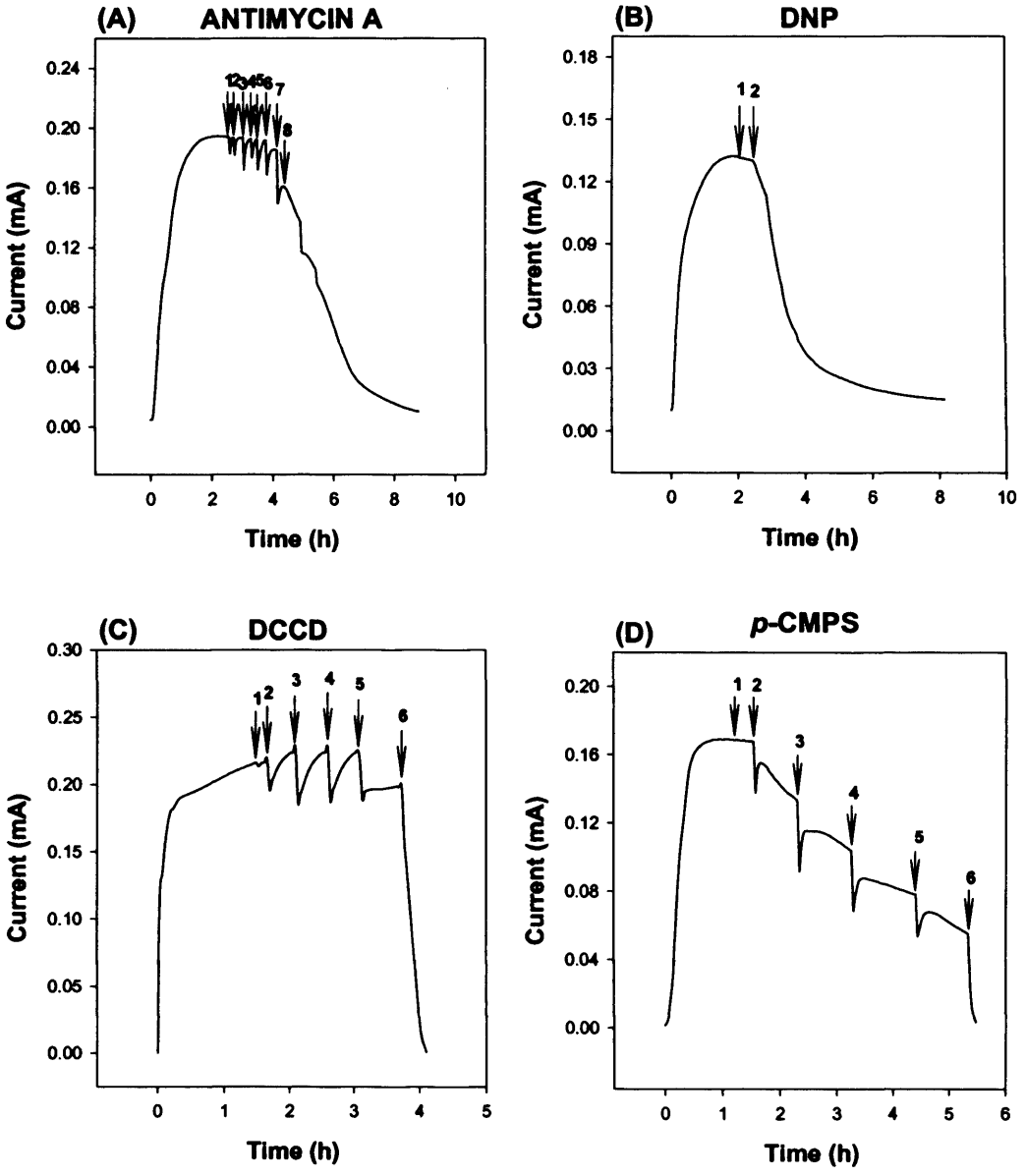

Figure 2.21 Current generation from the fuel cell fed with artificial wastewater and challenged with respiratory inhibitors. Inhibitors were added to the anode in increasing amounts at the points marked with arrows; (A) Antimycin A (1-2, 2-4, 3-8, 4-24, 5-56, 6-120, 7-340, 8-680 μM); (B) DNP (1-80, 2-240 μM); (C) DCCD (1-30, 2-60, 3-120, 4-280, 5-600, 6-1000 μM); (D) *p*-CMPS (1-10, 2-20, 3-40, 4-80, 5-160, 6-320 μM).

2.3.4. Effects of different electron donors and acceptors

2.3.4.1. Use of organic acids as fuel

The microbial fuel cell was operated using artificial wastewater, where main constituents were glucose and glutamic acid. Additions of various substrates were made to the fuel cell under continuous load (1 KΩ) (Figure 2.22). Current was generated immediately after the addition of various substrates. Sodium salts of a range of organic acids were used to prepare stock solutions and 0.25 ml of the latter were added to the anode compartment to measure current generation (Table 2.12). The highest current was obtained with pyruvate, citrate and acetate followed by propionate, lactate, glucose and iso-butyrate, in that order. However, the coulombic yield was highest with citrate followed by acetate, pyruvate, lactate, propionate and glucose. The yield was extremely low using iso-butyrate. These results suggested that the complex fuels were firstly metabolized by fermentative bacteria and then the metabolites from the fermentative bacteria are converted to electricity by the electrochemically-active bacteria.

Table 2.12 Effects of different substrates on current generation in the fuel cell.

Substrate (mM)	Theoretical coulomb[a] (C)	Experimental coulomb[b] (C)	Coulombic yield (%)
Acetate (5)	77	5.28 ± 0.16	6.85
Pyruvate (5)	96	5.26 ± 0.22	5.47
Lactate (10)	230	11.23 ± 0.25	4.88
Glucose (10)	460	11.62 ± 0.27	2.52
Citrate (5)	211	20.29 ± 0.95	9.61
Propionate (10)	268	11.67 ± 0.26	4.35
Iso-butyrate (5)	192	3.94 ± 0.23	2.05

[a]The different COD between initial and final COD depend on different substrates

[b]Data are presented as the mean ± S.D. (n=3)

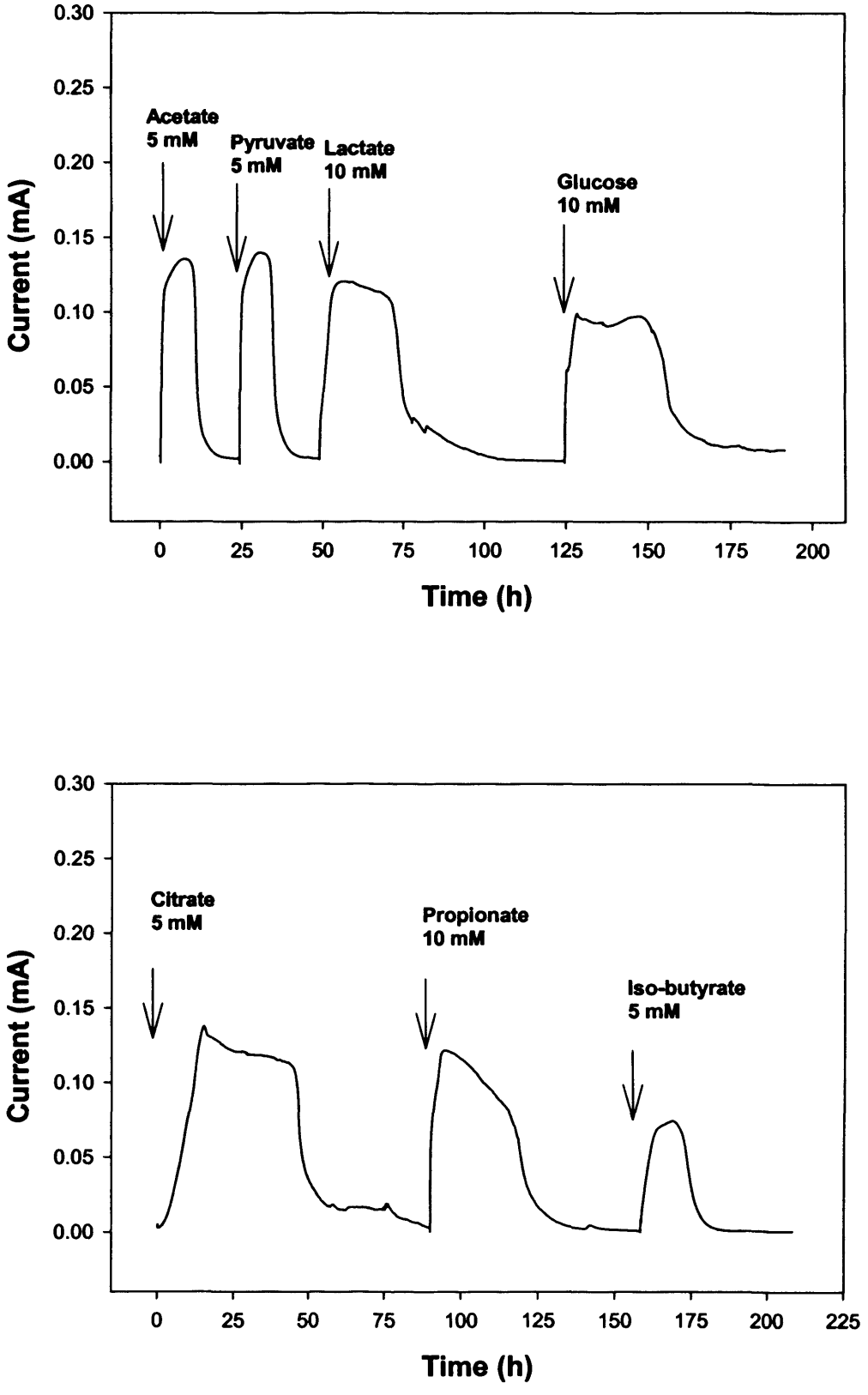

Figure 2.22 Current generation by the fuel cell fed with different substrates.

2.3.4.2. Effects of alternative electron acceptors

Previous results showed that oxidative phosphorylation inhibitors interfered with electron flow to the electrode in the fuel cell. The effects of natural electron acceptors on the performance of the fuel cell were tested using artificial wastewater as fuel. Fuel cells that had operated for over a year were used to test the effects of electron acceptors using air-saturated wastewater or adding nitrate, nitrite or sulphate.

2.3.4.2.1. Air

Air saturated and nitrogen gassed wastewater were mixed in different preparation to give a feed from 0 to 100% air saturation. The effect on current generation was tested. As shown in Table 2.13 and Figure 2.23, coulomb generation fell as the degree of air saturation increased. Because dissolved oxygen in an air-saturated solution is around 7-9 mg l^{-1}, which was low in comparison with the fuel added. The reduced coulomb might be due to the effect of dissolved oxygen on the electron transport system of microorganism.

Table 2.13 COD change and coulombic yield and air-saturation in the anode compartment.

Air saturation (%)	ΔCOD[a] (mg l^{-1})	Theoretical coulomb (C)	Experimental coulomb[b] (C)	Coulombic yield (%)
100	602 ± 9.48	112	6.16 ± 0.41	5.50
80	619 ± 21.92	114	8.39 ± 0.82	7.35
60	651 ± 6.34	124	7.76 ± 0.26	6.25
40	671 ± 5.65	130	8.21 ± 0.26	6.31
20	690 ± 2.82	134	8.26 ± 0.13	6.16
0	728 ± 1.64	143	9.85 ± 0.06	6.88

[a]The different COD between initial and final COD depend on air saturation wastewater volume

[b]Data are presented as the mean ± S.D. (n=2)

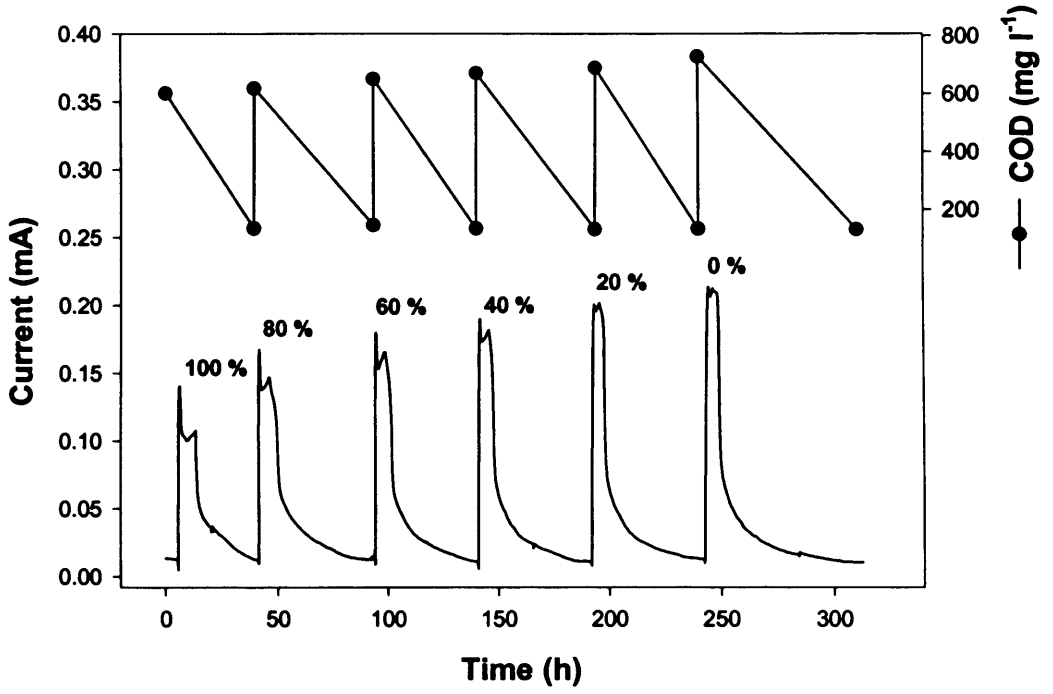

Figure 2.23 Current and COD change at different wastewater air saturations. Data are presented as the mean ± S.D. (n=2)

2.3.4.2.2. Nitrate

Similar experiments were conducted using wastewater with added nitrate. Coulomb production and current fell as the nitrate concentration increased (Figure 2.24) and nitrate was consumed completely (data not shown). Theoretically the COD needed for the complete oxidation of nitrate was about 25.6 mg l^{-1}. In this experiment, the amount of added COD was approximately 300 mg l^{-1} and theoretical coulomb output was about 90. However the fuel cell produced 12 C and the coulombic yield was 13.3%. The effect of nitrate on the current production would be same as the effect of nitrite (Figure 2.24) that has the capacity of inhibition of Fe(III) reduction and electron transfer to the electrode. The identities of inhibitory nitrogen oxides can be determined unequivocally from the data.

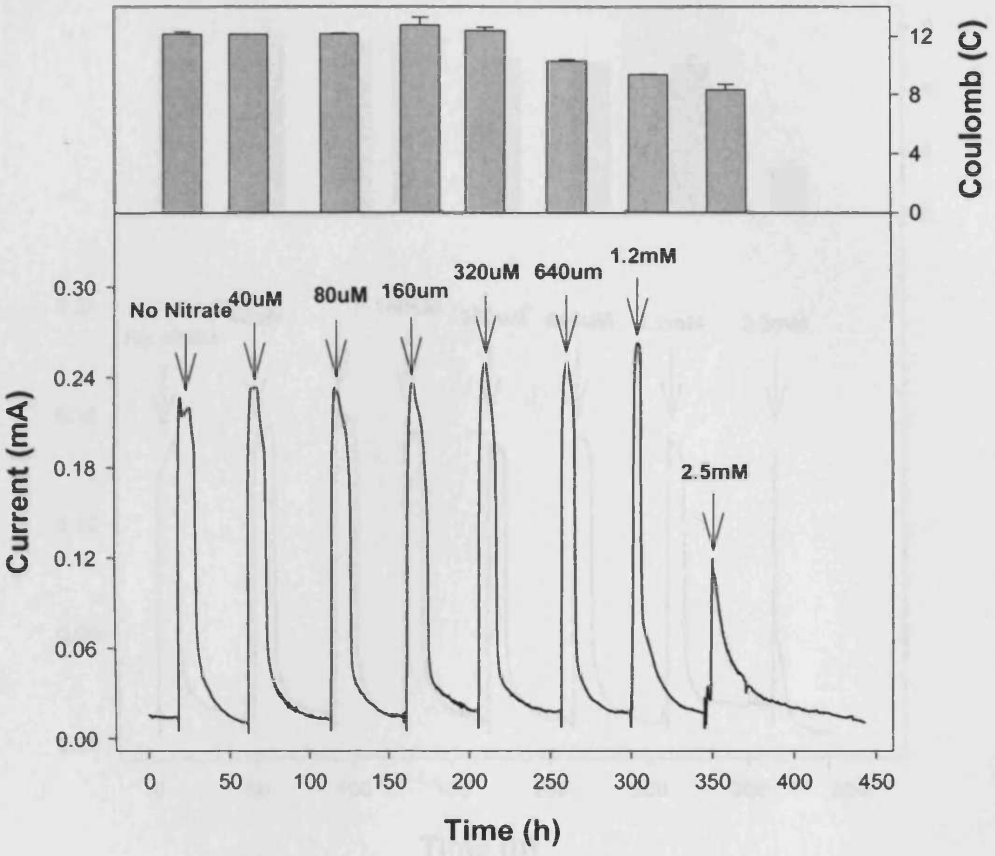

Figure 2.24 Performance of the fuel cell in the presence of different concentrations of nitrate. Data are presented as the mean ± S.D. (n=2)

2.3.4.2.3. Nitrite

A similar experiment to the previous one was conducted in the presence of nitrite. As shown in Figure 2.25, the inhibitory effect of nitrite was greater than with nitrate. The minimum inhibitory concentration was 1.2 mM and rapidly inhibited current generation at around 2.5 mM. Nitrite was an active inhibitor and also competed for reducing equivalent with electron transport to the electrode by the bacteria population. Current recovered immediately when no more nitrite was added (data not shown).

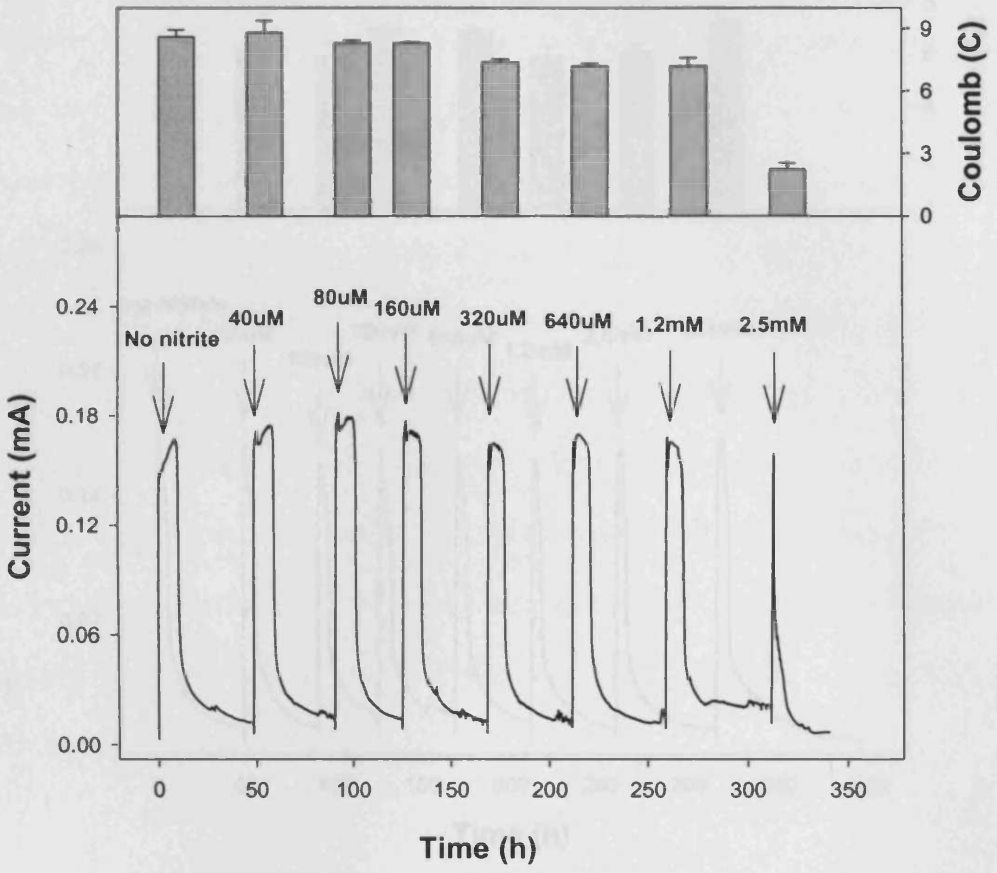

Figure 2.25 Performance of the fuel cell in the presence of different concentrations of nitrite. Data are presented as the mean ± S.D. (n=2)

2.3.4.2.4. Sulphate

Sulphate was added to the anode compartment as an electron acceptor and the current generated current. Measured current was not affected by sulphate addition (Figure 2.26). In addition the rate of COD decrease was not significantly affected by the treatment. High redox potential electron acceptors were probably consumed in the fuel cell, however sulphate was not.

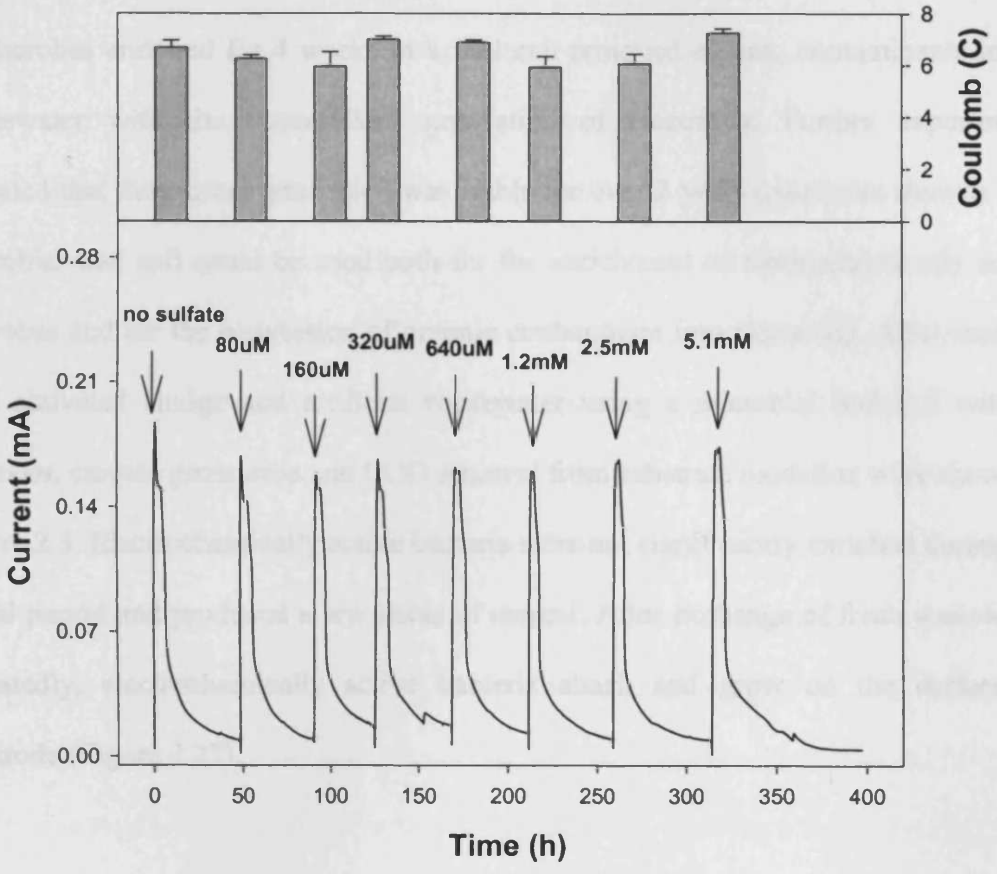

Figure 2.26 Performance of the fuel cell in the presence of different concentrations of sulphate. Data are presented as the mean ± S.D. (n=2)

2.4. Discussion

Microbes enriched for 4 weeks in a fuel cell removed organic contaminants in the wastewater with the concomitant generation of electricity. Further experiments revealed that the current generation was stable for over 2 years (result not shown). The microbial fuel cell could be used both for the enrichment of electrochemically active microbes and for the conversion of organic contaminant into electricity. After reaction with activated sludge and artificial wastewater using a microbial fuel cell without mediator, current generation and COD removal from substrate oxidation were shown in Figure 2.3. Electrochemically active bacteria were not significantly enriched during the initial period and produced a low value of current. After exchange of fresh wastewater repeatedly, electrochemically active bacteria attach and grow on the surface of electrode (Figure 2.27).

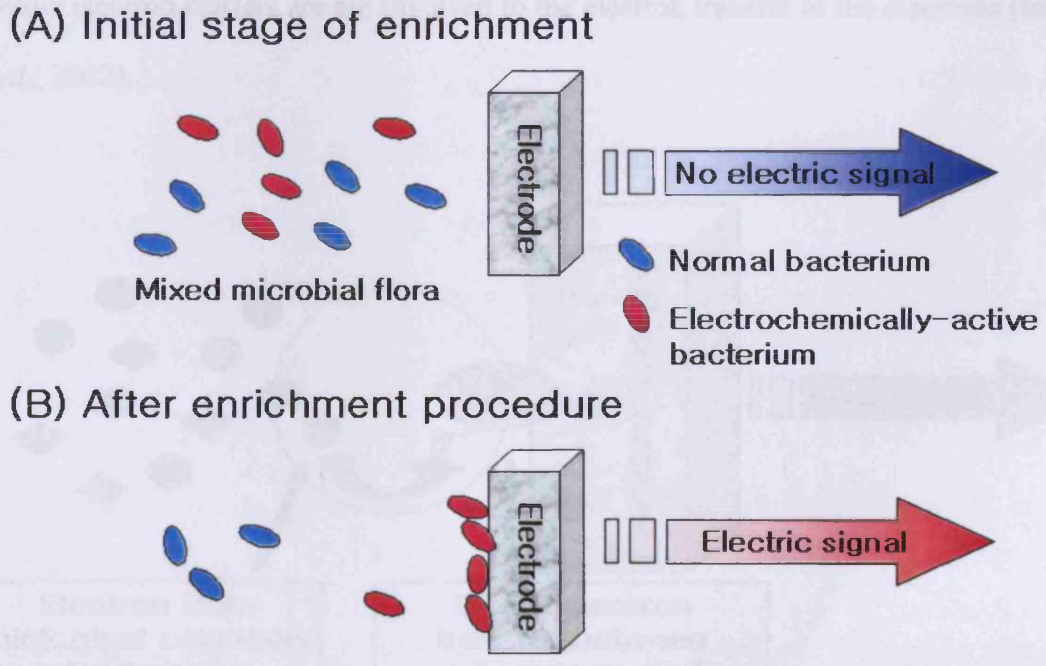

Figure 2.27 Proposed models for electrochemical enrichment method in a fuel cell.

Bacteria that have *c*-type cytochrome on the outer cell surface (membrane or cell wall) can under anaerobic conditions react with an electrode allow electrons to flow to the cathode (Myers and Myers, 1992; Kim *et al.*, 1999). After 4 weeks operation, current production stabilized once electrochemically active bacteria became associated with the electrode (Figure 2.28). Microbial fuel cells using aerobic sludge as inoculum with artificial wastewater as substrate also needs time for the enrichment of facultative anaerobic bacteria. Thus, the COD value of wastewater as substrate progressively decreased for 1 month operation. It is suggested that the activated sludge contained numerous metal reducing and electrochemically active bacteria.

Some of isolates from the microbial fuel cell were reported to be electrochemically active, and current was generated from a fuel cell using one of these, a strain of *Clostridium butyricum* (Park *et al.*, 2001). These results confirmed that electrically active microbes could be enriched in a fuel cell. Cell suspensions of the isolates were electrochemically active when measured using cyclic voltammetry, suggesting that soluble electron carriers are not involved in the electron transfer to the electrode (Bond *et al.*, 2002).

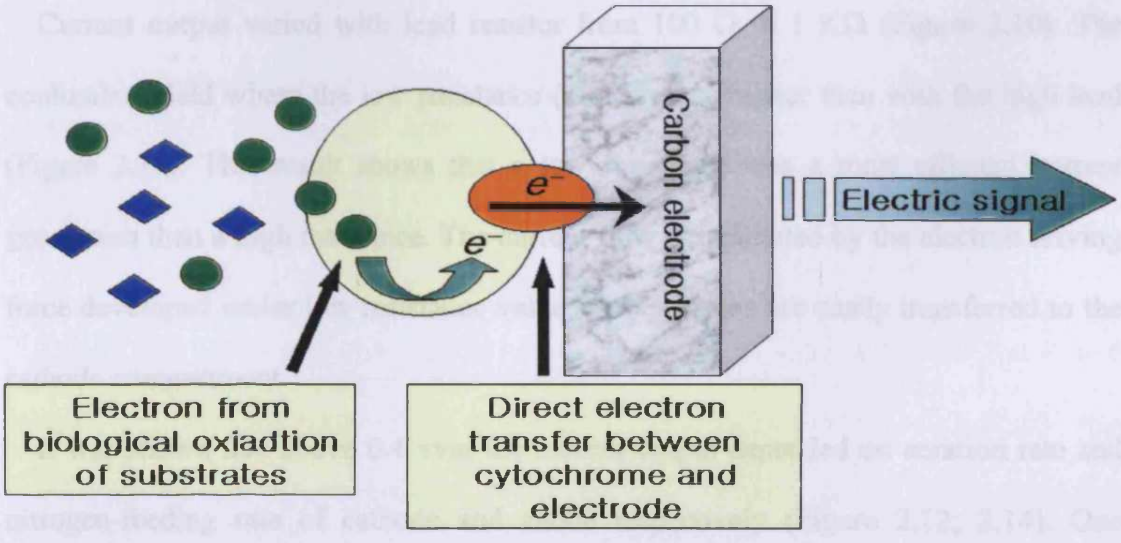

Figure 2.28 Proposed schematic diagram of principle of electrode reaction.

As the activity of bacteria is markedly dependent on pH, the output of the current may be affected by the pH in the anode compartment. The current generation is similar between pH 6.0 and 8.0 compared with pH 5.0 and 9.0 (Figure 2.6). Because pH 5.0 and 9.0 conditions are not suitable for growth and maintenance, we are expected current output to be low however current generation remained constant. It might be that the final pH in the anode compartment was due to neutrality because of reverse proton transfer from the cathode compartment. We conclude that this novel wastewater treatment system has the advantage of adapting to a broad range of pH values in the wastewater.

The influence of temperature on fuel cell operation was a varied slightly from 20℃ to 45℃ (Figure 2.8). Mesophilic bacteria may be enriched on the anode electrode because microbial fuel cell was operated above ambient temperatures (30℃). Bacteria on the electrode are affected by temperature, however current generation at 45℃ and 20℃ were similar associated. Although we do not understand exactly what happen, we assume that that thermophilic bacteria related with current generation are partially enriched on the electrode. Because high temperature (55℃) causes bacterial membrane damage, the current output could not be determined (data not shown).

Current output varied with load resistor from 100 Ω to 1 KΩ (Figure 2.10). The coulombic yield where the low resistance (100 Ω) was higher than with the high load (Figure 2.11). This result shows that a low resistance was a most efficient current generation than a high resistance. The current flow is facilitated by the electron driving force developed under low resistance value, and electrons are easily transferred to the cathode compartment.

It was shown that above 0.4 vvm the current output depended on aeration rate and nitrogen-feeding rate of cathode and anode respectively (Figure 2.12; 2.14). One limiting factor for current generation in a microbial fuel cell was maintenance of

anaerobic conditions in the anode and aerobic condition of cathode compartment respectively. In addition, electrode and cation ion exchange membrane areas were limiting factors for current output (Figure 2.16; 2.18). Throughout these results, several rate-limiting factors can be postulated and play an important part in fuel cell optimization for scale-up process (Figure 2.29).

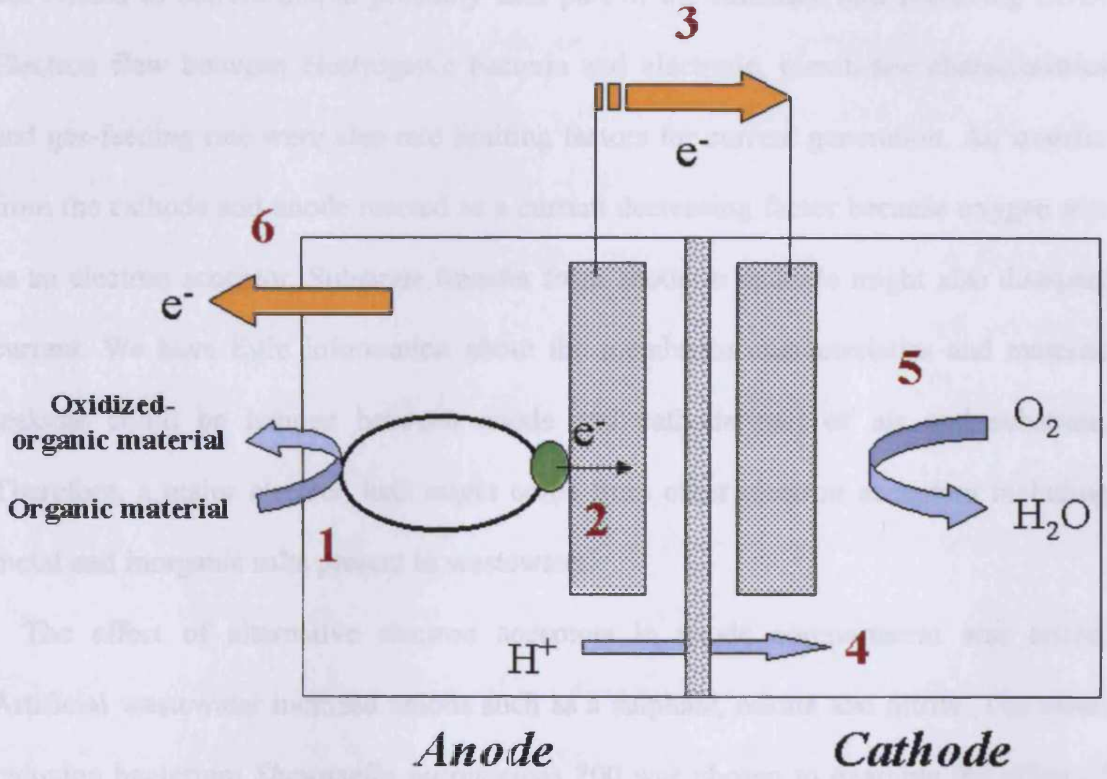

Figure 2.29 Possible rate limiting steps in a mediator-less microbial fuel cell. 1) fuel oxidation, 2) electron transfer to the electrode, 3) resistance, 4) proton permeability, 5) electron consumption at the cathode, and 6) electron leak at the anode.

The effects of operational conditions of a microbial fuel cell were tested and optimized for the best performance of a mediator-less microbial fuel cell as mentioned above. The optimal pH, temperature, resistance, cathode aeration rate, nitrogen gassing rate, and anode and cation ion exchange membrane areas were 7.0, 37℃, 1 KΩ, 0.6

vvm, 0.4 vvm and 5 cm^2, respectively. Then, these optimum conditions were used for all the other experiments in Chapter II, III and IV.

The coulomb conversion yield for a microbial fuel cell using activated sludge and artificial wastewater shows a low value (2-12%) compared with theoretical yield. One of explanations was the population ratio of bacteria related to current output. Bacteria not related to current output probably uses part of the substrate thus removing COD. Electron flow between electrogenic bacteria and electrode, membrane characteristics and gas-feeding rate were also rate limiting factors for current generation. Air transfer from the cathode and anode reacted as a current decreasing factor because oxygen acts as an electron acceptor. Substrate transfer from anode to cathode might also dissipate current. We have little information about the membrane characteristics and material leakage could be happen between anode and cathode part of air and substrate. Therefore, a major electron leak might come from other electron acceptors including metal and inorganic salts present in wastewater.

The effect of alternative electron acceptors in anode compartment was tested. Artificial wastewater included anions such as a sulphate, nitrate and nitrite. The metal reducing bacterium *Shewanella putrefaciens* 200 was chosen to examine the effect of alternative electron acceptors, including O_2, NO_3^- and NO_2^- on ferric iron reduction (DiChristina, 1992; Semple and Westlake, 1987). Results from earlier competition experiments with *S. putrefaciens* 200 demonstrated that the inhibitory effects of oxygen on Fe(III) reduction activity were due to preferential channeling of electrons to oxygen (Arnold *et al.*, 1990), whereas the inhibitory effects of nitrate on Fe(III) reduction activity were due to the chemical reoxidation of bacterially produced Fe(II) by the product of nitrate reduction, nitrite (Obuekwe *et al.*, 1981). In previous experiments, we expected that nitrate and nitrite might have an inhibitory effect because the electrode was a substitute for Fe(III) as electron acceptor and nitrate was itself a preferred

electron acceptor for anaerobic respiration among various metal reducing bacteria (Nealson and Krause, 1997). Nitrate was less efficient than nitrite however inhibition increased depending on concentration. Current generation was reduced because of electron transfer to both nitrate and nitrite. Nitrite could also be reacting as an inhibitor judging by the low coulomb output compared to expected results. The effect of sulphate on current generation was small even at higher concentrations. It might be the sulphate reducing bacteria were only a minor component of the population associated with the anode. From the results, alternative electron acceptors might cause the major leak of electron under anaerobic conditions in the anode compartment.

Current generation was inhibited by various metabolic inhibitors and by high redox potential electron acceptors. The data from metabolic inhibitor studies are consistent with the postulated mechanisms by which specific inhibitors interfere with electron transport to the electrode in a microbial fuel cell. Assuming that electrons generated and current come from electrochemically active bacteria attached to the electrode and the metabolic inhibitors block electron transport by binding at a single site, the kinetics of electron transport can be reduced in two simplified cases. i) A site of inhibition is also the rate-limiting step for electron transport in the absence of an inhibitor. ii) An inhibitor acts at a site other than the rate-limiting site or enzyme. Case (i) would hold, for example, if electron transport were limited at the NADH-Q oxidoreductase level by the inhibition quinacrine dihydrochloride, rotenone, and amytal or if respiration rate limits were imposed by cytochrome oxidase which were inhibited by azide (N_3^-), cyanide (CN^-) or CO. Case (ii) would hold for all inhibitors if the uninhibited respiration rate were limited to the rate of dissipation of the proton motive force. The mathematics of these two situations is fundamentally different at low inhibitor levels, because in case (ii) some level of inhibitor addition can be tolerated without diminishing the overall respiration rate. In case (i) any level of inhibitor binding would,

in theory, lower the respiration rate.

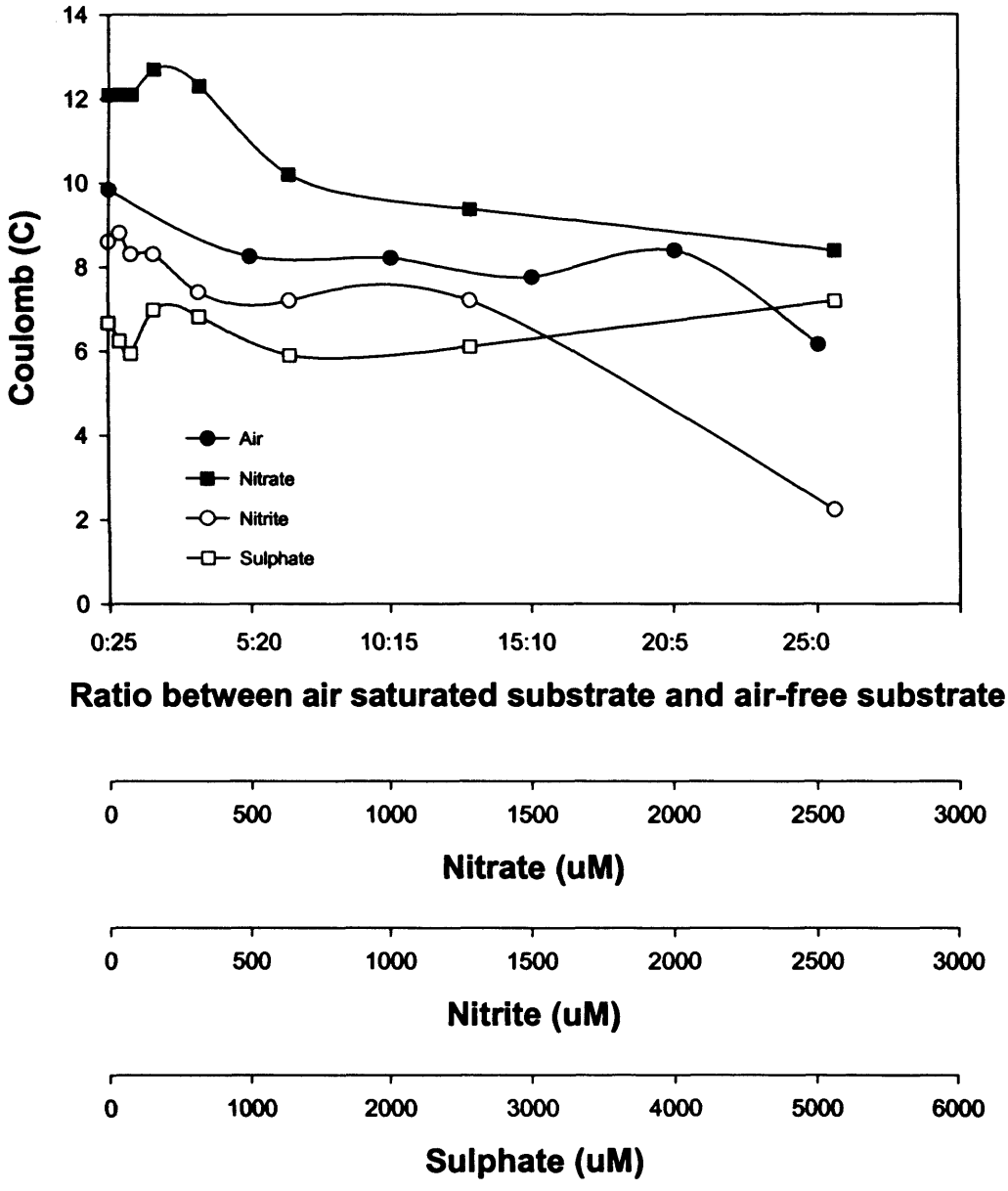

Figure 2.30 The effects of alternative electron acceptors at different concentrations.

In *Shewanella putrefaciens* 200, the dissimilatory iron reduction capacity increased nearly 8-fold through growth under oxygen limited conditions (Arnold *et al.*, 1986).

Electron transfer in the presence of specific respiratory inhibitors indicated that the species harbors both inducible and constitutive Fe(III)-reductase activities. Iron reduction via the constitutive system was blocked by dicyclohexylcarbodiimide (DCCD), 2-heptyl-4-hydroxyquinoline-*N*-oxide (HQNO), dicumarol and quinacrine. However, the induced electron transport system was not inhibited by DCCD. The inability of DCCD to interrupt dissimilatory iron reduction among cells grown at low oxygen tension suggests that electron transport via the high-rate, inducible iron reductase system is not coupled to oxidative phosphorylation (Arnold *et al.*, 1986). Thermodynamics indicate that dissimilatory iron reduction occurs via an abbreviated electron transport chain (Wehnder and Stumm, 1988). Inhibitor studies suggest that the constitutive Fe(III)-reductase activity is located farther along the electron transport chain than is its inducible counterpart.

The inhibitory effects of *p*-CMPS (*p*-chloromercuriphenylsulphonate) on whole cells agree with its effects on outer membrane ferric reductase, and imply a role for at least one iron-sulphur protein (Myers and Myers, 1994; Bragg, 1974). 0.32 mM *p*-CMPS inhibited current generation (Figure 2.21). This is suggesting that *p*-CMPS blocked the sulphydryl center of enzyme activity in the electrochemically active microbes.

Azide and cyanide anions can form very stable complexes with ferric heme iron and have been used extensively to probe the active site structure of the metal coordination positions in heme-proteins (Iizuka and Kotani 1968). The lack of effect by azide agrees with invitro ferric reductase data (Myers and Myers, 1993) (Figure 2.20) and with whole cells of *Shewanella putrefaciens* 200 (Arnold *et al.*, 1986) because azide inhibits cytochrome *c* oxidase part of the terminal electron transport chain to oxygen under aerobic condition and infers that Fe(III) reductase is distinct from the aerobic electron acceptor pathway (DiChristina, 1992). Though current generation fell slightly with cyanide at concentrations up to 0.16 mM, cyanide effects were significant at 3.0 mM of

concentration (Figure 2.20). These results also agree with its lack of activity on outer membrane ferric reductase and formate dehydrogenase related with Fe(III) reductase (Myers and Myers, 1993).

The inhibition by HQNO and antimycin A agree with previous findings in which these agents inhibited ferric reductase activity of the outer membrane (Myers and Myers, 1993) and Fe(III)-dependent proton translocation of *S. putrefaciens* MR-1 cells (Myers and Nealson, 1990). HQNO also inhibited Fe(III) reduction by *S. putrefaciens* 200 cells because of inhibitory effect on cytochrome *b* site which is located downstream of electron transport system (Obuekwe *et al.*, 1981). Antimycin A, a natural antibiotic from *Streptomyces*, specifically inhibits the electron transfer activity of Q-cytochrome *c* oxidoreductase (collectively called the bc-1 complex) in most respiratory and photosynthetic organisms. Because of high specificity and strong affinity, antimycin A has been widely used in functional studies of the cytochrome *b* with this inhibitor bound to the mitochondrial bc-1 complex. Then, the phenomenon of oxidant-induced reduction of cytochrome *b* can be observed, which provides strong experimental support for the proton motive Q cycle hypothesis. The specific interaction of antimycin A with the mitochondrial bc-1 complex has been studied by structure activity analysis using either synthetic analogues of the inhibitor (Tokutake *et al.*, 1994; Vonjagow and Link, 1986). Antimycin A had no measurable effect on current production at low concentrations, however it inhibited immediately at 340 μM (Figure 2.21).

0.5 mM Rotenone was ineffective, but the current dropped around 3.5 mM of concentration and was essentially zero at 10 mM rotenone (Figure 2.20). Rotenone inhibits electron transfer between the Fe-S cluster and ubiquinone, as indicated by electron paramagnetic resonance (EPR) and NADH-Q oxidoreductase activity of the complex I site. NADH-Q oxidoreductases in the eukaryotic mitochondrial and bacterial

respiratory chains can be divided into two groups, depending on whether they have NADH dehydrogenase-1 (NDH-1) or do not have NADH dehydrogenase-2 (NDH-2), plus an energy-coupling site, in which redox energy is converted to electrochemical proton potential across the coupling membrane. NDH-1 is inhibited by many specific inhibitors such as rotenone, capsaicin, 2-heptyl-4-hydroxyquinoline-*N*-oxide (HQNO), 1-methyl-4-phenyl-pyridinium (MPP), and ptericidin A. NDH-2 is completely resistant to NDH-1 type-inhibitors which can react on or near the ubiquinone-binding site. There is more than one binding site for rotenone-type inhibitors on complex I as has been concluded indirectly from kinetic studies. The number of binding sites that could be identified matched exactly the amount of inhibitor needed to completely block the activity of complex I, and in all cases of competitive binding, inhibitors were always displaced completely. Thus, if there were two inhibitor binding sites per complex I, they would have to be indistinguishable in terms of ligand affinity. In the absence of compelling evidence, the view is in favor of such unusual binding site heterogeneity. It should be noted that as rotenone was increased inhibition activity depended on concentration because of its competitive binding action.

DNP (2,4-dinitrophenol) inhibited at 0.24 mM (Figure 2.21). The tight coupling of electron transport and oxidative phosphorylation can be disrupted (uncoupled) by DNP and certain other acidic aromatic compounds. The acceleration of electron transport would be expected only if the transport kinetics were limited by the rate of dissipation of the proton motive force. We anticipated that current production was increased because the Δp was dissipated and respiratory activity accelerates to maintain it. However, the reverse was the case. The reason for this may be membrane distortion or interference due to DNP addition and not related to oxidative phosphorylation associated with electron transport to the electrode via the electrochemically active community in the fuel cell. ATPase was irreversibly inhibited by the carboxyl

activating reagent, dicyclohexylcarbodiimide (DCCD) and by oligomycin. 1000 μM DCCD (dicyclohexylcarbodiimide) inhibited current production (Figure 2.21). DCCD inhibited electron transport by electrochemically active bacteria under anaerobic conditions in the microbial fuel cell. Inhibition of current generation by ATPase inhibitors and uncouplers suggests that electron transfer to the electrode requires a reverse electron transport step. Another explanation is that the chemicals inhibited the fermentative metabolism, which plays a crucial role in fuel cell energetic. Inhibition data support the schematic representation of electron transport to Fe(III) or electrode and transport inhibition in microbial fuel cell (Figure 2.31).

Taken together the metabolic inhibitor studies suggest that oxidative phosphorylation is probably linked via a constitutive pathway to the electrode. This result supports the physical picture of inductive and constitutive branches for electron transfer to the electrode. The more energetically favorable branch is linked to oxidative phosphorylation via proton translocation. On the other hand, the shorter branch might serve as an electron sink for cellular reducing power. It also suggested from inhibitor experiments that electron transport to the electrode may be another anaerobic respiratory pathway, and suggested that current generation is bacterial activity which was enriched on the electrode.

We have shown that electrochemically active bacteria could be enriched using an electrochemical fuel cell, and that this system could almost completely remove organic contaminants from wastewater with concomitant electricity generation. This activity was inhibited by various microbial growth inhibitors as already discussed. Furthermore, metabolic inhibitor results suggested that the current generation seem to be associated with bacterial activity on the electrode, and could be regarded as a novel form of anaerobic respiration.

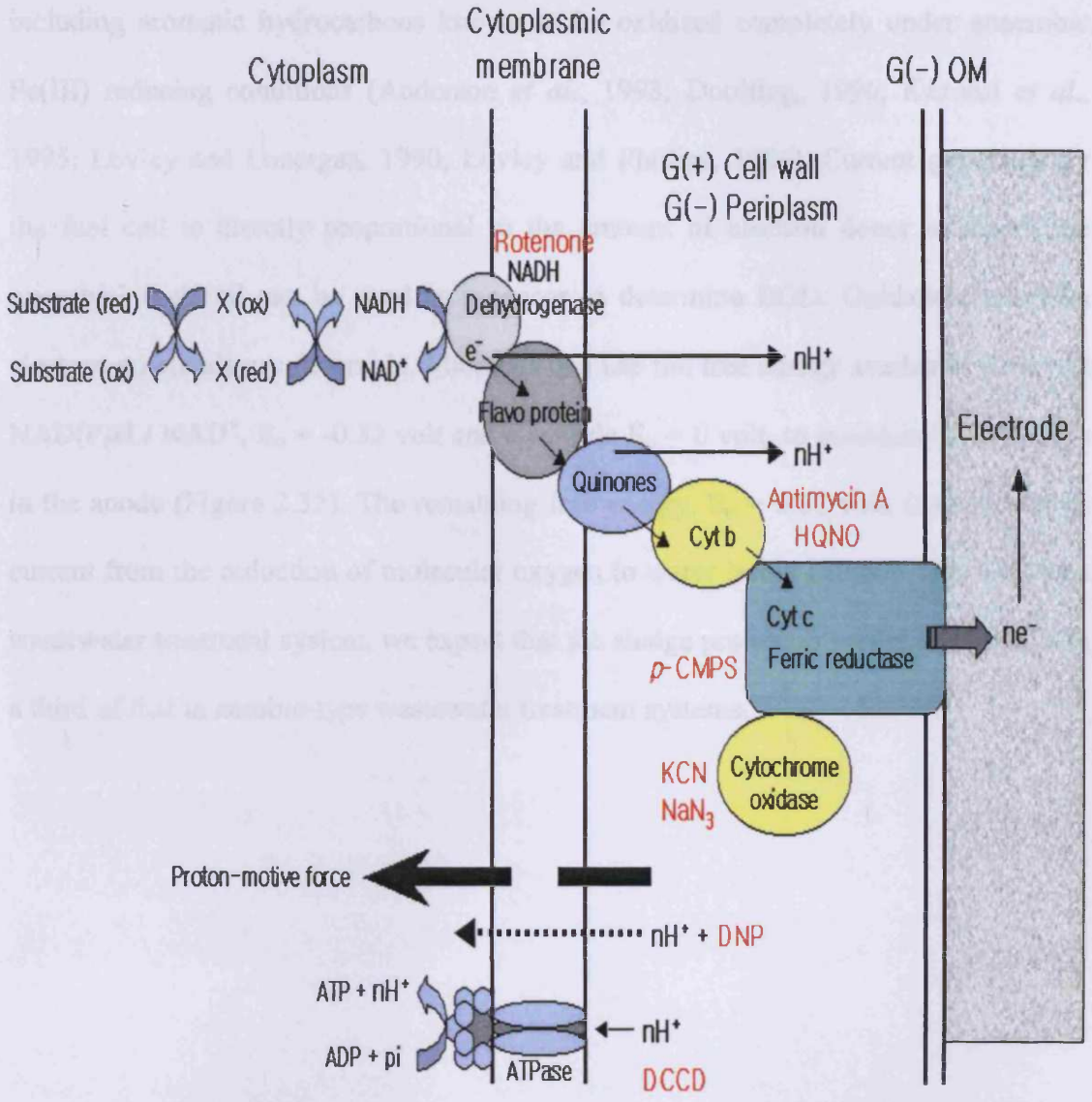

Figure 2.31 Schematic representation of electron and proton transport in the fuel cell. (HQNO: 2-heptyl-4-hydroxyquinolone-*N*-oxide DCCD: Dicyclohexylcarbodiimide DNP: 2,4-dinitrophenol *p*-CMPS: *p*-chloromercuriphenylsulphonate)

Microbial fuel cells enriched in the same way could be used to develop a novel wastewater treatment process. This would convert a major part of the energy in organic contaminants into electricity leading to a significant reduction in sludge production. It

would also be interesting to see if such system could be used to oxidize xenobiotics including aromatic hydrocarbons known to be oxidized completely under anaerobic Fe(III) reducing conditions (Anderson *et al.*, 1998; Doolfing, 1996; Kazumi *et al.*, 1995; Lovley and Lonergan, 1990; Lovley and Phillips, 1986). Current generated by the fuel cell is directly proportional to the amount of electron donor oxidised, the microbial fuel cell can be used as a sensor to determine BOD. Oxidation/reduction electron potentials are favorable. Microbes can use the free energy available: 0.32 volt NAD(P)H / NAD^+, $E_o' = -0.32$ volt and electrode $E_o' = 0$ volt, to maintain the microbes in the anode (Figure 2.32). The remaining free energy, $E_o' = 0.82$ volt, is converted to current from the reduction of molecular oxygen to water in the cathode. If it used as a wastewater treatment system, we expect that the sludge production reduced to less than a third of that in aerobic-type wastewater treatment systems.

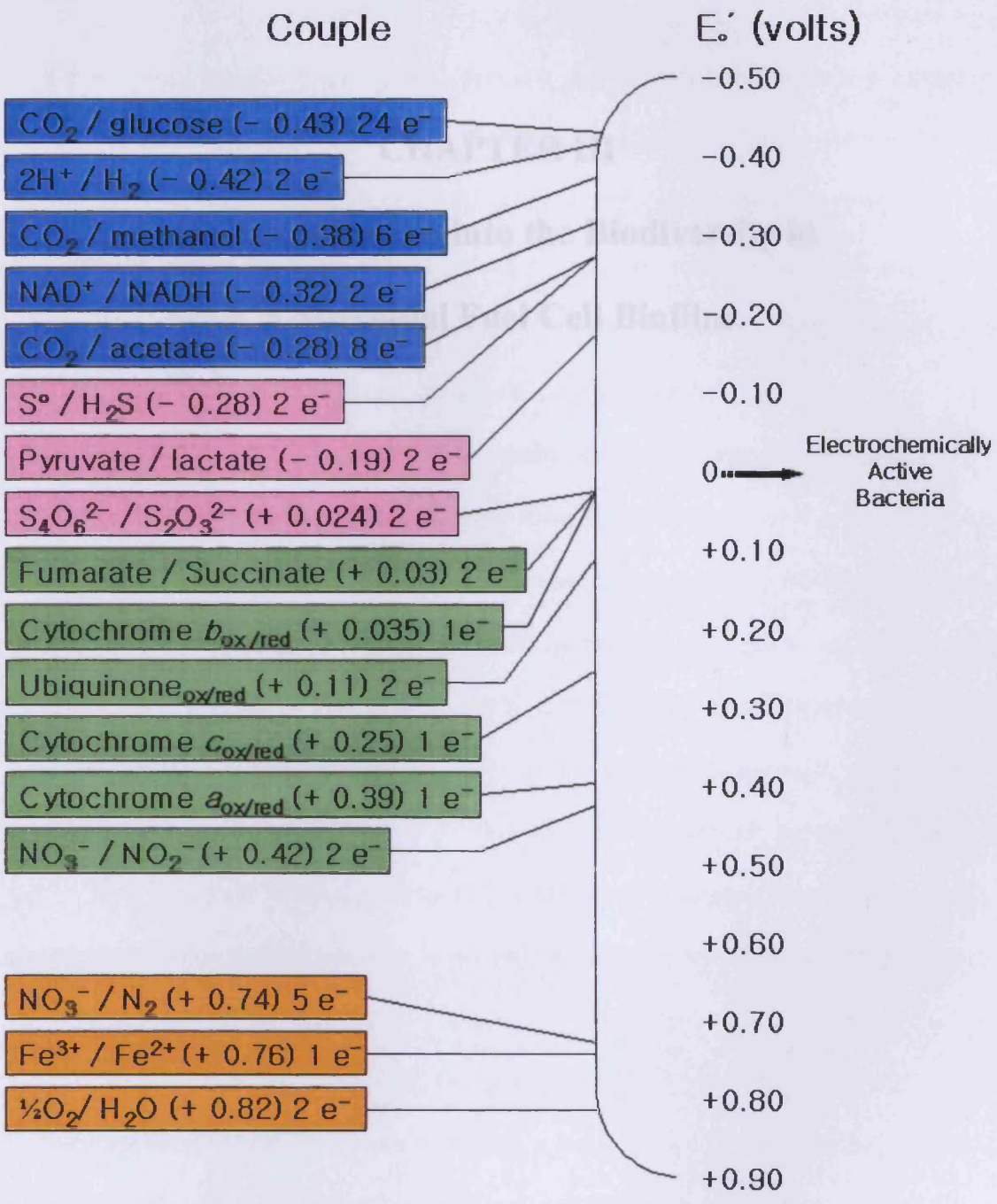

Figure 2.32 Standard mid-point potentials for important redox couple. Oxidation and reduction couples are arranged from the strongest reluctant (negative reduction potentials) at the top, to the strongest oxidants (positive reduction potentials) at the bottom. Electrochemically active bacteria enriched from the bacteria fuel cell were located around 0 volt (Brock *et al.*, 1994).

CHAPTER III

An Investigation into the Biodiversity in a Microbial Fuel Cell Biofilm

3.1. Introduction

A microbial fuel cell is an electrochemical device which converts the chemical energy of fuel to electrical energy by the metabolic or catalytic energy of microorganisms (see Chapter I and Kim *et al.*, 2002; Park and Zeikus, 2000). The electrons available through the metabolism of the electron donors (fuel) by microorganisms are transferred to the anode of the fuel cell, and then to the cathode through the circuit, where they reduce the oxidant (Allen and Bennetto, 1993), consuming protons available through the membrane from the anode. There are at least two types of microbial fuel cells. One involves the utilization of electrochemically active bacteria such as *Shewanella putrefaciens* (Kim *et al.*, 2002), *Clostridium butyricum* (Park *et al.*, 2001), *Aeromonas hydrophila* (Pham *et al.*, 2003), and *Geobacter sulfurreducens* (Bond and Lovley, 2003), and another involves the use of mediators which facilitate electron transfer between bacterial cell and the electrode (Park and Zeikus, 2000; Tayhas *et al.*, 1994). A microbial fuel cell system can be used for various purposes including bacterial activity monitoring (Kim *et al.*, 2003), electricity generation in a local area, and wastewater treatment processes with activated sludge as a source of bacteria.

Recently, the iron-reducing bacteria which use ferric iron [Fe(III)] as their electron acceptor (Caccavo *et al.*, 1994; DiChristina and DeLong, 1994; Myers and Myers, 1992; Lovley, 1991), has been attracting attention as a bacterial source for mediator-less microbial fuel cell development (Kim *et al.*, 2002; Park *et al.*, 2001). The typical Fe(III)-reducers, *Shewanella putrefaciens* (Dollhopf *et al.*, 2000; Hyun *et al.*, 1999), *Geobacter metallireducens* (Lovley *et al.*, 1993a), *Geovibrio ferrireducens* (Caccavo *et al.*, 1996a), and *Desulfotomacum reducens* (Tebo and Obraztsova, 1998), are able to

conserve energy for growth by coupling the oxidation of organic acids, aromatic hydrocarbons and H_2 to Fe(III) reduction by direct contact between the bacterial cell and Fe(III) minerals (DiChristina and DeLong, 1994; Hitchens, 1989; Lovley *et al.*, 1989b). Studies with Fe(III)-reducers showed that *Shewanella* and members of the *Geobacteraceae* could be applied to the construction of mediator-less microbial fuel cells (Kim *et al.*, 1999b; Bond and Lovley, 2003). It was proposed that these organisms were directly transferring electrons to the electrode surface (Bond and Lovley, 2003). Furthermore, *Shewanella putrefaciens* localizes the majority of its membrane-bound cytochromes on its outer membrane under anaerobic growth conditions (Arnold *et al.*, 1990; Myers and Myers, 1992; Myers and Myers, 1997). Redox proteins with electrochemical activity are also believed to be involved in the electro-chemical reaction between the bacterial cell and the electrode surface (Pham *et al.*, 2003).

Activated sludge is a well known example of a complex microbial community and also contains a large population of Fe(III)-reducing bacteria (Nielsen *et al.*, 1997; Nielsen, 1996; Rasmussen and Nielsen, 1996). A number of microorganisms present in activated sludge plants have been particularly interesting to microbiologists, but the significance of their activity in diverse environments is not well understood. In recent studies, activated sludge containing large amount of Fe(III)-reducers has been successfully used to generate electricity in a microbial fuel cell system (Park *et al.*, 2001). Based on findings isolating Fe(III)-reducers with electrochemical activity from the microbial fuel cell (Pham *et al.*, 2003; Park *et al.*, 2001), it has been proposed that electrochemically active bacteria are widespread on the electrode surface, and that their electrochemical activity is linked to anaerobic respiration. Thus, an investigation into biodiversity in a microbial fuel cell biofilm might identify the organisms in activated sludge that can conserve energy by oxidizing organic compounds using an electrode as

the direct electron acceptor.

Numerous culture-based studies have isolated and identified bacteria from microbial fuel cell biofilms (Pham *et al.*, 2003; Park *et al.*, 2001). They have provided insight into the diversity of the latter. However, conventional microbiological methods are always selective and cannot provide complete information on the true community structure. Consequently, recent developments in cultivation-independent techniques, such as the ribosomal RNA (rRNA) approach (Olsen *et al.*, 1986), now permit considerably more detailed and accurate analysis of mixed microbial communities. In particular, sequence variation in rRNA has been exploited to infer phylogenetic relationship among microorganisms (Woese, 1987) and for designing specific nucleotide probes to detect individual microbial taxa in natural habitats (Amann *et al.*, 1992; Giovannoni *et al.*, 1988).

In this Chapter, several molecular techniques have been used to gain a better understanding of the microbial community and the potential role of these bacteria in a microbial fuel cell. In view of the estimate that <1% of bacteria in nature can be cultured (Giovannoni and Rappé, 2000; Amann *et al.*, 1995), the analysis of 16S ribosomal DNA (rDNA) clone libraries with restriction fragments length polymorphism (RFLP) represents the best method for examining microbial diversity in a fuel cell biofilm. Denaturing gradient gel electrophoresis (DGGE) allows one to analyse the shift in microbial communities when sampled at different times (Muyzer *et al.*, 1993; Amann *et al.*, 1990a), and fluorescent *in situ* hybridization (FISH) with rRNA-targeted oligonucleotide probes (Snaidr *et al.*, 1997) were used to directly analyse the community structure of a biofilm.

The aim of this study was to characterize the enriched microbial population in the biofilm of graphite-felt anode of the fuel cell via 16S rRNA gene RFLP/sequencing analysis, PCR-DGGE and FISH, and to analyse the surface of enriched electrode biofilm using microscopy.

3.2. Materials and methods

3.2.1. Collection of electrode samples

Both anode and cathode electrodes of the microbial fuel cell consisted of graphite felt (50×50×3 mm^3 in dimension, GF series, Electrosynthesis, E. Amherst, NY, U.S.A.). Three pieces of anode electrode (1 cm^2) were removed from the same microbial fuel cell. One was collected at start-up; a second was collected from the fuel cell after enrichment for 6 months using activated sludge obtained from Ponthir sewage treatment works (Gwent, UK) using artificial wastewater as electron donor (Table 2.1), whilst the last was collected from same cell after 11 months operation.

3.2.2. The microbial fuel cell

Fuel cells were constructed from transparent polyacrylic material and were similar to those used previously (Allen and Bennetto, 1993; Delaney *et al.*, 1984). The fuel cells had 20 ml capacity electrode compartments measuring 50×57×7 mm^3 (Figure 2.1). Each cell compartment had three ports at the top: for the electrode wire, the addition and removed of solutions, and for gassing. The two compartments of each cell were separated by a cation-permeable ion exchange membrane (model 55165, BDH Lab supplies, Dorset, UK) sealed between 2 mm thick silicon rubber gaskets. Contact between the electrodes and the ion-exchange membrane was prevented by inclusion of thin plastic bars (2×2×5 mm^3). The anode compartment was loaded with 20 ml of freshly prepared artificial wastewater adjusted to pH 7.0 plus aerobic sewage activated sludge and the cathode compartment contained 50 mM Na-phosphate buffer (pH 7.0) in 0.1 M NaCl (Kim *et al.*, 1999b). Nitrogen and air were continuously purged through anode and cathode compartments to maintain anaerobic or aerobic conditions respectively, at the rate of 15 ml min^{-1}. The microbial fuel cell was immersed in a water

bath to maintain temperature (37℃). Potential change was recorded using a digital voltameter (Model 2000-20, Keithley, Cleveland, U.S.A.) linked to the multichannel scanner (Model 2000-SCAN, Keithley). Current was obtained from time-dependence of the cell voltage at a fixed resistive load (1 KΩ). Data were recorded every 120 s on an IBM compatible personal computer having an IEEE488 interface (Model KPC-488.2AT, Keithley) and a cable (Model CTMGPIB-1, Keithley). The operational conditions optimized in Chapter II were used for all experiments in Chapter III.

3.2.3. Restriction fragments length polymorphism (RFLP) analysis

3.2.3.1. Total DNA extraction of attached bacteria on electrode

The DNA extraction procedure is modified from the method of Zhou *et al.* (1996). Total DNA was extracted directly from the anode electrode samples. One gram of electrode sample was centrifuged for 10 min at 14,000 r.p.m. and 250 mg acid washed glass bead (Stratagene, La Jolla, U.S.A.) were added to the sediment, which was then resuspended in 1 ml buffer A [100 mM Tris-HCl, 100 mM EDTA, 100 mM phosphate buffer, 1.5 M NaCl, 1% CTAB (hexadecyltrimethyl ammonium bromide), 3 μl proteinase K (5 mg ml^{-1}), 2 μl lysozyme (50 mg ml^{-1}) at pH 8.0]. Cell lysis took place after shaking for 20 min on a flatform shaker at full speed. Then, 120 μl 20% SDS (sodium dodecylsulphate) were added and incubated for 30 min at 65℃. After centrifugation at 6,000 r.p.m. for 5 min, the supernatant was then transferred to a new tube, where impurities were extracted using 300 μl chloroform/isoamyl alcohol (24/1) and the DNA precipitated with 0.6 volumes of isopropanol at room temperature for 30 min. The precipitates were spun down at 14,000 r.p.m. for 10 min, rinsed in 300 μl 70% ethanol, dried in a vacuum desiccator and resuspended in 100 μl 10 mM Tris buffer (pH 8.5). DNA from electrode was stored at 4℃.

3.2.3.2. PCR amplification of 16S rRNA genes

DNA directly extracted from the electrode DNA was used as template in PCRs using primers 27F (5'-AGA GTT TGA TCM TGG CTC AG-3') and 1387R (5'-GGG CGG WGT GTA CAA GGC-3') to amplify 16S rDNA (Marchesi *et al.*, 1998). A typical 50-µl PCR mixture contained 20 pmol of each forward and reverse primer, 250 µM (each) deoxynucleotide triphosphates, 1 U of Biotaq DNA polymerase (Bioline, London, UK), PCR buffer (Bioline), 1.5 mM $MgCl_2$, and approximately 250 ng of template DNA. PCR was performed using an MJ Research PTC-200 machine and analysed on a 1% agarose gel. The cycles used were as follows: 1 cycle at 95℃ for 5 min; 29 cycles at 92℃ for 45 s, 55℃ for 45 s, and 75℃ for 45s; followed by 1 cycle at 75℃ for 20 min.

3.2.3.3. Clone library construction

The "TA" cloning kit procedure allowed direct insertion of a PCR product into the plasmid vector pGEM-T® Easy (Promega, Madison, WI, U.S.A.). The use of a thermostable Taq DNA polymerase, which added single deoxyadenine (dA) overhangs to the 3' end of the PCR product, resulted in efficient ligation of the foreign DNA into the linearised vector, containing 3' terminal thymidines. Amplicons were used in a ligation reaction mixture comprising 1 µl of T4 DNA ligase (3 U μl^{-1}), 5 µl of 2× rapid ligation buffer, 1 µl of pGEM-T® easy vector (50 ng), 1 µl of amplicons (250 ng), and 2 µl of sterile water from TA Cloning Kit (Promega). The mixture tube was incubated overnight at 4℃ to allow ligation to proceed.

Bacterial transformation of *Escherichia coli* strain JM109 high efficiency competent cells, provided with the vector system, was carried out as follows: 2 µl of the ligation reaction was mixed gently with the cell suspension (50 µl) and incubated on ice for 20 min. The cells treated by heat shock (45 s at 42℃) and transferred to ice (2 min) before addition of 150 µl SOC medium (2% tryptone; 0.5% yeast extract; 10 mM NaCl; 2.5

mM KCl; 10 mM $MgCl_2$; 10 mM $MgSO_4$; 20 mM glucose). They were then incubated for 1 h at 37℃ in an orbital shaker. A volume of 100 µl of transformed cells was spread-inoculated onto LB agar plates containing ampicillin (50 µg ml^{-1}), 5-bromo-4-chloro-3-indolyl-β-D-galactopyranoside (X-gal, 20 µl of 50 mg ml^{-1}) and isopropyl-β-D-thiogalactopyranoside (IPTG, 100 µl of 100 mM), which were incubated at 37℃ for 16 h and then stored at 4℃. Recombinant transformants colonies selected by blue-white screening were streaked on fresh LB agar plates for a further round of selection and clonal growth and placed in LB broth (5 ml) containing ampicillin (50 µg ml^{-1}). Each of the white colonies were grown overnight in an orbital shaker at 37℃ in preparation for plasmid isolation.

Plasmid isolation was carried out by alkaline lysis using the Wizard™ *Plus* SV Minipreps DNA purification systems (Promega), as described by the manufacturer. Clones treated with restriction enzyme *Rsa*I (Promega) and *Cfo*I. The digestion mixture consisted of 1 µl of *Rsa*I and *Cfo*I enzyme (10 U $µl^{-1}$), 1 µl of C- or B-buffer (Promega), 3 µl of sterile water and 5 µl of plasmid was inserted into the 16S rDNA. The reaction was carried out at 37℃ for 2 h. The restriction digested fragments were visualized by electrophoresis in a 1% agarose gel for 1 h at 80 V.

3.2.3.4. Sequencing of clones

The clone library was initially analysed by partial sequencing of chosen clones by restriction fragments length polymorphism (RFLP) analysis. Plasmid DNA was sequenced using an ABI PRISM 3100-Genetic Analyzer (Applied Bio-systems, Foster City, CA, U.S.A.) with fluorescent primer labeling using near-infrared IRD800 according to the manufacturer's instructions. Automated sequencer was used to separate amplified fragments and to read the sequences.

3.2.3.5. Phylogenetic analysis

Sequences were analysed using the BLAST search program (Altschul *et al.*, 1997) from the National Center for Biotechnology Information website (http://www.ncbi.nlm.nih.gov) and also compared for chimera formation with Check_Chimera software of the Ribosomal Database Project (RDP) II. Non-chimeric sequences were compared to the RDP SSU_Prok data set (release 8.0) using the Sequence_Match analysis service (http://rdp.cme.msu.edu/). Clone 16S rDNA sequences, their closest relatives identified from database searches, and appropriate type strain sequences were aligned with CLUSTAL W (Thompson *et al.*, 1994). Reference sequences were obtained from the RDP Select_Sequence function and the GenBank database. Evolutionary distances were calculated by the method of Jukes and Cantor (Jukes and Cantor, 1969) and phylogenetic trees were constructed by the neighbor-joining method with TREECON for Windows (van de Peer and Wachter, 1994), including bootstrap analysis (Felsenstein, 1985).

3.2.4. Denaturing gradient gel electrophoresis (DGGE) of electrode samples

3.2.4.1. PCR amplification of 16S rDNA fragments

Primers complementary to conserved regions were used to amplify a 194-bp fragment of the 16S rDNA corresponding to nucleotides GC-341F to 534R in *Escherichia coli* sequence (Muyzer *et al.*, 1993). The nucleotide sequence of the forward primer, which is specific for eubacteria (5'-CCT ACG GGA GGC AGC AG-3'), contains at its 5' end a 40 - base GC clamp (5'-CGC CCG CCG CGC GCG GGC GGG GCG GGG GCA CGG GGG G-3') to stabilize the melting behavior of the DNA fragments (Sheffield *et al.*, 1989). The universal consensus sequence (5'-ATT ACC GCG GCT GCT GG-3') was used as a reverse primer. A typical 50-µl PCR mixture contained 20 pmol of each forward and reverse primer, 250 µM (each) of

deoxynucleotide triphosphates, 1 U of Biotaq DNA polymerase (Bioline), PCR buffer (Bioline), 1.5 mM $MgCl_2$, and approximately 250 ng of template DNA. PCR was performed using a MJ Research PTC-200 machine and analysed on a 1.5 % agarose gel. The cycles used were as follows: 1 cycle at 95℃ for 10 min; 19 cycles at 95℃ for 1 min, 65℃ for 45 s, and 72℃ for 45 s; 19 cycles at 95℃ for 1 min, 55℃ for 45 s, and 72℃ for 45 s; followed by 1 cycle at 72℃ for 10 min. To increase the specificity of the amplification and to reduce the formation of spurious products, a "touchdown" PCR was performed. A touchdown PCR is a PCR in which the annealing temperature is set 10℃ above the expected annealing temperature (65℃) and decreased by 0.5℃ every second cycle until a touchdown of 55℃ (Rölleke *et al.*, 1996). All PCR products (5-µl volumes) were analysed by electrophoresis in 2% (w/v) agarose gels (Sambrook *et al.*, 1989) before DGGE analysis was performed

3.2.4.2. Analysis of PCR products by DGGE

DGGE was performed with Dcode Universal Mutation Detection System (Bio-Rad Laboratories) which is based on the Bio-Rad Protean II system and PCR products were separated using this system. 1 mm-thick (16×10 cm glass plates) polyacrylamide gels made of 10% (w/v) polyacrylamide gradient [acrylogel 2.6 solution; acrylamide-*N,N'*-methylenebisacrylamide (37.5:1); BDH Laboratory Supplies, Poole, UK]. DGGE gels contained a 30 to 60% denaturant gradient of urea and formamide solution increasing in the direction of electrophoresis [100% denaturant is defined as 7 M urea with 40% (v/v) formamide]. Gels were polymerized with ammonium persulphate (APS) (Fisher Scientific, UK) and *N,N,N',N'*-tetramethyl-ethylenediamine (TEMED) (Sigma, UK) according to manufacturer's instructions. Gels were poured with the aid of a Model 475 gradient delivery system (Bio-Rad, Hercules, CA, U.S.A.) and prepared with, and electrophoresed in, 1× TAE buffer (pH 8.0; 40 mM Tris base, 20 mM acetic acid, 1 mM

EDTA) and run at 60℃ for 5 h at 200 V. After electrophoresis, the polyacrylamide gels were stained for 20 min in 1× TAE containing SYBRGold nucleic acid gel stain 10000× concentrate in DMSO (Molecular Probes, Leiden, The Netherlands) and the UV gel image was captured by using a Gene Genius Bio Imaging System (Syngene, Cambridge, UK).

3.2.5. Fluorescent *in situ* hybridization (FISH) of electrode samples

3.2.5.1. Fixation of electrode samples

Electrode samples were fixed in 50% ethanol at 4℃ for 24 h (Amann *et al.*, 1990a). Fixed samples were spotted on precleaned teflon-coated microscope slides (BDH Laboratory Supplies, Poole, UK), air-dried at 37℃ for 2 h and dehydrated in an ethanol series (50%, 80% and 95% ethanol, 3 min in each).

3.2.5.2. DAPI staining

Two teflon-coated microscope slides were prepared for direct counts of the enriched electrode samples, and another sixteen slides were prepared for the dual staining procedure. Fixed samples spotted were stained for 10 min at 22℃ with 8 μl of the DNA-binding dye 4', 6-diamidino-2-phenylindole (DAPI: 0.7 mg ml^{-1}), and then rinsed with deionized water to completely remove excess stain, and air dried (Hicks *et al.*, 1992; Wagner *et al.*, 1993). These slides were mounted in Citifluor (Citifluor Ltd, London, UK) or Vectashield (Vector Inc, CA, U.S.A.) as an enhancer. Total cells were detected with a Carl Zeiss LSM-410 confocal scanning laser microscope (Carl Zeiss Inc., Thornwood, NY) fitted for epifluorescence microscopy. The cells remaining sixteen slides were prepared for hybridization with one fluorescent eubacterial probe and seven eukaryotic oligonucleotide probes.

3.2.5.3. Oligonucleotide probes

Alignments of rRNA gene sequences were screened for signature positions characteristic of the alpha-, beta-, and gamma-subclasses of *Proteobacteria*, *Bacteroidetes*, *Actinobacteria*, *Firmicutes* and *Planctomycetes*. Oligonucleotides complementary to selected regions were synthesized with a fluorescein isothiocyanate (FITC), tetramethylrhodamine-5-isothiocyanate (TRITC) and CY3 at the 5'-end (MWG Biotech; Ebersberg, Germany) (Amann *et al.*, 1990b). Sequences and target sites are presented in Table 3.1.

3.2.5.4. *In situ* hybridization and probe-specific cell counts

The hybridization buffer (360 µl of 5 M NaCl, 40 µl of 1 M Tris-HCl, 2 µl of 10% SDS, 400 or 700 µl of formamide, 1198 or 898 µl of autoclaved milli-Q water) was prepared in 2-ml microcentrifuge tubes at the time of use which allowed 8:1 to each well on the slide and the remainder in the hybridization tube for keeping the chamber in the tube moist. 8 µl hybridization buffer [0% (for probes EUB338a.b.c., HGC906), 20% (for probes ALF1b), and 35% (for probes BET42a, GAM42a, CF319b, LGC354a.b.c., PLA46)] was added to each well on the slide, the remainder was used to moisten a tissue paper in the 50-ml tube. Then 1 µl of oligonucleotide probes at 25 ng μl^{-1} were added and mixed carefully. Since single mismatch discrimination was required for probes BET42a and GAM42a (see Table 3.1), the different amounts (0.25 µg, 2.5 µg) of unmodified oligonucleotide GAM42a as competitor to the hybridization solution containing 25 ng labeled probe BET42a was added (Manz *et al.*, 1992). The slide was placed into the 50-ml tube containing the moistened tissue and put into a hybridization oven at 46℃ for 2 h. After hybridization, the slides were carefully removed from the tube and rinsed immediately in prewarmed (48℃) washing buffer (2150 or 700 µl of 5 M NaCl, 1 ml of 1 M Tris-HCl, 43.8 ml Milli-Q water, 50 µl of

Table 3.1 Sequence, target sites and specificities of rRNA-targeted oligonucleotide probes used for whole-cell hybridization.

Probe	Label	Target group	Sequence (5'→3')	Target[a]	%GC	Tm[b]	%FA[c]	Reference
EUB338a	Fluorescein	*Bacteria*	GCT GCC TCC CGT AGG AGT	16S rRNA	66.7	60.5	0	Amann *et al.*, 1990b
EUB338b	Fluorescein	*Bacteria*	GCA GCC ACC CGT AGG TGT	16S rRNA	66.7	60.5	0	Daims *et al.*, 1999
EUB338c	Fluorescein	*Bacteria*	GCT GCC ACC CGT AGG TGT	16S rRNA	66.7	60.5	0	Daims *et al.*, 1999
ALF1b	Cy3	α-*Proteobacteria*	CGT TCG (CT)TC TGA GCC AG	16S rRNA	61.8	56.4	20	Manz *et al.*, 1996
BET42a	Cy3	β-*Proteobacteria*	GCC TTC CCA CTT CGT TT	23S rRNA	52.9	52.8	35	Manz *et al.*, 1996
GAM42a	Cy3	γ-*Proteobacteria*	GCC TTC CCA CAT CGT TT	23S rRNA	52.9	52.8	35	Manz *et al.*, 1996
CF319a	Cy3	*Bacteroidetes*	TGG TCC GTG TCT CAG TAC	16S rRNA	55.6	56	35	Manz *et al.*, 1994
CF319b	Cy3	*Bacteroidetes*	TGG TCC GTA TCT CAG TAC	16S rRNA	50	53.7	35	Manz *et al.*, 1994
BAC303	Cy3	*Bacteroides*	CCA ATG TGG GGG ACC TT	16S rRNA	58.8	55.2	35	Manz *et al.*, 1994
HGC906	Rhodamine	*Actinobacteria*	GAG TAC GGC CGC AAG GCT A	16S rRNA	63.2	61	0	This study
HGC69a	Cy3	*Actinobacteria*	TAT AGT TAC CAC CGC CGT	23S rRNA	50	53.7	35	Roller *et al.*, 1994
LGC354a	Cy3	*Firmicutes*	TGG AAG ATT CCC TAC TGC	16S rRNA	50	53.7	35	Meier *et al.*, 1999
LGC354b	Cy3	*Firmicutes*	CGG AAG ATT CCC TAC TGC	16S rRNA	55.6	56	35	Meier *et al.*, 1999
LGC354c	Cy3	*Firmicutes*	CCG AAG ATT CCC TAC TGC	16S rRNA	55.6	56	35	Meier *et al.*, 1999
PLA46	Cy3	*Planctomycetes*	GAC TTG CAT GCC TAA TCC	16S rRNA	50	53.7	35	Neef *et al.*, 1998
1501B	Cy3	Outer membrane cytochrome *c*	GCA TTT GGA ACG TCG TAG GT		50	60		This study

[a]Position in the rRNA of *Escherichia coli*.

[b]Optimal hybridization temperature (℃).

[c]Formamide concentration in hybridization buffer.

10% SDS) at 48℃ (Seviour and Blackall, 1999). Slides were placed into the washing buffer tube and into water bath at 48℃ for 20 min. After the wash, the slides were removed, gently rinsed in deionized water from a wash bottle, and quickly dried. Before examination the slides were mounted in Citifluor (Citifluor Ltd, London, UK) or Vectashield (Vector Inc, CA, U.S.A.) as an enhancer. Fluorescence was detected with a Carl Zeiss LSM-410 confocal scanning laser microscope (Carl Zeiss Inc., Thornwood, NY) fitted for epifluorescence microscopy. Samples were examined using the 488 nm line of a dual line argon ion laser with a filter BP515-545 and 10×, 40× and 100× objective lenses.

The total and probe-specific cells were counted by manual counting with quadrates. The method of enumeration is to count the number of cells within squares on a 10 × 10 graticule. The number of bacteria (T) is calculated from the mean number of bacteria per graticule area (N), filteration area (A_f), volume of sample filtered (V) and the graticule area (a) by the formula $T = NA_f / aV$. The precision of the count depends on the number of bacteria and not the number of microscope fields counted (Fry, 1990). The 95% confidence intervals are approximately twice the square root of the number counted, thus are 10% for 400 cells and 20% for 100 cells and 36% for 30 cells (Jones, 1979). For this reason most researchers count 400 bacteria per membrane filter to get more reliable results. For each probe, 999 ± 69.5 cells stained with the bacterial probe EUB338 were enumerated. 360 ± 23.2 cells of all DAPI-stained cells hybridized with probe for α-*Proteobacteria* (ALF1b). Other members of the *Proteobacteria* hybridizing with probes for the beta subclass (BET42a) and the gamma subclass (GAM42a) constituted 49 ± 9.4 and 131 ± 40.5 cells, respectively. The probe CF319b, specific for most members of the *Bacteroidetes* group, bound to 345 ± 126.3 cells and probe HGC906 and LGC354, which is complementary to a 16S rRNA signature of bacteria with a high and low DNA G+C content, bound to 65 ± 23.1 and 199 ± 45.1 cells. The

probe PLA46 related to *Planctomycetes* also bound to 16 ± 4.5 cells.

3.2.6. Microscopy

Anode electrode (graphite felt) was partially removed from a microbial fuel cell which had been enriched for more than 6 months for the microscopic observations.

3.2.6.1. Low vacuum electron microscopy (LVEM)

1 cm^2 samples of the anode electrode were cut with a blade (0.5 cm^2) and put on nucleopore membrane (Whatman Co., pore size 0.2 μm). The samples were observed with low vacuum electron microscopy (JSM-5200LV, JEOL Co, Japan) without pretreatment.

3.2.6.2. Scanning electron microscopy (SEM)

1 cm^2 surface samples of the anode electrode were cut with a blade and embeded on nucleopore membrane (Whatman Co., pore size 0.2 μm). To observe small bacteria observation, the electrode was vortexed with phosphate buffer (pH 7.0) and filtered on to a membrane filter (Whatman Co., pore size 0.45 μm). Samples were fixed with 3% (v/v) glutaraldehyde in 100mM HEPES buffer (pH 6.8) containing 2 mM $MgCl_2$ for 1 h and then treated with 1% OsO_4 (w/v) for 2 h. The samples were dehydrated using 30, 50, 70, 80, 90 and 95% (v/v) of ethanol solutions for 20 min, respectively. Water was removed from the samples by critical point drying with CO_2.The dried samples were coated in a sputtering device (Eiko IB-3 ion coater, Tokyo, Japan), and examined in an SEM instrument (JSM-5200LV, JEOL, Tokyo, Japan) operating at less than 25 KV.

3.2.6.3. Transmission electron microscopy (TEM)

1 cm^2 electrode samples were vortexed to separate microbial cells. 0.5 ml of cell

suspension was mixed with an equal volume of 3% (v/v) glutaraldehyde solution in 100 mM HEPES buffer (pH 6.8) containing 2 mM $MgCl_2$ and kept for 2 h at room temperature. The cells were washed twice using HEPES buffer by centrifugation (10,000 r.p.m., for 5 min). The washed cell pellet was suspended in 1% (w/v) OsO_4 solution and incubated for 2 h at room temperature. OsO_4 solution was removed by washing using HEPES buffer. Samples were washed again twice in deionized water and 70% (v/v) ethanol for 15 min each, and transferred to 80 and 95% (v/v) ethanol, successively, for 15 min each. Finally, the cells were transferred to 100% ethanol and kept for 30 min at room temperature. The cells recovered from ethanol were embedded using LR white resin (Pelco, Co. Redding, CA, U.S.A.). The embedded block was left overnight at 60℃ and then sectioned using a microtome (Ultramicrotome, Sorvall MT-II, Wilmington, Delaware, U.S.A.) to 60-90 nm of thickness. The thin sections were stained using uranyl acetate (1 mM), lead citrate (1 mM) for 15, 10 min, respectively, and washed 0.02 M NaOH. TEM instrument (JEM-1210, JEOL, Tokyo, Japan) was operated at 80 KV.

3.2.6.4. Confocal scanning laser microscopy (CSLM)

A Carl Zeiss LSM-410 confocal scanning laser microscope (Carl Zeiss Inc., Thornwood, NY) was used to observe in 3-D the microbial population which developed on the graphite felt electrode. Felt samples were stained with acridine orange (0.02% final concentration) for 2-4 h, rinsed twice with distilled water and embeded with 1% agarose solution (Difco, U.S.A.) at 40℃ (the felt surface was nearly covered by agarose). Alternatively, the samples were stained with LIVE BacLight Bacterial Gram stain kit (L-7005, Molecular Probes, Leiden, The Netherlands). Samples were examined using the 488 nm line of a dual line argon ion laser with a filter BP515-545 and 10×, 40× and 100× objective lenses.

3.3. Results

3.3.1. Clone library construction

The early establishment stage of the fuel cell and the 6 and 11 month enriched electrode 16S rDNA clone libraries were constructed and contained a total of 173 clones. Library A (MFC-A) contained 39 clones and was made with primers 27F and 1387R, while Library B (MFC-B) contained 47 clones and Library C (MFC-C) contained 87 clones and were made with same primers.

3.3.1.1. Clone library analysis: RFLP and partial sequencing

In three clone libraries, a sample of 58 clones was selected for partial sequencing and phylogenetic analysis. Partial sequence length ranged from 472 to 1356 bp (median 914bp; 92%> 800 bp). All sequences were submitted to a RDP Sequence_Match query and a GenBank BLAST search to find their closest matches in the databases, and no chimeric sequences were found among the clones from MFC-A to MFC-C. Non-chimeric sequences were then used in the construction of phylogenetic trees. The inclusion of a range of partial sequence lengths did not alter the topology of the phylogenetic trees when compared to trees constructed from type strain sequences over 1200 bp.

Clone sequences analysed fell into nine major lineages of the domain *Bacteria* (Hugenholtz *et al.*, 1998). In Library A (MFC-A) from the initial operating stage electrode, *Prosthecobacter* phylotypes constituted the most abundant division with 30.8% (12/39) of the sequenced clones, followed by 28.2% (11/39) *Bacteroidetes*, 12.8% (5/39) α-*Proteobacteria* and 7.7% (3/39) δ-*Proteobacteria* group (Table 3.2; Figure 3.1). Six of the eight sequenced *Bacteroidetes* clones clustered in the RDP

Cytophaga group, one sequence clustered in the RDP *Sphingobacterium* group, and one sequence had a highest match in the RDP *Bacteriodes* group. Of the 2 α-*Proteobacteria* related sequences, one belonged to the RDP designated group *Azospirillum,* and the other to the *Rhodopila* group. One δ-*Proteobacteria* related sequence belonged to the RDP *Myxobacteria* group.

In Library B (MFC-B) from the 6 months enriched electrode, *Bacteroidetes* was the most abundant division with 25.5% (12/47) of the sequenced clones, followed by 19.2% (9/47) δ-*Proteobacteria*, 17.0% (8/47) α-*Proteobacteria*, 10.6% (5/47) green-sulfur bacteria, 8.5% (4/47) gram-positive bacteria, 6.4% (3/47) γ-*Proteobacteria*, 4.3% (2/47) β-*Proteobacteria*, 4.3% (2/47) *Cyanobacteria*, and 2.1% (1/47) *Prosthecobacter* group (Table 3.3; Figure 3.2). Three of the six sequenced α-*Proteobacteria* clones clustered in the RDP *Azospirillum* group, two sequences clustered in the RDP *Rhizobium-Agrobacterium* group, and one sequence had a highest match in the RDP *Rhodopila* group. Of the 5 *Bacteroidetes* related sequences, three sequences belonged to the RDP designated group *Cytophaga*, and two to *Bacteriodes*. Two of the four sequenced δ-*Proteobacteria* clones matched most closely the RDP *Desulfovibrio* group, and two to the *Desulfuromonas* group. Two β-*Proteobacteria* related sequences belonged to the RDP *Azoarcus* group, and two γ-*Proteobacteria* to the *Enteric and Relatives* group. One of the two sequenced gram-positive bacteria belonged to the RDP *Sporomusa* group, and one to the *Acidimicrobium* group. One green-sulfur bacteria related sequence belonged to the RDP *Chlorobium* group, and one *Cyanobacteria* to the *Gloeothece-Gloeocapsa* group.

In Library C (MFC-C) from the 11 months enriched electrode, γ-*Proteobacteria* was the most abundant division with 59.8% (52/87) of the sequenced clones, followed by

23.0% (20/87) gram-positive bacteria, 8.1% (7/87) *Fibrobacter* and *Acidobacterium*, 6.9% (6/87) α-*Proteobacteria*, and 1.2% (1/87) green non-sulfur bacteria (Table 3.4; Figure 3.3). Seven of the nine sequenced gram-positive bacteria clones clustered in the RDP *Clostridium botulinum* group, and two sequences clustered in *Acidimicrobium* group. Of the six α-*Proteobacteria* related sequences, five belonged to the RDP designated group *Rhizobium-Agrobacterium*, and one to the *Sphingomonas* group. Three γ-*Proteobacteria* related sequences belonged to the RDP *Xanthomonas* group, and three *Fibrobacter* and *Acidobacterium* to the *Acidobacterium capsulatum* group. One green non-sulfur bacteria related sequence matched most closely to the RDP *Thermus* group.

3.3.1.2. Phylogenetic affiliations of bacterial community members

A total of 58 clones were sequenced from the three clone libraries. The sequences were compared with GenBank and the closest match was determined as mentioned above (Table 3.2; 3.3; 3.4). A phylogenetic tree was constructed with the closest match and its related sequences (Figure 3.1; 3.2; 3.3). Phylogenetic analyses revealed that the clone sequences retrieved from the enriched electrode samples fell into eleven clusters. Dominant clone sequences were representatives of the γ-*Proteobacteria* (33.7%), *Firmicutes* (14.7%), *Bacteroidetes* (14.1%), α-*Proteobacteria* (11.7%), *Prosthecobacter* (8.0%), δ-*Proteobacteria* (7.4%), *Fibrobacter* and *Acidobacterium* (4.3%) and green-sulfur bacteria (3.1%) and similar to sequences from the β-*Proteobacteria*, *Cyanobacteria* and green non-sulfur bacteria.

The dominant clone sequence from the Library A (MFC-A) was related to the genus *Verrucomicrobium* and had a similarity (90%) to 16S rRNA genes from *V. spinosum*. Clone sequences related to the *Bacteroidetes* phylotypes were shown the similarity to sequences from the genera *Flavobacterium*, *Bacteroides* and *Cytophaga* in Figure 3.1.

Table 3.2 Closest matches of the initial operating stage microbial fuel cell electrode 16S rDNA clones [library A (MFC-A)] with sequences in the GenBank database according to the BLAST search program (Altschul *et al.*, 1997) in the national Centre for Biotechnology Information (NCBI) website (*http://www.ncbi.nlm.nih.gov*).

RDP division	RDP group	Clone designation (MFC-A)	GenBank closest match	% similarity
Bacteroidetes	*Cytophaga*	MFC-A3	*Flavobacterium limicola*	93
		MFC-A5	Uncultured bacterium FukuN36	95
		MFC-A6, A12	*Flavobacterium aquatile*	95-96
		MFC-A11	Antarctic bacterium R-8963	95
		MFC-A15	*Flavobacterium* sp. EP241	96
	Sphingobacterium	MFC-A16	Uncultured bacterium clone TLM	94
	Bacteriodes	MFC-A14	*Bacteroides* sp. AR20	97
α-*Proteobacteria*	*Azospirillum*	MFC-A1	Endosymbiont of *Acanthamoeba* sp	94
	Rhodopila	MFC-A7	Uncultured alpha proteobacterium	91
δ-*Proteobacteria*	*Myxobacteria*	MFC-A8	*Nannocystis exedens*	90
Prosthecobacter	*Prosthecobacter*	MFC-A2	Uncultured *Verrucomicrobia* bacterium	90

Table 3.3 Closest matches of the 6 months enriched electrode 16S rDNA clones [library B (MFC-B)] with sequences in the GenBank database according to the BLAST search program (Altschul *et al.*, 1997) in the national Centre for Biotechnology Information (NCBI) website (*http://www.ncbi.nlm.nih.gov*).

RDP division	RDP group	Clone designation (MFC-B)	GenBank closest match	% similarity
Bacteroidetes	*Cytophaga*	MFC-B1, B23	Uncultured eubacterium WCHB1-32	86
		MFC-B21	*Flavobacterium* sp. cpw707	98
	Bacteriodes	MFC-B6	Uncultured eubacterium WCHB1-29	92
		MFC-B24	Bacterium mpn-isolate group 6	88
α-*Proteobacteria*	*Azospirillum*	MFC-B2	Uncultured rape rhizosphere bacterium wr0007	96
		MFC-B12, B13	*Azospirillum* sp.	98
	Rhizobium-Agrobacterium	MFC-B7	Alpha proteobacterium F0723	97
		MFC-B22	Uncultured rape rhizosphere bacterium wr0006	97
	Rhodopila	MFC-B9	Uncultured bacterium GKS2-218	94
β-*Proteobacteria*	*Azoarcus*	MFC-B3	*Dechlorosoma* sp. Iso1	99
		MFC-B16	*Azoarcus* sp. BS2-3	99
γ-*Proteobacteria*	*Enterics and Relatives*	MFC-B15	*Klebsiella ornithinolytica* strain ATCC 31898	99
		MFC-B25	*Enterobacter aerogenes*	98
δ-*Proteobacteria*	*Desulfovibrio*	MFC-B10, B20	*Lawsonia intracellularis*	92
	Desulfuromonas	MFC-B14, B19	*Geobacter* sp	98
Gram-positive bacteria	*Sporomusa*	MFC-B8	*Anaerovibrio burkinabensis* DSM 6283(T)	98
	Acidimicrobium	MFC-B11	Uncultured rape rhizosphere bacterium wr0198	95
Cyanobacteria	*Gloeothece-Gloeocapsa*	MFC-B5	Rhizosphere soil bacterium clone RSC-II-6	93
Green-sulfur bacteria	*Chlorobium*	MFC-B4	Uncultured bacterium PENDANT-20	92
Prosthecobacter	*Prosthecobacter*	MFC-B18	Uncultured eubacterium AA08	92

Table 3.4 Closest matches of the 11 months enriched electrode 16S rDNA clones [library C (MFC-C)] with sequences in the GenBank database according to the BLAST search program (Altschul *et al.*, 1997) in the national Centre for Biotechnology Information (NCBI) website (*http://www.ncbi.nlm.nih.gov*).

RDP division	RDP group	Clone designation (MFC-C)	GenBank closest match	% similarity
Fibrobacter and Acidobacterium	*Acidobacterium capsulatum*	MFC-C4	Uncultured bacterium SJA-149	94
		MFC-C13	Uncultured eubacterium WD281	93
		MFC-C15	Uncultured eubacterium WD247	93
α-*Proteobacteria*	*Rhizobium-Agrobacterium*	MFC-C5, C16	*Mesorhizobium* sp WG	98-99
		MFC-C14	*Rhodoplanes elegans*	99
		MFC-C19	Uncultured alpha proteobacterium	96
		MFC-C22	Uncultured rape rhizosphere bacterium wr0006	98
	Sphingomonas	MFC-C9	*Sphingomonas* sp. oral clone AW030	96
γ-*Proteobacteria*	*Xanthomonas*	MFC-C1, C3, C12	Gamma proteobacterium A40-1	95-98
Gram-positive bacteria	*Clostridium botulinum*	MFC-C2, C10	*Clostridium disporicum*	97
		MFC-C6, C11, C18	*Clostridium thiosulforeducens*	93-94
		MFC-C8	*Clostridium butyricum* (NCIMB8082) rrn gene	95
		MFC-C23	*Anaerobacter polyendosporus*	92
	Acidimicrobium	MFC-C7, C17	*Desulfosporosinus* sp. S8	84-85
Green non-sulfur bacteria	*Thermus*	MFC-C20	*Meiothermus ruber*	92

Figure 3.1 Phylogenetic tree illustrating the relationship between the closest relatives in the RDP and GenBank databases of 16S rDNA gene sequences from the initial operating stage microbial fuel cell electrode. 16S rRNA gene sequences were aligned using CLUSTAL W, and the tree was constructed by the neighbor-joining program from a similarity matrix of pair-wise comparisons made by the Jukes-Cantor algorithm in TREECON. The tree was rooted with the *Euryarchaeota Methanoculleus olentangyi*. Bootstrap values over 70, from 100 replicate trees, are shown at the nodes. The scale bar represents 10% difference in nucleotide sequence.

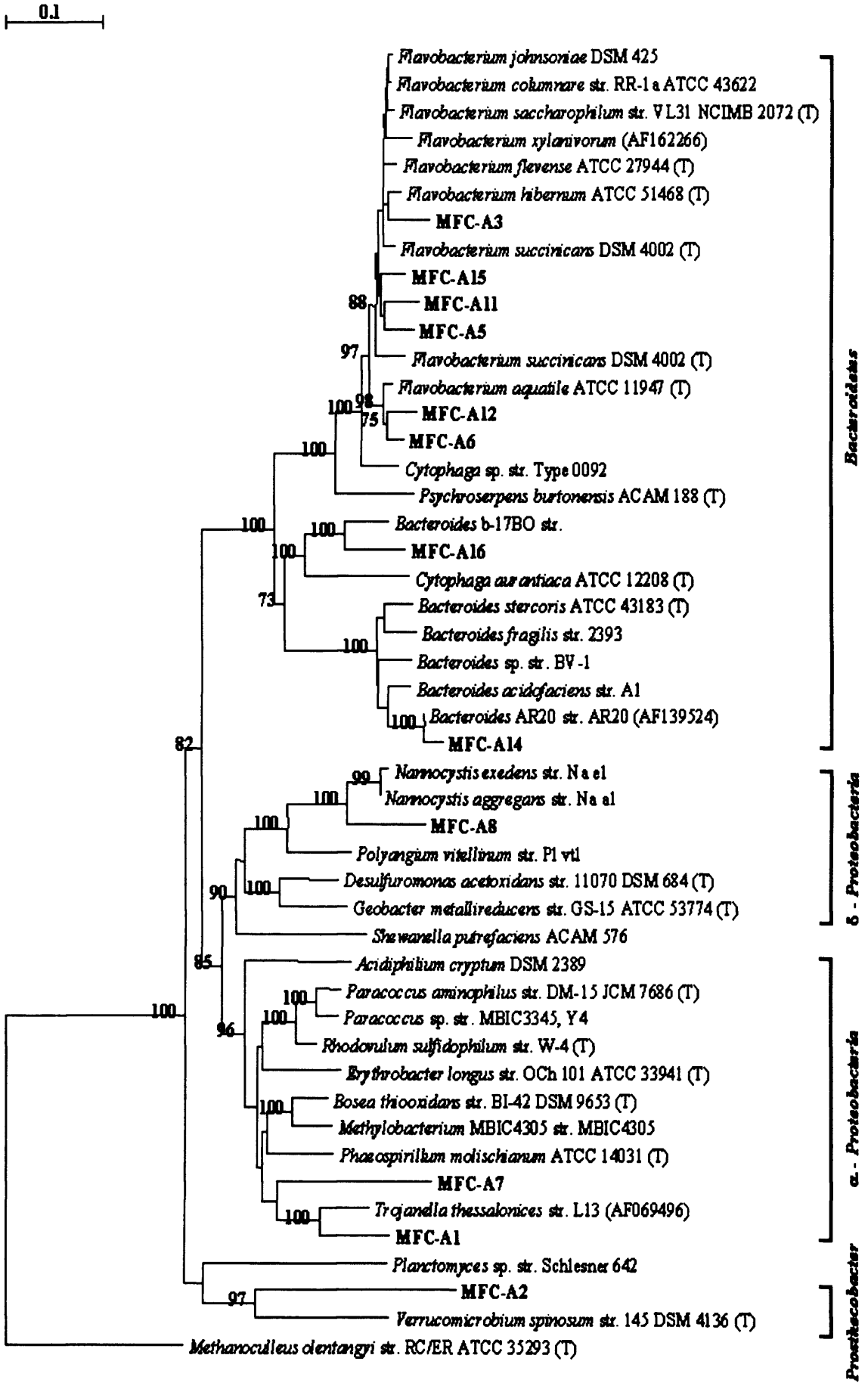
0.1
Flavobacterium johnsoniae DSM 425
Flavobacterium columnare str. RR-1 a ATCC 43622
Flavobacterium saccharophilum str. VL31 NCIMB 2072 (T)
Flavobacterium xylanivorum (AF162266)
Flavobacterium flevense ATCC 27944 (T)
Flavobacterium hibernum ATCC 51468 (T)
MFC-A3
Flavobacterium succinicans DSM 4002 (T)
MFC-A15
MFC-A11
MFC-A5
Flavobacterium succinicans DSM 4002 (T)
Flavobacterium aquatile ATCC 11947 (T)
MFC-A12
MFC-A6
Cytophaga sp. str. Type 0092
Psychroserpens burtonensis ACAM 188 (T)
Bacteroides b-17BO str.
MFC-A16
Cytophaga aurantiaca ATCC 12208 (T)
Bacteroides stercoris ATCC 43183 (T)
Bacteroides fragilis str. 2393
Bacteroides sp. str. BV-1
Bacteroides acidofaciens str. A1
Bacteroides AR20 str. AR20 (AF139524)
MFC-A14
Nannocystis exedens str. Na e1
Nannocystis aggregans str. Na a1
MFC-A8
Polyangium vitellinum str. Pl vt1
Desulfuromonas acetoxidans str. 11070 DSM 684 (T)
Geobacter metallireducens str. GS-15 ATCC 53774 (T)
Shewanella putrefaciens ACAM 576
Acidiphilium cryptum DSM 2389
Paracoccus aminophilus str. DM-15 JCM 7686 (T)
Paracoccus sp. str. MBIC3345, Y4
Rhodovulum sulfidophilum str. W-4 (T)
Erythrobacter longus str. OCh 101 ATCC 33941 (T)
Bosea thiooxidans str. BI-42 DSM 9653 (T)
Methylobacterium MBIC4305 str. MBIC4305
Phaeospirillum molischianum ATCC 14031 (T)
MFC-A7
Trojanella thessalonices str. L13 (AF069496)
MFC-A1
Planctomyces sp. str. Schlesner 642
MFC-A2
Verrucomicrobium spinosum str. 145 DSM 4136 (T)
Methanoculleus olentangyi str. RC/ER ATCC 35293 (T)
Bacteroidetes
δ - Proteobacteria
α - Proteobacteria
Prosthecobacter

Figure 3.2 Phylogenetic tree illustrating the relationship between the closest relatives in the RDP and GenBank databases of 16S rDNA gene sequences from 6 months enriched microbial fuel cell electrode. 16S rRNA gene sequences were aligned using CLUSTAL W, and the tree was constructed by the neighbor-joining program from a similarity matrix of pair-wise comparisons made by the Jukes-Cantor algorithm in TREECON. The tree was rooted with the *Euryarchaeota Methanoculleus olentangyi*. Bootstrap values over 70, from 100 replicate trees, are shown at the nodes. The scale bar represents 10% difference in nucleotide sequence.

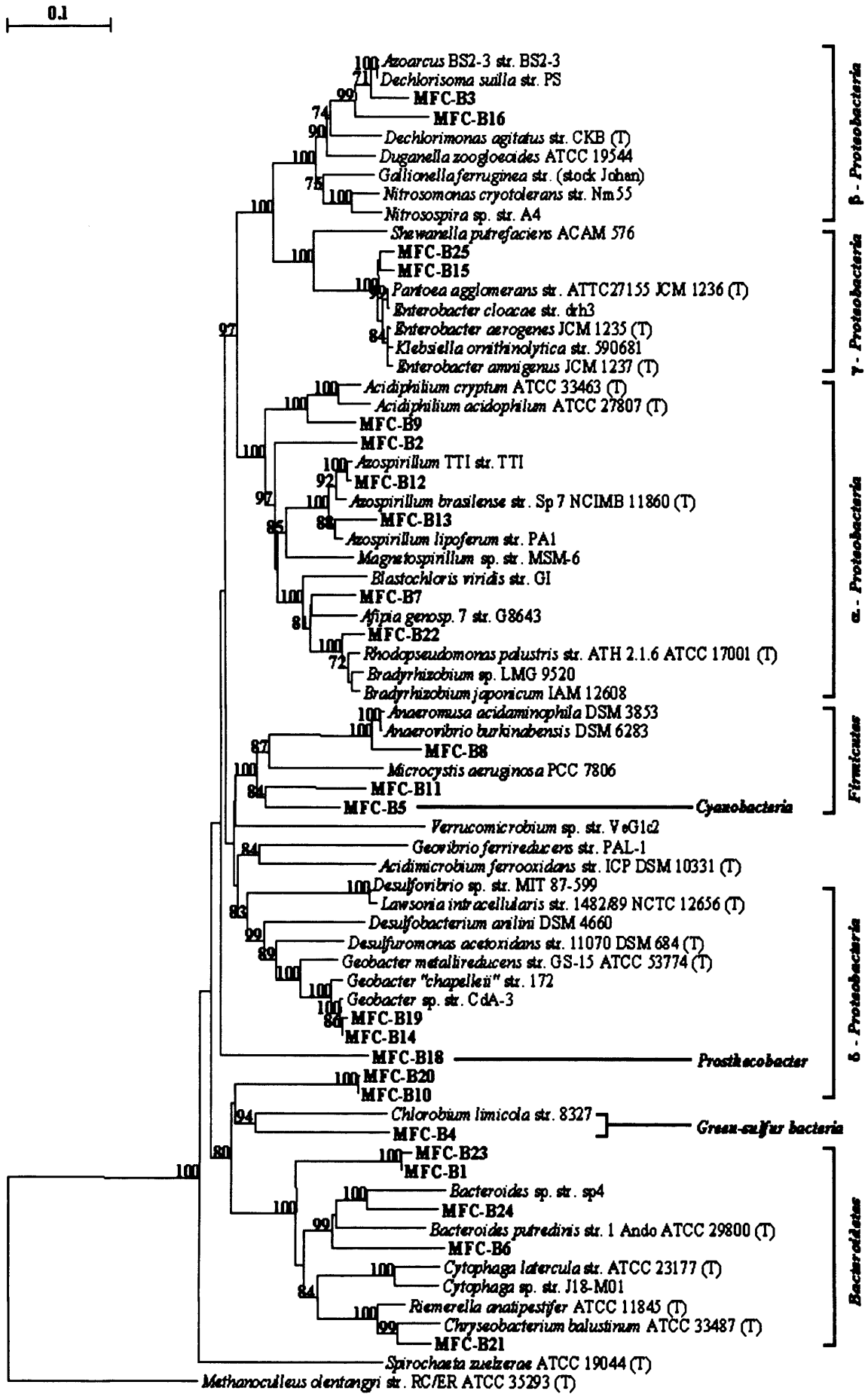
0.1
Azoarcus BS2-3 str. BS2-3
Dechlorisoma suilla str. PS
MFC-B3
MFC-B16
Dechlorimonas agitatus str. CKB (T)
Duganella zoogloecides ATCC 19544
Gallionella ferruginea str. (stock Johan)
Nitrosomonas cryotolerans str. Nm55
Nitrosospira sp. str. A4
Shewanella putrefaciens ACAM 576
MFC-B25
MFC-B15
Pantoea agglomerans str. ATTC27155 JCM 1236 (T)
Enterobacter cloacae str. drh3
Enterobacter aerogenes JCM 1235 (T)
Klebsiella ornithinolytica str. 590681
Enterobacter amnigenus JCM 1237 (T)
Acidiphilium cryptum ATCC 33463 (T)
Acidiphilium acidophilum ATCC 27807 (T)
MFC-B9
MFC-B2
Azospirillum TTI str. TTI
MFC-B12
Azospirillum brasilense str. Sp 7 NCIMB 11860 (T)
MFC-B13
Azospirillum lipoferum str. PA1
Magnetospirillum sp. str. MSM-6
Blastochloris viridis str. GI
MFC-B7
Afipia genosp. 7 str. G8643
MFC-B22
Rhodopseudomonas palustris str. ATH 2.1.6 ATCC 17001 (T)
Bradyrhizobium sp. LMG 9520
Bradyrhizobium japonicum IAM 12608
Anaeromusa acidaminophila DSM 3853
Anaerovibrio burkinabensis DSM 6283
MFC-B8
Microcystis aeruginosa PCC 7806
MFC-B11
MFC-B5
Cyanobacteria
Verrucomicrobium sp. str. VeG1c2
Geovibrio ferrireducens str. PAL-1
Acidimicrobium ferrooxidans str. ICP DSM 10331 (T)
Desulfovibrio sp. str. MIT 87-599
Lawsonia intracellularis str. 1482/89 NCTC 12656 (T)
Desulfobacterium anilini DSM 4660
Desulfuromonas acetoxidans str. 11070 DSM 684 (T)
Geobacter metallireducens str. GS-15 ATCC 53774 (T)
Geobacter "chapelleii" str. 172
Geobacter sp. str. CdA-3
MFC-B19
MFC-B14
MFC-B18
Prosthecobacter
MFC-B20
MFC-B10
Chlorobium limicola str. 8327
MFC-B4
Green-sulfur bacteria
MFC-B23
MFC-B1
Bacteroides sp. str. sp4
MFC-B24
Bacteroides putredinis str. 1 Ando ATCC 29800 (T)
MFC-B6
Cytophaga latercula str. ATCC 23177 (T)
Cytophaga sp. str. J18-M01
Riemerella anatipestifer ATCC 11845 (T)
Chryseobacterium balustinum ATCC 33487 (T)
MFC-B21
Spirochaeta zuelzerae ATCC 19044 (T)
Methanoculleus olentangyi str. RC/ER ATCC 35293 (T)
β - Proteobacteria
γ - Proteobacteria
α - Proteobacteria
Firmicutes
δ - Proteobacteria
Bacteroidetes

Figure 3.3 Phylogenetic tree illustrating the relationship between the closest relatives in the RDP and GenBank databases of 16S rDNA gene sequences from 11 months enriched microbial fuel cell electrode. 16S rRNA gene sequences were aligned using CLUSTAL W, and the tree was constructed by the neighbor-joining program from a similarity matrix of pair-wise comparisons made by the Jukes-Cantor algorithm in TREECON. The tree was rooted with the *Euryarchaeota Methanoculleus olentangyi*. Bootstrap values over 70, from 100 replicate trees, are shown at the nodes. The scale bar represents 10% difference in nucleotide sequence.

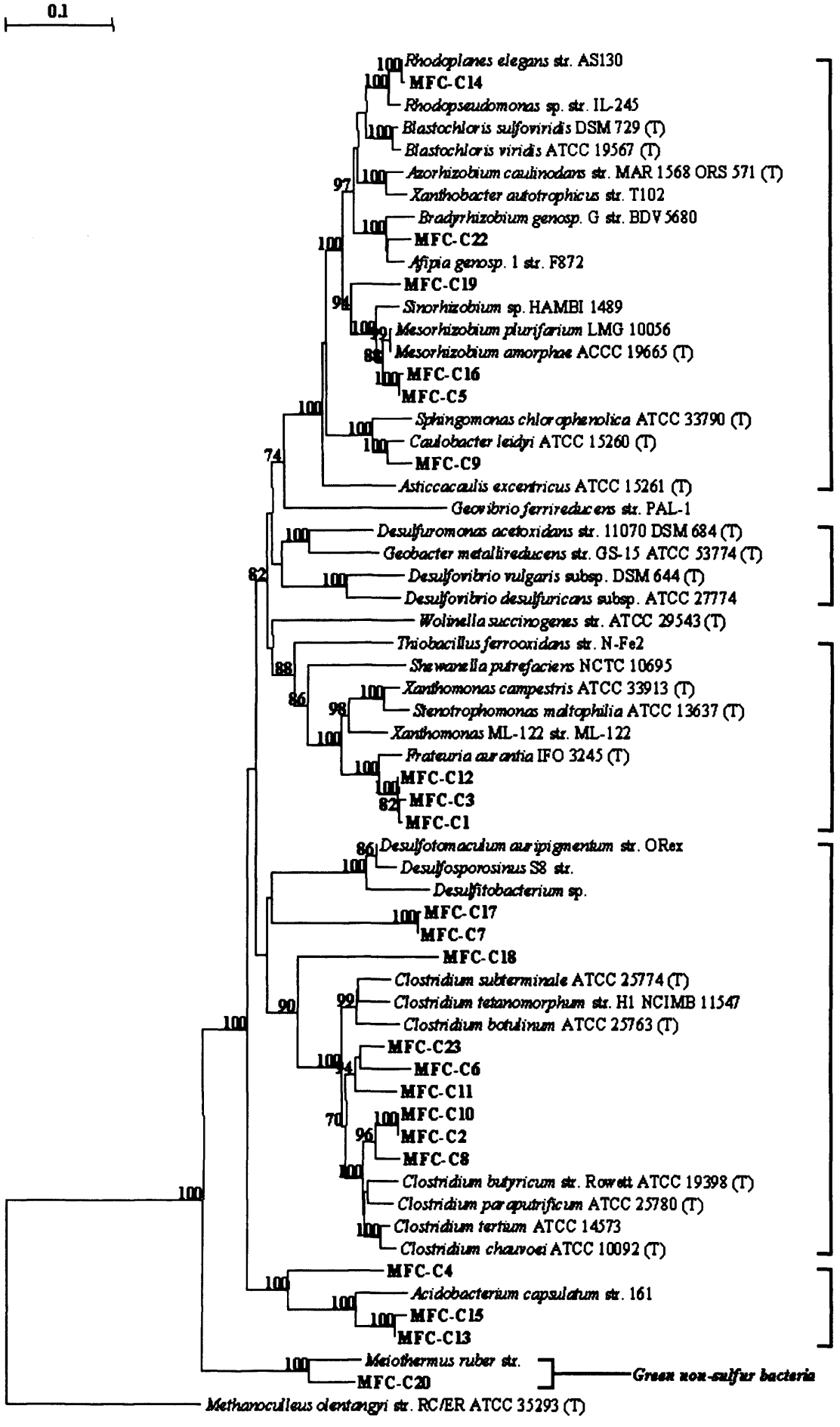
0.1
Rhodoplanes elegans str. AS130
MFC-C14
Rhodopseudomonas sp. str. IL-245
Blastochloris sulfoviridis DSM 729 (T)
Blastochloris viridis ATCC 19567 (T)
Azorhizobium caulinodans str. MAR 1568 ORS 571 (T)
Xanthobacter autotrophicus str. T102
Bradyrhizobium genosp. G str. BDV 5680
MFC-C22
Afipia genosp. 1 str. F872
MFC-C19
Sinorhizobium sp. HAMBI 1489
Mesorhizobium plurifarium LMG 10056
Mesorhizobium amorphae ACCC 19665 (T)
MFC-C16
MFC-C5
Sphingomonas chlorophenolica ATCC 33790 (T)
Caulobacter leidyi ATCC 15260 (T)
MFC-C9
Asticcacaulis excentricus ATCC 15261 (T)
Geovibrio ferrireducens str. PAL-1
Desulfuromonas acetoxidans str. 11070 DSM 684 (T)
Geobacter metallireducens str. GS-15 ATCC 53774 (T)
Desulfovibrio vulgaris subsp. DSM 644 (T)
Desulfovibrio desulfuricans subsp. ATCC 27774
Wolinella succinogenes str. ATCC 29543 (T)
Thiobacillus ferrooxidans str. N-Fe2
Shewanella putrefaciens NCTC 10695
Xanthomonas campestris ATCC 33913 (T)
Stenotrophomonas maltophilia ATCC 13637 (T)
Xanthomonas ML-122 str. ML-122
Frateuria aurantia IFO 3245 (T)
MFC-C12
MFC-C3
MFC-C1
Desulfotomaculum auripigmentum str. ORex
Desulfosporosinus S8 str.
Desulfitobacterium sp.
MFC-C17
MFC-C7
MFC-C18
Clostridium subterminale ATCC 25774 (T)
Clostridium tetanomorphum str. H1 NCIMB 11547
Clostridium botulinum ATCC 25763 (T)
MFC-C23
MFC-C6
MFC-C11
MFC-C10
MFC-C2
MFC-C8
Clostridium butyricum str. Rowett ATCC 19398 (T)
Clostridium paraputrificum ATCC 25780 (T)
Clostridium tertium ATCC 14573
Clostridium chauvoei ATCC 10092 (T)
MFC-C4
Acidobacterium capsulatum str. 161
MFC-C15
MFC-C13
Meiothermus ruber str.
MFC-C20
Green non-sulfur bacteria
Methanoculleus olentangyi str. RC/ER ATCC 35293 (T)
α - Proteobacteria
δ - Proteobacteria
γ - Proteobacteria
Firmicutes
Fibrobacter & Acidobacterium

The second dominant clone sequences affiliated with δ-*Proteobacteria* from the Library B (MFC-B) were related to the genus *Geobacter* and had a similarity (96-98%) to 16S rRNA genes from a microorganism isolated from surface sediments (*Geobacter* sp.) (Cummings *et al.*, 2000) and sequence identified in Fe(III)-reducing bacteria (*G. metallireducens*) (Nevin and Lovley, 2000; Lovley *et al.*, 1993a) (Figure 3.2). About two-thirds of clone sequences retrieved from the Library C (MFC-C) were dominantly related to the γ-*Proteobacteria* and had high similarity (95-98%) to 16S rRNA genes from *Frateuria aurantia* (Lisdiyanti *et al.*, unpublished data) and Gamma proteobacterium A40-1 (Curtis *et al.*, 2002) isolated from acidic (pH 2.9) soils. Several clone sequences affiliated with *Firmicutes* were related to the genera *Clostridium*, *Desulfosporosinus*, *Desulfitobacterium* and *Desulfotomaculum* (Figure 3.3). One of clone sequences shared with 95% similarity to *Clostridium butyricum* (Park *et al.*, 2001), Fe(III)-reducing bacteria isolated from mediator-less microbial fuel cell.

3.3.2. DGGE analysis of the microbial population in the microbial fuel cell

DNA extracted from the electrode was amplified by PCR using primers for 16S rDNA and the amplicon was compared by DGGE with that of sewage activated sludge used as the inoculum. DGGE profiles of the fuel cell electrode were obtained for each period and revealed that the population of electrochemically active bacteria, associated with generating electricity in the fuel cell, had changed significantly over the 11 months period as it showed quite a different banding pattern (Figure 3.4), suggesting that the electrode contained a different bacterial population from that of the inoculum [sewage activated sludge (lane S) and starch processing activated sludge (lane St)]. Clearly some bacteria had been enriched during the operation of the microbial fuel cell.

The electrode samples and control strains (*E. coli* and *Shewanella putrefaciens* IR1

as an iron reducing organism with electrochemical activity) were subjected to DGGE analysis using a 30-60% denaturing gradient solution. Different polyacrylamide gel percentage by acrylamide/bis mix, varying denaturing gradient solution, electrophoresis running temperature, voltage and time, as well as stain solutions were analysed to determine the optimal DGGE conditions to characterize the microbial populations (Muyzer *et al.*, 1993).

The DGGE profile from the first start-up stage electrode sample (lane S) showed that many different species were presented over the 30-60% denaturing gradient (Figure 3.4). The DGGE patterns from the 6 and 11 months-enriched electrode DNA (lanes 1 and 6) showed about 40 distinguishable bands, which originally derived from bacteria present in sewage activated sludge. The background smear may contain more bands, which are not clearly distinguishable. When comparing the DGGE pattern originating the start-up stage electrode, absent or missing bands can be seen in both lanes. This suggests that aerobic and non-electrochemically active bacteria could be wash out of the electrode during the anaerobic operation.

DGGE with 22 clones from the 11 months enriched electrode was performed and each clone was then matched with the bacterial profile of the PCR product obtained after amplification of the same electrode sample and identified by sequencing clones (Figure 3.5). Each band in the electrophoresis pattern presumably originates from one bacterial species present in the original material. Theoretically, bands at the same position in the electrophoresis pattern contain DNA fragments with identical sequences (Teske *et al.*, 1996). However, this should be confirmed by direct sequencing of the bands. Furthermore, overlapping fragments with different sequences cannot be excluded in DGGE separation patterns derived from complex bacterial populations.

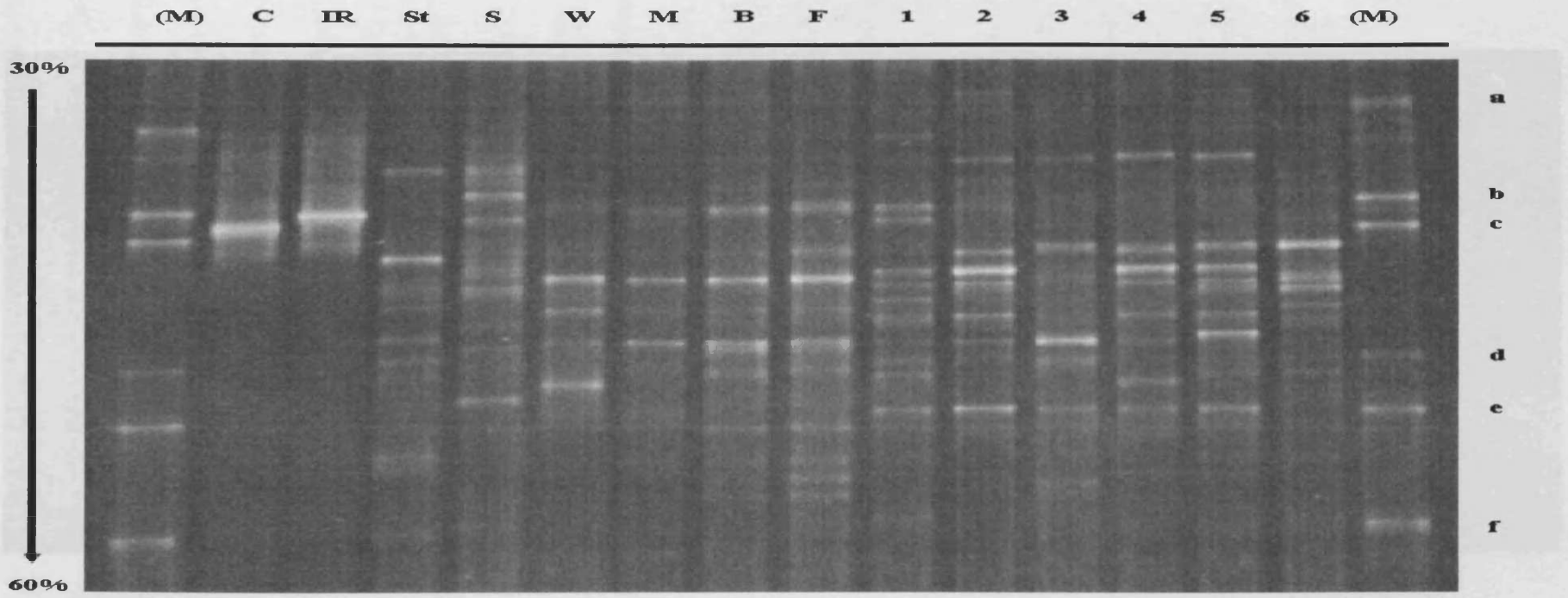

Figure 3.4 DGGE analysis of PCR-amplified 16S rDNA fragments from sewage activated sludge and the enriched electrode. Lane C : *E. coli*, lane IR : *Shewanella putrefaciens* IR1, lane St : starch processing wastewater enriched electrode, lane S : sewage activated sludge (initial operating stage electrode), lane W : planktonic community in the cell, lane M : ion-exchange membrane biofilm, lane B : clump part of electrode, lane F : biofilm part of electrode, lane 1 : 6 months enriched electrode, lane 6 : 11 months enriched electrode, and lanes 2, 3, 4, 5 : each electrode from different microbial fuel cells. Marker lanes labeled "(M)". Marker bands are PCR products from pure cultures isolated from the environment. Species assignment for each band from top to bottom is as follows (a) *Pseudomonas*, (b) *Commamonas*, (c) *Staphylococcus*, (d) *Bacillus*, (e) *Arthrobacter*, (f) *Bacillus*.

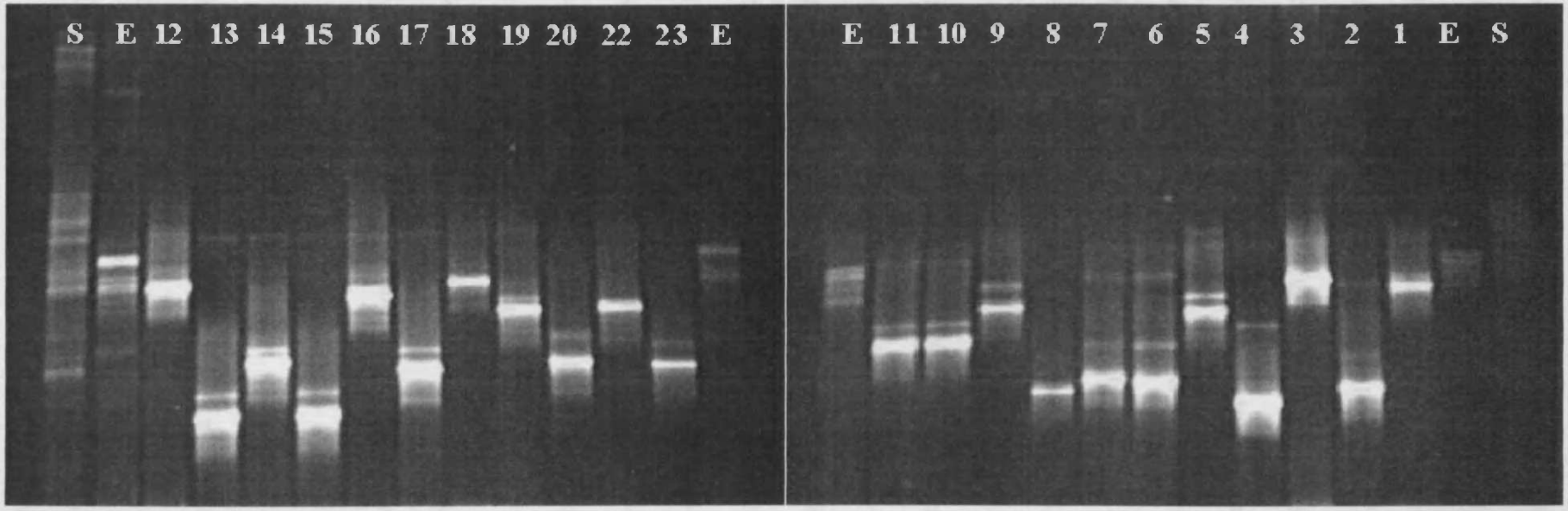

Figure 3.5 DGGE profiles of PCR-amplified 16S rRNA gene sequence from individual clones in the 16S rRNA gene library constructed from the 11 months enriched electrode. The lanes contained DNA template samples as follows: S, original sewage activated sludge; E, 11 months enriched electrode biomass; number (1-23), each clone in the 16S rRNA gene library constructed from the 11 months enriched electrode. The denaturing gradient of the gel is 30% (at the top) to 60% (at the bottom). Gels were stained using SYBR Gold from Molecular Probes.

3.3.3. *In situ* analysis of the enriched electrode sample

Typical microorganisms which constitute activated sludge are thought to be protista and bacteria (Dias and Bhat, 1964). The 6 months enriched electrode sample using activated sludge was first analysed by DAPI staining and *in situ* hybridization, and then the proportion of target species to the total bacteria was quantified. Hybridization with the seven group-specific probes resulted in the straightforward detection of stained individual cells. Signals obtained with all the oligonucleotide probes were strong and indicated high cellular rRNA contents (Figure 3.6). Enumeration of DAPI-stained cells revealed a total cell count of $1.7 \pm 0.3 \times 10^6$ ml^{-1}. 61 ± 4.2% of the cells visualized by DAPI could be detected with the bacterial probe EUB338. 22 ± 1.4% of all DAPI-stained cells hybridized with probe for α-*Proteobacteria* (ALF1b). Other members of the *Proteobacteria* hybridizing with probes for the beta subclass (BET42a) and the gamma subclass (GAM42a) constituted 3 ± 0.6 and 8 ± 2.4% of the cells, respectively. The probe CF319b, specific for most members of the *Bacteroidetes* group, bound to 21 ± 7.7%, and probe HGC906 and LGC354, which is complementary to a 16S rRNA signature of bacteria with a high and low DNA G+C content, bound to 4 ± 1.4 and 12 ± 2.7% of all DAPI-stained cells. The probe PLA46 related to *Planctomycetes* also bound to 1 ± 0.3% of all DAPI-stained cells. The sum of the group-specific counts was, at 71%, higher than the percentage of cells hybridizing with the bacterial probe EUB338 (61%). This might be due to an underestimation of the total cell count as determined by DAPI staining.

Bacteroidetes and α-*Proteobacteria* were the predominant bacterial group present in the enriched electrode sample. Other groups, such as γ-*Proteobacteria*, *Firmicutes* (low G+C DNA content group of Gram positive bacteria), β-*Proteobacteria*, *Actinobacteria* (high G+C DNA content group of Gram positive bacteria) and *Planctomycetes*

constituted smaller fractions. This predominance of *Proteobacteria* in municipal wastewater treatment plants has been reported (Wagner *et al.*, 1993; Manz *et al.*, 1994), but some activated sludge treating industrial or synthetic wastewaters have quite different compositions (Manz *et al.*, 1994) and anaerobic operating condition, resistance and temperature in a microbial fuel cell may affect the bacterial community structures at group level.

We also compared the community structure of the enriched electrode sample as determined by *in situ* hybridization with the composition of the clone library (Figure 3.7). These result shows that the ratio of seven groups against the EUB probe is nearly the same as the composition of the clone library. The *Planctomycetes* showed virtually no hybridization signals with the electrode sample, which is in accordance with 16S rRNA sequences from the clone library.

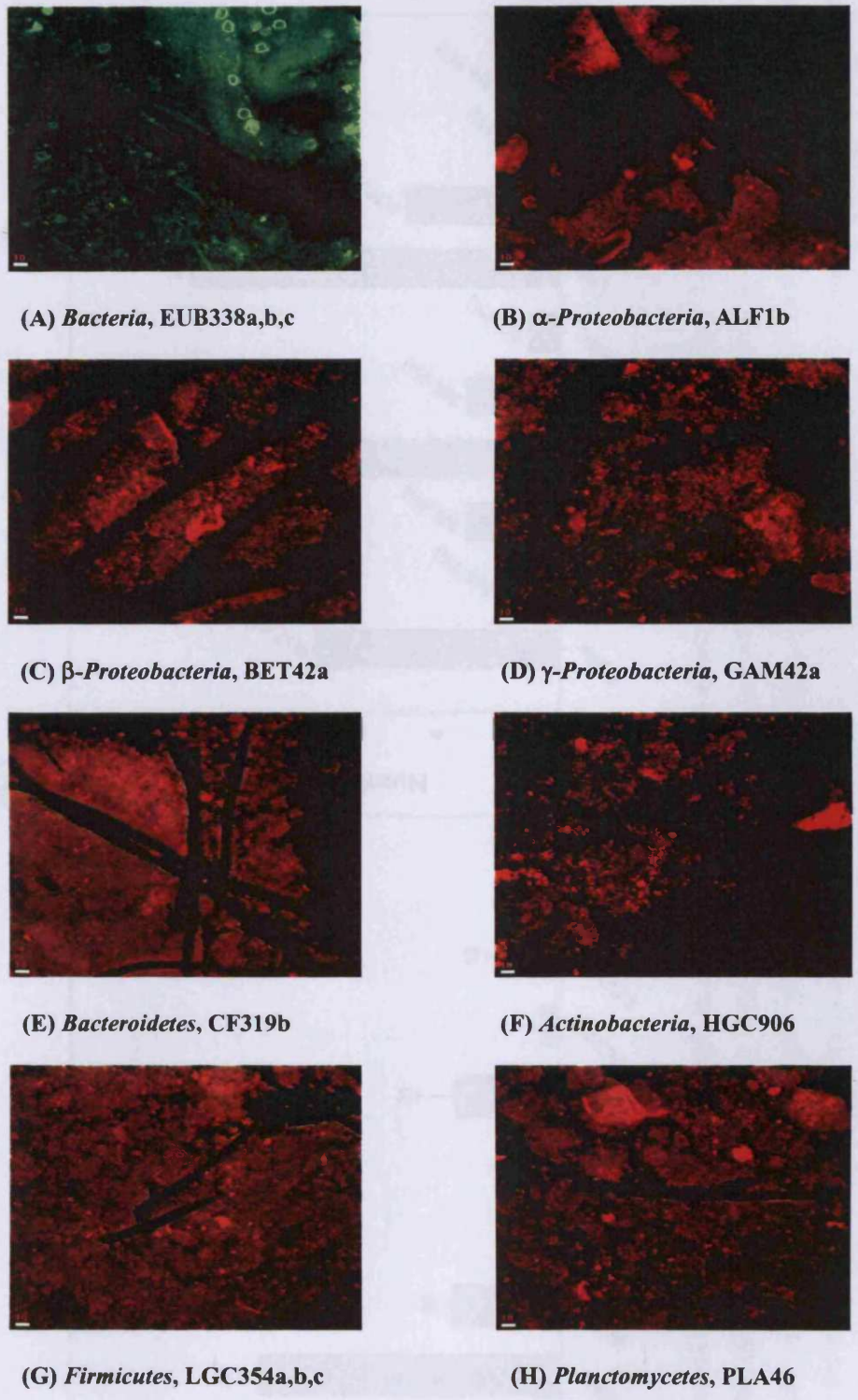

(A) *Bacteria*, EUB338a,b,c

(B) α-*Proteobacteria*, ALF1b

(C) β-*Proteobacteria*, BET42a

(D) γ-*Proteobacteria*, GAM42a

(E) *Bacteroidetes*, CF319b

(F) *Actinobacteria*, HGC906

(G) *Firmicutes*, LGC354a,b,c

(H) *Planctomycetes*, PLA46

Figure 3.6 Micrographs of the enriched electrode after *in situ* hybridization with fluorescently labeled oligonucleotide probes.

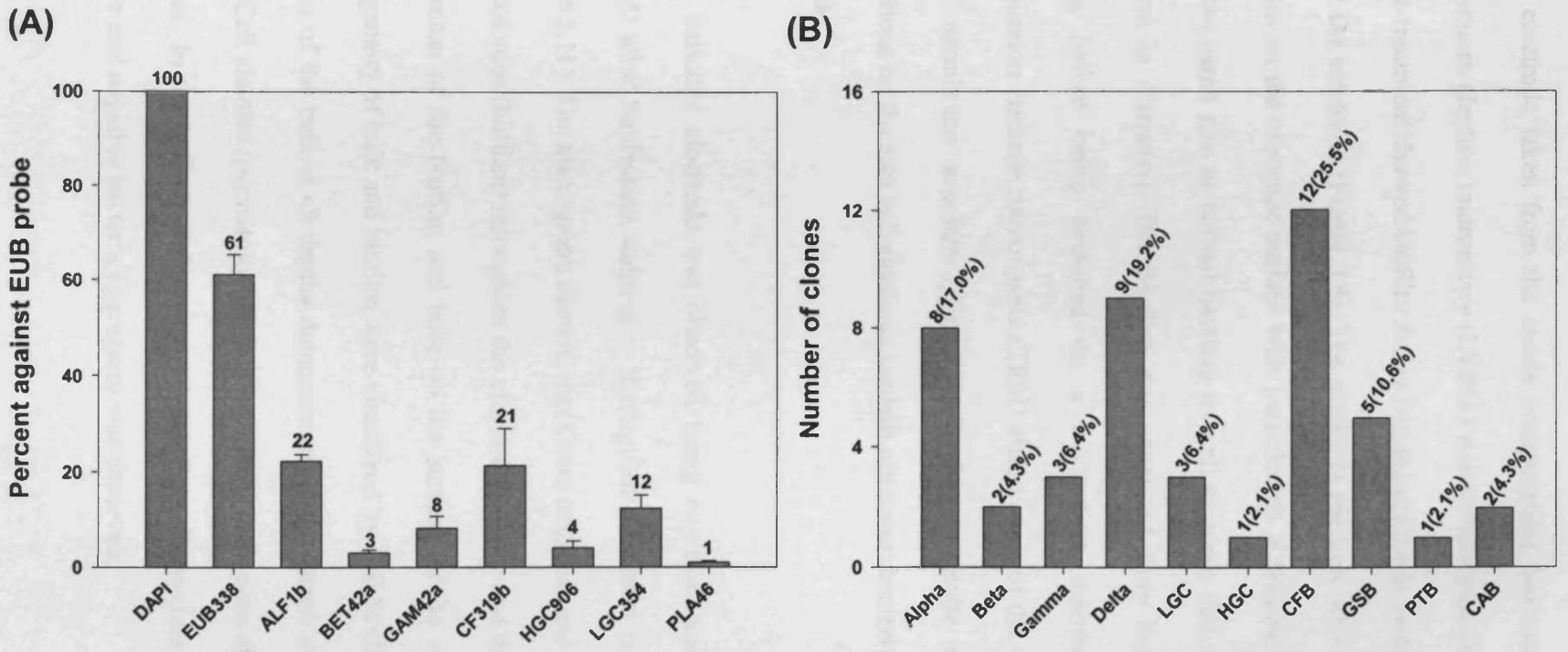

Figure 3.7 Comparison of the community structure in the 6 months enriched electrode sample as determined by *in situ* hybridization and the composition of the clone library. (A) *In situ* hybridization with oligonucleotide probes. The bars represent hybridization percent against the EUB probe. (B) Phylogenetic analysis of the clone library. Alpha: α-*Proteobacteria*, Beta: β-*Proteobacteria*, Gamma: γ-*Proteobacteria*, Delta: δ-*Proteobacteria*, LGC: *Firmicutes* (Gram-positive bacteria with a low DNA G+C content), HGC: *Actinobacteria* (Gram-positive bacteria with a high DNA G+C content), CFB: *Bacteroidetes*, GSB: *Green-sulfur bacteria*, PTB: *Prosthecobacter*, CAB: *Cyanobacteria*. Error bars represent standard deviation (n=2).

3.3.4. Morphological characteristics of biomass enriched on the electrode

The electrode taken from the anode compartment was examined microscopically. Low vacuum electron microscopy (LVEM) which facilitates direct observation without any pre-treatment showed biofilm formed on the electrode surface and clumps scattered around the electrode (Figure 3.8). The scanning electron microscopy (SEM) showed a thin film on the electrode surface with particles on it (Figure 3.9). The particles were about the same size as normal bacteria as well as some that were much smaller (0.2-0.45 μm in diameter). The biofilm was separated from the electrode by vigorous shaking before being collected on a nucleopore membrane filter (0.45 μm). Transmission electron microscopic (TEM) observation of the small particles showed a bilayer membrane structure (Figure 3.10). These results show that the bacterial populations on the fuel cell electrode contain ultramicrobacteria as well as normal sized bacteria.

The enriched electrode was observed using confocal scanning laser microscopy (CSLM) after fluorescent staining to distinguish the Gram reaction of the organisms (Figure 3.11). The micrograph showed that Gram negative and positive bacteria formed microcolonies (biofilm) throughout the electrode surface and the microbial clumps. The distribution of the biofilm and bulk on the surface of the electrode and the spatial heterogeneity of bulk and biofilm were visualized by CSLM (Figure 3.11). Optical thin sections of the bulk at all depths demonstrated the presence of bulk structure (Figure. 3.12). Cell clusters (microcolonies) and individual cells were distributed throughout the structure. In the optical section over 50 μm from the surface of electrode, the Gram positive and negative bacteria aggregates was observed.

(A)

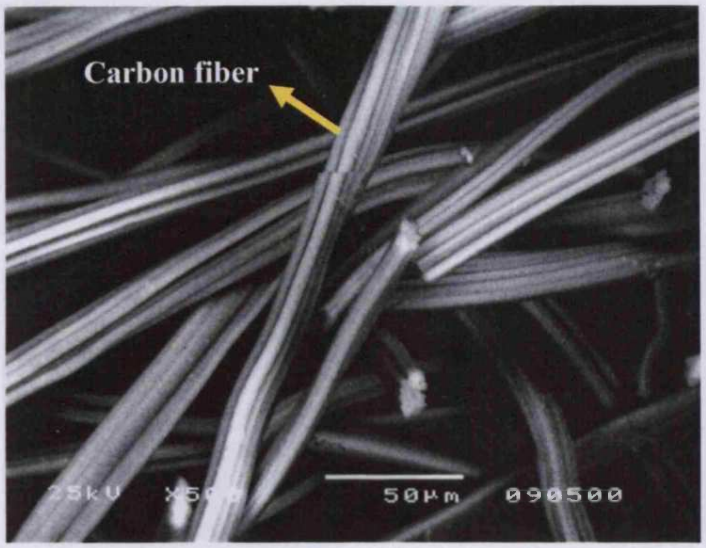

(B)

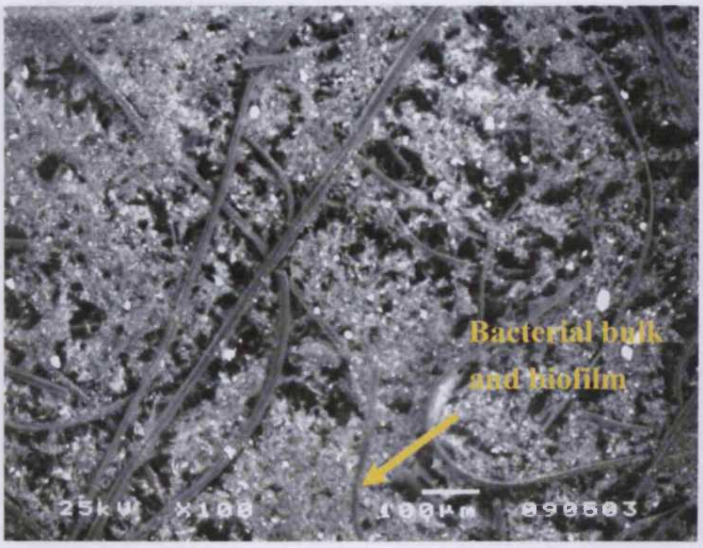

Figure 3.8 Low vacuum electron micrographs (LVEM) of the anode electrode. A) carbon fiber electrode sample, B) sample after enrichment for 6 months showing biofilm and bulk structure formed on the electrode.

(A)

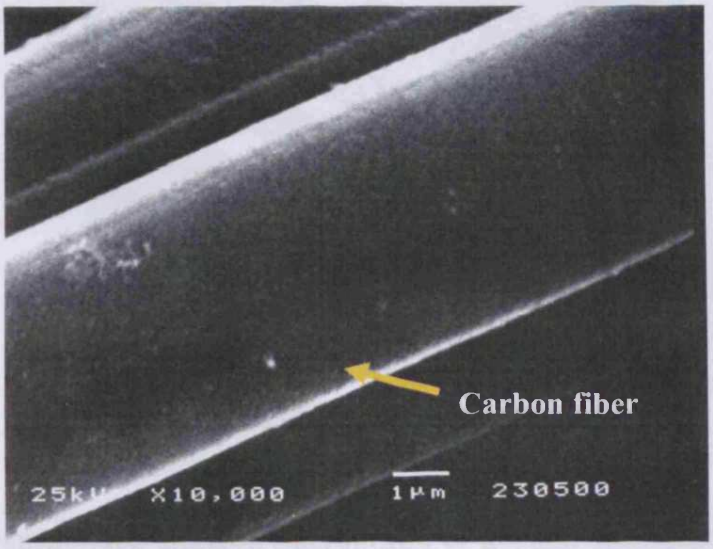

(B)

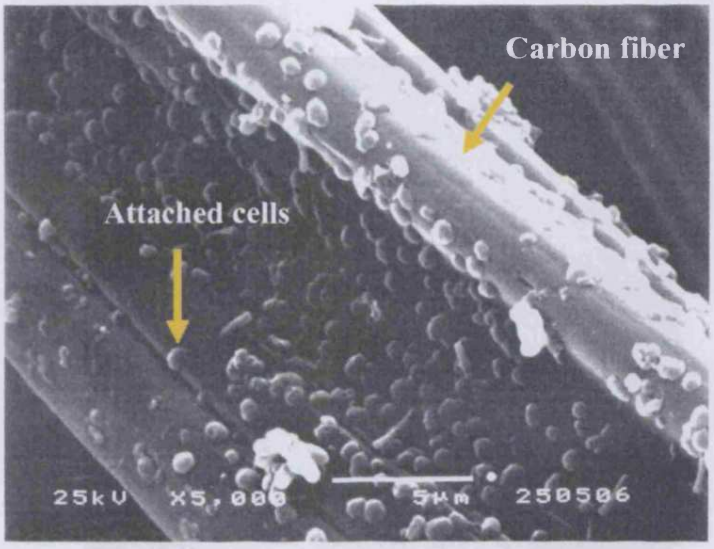

Figure 3.9 Scanning electron micrographs (SEM) of electrode. A) carbon fiber electrode sample before enrichment, B) surface of the enriched electrode with normal and small size bacteria.

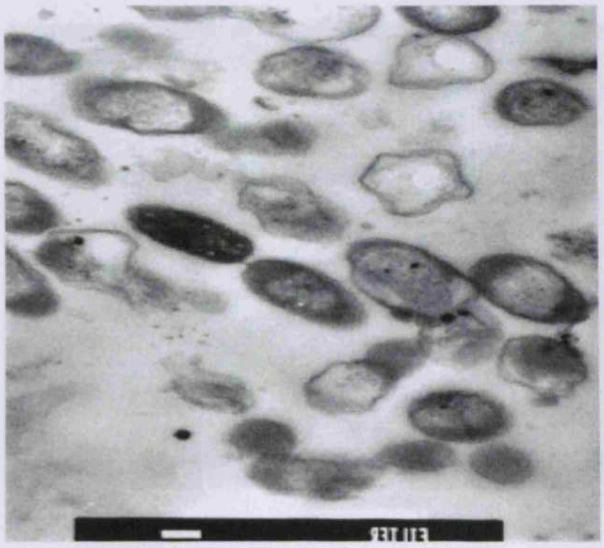

Figure 3.10 Transmission electron micrograph of normal and small size (0.2–0.45 μm in diameter) bacteria on the surface of the electrode. Bar size: 0.1 μm.

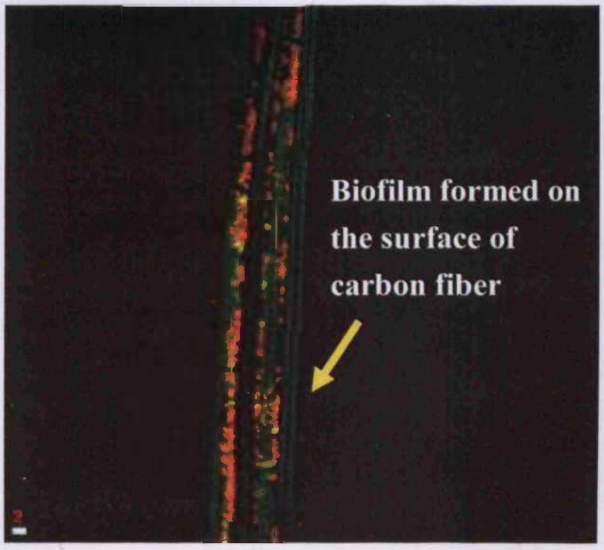

Figure 3.11 Confocal scanning laser micrographs (CSLM) of electrode. The image was showed using by the fluorescent staining to distinguish the Gram staining of the bacteria (red colour: Gram positive bacteria, green colour: Gram negative bacteria). Bar: 2 μm.

Top **bottom (electrode)**

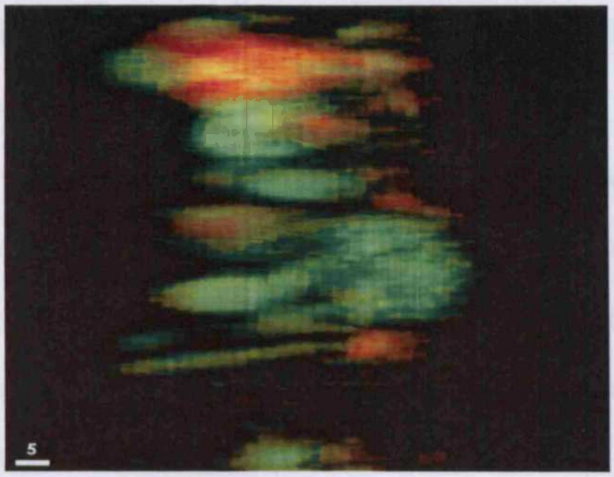

Figure 3.12 CSLM of a bacterial clump which formed on the electrode. The photograph shows that the bacterial bulk and biofilm on the anode electrode consist of bacterial clusters and microcolonies of Gram positive and negative bacteria. Bar: 5 μm.

3.4. Discussion

Microbial communities of a microbial fuel cell biofilm have not been investigated using molecular techniques. Recent studies have shown that a conventional microbiological approach analysing the microbial communities of biofilm is insufficient (Pham *et al.*, 2003; Park *et al.*, 2001). Studies on microbial fuel cells were limited to electricity generation and the metabolic characteristics of the population. As far as we know, there are only a few previous studies that have retrieved 16S rDNA sequences from microbial fuel cell biofilm (Bond *et al.*, 2002; Tender *et al.*, 2002; Kim, 2002). We investigated electrode-reducing microorganisms involved in harvesting energy using molecular techniques, and found that microbial community structure depends on the bacterial source and on the electron donor used in such fuel cells. As discussed below, these findings greatly expand the potential for using microbes to convert organic matter to electricity since previously described microbial fuel cells did not effectively oxidize the organic fuel and most required the addition if electron transfer-mediating compounds.

Clone libraries are an effective way of retrieving bacterial 16S rDNA sequences from a diverse environment, but concern has been expressed over their ability to accurately represent the overall composition of such communities. Problems inherent to the construction of a clone library include: sample handling (Rochelle *et al.*, 1994), biased DNA extraction, differing rRNA gene copy numbers (Farrelly *et al.*, 1995), biased PCR amplification (Reysenbach *et al.*, 1992), chimera formation (Kopczynski *et al.*, 1994), and biased cloning efficiencies for different sequences (Rainey *et al.*, 1994). Sequencing indicated that the DNA extraction method used in this study successfully lysed a wide range of bacteria. In addition, the use of two primer sets, 27F and 1387R

in the PCR amplification from the enriched electrode and 341F and 534R for PCR-DGGE analysis, potentially limited biases associated with FISH. Diversity of bacterial sequences within the environment can also be underestimated by the particular methodological approach used and especially by the choice of suitable PCR primers employed (Marchesi *et al.*, 1998; Schmalenberger *et al.*, 2001). Using the computer software PRIMROSE (Ashelford *et al.*, 2002) and OligoCheck in conjunction with the RDP database, it was possible to determine primer coverage as a percentage of the target taxon from relevant sequence information. In this study the primers 27F and 1387R showed 29.8% and 93.6% respectively coverage of *Bacteria*, respectively. The primers for PCR-DGGE analysis were considerably better and matched with 98.5% (341F) and 91.6% (534R) of bacterial 16S rDNA sequences in the database.

Sequencing and FISH of the enriched electrode sample gave very similar results, suggesting that either method was acceptable for predicting division level abundances (Figure 3.7). Partial sequencing of 58 clones and grouping of the entire clone library predicted γ-*Proteobacteria* and *Bacteroidetes* were the most abundant divisions in the clone library, followed by Gram-positive bacteria, α-*Proteobacteria*, *Prosthecobacter*, δ-*Proteobacteria*, *Fibrobacter* and *Acidobacterium*, green-sulfur bacteria, and β-*Proteobacteria* group. This result is different from those of Bond *et al.* (2002), who reported that δ-*Proteobacteria* was the major group in a microbial fuel cell enriched with acetate in sea water. This difference might be due to differences in electron donors used or in the salt concentration. In many environments, especially sewage activated sludge and a variety sediments, many Fe(III)-reducing bacteria with electrochemical activity were found in the gamma and delta subclass of the *Proteobacteria*. These include *Geobacter sulfurreducens* (Bond and Lovley, 2003), *Shewanella putrefaciens* (Nielsen *et al.*, 1997) and *Desulfuromonas acetoxidans* and all these could transfer

electrons to other insoluble electron acceptors, such as Fe(III) oxides (Lonergan *et al.*, 1996). In this study this led to operating the fuel cell with activated sludge and to the enrichment of Fe(III)-reducers with electrochemical activity under the conditions employed for power generation. Finding types of Fe(III)-reducing bacteria with electrochemical activity like the family *Geobacteraceae* in 16S rDNA clone libraries strongly supports this approach (Table 3.3). The rise in *Proteobacteria*, especially γ- and δ-*Proteobacteria* with a concomitant fall in *Bacteroidetes* commonly found in activated sludge suggested that the enriched population might be adapted to optimize energy generation. It was not clear whether the electrochemically active bacteria enriched in the fuel cell were actually Fe(III)-reducers. However, a culture-dependent approach with metabolic activity tests including Fe(III) reduction and cyclic voltammetry might confirm this possibility.

Analysis of the 16S rDNA PCR fragments using DGGE is another valuable analytical method, however selection bias might occur. DGGE as a technique for studying microbial diversity is superior to cloning and subsequent sequencing of PCR amplified rDNA or ribosomal copy DNA fragments. First, it provides an immediate display of the constituents of a population in both a qualitative and a semiquantitative way, and second, it is less time-consuming and laborious (Muyzer *et al.*, 1993). As mentioned above, many factors affect bias in the PCR must be taken into account when analysing DGGE gels. For example, the choice of suitable primers, the efficiency and evenness of amplification of diverse sequences or rRNA gene copy number (Von Wintzingerode *et al.*, 1997). For further characterization of the bands observed, DNA fragments can be excised from the DGGE gel, reamplified, and sequenced directly, without the PCR product being cloned first. Care must be taken because the band may not be a single fragment and if more than one sequence is present poor sequence data

will be the result. Regardless of this weakness, it is a rapid and efficient approach for the analysis of mixed microbial populations from natural environments.

The banding patterns observed in the DGGE gels were complex, indicating the presence of a diverse bacterial community over the sampling time. The number of bands changed between electrodes enriched with artificial wastewater (Figure 3.4; lane S, 1 and 6) and starch processing wastewater (lane St), and between early electrode sample (lane S) and enriched electrodes (lane 1 and 6). It is believed that a number of fermentative bacteria with non-electrochemical activity, present on the surface of the electrode, were washed out during the enrichment process. Those bacteria will be fermented with oxygen, which diffuse through the ion-exchange membrane in the fuel cell. Therefore, electrochemically active bacteria might be firmly attached to anode in the fuel cell. 16S rDNA extracted from initial operating stage electrode produced at least 27 bands, some of which matched those in the 6 and 11 months enriched electrode using artificial wastewater as the fuel. Whilst the bands (lane S) from sewage activated sludge in the early stage electrode were distributed in the middle of the gel, bands (lane 1 and 6) from the adapted electrodes were distributed over a wider range of denaturants. Increase in the band extensity and distinguishment of fragments from the enriched electrode suggested that the selection process has promoted the dominance of certain microbial populations during the process. These results demonstrate that the bacterial population in the fuel cell is significantly different from the early stage electrode and activated sludge used to inoculate the fuel cell. Many bands in the low denaturant region was observed in the enriched electrode. Results with the 16S rDNA clone library (Table 3.4) show that strains with low G+C content appeared during the enrichment process. It would also be interesting to see if gram-positive bacteria with low G+C content are involved in generation of electricity. Park *et al.* (2001) reported that

Clostridium butyricum isolated from a mediator-less microbial fuel cell using starch processing wastewater as the fuel, successfully operated a fuel cell in a pure culture. Sequencing those bands from the DGGE gel might give a more reliable assessment of the microbial community structure in the fuel cell. More bands appeared in the electrode fed with artificial wastewater and sewage activated sludge than in the electrode fed with starch processing wastewater. These results suggest that microbial fuel cells fed with sewage activated sludge contain more fermentative bacteria in addition to the electrochemically active bacteria.

Fluorescently labled oligonucleotide probes were used for the *in situ* enumeration of important phylogenetic groups. The initial *in situ* probing was performed mainly to evaluate in an early stage of the study the representativeness of an rDNA library constructed from the sample examined. As mentioned above, results of 16S rDNA library in comparison with that of the *in situ* probing of the enriched electrode sample showed good agreement (Table 3.7). However, it is obvious that when group-specific probes based on cultured bacteria are used, only those populations that are looked for will be detected. In contrast, if it is assumed that the primers used for PCR are fairly general, rDNA libraries should not be biased towards known groups since they rely on direct rRNA gene retrieval (Snaidr *et al.*, 1997). With FISH on the enriched electrode, 61% of total microorganisms (stained with DAPI) were detectable with bacterial probe Eub338. This value might be lower in the old electrode enriched with artificial wastewater. FISH is known to detect only cells with a sufficient number of ribosomes (Amann *et al.*, 1995). Results obtained by DGGE indicated that the composition of the bacterial community on the enriched electrode was relatively stable after 6 months of operation. Therefore, we assume that the enrichment process is mainly driven by multiplication of electrochemically active bacteria and non-electrochemically active

bacteria lose activity with time that they are no longer detectable by FISH.

For the detection of *c*-type cytochromes, which are specifically involved in metal reduction, we designed specific nucleotide primers as named 1501B (Beliaev and Saffarini, 1998; Myers and Myers, 1992). In other studies, several proteins such as MtrA, MtrB and MtrC have been identified that are involved in Fe(III) and Mn(IV) reduction. MtrA is a periplasmic decahaem *c*-type cytochrome that appears to be part of the electron transport chain, which leads to Fe(III) and Mn(IV) reduction. MtrC appears to be required for the activity of the terminal Fe(III) reductase (Beliaev *et al.*, 2001). Though the mechanisms of electron transfer leading to metal reduction are poorly understood, we supposed that the location of Fe(III) reductases on the outer membrane is predicted to be an advantage for metal reducing bacteria and are a way of dealing with insoluble electron acceptors such as the electrode used in this study. However, we failed to amplify *c*-type cytochrome gene from the enriched electrode. Reasons for this failure might be that the primers are only targeted on specific Fe(III)-reducing bacteria such as *Shewanella putrefaciens* or that the proportion of Fe(III)-reducer is low rate in this microbial community.

Electron microscopic observation showed a typical biofilm structure on the electrode surface. Low vacuum electron microscopic observation revealed that the anode retrieved from the enriched fuel cell with artificial wastewater and activated sludge was covered with a thick biofilm, and microbial clumps loosely associated with the electrode. Since electron transfer to the electrode requires direct contact between microbial cells and the electrode, it is plausible that the fermentative bacteria in the clumps convert the complex organic contaminants to simple fatty acids and alcohols which were then used by electrochemically active biofilm bacteria. Scanning electron

micrographs of the electrode showed ultramicrobacterium-like particles in the biofilm formed. The particles were shown to possess bilayer membrane structures by transmission electron microscopy. It is not clear if the ultramicrobacteria represent the resting stage of normal bacteria or vegetative cells of novel bacteria (Kaprelyants *et al.*, 1993). Gram positive and Gram negative bacterial micro-colonies were observed in the biofilm and in microbial clumps under a confocal scanning laser microscope.

In conclusion, I have shown electrochemically active bacteria were enriched from activated sewage sludge taken from an aerobic digester, using artificial wastewater as an electron donor. The microbial diversity of the electrode biofilm was investigated by PCR-DGGE using bacterial 16S rRNA gene fragments and FISH with 8 oligonucleotide probes. A 16S rRNA gene library was also constructed with detailed RFLP and sequence analysis indicating that γ-*Proteobacteria* and *Bacteroidetes* followed by Gram-positive bacteria were the most abundant divisions within the clone library. Electron microscopic observations showed that the electrode had a microbial biofilm attached to its surface along with loosely associated microbial clumps. It was suggested that these microbial clumps consist of fermentative bacteria that ferment the complex fuel into simple fermentation products. These products could then be used as substrates for the electrochemically active bacteria within the biofilm to generate electricity. Based on these findings it is proposed that electrochemically active bacteria are widespread in the fuel cells, and that their electrochemical activity is linked to a form of anaerobic respiration.

CHAPTER IV

Isolation and Taxonomic Characterization of a Novel Fe(III)-Reducing Bacterium with Electrochemical Activity in a Microbial Fuel Cell Biofilm

The work has been preparing in modified form as:

Kim, G.T., Webster, G., Kim, H.J., Kim, B.H., Wimpenny, J.W.T. & Weightman, A.J. (in prep). Bacterial community structure, compartmentalization and activity in a microbial fuel cell biofilm. *Environmental Microbiology*

The partial work related to isolation of Fe(III)-reducing bacteria has been submitted:

Kim, G.T., Hyun, M.S., Chang, I.S., Kim, H.J., Park, H.S., Kim, B.H., Kim, S.D., Wimpenny, J.W.T. & Weightman, A.J. (submitted). Dissimilatory Fe(III) reduction by electrochemically active lactic acid bacterium phylogenetically related to *Enterococcus gallinarum* isolated from submerged soil. *Journal of Applied Microbiology*

4.1. Introduction

A microbial fuel cell is an electrochemical device that converts chemical energy to electrical energy with the aid of the catalytic activity of electrochemically active microorganisms (Kim *et al.*, 2002). Several electron-transfer mediators have been used to facilitate electron transfer between an electrode and electrochemically inactive microorganisms (Kim and Kim, 1988). In contrast mediator-less microbial fuel cells using electrochemically active microorganisms (EAM) can transfer electrons to graphite anodes directly. A similar device was successfully used to enrich a microbial consortium that reduced the chemical oxygen demand (COD) of wastewater collected from a starch-processing plant (Park *et al.*, 2001).

Electrochemical techniques including cyclic voltammetry have been used to characterize redox proteins including cytochromes (Kazlauskaite *et al.*, 1996). In general, bacterial cells are electrochemically inactive as their cell wall structures consist of non-conducting material such as lipid and peptidoglycan. Such cells can be modified with hydrophobic conducting polymers to induce electrochemical activity (Park *et al.*, 1997). An Fe(III)-reducing bacterium *Shewanella putrefaciens* is known to localize the majority of its membrane-bound cytochromes on its outer membrane (Myers and Myers, 1992), which are believed to be involved in the reduction of water-insoluble Fe(III). Intact cells of anaerobically grown *S. putrefaciens* were electrochemically active (Kim *et al.*, 1999b) and the bacterium could grow on lactate in a fuel cell-type of electrochemical cell without added electron acceptor (Kim *et al.*, 1999).

Iron is universally present in most ecosystems, and the microbial reduction of Fe(III)

plays an important role in the biogeochemistry of these systems. Many microorganisms are able to conserve energy for growth by coupling the oxidation of organic acids, aromatic hydrocarbons and H_2 to Fe(III) reduction, e.g., fermentative bacteria and some sulphate reducers (Nielsen *et al.*, 2002). These include species of the genera *Geobacter* (Lovley *et al.*, 1993a; Caccavo *et al.*, 1996a), *Shewanella* (Lovley *et al.*, 1989b; Hyun *et al.*, 1999) and a sulphate reducing bacterium, *Desulfotomacum reducens* (Tebo and Obraztsova, 1998). The enterobacterium, *Klebsiella oxytoca*, isolated from sediments under an iron mat, catalyze oxidation of Fe(II) in acidic and near-neutral solutions to produce iron hydroxides (Baldi *et al.*, 2001). In the metabolism of a photosynthetic bacterium, *Rhodobacter capsulatus,* Fe(III) acts as an auxiliary oxidant with physiological importance for redox poising under anaerobic photoheterotrophic growth conditions (Dobbin *et al.*, 1996). Recently, a number of Fe(III) reducing bacteria with electrochemical activity were isolated from a microbial fuel cell, e.g., *Clostridium butyricum* (Park *et al.*, 2001) and *Aeromonas hydrophila* (Pham *et al.*, 2003).

For several years, researchers have examined the microbial populations of microbial fuel cell biofilm in order to understand their electrochemical roles (Lee *et al.*, 2003; Tender *et al.*, 2002; Bond *et al.*, 2002). When microbial diversity is studied by conventional microbiological techniques, such as cultivation of bacteria on solid media, these results are quite biased, because a majority of microorganisms are not cultivated. Over the last decade, cultivation-independent methods based on direct PCR amplification and analysis of ribosomal RNA genes have been developed and allowed a more comprehensive analysis of microbial communities in comparison with cultivation based techniques. The amplified fragments of 16S rRNA genes and the analysis of these genes by denaturing gradient gel electrophoreseis (DGGE) and construction of clone libraries, which can be screened by restriction fragments length polymorphism

(RFLP) before sequencing, have been frequently used to examine the microbial diversity of environmental samples and to monitor changes in microbial communities (Muyzer *et al.*, 1993; Lee *et al.*, 2003).

Previous studies on the analysis of microbial communities firmly attached to the electrode harvesting electricity from a variety of sediments and activated sludge showed that electricity generation results in specific enrichment of microorganisms in the delta subclasss of the *Proteobacteria* colonizing the anode of the fuel cell (Bond *et al.*, 2002; Lee *et al.*, 2003). They have also suggested that members of the *Geobacteraceae* can use electrodes as terminal electron acceptors for anaerobic respiration. These members were most closely related to Fe(III)- and sulphate-reducing microorganisms noted above. Several microorganisms in the family of *Geobacteraceae* such as *Geobacter sulfurreducens* (Bond and Lovley, 2003) and *Desulfuromonas acetoxidans* (Bond *et al.*, 2002) were successfully used to generate an electrical current. These results clearly show that Fe(III)-reducing microorganisms can be active in microbial fuel cell.

In the present study, the mediator-less microbial fuel cell was used to enrich electrochemically active microbes on artificial wastewater containing glucose and glutamic acid as the electron donor. These cells have been operated for over 18 months. To investigate the specific enrichment of microorganisms in the fuel cell, the microbial community from the anode compartment was characterized using cultivation and cultivation-independent techniques (Figure 4.1). The isolate, WG2, used in this study was one of the colonies which formed on a solid media, with glucose as electron donor and ferric pyrophosphate as electron acceptor. The isolate was classified as a strain of the genus *Klebsiella* which was able to reduce insoluble Fe(III). Cyclic voltammetry

and fuel cell techniques were used to characterize its electrochemical activity of bacterial isolates obtained using this approach.

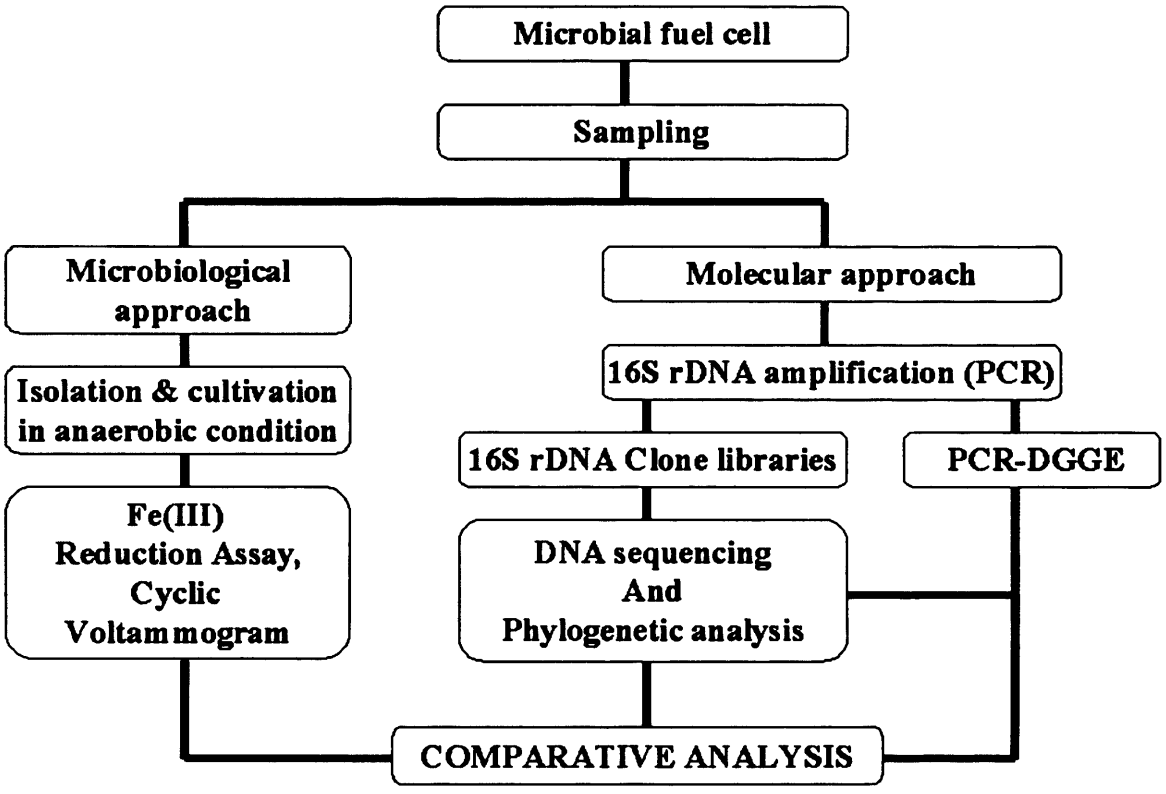

Figure 4.1 A flow diagram illustrating the experimental approach employed in Chapter IV, to investigate and compare the microbial diversity in a fuel cell fed with artificial wastewater for 18 months.

4.2. Materials and methods

4.2.1. Sampling

For the collection of microbial clumps and biofilm from the electrode, the anode (1 cm^2) was collected. It was transferred to a universal tube containing anaerobically prepared 10 ml sterile saline solution. The tube was shaken gently by hand to remove clumps from the electrode before transferring the suspension to a sterile anaerobic universal tube. Fresh saline solution was added to the tube containing the electrode and the latter was shaken vigorously to obtain a suspension of cells from the biofilm. Planktonic community in the anode compartment of the fuel cell and ion exchange membrane biofilm were also collected directly from the same microbial fuel cell (Figure 4.2).

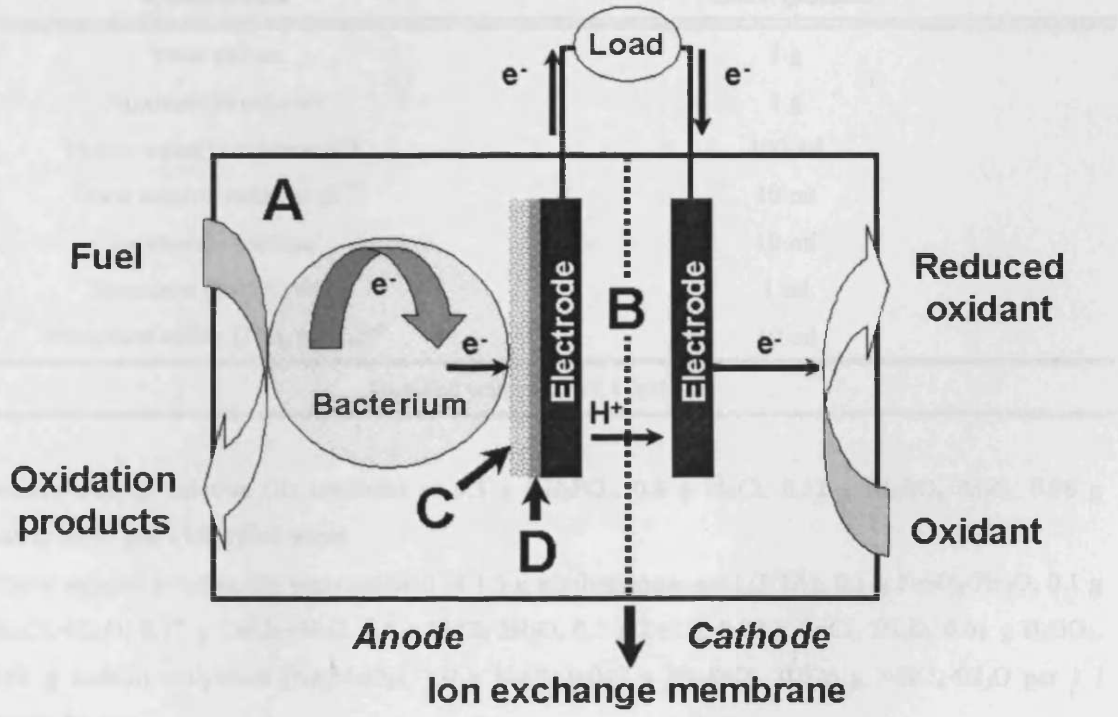

Figure 4.2 The sampling site from the anode part of microbial fuel cell. A) planktonic community in the anode compartment, B) membrane biofilm, C) clump part on the electrode, and D) biofilm part on the electrode.

4.2.2. Mediator-less microbial fuel cell and enrichment

The method for construction and operation of mediator-less microbial fuel cells is described in Chapter II. They were inoculated with activated sludge collected from Ponthir sewage treatment works (Gwent, UK) and fed continuously with artificial wastewater containing glucose and glutamate. The operational conditions optimized in Chapter II were used for all experiments in Chapter IV. The cell suspension was fed with PBBM (Table 4.1) containing 10 mM glucose (Schink and Bomar, 1992). The cell was connected through a resistance of 1 KΩ to measure the potential drop between the anode and cathode as current.

Table 4.1 The composition of phosphate-buffered basal medium (PBBM).

Components	PBBM medium
Yeast extract	1 g
Ammonium chloride	1 g
Macro-mineral solution (II)[a]	100 ml
Trace mineral solution (II)[b]	10 ml
1× vitamin solution[c]	10 ml
Resazurin (0.02%, w/v)	1 ml
Phosphate buffer (1 M, pH 7.2)[d]	10 ml
Distilled water up to 1 l (pH 7.2)	

[a]Macro-mineral solution (II) consisted of 0.3 g KH_2PO_4, 0.6 g NaCl, 0.12 g $MgSO_4 \cdot 7H_2O$, 0.08 g $CaCl_2 \cdot 2H_2O$ per 1 l distilled water.

[b]Trace mineral solution (II) was consisted of 1.5 g nitrilotriacetic acid (NTA), 0.1 g $FeSO_4 \cdot 7H_2O$, 0.1 g $MnCl_2 \cdot 4H_2O$, 0.17 g $CoCl_2 \cdot 6H_2O$, 0.1 g $CaCl_2 \cdot 2H_2O$, 0.1 g $ZnCl_2$, 0.02 g $CuCl_2 \cdot 2H_2O$, 0.01 g H_3BO_3, 0.01 g sodium molybdate (Na_2MoO_3), 1.0 g NaCl, 0.017 g Na_2SeO_3, 0.026 g $NiSO_4 \cdot 6H_2O$ per 1 l distilled water.

[c]1× vitamin solution was consisted of 0.002 g biotin, 0.002 g folic acid, 0.010 g B6 (pyridoxine HCl), 0.005 g B1 (thiamine HCl), 0.005 g B2 (riboflavin), 0.005 g nicotinic acid (niacin), 0.005 g pantothenic acid, 0.0001 g B12 (cyanocobalamin) crystalline, 0.005 g PABA (*p*-aminobenzoic acid), 0.005 g lipoic acid (thioctic) per 1 l distilled water.

[d]1 M phosphate buffer consisted of 136.09 g KH_2PO_4, 358.14 g K_2HPO_4 per 1 l distilled water.

4.2.3. DNA extraction

Total chromosomal DNA was extracted from the planktonic community and membrane biofilm as well as the clump and biofilm part of the anode from a fuel cell fed with artificial wastewater containing glucose and glutamate. Extraction procedures were carried out as described in Chapter III. A freeze-thaw DNA extraction method was also used for the isolates (McCaig *et al.*, 1994). 1 ml of culture was centrifuged at 13,000 r.p.m. for 5 min and it was added 100 µl of 5% (w/v) Chelex 100 (Bio-Rad, Hercules, CA, U.S.A.) before the precipitate was resuspended. Tubes were boiled for 5 min and then placed on ice for 5 min. This was repeated twice before centrifuging the cells for another 5 min. To quantify DNA yield, extracts were examined by agarose (1.2% w/v) gel electrophoresis, stained with 0.5 µg ml^{-1} ethidium bromide and compared to a HyperLadder I DNA quantification marker (Bioline, London, UK).

4.2.4. PCR amplification of 16S rDNA gene sequences

Amplification of 16S rDNA genes from the extracted DNA was performed using the following primer combinations in a nested PCR with 27F-1492R (5'-GGTTACCTTGTTACGACT T-3') (DeLong, 1992) and GC-341F-534R (Rölleke *et al.*, 1996). Primary amplification reactions (27F-1492R) were performed with 20 pmol $µl^{-1}$ of primers, 1 µl of DNA template, 1× reaction buffer (Bioline), 1.5 mM $MgCl_2$, 1 U Biotaq DNA polymerase (Bioline), 250 µM each dNTP in a 50-µl PCR reaction mixture with molecular grade water. Reaction mixtures were held at 95℃ for 2 min followed by 30 cycles of 94℃ for 30 s, 52℃ for 30 s and 72℃ for 90 s plus 1 s per cycle, with a final extension step of 5 min at 72℃. The secondary (nested) PCR amplification step (GC-341F-534R) for the diversity analysis using DGGE was carried out as described in Chapter III. Primers used in this study were analysed using PRIMROSE version 1.1.3. (Ashelford *et al.*, 2002) and OligoCheck computer

softwares to check the coverage of the primer within the bacterial domain of the RDP database (release 8.1), Ribosomal Project-II (http://www.rdp.cme.msu.edu/).

4.2.5. 16S rDNA gene sequencing and phylogenetic analysis

Amplicons generated using the primer pair 27F-1492R were cloned using pCR®2.1-TOPO® vector (Invitrogen, Groningen, The Netherlands) and transformed into chemically competent TOP10 One Shot® *E. coli* (Invitrogen). The transformed culture was plated on LB agar medium containing 50 μg ml^{-1} kanamycin and 50 mg ml^{-1} X-gal. Kanamycin-resistant and β-galactosidase-negative clones were transferred to a liquid medium of the same composition. Plasmids were purified by the Wizard® *Plus* SV Minipreps DNA purification systems (Promega) and analysed for RFLP using enzyme pairs (*RsaI*/*CfoI*) to select different clones. Selected clones were sequenced with 27F-1492R primers using an ABI PRISM 3100-Genetic Analyzer (Applied Bio-systems, Foster City, CA, U.S.A.). Partial 16S rDNA sequences were subjected to a NCBI BLASTN (http://www.ncbi.nlm.nih.gov/blast/) search to identify sequences with highest similarity and compared for chimera formation with Check_Chimera software of the Ribosomal Database Project (RDP) II. Clone 16S rDNA sequences, their closest relatives identified from database searches, and appropriate type strain sequences were aligned with CLUSTAL W (Thompson *et al.*, 1994). Reference sequences were obtained from the RDP Select_Sequence function and the GenBank database. Evolutionary distances were calculated by the method of Jukes and Cantor (Jukes and Cantor, 1969). Phylogenetic trees were constructed by the neighbor-joining method with TREECON for Windows (van de Peer and Wachter, 1994), including bootstrap analysis (Felsenstein, 1985).

4.2.6. DGGE analysis of bacterial diversity

DGGE was carried out on the nested PCR products to check for bacterial diversity as previously described (Schäfer and Muyzer, 2000; Webster *et al.*, 2002). PCR products were separated using 8% (w/v) polyacrylamide gels with a denaturant gradient between 30% and 60%. One hundred percent denaturing conditions are defined as 7 M urea and 40% (v/v) formamide. Gels were poured with the aid of a 50 ml volume Gradient Mixer (Fisher Scientific, Loughborough, UK) and electrophoresis done at 200 V for 5 h at 60℃. Polyacrylamide gels were stained with SYBRGold nucleic acid gel stain (Molecular Probes, Leiden, The Netherlands) for 30 min and viewed under UV. Gel images were captured with a Gene Genius Bio Imaging System (Syngene, Cambridge, UK). For further characterization of the DGGE bands observed, excised DGGE bands were re-amplified by PCR, confirmed by DGGE and the re-amplified products sequenced directly with 341F or 534R primer.

4.2.7. Isolation of the Fe(III)-reducing bacteria

The bacterial strains used in the study were isolated from the anode biofilm (Figure 4.1). A piece (1 cm^2) of anode electrode (50×50×3 mm^3 in dimension, Graphite felt, GF series, Electrosynthesis, Amherst, NY, U.S.A.) was transferred to a universal tube containing 10 ml sterile anaerobic saline solution and shaken vigorously to separate microbial cells from the biofilm. The suspension was serially diluted and plated on PBBM (Schink and Bomar, 1992) containing 10 mM glucose and 20 mM ferric pyrophosphate as electron donor and acceptor in a MACS anaerobic workstation (Don Whitley Scientific Limited, UK). Colonies which appeared on the plate were isolated to test their Fe(III)-reducing activities. Some colonies formed haloes around them on the plate, due to Fe(III) reduction (Coates *et al.*, 1996).

4.2.8. Culture conditions of the bacterial isolate

Anaerobic techniques were used throughout the study (Hungate, 1969). The PBBM was used to cultivate and maintain the culture (Table 4.1). The medium was anaerobically dispensed into pressure tubes (2.5×15 cm, Bellco Glass Inc.) or serum vials (160 ml, Wheaton Scientific Co., Millville, NJ, U.S.A.) which were stoppered with butyl rubber bungs (Bellco Glass Inc.) and crimped with aluminum caps. Solid medium was prepared by adding 2% agar to PBBM. Glucose was used as an electron donor at a final concentration of 5-10 mM with or without an electron acceptor. Amorphous ferric oxyhydroxide [Fe(O)OH] was prepared according to McLaughlin *et al.* (1981) and added as an electron acceptor (10 g l^{-1}) to the medium. Ferric citrate or ferric pyrophosphate were used as a soluble Fe(III) to prepare solid medium. Luria-Bertani (LB) medium was used for cultivation and maintenance of the isolate under anaerobic conditions. All cultures were prepared and inoculated at 30℃.

4.2.9. Morphological characterization of the bacterial isolates

A light microscope (A Vickers Instrument, UK) was used to determine the Gram reaction (Harold, 1994). Grown cells in LB medium for 24 h were stained with crystal violet and then treated with an iodine solution as a mordant. The intensely stained cells were then washed with ethanol. In order to make the contrast between the two obvious results (Gram positive and negative), the preparation was counterstained with a contrasting red dye, safranin O. The stained cells were observed by light microscope with *Bacillus* sp. and *E. coli* as Gram positive and negative control strains, respectively. A non-staining method was also used to determine Gram reaction (Buck, 1982).

4.2.10. Total culturable counts

The total number of culturable bacteria was calculated by a colony forming unit

(CFU) method (Hanson, 1994). PBBM containing 20 mM ferric pyrophosphate was used for colony counts and 10 mM glucose, 20 mM lactate and 20 mM acetate respectively were added as electron donor. A piece of the electrode taken from the fuel cell enriched for 18 months was placed in a universal tube containing anaerobically prepared 10 ml sterile saline solution. The tube was shaken gently by hand to remove clumps from the electrode shown in Figure 3.9(B) before the suspension was transferred to a sterile anaerobic universal tube. Fresh saline solution was added to the tube containing the electrode and the latter was shaken vigorously to obtain a suspension of cells from the biofilm. Suspensions were diluted serially to count the colony forming units on PBBM plates with or without ferric pyrophosphate as electron acceptor. Planktonic community in the anode compartment of the fuel cell and ion exchange membrane biofilm were transferred directly to a sterile anaerobic saline solution for counting the colony forming units on PBBM plates. 100 µl aliquots of each sample were spread onto PBBM. The plates were incubated at 30℃ for 7 days, and colonies were counted every 48 h.

4.2.11. Cyclic voltammetry testing

Bacterial cells grown in LB medium containing 20 mM ferric citrate for 72 h under anaerobic conditions were harvested, washed three times and suspended in 50 mM anaerobic phosphate buffer containing 100 mM NaCl (Kim *et al.*, 1999b). The cyclic voltammograms of the cell suspensions were obtained using a potentiostat (CV-50W, BAS, West Lafayette, IN, U.S.A.) interfaced to a personal computer with the software supplied by the manufacturer (Park *et al.*, 2001). A glassy carbon working electrode (2 mm diameter, MF-2012, BAS), a platinum counter electrode (MW-4130, BAS), and an Ag/AgCl reference electrode (MF-2052, BAS) were used in an electrochemical cell with a working volume of 5 ml. The working electrode was polished with aluminium-

water slurry on cotton wool before each measurement. Oxygen-free nitrogen was gassed through the cell for 10 min before measurements. The scan rate of 100 mV s^{-1} was employed over the range from 0.8 to –0.8 V.

4.2.12. Chemical analyses

Fe(III) reduction was monitored spectrophotometrically by ferrozine assay of HCl-extractable Fe(II) (Phillips and Lovley, 1987). 0.5 ml of culture was mixed with 1 ml of HCl solution (0.5 N), and was incubated for 15 min at room temperature before being centrifuged (10,000 r.p.m., for 5 min). 1 ml of supernatant and 1 ml of ferrozine solution [1 g l^{-1} in 50 mM HEPES buffer (pH 7.0)] was reacted for 15 min before the optical density was read at 562 nm. Fresh medium was used as a control instead of culture. The Fe(III) reduction was calculated using a previously derived Fe(II) concentration versus optical density calibration curve. Ferrous ethylenediammonium sulfate tetrahydrate ($C_2H_{10}N_2O_4SFeSO_4 \cdot 4H_2O$, Fluka Chemie AG, Switzerland) was used as standard Fe(II). Glucose was quantified using a PGO-enzymatic glucose kit (Young-dong Pharm. Co., Seoul, Korea).

4.3. Results

4.3.1. 16S rRNA gene library construction

16S rDNA clone libraries were constructed containing a total of 301 clones from the planktonic community in the fuel cell (MFC-D), ion exchange membrane biofilm (MFC-E), the bacterial clump part of the electrode (MFC-F), and the electrode biofilm (MFC-G). Library D (MFC-D) contained 71 clones and was constructed using primers 27F and 1492R, while Library E (MFC-E) contained 72 clones, Library F (MFC-F) 80 and Library G (MFC-G) 78 clones were made with the same primers.

4.3.1.1. 16S rRNA gene libraries obtained from the fuel cell

In four clone libraries, 110 clones were selected for partial sequencing and phylogenetic analysis. Partial sequence length ranged from 1072 to 1371 bp (median 1222 bp; 100% > 800 bp). All sequences were submitted to a RDP Sequence_Match query and a GenBank BLAST search to find their closest matches in the databases, and no chimeric sequences were found among the clones from MFC-D to MFC-G. Non-chimeric sequences were then used in the construction of phylogenetic trees. A comparison of the bacterial community structure in the fuel cell fed with artificial wastewater for 18 months is shown in Figure 4.3.

In Library D (MFC-D) from the planktonic community in the fuel cell, *Bacterioidetes* phylotypes constituted the most abundant phylum with 49.3% (35/71) of the sequenced clones, followed by 25.3% (18/71) *Spirochaetes*, 18.3% (13/71) β-*Proteobacteria*, 5.6% (4/71) *Firmicutes* and 1.4% (1/71) γ-*Proteobacteria* (Table 4.2; Figure 4.4). Four of the nine sequenced *Bacteroidetes* clones clustered in the RDP *Porphyromonadaceae* family group, four sequences clustered in the RDP

Bacteroidaceae family and one sequence had its highest match in the RDP *Flavobacteriaceae* family. Six *Spirochaetes* related sequences belonged to the RDP designated family *Spirochaetaceae*. Four of the five sequenced β-*Proteobacteria* clones clustered in the RDP *Rhodocyclaceae* family and one sequence had a highest match in the RDP *Comamonadaceae* family. Three *Firmicutes* related sequences belonged to the RDP *Peptococcaceae* family and one γ-*Proteobacteria* related sequence to the RDP *Xanthomonadaceae* family.

In Library E (MFC-E) from ion exchange membrane biofilm in the fuel cell, *Firmicutes* was the most abundant phylum with 45.8% (33/72) of the sequenced clones, followed by 19.4% (14/72) *Bacteroidetes*, 19.4% (14/72) β-*Proteobacteria*, 8.3% (6/72) α-*Proteobacteria*, 5.6% (4/72) γ-*Proteobacteria* and 1.4% (1/72) *Planctomycetes* (Table 4.3; Figure 4.5). Six *Firmicutes* related sequences belonged to the RDP *Clostridiaceae* family. Of the five *Bacteroidetes* related sequences, two belonged to the RDP designated family *Porphyromonadaceae*, two to *Flavobacteriaceae* and one to *Flexibacteraceae*. Eight β-*Proteobacteria* related sequences belonged to the RDP *Rhodocyclaceae* family. Four α-*Proteobacteria* related sequences belonged to the RDP *Sphingomonadaceae* (two sequences), *Rhodospirillaceae* (one sequence) and *Brucellaceae* (one sequence), respectively. Of the three γ-*Proteobacteria* related sequences, one sequence belonged to the RDP *Methylococcaceae* family, another to *Pseudomonadaceae*, and the other to *Xanthomonadaceae*. One *Planctomycetes* related sequence belonged to the RDP *Planctomycetaceae* family group.

In Library F (MFC-F) from bacterial clumps from the electrode fed with artificial wastewater for 18 months, *Bacteroidetes* was the most abundant phylum with 32.5%

(26/80) of the sequenced clones, followed by 27.5% (22/80) β-*Proteobacteria*, 15.0% (12/80) γ-*Proteobacteria*, 7.5% (6/80) α-*Proteobacteria*, 6.3% (5/80) *Acidobacteria*, 5.0% (4/80) *Firmicutes*, 3.8% (3/80) unclassified bacteria and 2.5% (2/80) *Genera_incertae_sedis* "TM7" (Table 4.4; Figure 4.6). Three of the five sequenced *Bacteroidetes* clones clustered in the RDP *Flavobacteriaceae* family, one sequence clustered in *Porphyromonadaceae* family, and the other in *Bacteriodaceae* family. Eleven β-*Proteobacteria* related sequences belonged to the RDP *Rhodocyclaceae* family (seven sequences), *Alcaligenaceae* (one sequence), *Comamonadaceae* (one sequence), *Oxalobacteraceae* (one sequence), and *Genera_incertae_sedis* (one sequence), respectively. Of the four γ-*Proteobacteria* related sequences, two belonged to the RDP *Enterobacteriaceae* family, another one sequence to *Legionellaceae*, and the other to *Xanthomonadaceae*. Three α-*Proteobacteria* related sequences belonged to the RDP *Rhodobacteraceae*, *Brucellaceae*, and *Sphingomonadaceae*, respectively. Three *Firmicutes* related sequences matched most closely to the RDP *Clostridiaceae* family group. One *Acidobacteria* related sequence belonged to the RDP *Acidobacteriaceae* family.

In Library G (MFC-G) from biofilm of the electrode in the fuel cell, *Bacteroidetes* was the most abundant phylum with 29.5% (23/78) of the sequenced clones, followed by 29.5% (23/78) β-*Proteobacteria*, 19.2% (15/78) γ-*Proteobacteria*, 11.5% (9/78) α-*Proteobacteria*, 3.8% (3/78) *Acidobacteria*, 2.6% (2/78) *Firmicutes*, 1.3% (1/78) δ-*Proteobacteria*, 1.3% (1/78) *Genera_incertae_sedis* "TM7" (Hugenholtz *et al.*, 2001) and 1.3% (1/78) unclassified bacteria (Table 4.5; Figure 4.7). Two of the five sequenced *Bacteroidetes* clones clustered in the RDP *Flavobacteriaceae* family, another two sequences clustered in *Flexibacteraceae* family, and the other one in *Porphyromonadaceae* family. Ten β-*Proteobacteria* related sequences belonged to the

RDP *Rhodocyclaceae* family (eight sequences), *Comamonadaceae* (one sequence), and *Burkholderaceae* (one sequence), respectively. Of the four γ-*Proteobacteria* related sequences, two belonged to the RDP *Enterobacteriaceae* family, and another two sequences to *Pseudomonadaceae*. Five α-*Proteobacteria* related sequences belonged to the RDP *Sphingomonadaceae* (two sequences), *Brucellaceae*, and *Methylocystaceae*, respectively. Two *Firmicutes* related sequences matched most closely to the RDP *Clostridiaceae* family group. One *Acidobacteria* related sequence belonged to the RDP *Acidobacteriaceae* family and one δ-*Proteobacteria* to *Desulfovibrionaceae*.

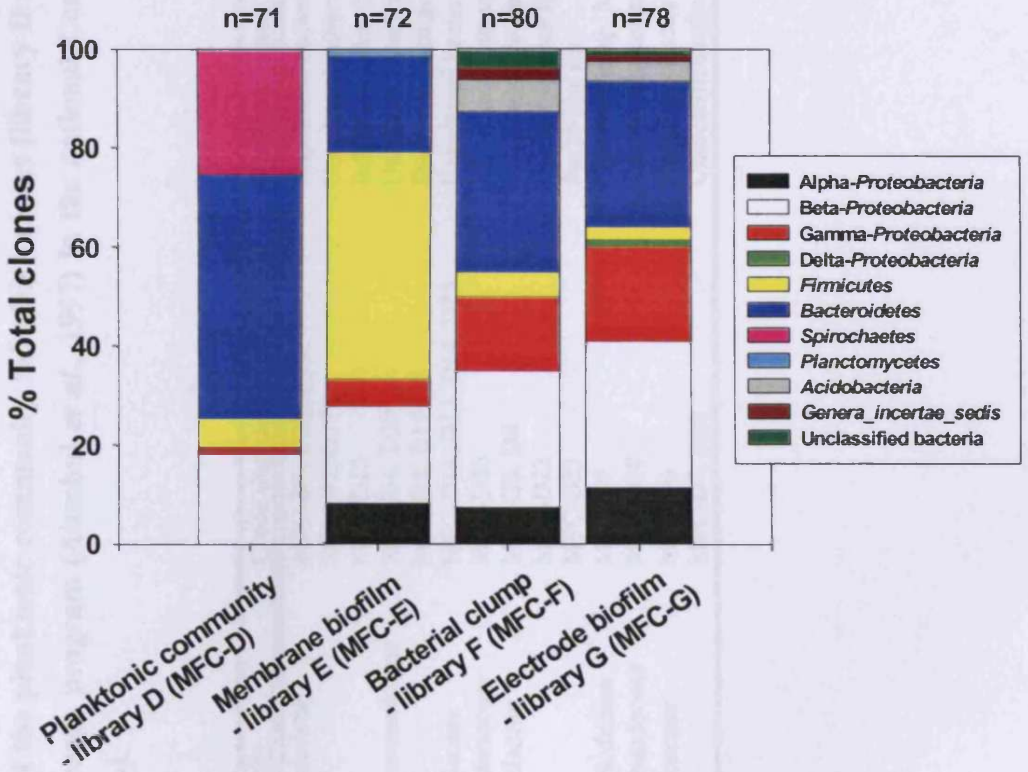

Figure 4.3 Comparison of the bacterial community structure in the fuel cell fed with artificial wastewater for 18 months. 16S rDNA clone library was constructed using primers 27F and 1492R. Composition of the 16S rDNA clone library was estimated by RFLP and partial sequencing of 110/301 clones. N indicated the number of clone in each 16S rDNA clone library.

Table 4.2 Closest matches of the planktonic community 16S rDNA clones [library D (MFC-D)] with sequences in the GenBank database according to the BLAST search program (Altschul *et al.*, 1997) in the national Centre for Biotechnology Information (NCBI) website (*http://www.ncbi.nlm.nih.gov*).

RDP phylum	RDP family	Clone designation (MFC-D)	GenBank closest match	% similarity
Spirochaetes	*Spirochaetaceae*	MFC-D1, D25, D28	Uncultured bacterium SJA-102	94, 95, 95
		MFC-D2, D17	Uncultured eubacterium WCHB1-91	93, 97
		MFC-D13	Sulfate-reducing bacterium F1-7b	97
Bacteroidetes	*Porphyromonadaceae*	MFC-D4, D20	Uncultured Bacteroidetes bacterium clone BIci 17	98, 96
		MFC-D5, D19	*Dysgonomonas gadei* strain 1145589	94, 94
	Bacteroidaceae	MFC-D14, D15, D16, D27	Uncultured bacterium partial 16S rRNA gene clone IIB-27	98, 98, 98, 96
	Flavobacteriaceae	MFC-D26	*Flavobacterium* sp. cpw707	98
β-*Proteobacteria*	*Rhodocyclaceae*	MFC-D3, D8	*Propionivibrio limicola* 16S rRNA gene	94, 96
		MFC-D22	*Dechloromonas* sp.	94
		MFC-D23	*Bacterium* str.	99
	Comamonadaceae	MFC-D9	*Comamonas* sp. MBIC3885 gene	99
γ-*Proteobacteria*	*Xanthomonadaceae*	MFC-D10	*Stenotrophomonas* sp. LMG 19833	99
Firmicutes	*Peptococcaceae*	MFC-D6	Uncultures bacterium partial 16S rRNA gene clone IA-10	98
		MFC-D7, D29	Unidentified eubacterium from anoxic bulk soil clone BSV24	89, 90

Table 4.3 Closest matches of the membrane biofilm 16S rDNA clones [library E (MFC-E)] with sequences in the GenBank database according to the BLAST search program (Altschul *et al.*, 1997) in the national Centre for Biotechnology Information (NCBI) website (*http://www.ncbi.nlm.nih.gov*).

RDP phylum	RDP family	Clone designation (MFC-E)	GenBank closest match	% similarity
Bacteroidetes	*Porphyromonadaceae*	MFC-E16, E33	Uncultured Bacteroidetes bacterium clone BIci 17	99, 98
	Flavobacteriaceae	MFC-E6, E13	*Flavobacterium* sp. cpw707	94, 98
	Flexibacteraceae	MFC-E20	Uncultured eubacterium WCHB1-32	88
α-*Proteobacteria*	*Sphingomonadaceae*	MFC-E12, E18	*Malawimonas jakobiformis* mitochondrial DNA	98, 98
	Rhodospirillaceae	MFC-E22	*Caedibacter caryophila*	93
	Brucellaceae	MFC-E29	Alpha proteobacterium TA12-21	92
β-*Proteobacteria*	*Rhodocyclaceae*	MFC-E10	*Dechlorosoma* sp. Iso1	99
		MFC-E11	*Azonexus fungiphilus*	98
		MFC-E14, E21, E25	*Bacterium* str. 51885	99, 98, 98
		MFC-E19, E31	Uncultured bacterium SJA-10	98, 97
		MFC-E30	*Zoogloea* sp. strain DhA-35	99
γ-*Proteobacteria*	*Methylococcaceae*	MFC-E8	Uncultured bacterium clone HTA4	92
	Pseudomonadaceae	MFC-E17	Uncultured gmma proteobacterium clone 8-10	93
	Xanthomonadaceae	MFC-E26	*Stenotrophomonas maltophilia* strain e-a21	95
Firmicutes	*Clostridiaceae*	MFC-E1, E2, E7, E9	Uncultured Pietermaritzburg bacterium Y14-5	98, 98, 96, 97
		MFC-E4	Unidentified Cytophagales/green sulfur bacterium OPB56	95
		MFC-E23	Unidentified bacterium clone 4955	91
Planctomycetes	*Planctomycetaceae*	MFC-E15	*Planctomyces* sp. strain BD1-23	94

Table 4.4 Closest matches of the bacterial clump 16S rDNA clones [library F (MFC-F)] with sequences in the GenBank database according to the BLAST search program (Altschul *et al.*, 1997) in the national Centre for Biotechnology Information (NCBI) website (*http://www.ncbi.nlm.nih.gov*).

RDP phylum	RDP family	Clone designation (MFC-F)	GenBank closest match	% similarity
Bacteroidetes	*Porphyromonadaceae*	MFC-F4	Uncultured bacterium clone IA-16	91
	Bacteriodaceae	MFC-F16	*Dysgonomonas gadei* strain 1145589	92
	Flavobacteriaceae	MFC-F17	*Flavobacterium* sp. cpw707	95
		MFC-F10, F11	Unidentified Cytophagales/green sulfur bacterium OPB56	88, 89
α-*Proteobacteria*	*Rhodobacteraceae*	MFC-F7	*Achromobacter* sp. LMG5430	93
	Brucellaceae	MFC-F23	*Ochrobactrum* sp. 4FB9	95
	Sphingomonadaceae	MFC-F28	*Malawimonas jakobiformis* mitochondrial DNA	98
β-*Proteobacteria*	*Alcaligenaceae*	MFC-F1	*Alcaligenes* sp.	99
	Genera_incertae_sedis	MFC-F2	*Thiomonas* sp.	95
	Rhodocyclaceae	MFC-F8, F19, F27	*Azonexus fungiphilus*	94, 98, 99
		MFC-F20, F26	*Dechlorosoma* sp. Iso1	99, 93
		MFC-F21	*Bacterium* str. 51885	98
		MFC-F29	*Azoarcus* sp. BS2-3	99
	Comamonadaceae	MFC-F14	*Comamonas* sp. MBIC3885 gene	92
	Oxalobacteraceae	MFC-F15	*Janthinobacterium lividum*	95
γ-*Proteobacteria*	*Legionellaceae*	MFC-F6	*Legionella fairfieldensis*	95
	Xanthomonadaceae	MFC-F13	*Nevskia ramose*	99
	Enterobacteriaceae	MFC-F18	*Klebsiella oxytoca*	95
		MFC-F22	*Klebsiella ornithinolytica*	95
Firmicutes	*Clostridiaceae*	MFC-F5	*Alkalliphilus auruminator*	93
		MFC-F9	Uncultured bacterium mle1-12	91
		MFC-F12	*Clostridiaceae* str. A4d gene	97
Genera_incertae_sedis "TM7"	*TM7*	MFC-F25	Uncultured soil bacterium clone C129	89
Acidobacteria	*Acidobacteriaceae*	MFC-F24	Bacterium species clone Ep_T1.172	92
Unclassified bacteria		MFC-F3	Uncultured Pietermaritzburg bacterium Y14-5	95

Table 4.5 Closest matches of the electrode biofilm 16S rDNA clones [library G (MFC-G)] with sequences in the GenBank database according to the BLAST search program (Altschul *et al.*, 1997) in the national Centre for Biotechnology Information (NCBI) website (*http://www.ncbi.nlm.nih.gov*).

RDP phylum	RDP family	Clone designation (MFC-G)	GenBank closest match	% similarity
Bacteroidetes	*Flavobacteriaceae*	MFC-G1, G18	*Flavobacterium* sp. cpw707	95, 98
	Porphyromonadaceae	MFC-G6	*Dysgonomonas gadei* strain 1145589	91
	Flexibacteraceae	MFC-G32	Uncultured bacterium clone Biai2	93
		MFC-G28	Unidentified Cytophagales/green sulfur bacterium OPB56	88
α-*Proteobacteria*	*Sphingomonadaceae*	MFC-G25, G27	*Malawimonas jakobiformis* mitochondrial DNA	95, 98
		MFC-G26	*Sphingomonas asaccharolytica*	93
	Brucellaceae	MFC-G12	*Ochrobactrum* sp. 4FB9	95
	Methylocystaceae	MFC-G21	*Methylocystis parvus*	94
β-*Proteobacteria*	*Rhodocyclaceae*	MFC-G3, G24	*Azonexus fungiphilus*	98, 99
		MFC-G4, G22	*Dechlorosoma* sp. Iso1	99, 93
		MFC-G5, G16, G20	*Bacterium* str. 51885	98, 98, 98
		MFC-G31	*Azoarcus* sp. BS2-3	99
	Comamonadaceae	MFC-G29	*Acidovorax* sp.	96
	Burkholderiaceae	MFC-G11	*Burkholderia* sp.	96
γ-*Proteobacteria*	*Enterobacteriaceae*	MFC-G2	*Klebsiella oxytoca*	95
		MFC-G7	*Klebsiella ornithinolytica*	95
	Pseudomonadaceae	MFC-G8	Uncultured gamma proteobacterium clone Biyi3	89
		MFC-G30	Gamma proteobacterium WJ2	92
δ-*Proteobacteria*	*Desulfovibrionaceae*	MFC-G17	*Desulfovibrio intestinalis*	95
Firmicutes	*Clostridiaceae*	MFC-G10	Uncultured soil bacterium 480-2	90
		MFC-G23	*Alkalliphilus auruminator*	96
Genera_incertae_sedis "TM7"	*TM7*	MFC-G19	Uncultured soil bacterium clone C129	89
Acidobacteria	*Acidobacteriaceae*	MFC-G15	Bacterium species clone Ep_T1.172	92
Unclassified bacteria		MFC-G13	Unidentified eubacterium clone vadinBA07	90

Figure 4.4 Phylogenetic tree illustrating the relationship between closest relatives in the RDP and GenBank databases for 16S rDNA gene sequences from the planktonic community in the fuel cell. 16S rRNA gene sequences were aligned using CLUSTAL W, and the tree was constructed by the neighbor-joining program from a similarity matrix of pair-wise comparisons made by the Jukes-Cantor algorithm in TREECON. The tree was rooted with the *Euryarchaeota Methanoculleus olentangyi*. Bootstrap values over 70, from 100 replicate trees, are shown at the nodes. The scale bar represents 10% difference in nucleotide sequence.

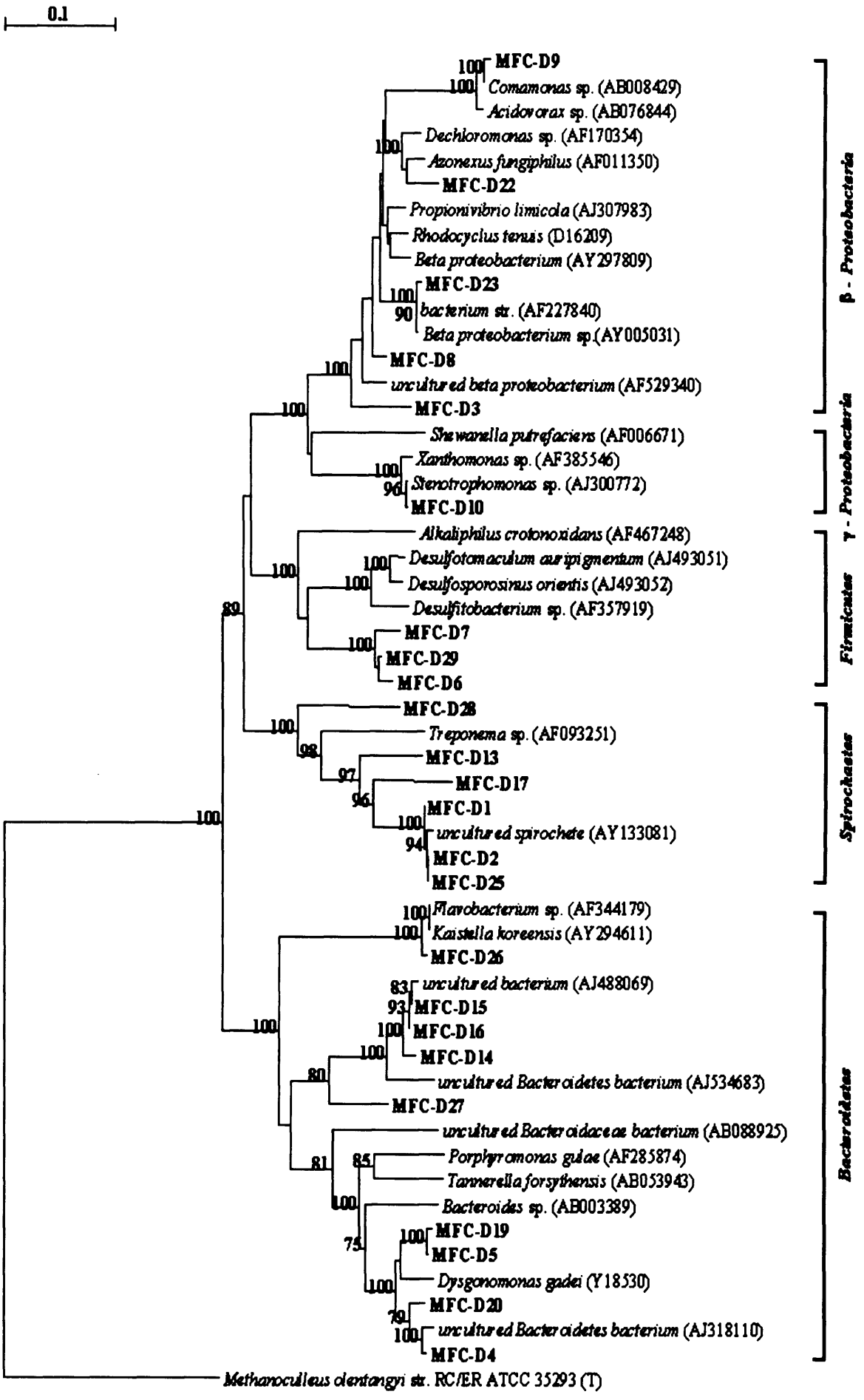
0.1
MFC-D9
Comamonas sp. (AB008429)
Acidovorax sp. (AB076844)
Dechloromonas sp. (AF170354)
Azonexus fungiphilus (AF011350)
MFC-D22
Propionivibrio limicola (AJ307983)
Rhodocyclus tenuis (D16209)
Beta proteobacterium (AY297809)
MFC-D23
bacterium str. (AF227840)
Beta proteobacterium sp (AY005031)
MFC-D8
uncultured beta proteobacterium (AF529340)
MFC-D3
β - Proteobacteria
Shewanella putrefaciens (AF006671)
Xanthomonas sp. (AF385546)
Stenotrophomonas sp. (AJ300772)
MFC-D10
γ - Proteobacteria
Alkaliphilus crotonoxidans (AF467248)
Desulfotomaculum auripigmentum (AJ493051)
Desulfosporosinus orientis (AJ493052)
Desulfitobacterium sp. (AF357919)
MFC-D7
MFC-D29
MFC-D6
Firmicutes
MFC-D28
Treponema sp. (AF093251)
MFC-D13
MFC-D17
MFC-D1
uncultured spirochete (AY133081)
MFC-D2
MFC-D25
Spirochaetes
Flavobacterium sp. (AF344179)
Kaistella koreensis (AY294611)
MFC-D26
uncultured bacterium (AJ488069)
MFC-D15
MFC-D16
MFC-D14
uncultured Bacteroidetes bacterium (AJ534683)
MFC-D27
uncultured Bacteroidaceae bacterium (AB088925)
Porphyromonas gulae (AF285874)
Tannerella forsythensis (AB053943)
Bacteroides sp. (AB003389)
MFC-D19
MFC-D5
Dysgonomonas gadei (Y18530)
MFC-D20
uncultured Bacteroidetes bacterium (AJ318110)
MFC-D4
Bacteroidetes
Methanoculleus olentangyi str. RC/ER ATCC 35293 (T)

Figure 4.5 Phylogenetic tree illustrating the relationship between closest relatives in the RDP and GenBank databases for 16S rDNA gene sequences from ion exchange membrane biofilm. 16S rRNA gene sequences were aligned using CLUSTAL W, and the tree was constructed by the neighbor-joining program from a similarity matrix of pair-wise comparisons made by the Jukes-Cantor algorithm in TREECON. The tree was rooted with the *Euryarchaeota Methanoculleus olentangyi*. Bootstrap values over 70, from 100 replicate trees, are shown at the nodes. The scale bar represents 10% difference in nucleotide sequence.

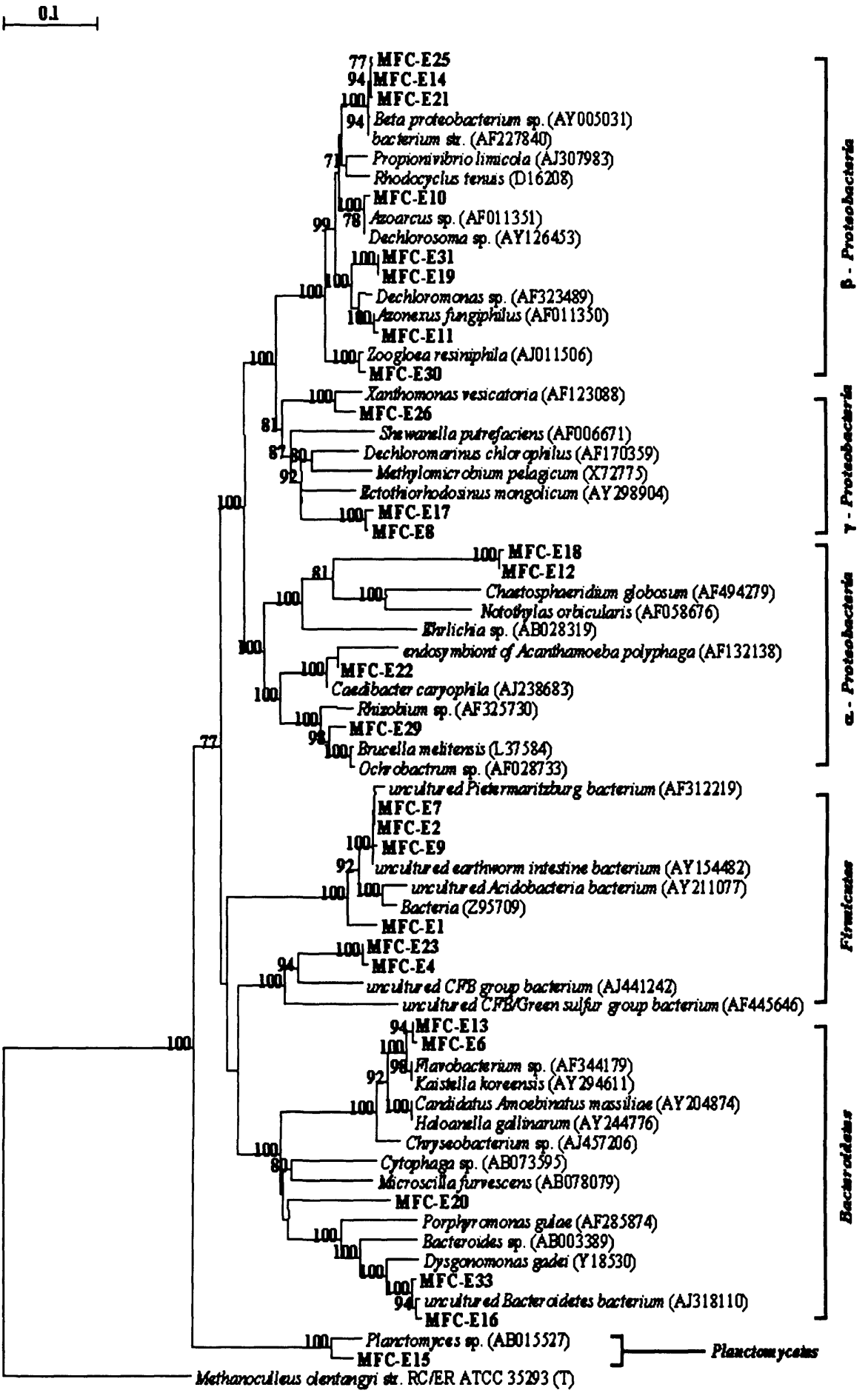
0.1
MFC-E25
MFC-E14
MFC-E21
Beta proteobacterium sp. (AY005031)
bacterium str. (AF227840)
Propionivibrio limicola (AJ307983)
Rhodocyclus tenuis (D16208)
MFC-E10
Azoarcus sp. (AF011351)
Dechlorosoma sp. (AY126453)
MFC-E31
MFC-E19
Dechloromonas sp. (AF323489)
Azonexus fungiphilus (AF011350)
MFC-E11
Zoogloea resiniphila (AJ011506)
MFC-E30
β - Proteobacteria
Xanthomonas vesicatoria (AF123088)
MFC-E26
Shewanella putrefaciens (AF006671)
Dechloromarinus chlorophilus (AF170359)
Methylomicrobium pelagicum (X72775)
Ectothiorhodosinus mongolicum (AY298904)
MFC-E17
MFC-E8
γ - Proteobacteria
MFC-E18
MFC-E12
Chaetosphaeridium globosum (AF494279)
Notothylas orbicularis (AF058676)
Ehrlichia sp. (AB028319)
endosymbiont of Acanthamoeba polyphaga (AF132138)
MFC-E22
Caedibacter caryophila (AJ238683)
Rhizobium sp. (AF325730)
MFC-E29
Brucella melitensis (L37584)
Ochrobactrum sp. (AF028733)
α - Proteobacteria
uncultured Pietermaritzburg bacterium (AF312219)
MFC-E7
MFC-E2
MFC-E9
uncultured earthworm intestine bacterium (AY154482)
uncultured Acidobacteria bacterium (AY211077)
Bacteria (Z95709)
MFC-E1
MFC-E23
MFC-E4
uncultured CFB group bacterium (AJ441242)
uncultured CFB/Green sulfur group bacterium (AF445646)
Firmicutes
MFC-E13
MFC-E6
Flavobacterium sp. (AF344179)
Kaistella koreensis (AY294611)
Candidatus Amoebinatus massiliae (AY204874)
Haloanella gallinarum (AY244776)
Chryseobacterium sp. (AJ457206)
Cytophaga sp. (AB073595)
Microscilla furvescens (AB078079)
MFC-E20
Porphyromonas gulae (AF285874)
Bacteroides sp. (AB003389)
Dysgonomonas gadei (Y18530)
MFC-E33
uncultured Bacteroidetes bacterium (AJ318110)
MFC-E16
Bacteroidetes
Planctomyces sp. (AB015527)
MFC-E15
Planctomycetes
Methanoculleus olentangyi str. RC/ER ATCC 35293 (T)

Figure 4.6 Phylogenetic tree illustrating the relationship between closest relatives in the RDP and GenBank databases for 16S rDNA gene sequences from the bacterial clump part of electrode. 16S rRNA gene sequences were aligned using CLUSTAL W, and the tree was constructed by the neighbor-joining program from a similarity matrix of pair-wise comparisons made by the Jukes-Cantor algorithm in TREECON. The tree was rooted with the *Euryarchaeota Methanoculleus olentangyi*. Bootstrap values over 70, from 100 replicate trees, are shown at the nodes. The scale bar represents 10% difference in nucleotide sequence.

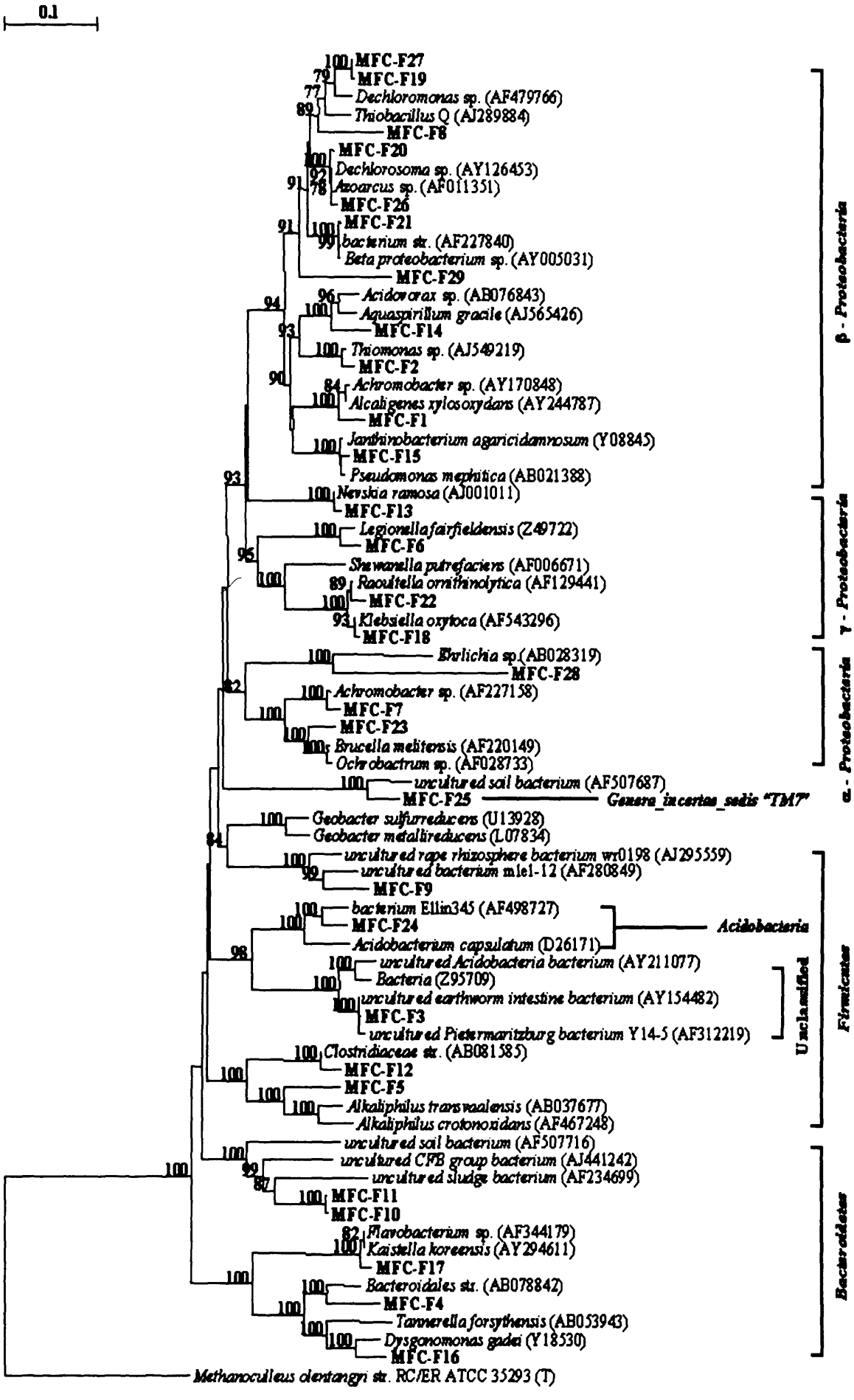
0.1
MFC-F27
MFC-F19
Dechloromonas sp. (AF479766)
Thiobacillus Q (AJ289884)
MFC-F8
MFC-F20
Dechlorosoma sp. (AY126453)
Azoarcus sp. (AF011351)
MFC-F26
MFC-F21
bacterium str. (AF227840)
Beta proteobacterium sp. (AY005031)
MFC-F29
Acidovorax sp. (AB076843)
Aquaspirillum gracile (AJ565426)
MFC-F14
Thiomonas sp. (AJ549219)
MFC-F2
Achromobacter sp. (AY170848)
Alcaligenes xylosoxydans (AY244787)
MFC-F1
Janthinobacterium agaricidamnosum (Y08845)
MFC-F15
Pseudomonas mephitica (AB021388)
Nevskia ramosa (AJ001011)
MFC-F13
Legionella fairfieldensis (Z49722)
MFC-F6
Shewanella putrefaciens (AF006671)
Raoultella ornithinolytica (AF129441)
MFC-F22
Klebsiella oxytoca (AF543296)
MFC-F18
Ehrlichia sp. (AB028319)
MFC-F28
Achromobacter sp. (AF227158)
MFC-F7
MFC-F23
Brucella melitensis (AF220149)
Ochrobactrum sp. (AF028733)
uncultured soil bacterium (AF507687)
MFC-F25
Genera_incertae_sedis "TM7"
Geobacter sulfurreducens (U13928)
Geobacter metallireducens (L07834)
uncultured rape rhizosphere bacterium wr0198 (AJ295559)
uncultured bacterium mle1-12 (AF280849)
MFC-F9
bacterium Ellin345 (AF498727)
MFC-F24
Acidobacterium capsulatum (D26171)
Acidobacteria
uncultured Acidobacteria bacterium (AY211077)
Bacteria (Z95709)
uncultured earthworm intestine bacterium (AY154482)
MFC-F3
uncultured Pietermaritzburg bacterium Y14-5 (AF312219)
Unclassified
Clostridiaceae str. (AB081585)
MFC-F12
MFC-F5
Alkaliphilus transvaalensis (AB037677)
Alkaliphilus crotonoxidans (AF467248)
uncultured soil bacterium (AF507716)
uncultured CFB group bacterium (AJ441242)
uncultured sludge bacterium (AF234699)
MFC-F11
MFC-F10
Flavobacterium sp. (AF344179)
Kaistella koreensis (AY294611)
MFC-F17
Bacteroidales str. (AB078842)
MFC-F4
Tannerella forsythensis (AB053943)
Dysgonomonas gadei (Y18530)
MFC-F16
Methanoculleus olentangyi str. RC/ER ATCC 35293 (T)
β - Proteobacteria
γ - Proteobacteria
α - Proteobacteria
Firmicutes
Bacteroidetes

Figure 4.7 Phylogenetic tree illustrating the relationship between closest relatives in the RDP and GenBank databases for 16S rDNA gene sequences from the electrode biofilm. 16S rRNA gene sequences were aligned using CLUSTAL W, and the tree was constructed by the neighbor-joining program from a similarity matrix of pair-wise comparisons made by the Jukes-Cantor algorithm in TREECON. The tree was rooted with the *Euryarchaeota Methanoculleus olentangyi*. Bootstrap values over 70, from 100 replicate trees, are shown at the nodes. The scale bar represents 10% difference in nucleotide sequence.

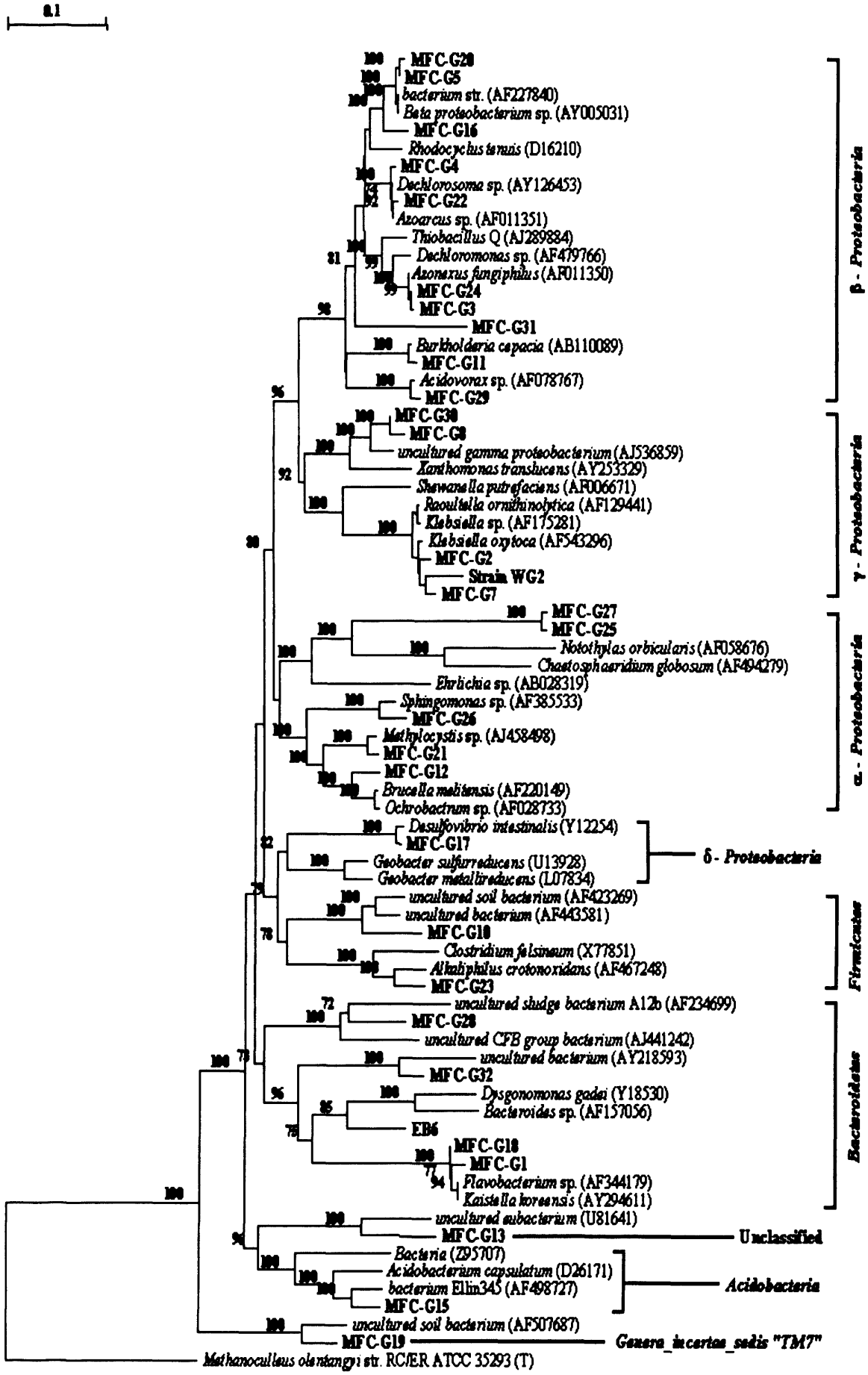
0.1
MFC-G28
MFC-G5
bacterium str. (AF227840)
Beta proteobacterium sp. (AY005031)
MFC-G16
Rhodocyclus tenuis (D16210)
MFC-G4
Dechlorosoma sp. (AY126453)
MFC-G22
Azoarcus sp. (AF011351)
Thiobacillus Q (AJ289884)
Dechloromonas sp. (AF479766)
Azonexus fungiphilus (AF011350)
MFC-G24
MFC-G3
MFC-G31
Burkholderia cepacia (AB110089)
MFC-G11
Acidovorax sp. (AF078767)
MFC-G29
β - Proteobacteria
MFC-G30
MFC-G8
uncultured gamma proteobacterium (AJ536859)
Xanthomonas translucens (AY253329)
Shewanella putrefaciens (AF006671)
Raoultella ornithinolytica (AF129441)
Klebsiella sp. (AF175281)
Klebsiella oxytoca (AF543296)
MFC-G2
Strain WG2
MFC-G7
γ - Proteobacteria
MFC-G27
MFC-G25
Nothoflas orbicularis (AF058676)
Chaetosphaeridium globosum (AF494279)
Ehrlichia sp. (AB028319)
Sphingomonas sp. (AF385533)
MFC-G26
Methylocystis sp. (AJ458498)
MFC-G21
MFC-G12
Brucella melitensis (AF220149)
Ochrobactrum sp. (AF028733)
α - Proteobacteria
Desulfovibrio intestinalis (Y12254)
MFC-G17
Geobacter sulfurreducens (U13928)
Geobacter metallireducens (L07834)
δ - Proteobacteria
uncultured soil bacterium (AF423269)
uncultured bacterium (AF443581)
MFC-G10
Clostridium felsineum (X77851)
Alkaliphilus crotonoxidans (AF467248)
MFC-G23
Firmicutes
uncultured sludge bacterium A12b (AF234699)
MFC-G28
uncultured CFB group bacterium (AJ441242)
uncultured bacterium (AY218593)
MFC-G32
Dysgonomonas gadei (Y18530)
Bacteroides sp. (AF157056)
EB6
MFC-G18
MFC-G1
Flavobacterium sp. (AF344179)
Kaistella koreensis (AY294611)
Bacteroidetes
uncultured eubacterium (U81641)
MFC-G13
Unclassified
Bacteria (Z95707)
Acidobacterium capsulatum (D26171)
bacterium Elm345 (AF498727)
MFC-G15
Acidobacteria
uncultured soil bacterium (AF507687)
MFC-G19
Genera_incertae_sedis "TM7"
Methanoculleus olentangyi str. RC/ER ATCC 35293 (T)

4.3.1.2. Phylogenetic affiliations of bacterial community members

Figure 4.3 shows the compositions of the bacterial community in the four compartment of the microbial fuel cell in terms of the major phyla and subdivisions that were present. The bacterial community in all compartments consisted of *Proteobacteria*, *Bacterioidetes*, *Firmicutes*, *Spirochaetes*, *Acidobacteria*, *Planctomycetes*, *Genera_incertae_sedis* "TM7" (Hugenholtz *et al.*, 2001) and unclassified bacteria. *Bacteriodetes* phylotypes constituted the most abundant division with 32.5% (98/301) of the sequenced clones, followed by 23.9% (72/301) β-*Proteobacteria*, 14.2% (43/301) *Firmicutes*, 10.6% (32/301) γ-*Proteobacteria*, 6.9% (21/301) α-*Proteobacteria*, 5.9% (18/301) *Spirochaetes*, 2.6% (8/301) *Acidobacteria*, 0.9% (3/301) *Genera_incertae_sedis* "TM7", 0.3% (1/301) δ-*Proteobacteria*, and 0.3% (1/301) *Planctomycetes*. Other sequences (1.3%) of the clone library could not be assigned to any known lineage of the domain *Bacteria*. The rise in *Proteobacteria*, especially γ-*Proteobacteria* and β-*Proteobacteria*, was concomitant with a fall in *Bacteroidetes* phylotypes in the MFC-F and MFC-G libraries. Figure 4.7 showed phylogenetic position of 30 selected clones retrieved from the Library G (MFC-G) with related taxa and other Fe(III)-reducing bacteria. It also showed strain WG2 with high Fe(III)-reducing and electrochemical activity isolated from the electrode biofilm was affiliated within the γ-*Proteobacteria* group in the phylogenetic tree as predicted by RDP and GenBank searches with Sequence_Match and BLAST. Strain WG2 and one clone sequence retrieved from the electrode biofilm shared 95-97% similarity to *Klebsiella oxytoca*, Fe(III)-reducing bacteria isolated from sediments under an iron mat (Baldi *et al.*, 2001). In addition, one clone affiliated to the δ-*Proteobacteria* group was only found within the Library G (MFC-G) and had high similarity (95%) to 16S rRNA genes from *Desulfovibrio intestinalis* (Frohlich *et al.*, 1999) isolated from hindgut contents of the lower termite *Mastotermes darwiniensis* and sequences identified in

sulphate- and U(VI)-reducing bacterium (Selenska-Pobell, 2002; Friedrich, 2002). It was also related with high identity to the genus *Desulfovibrio* recovered from mediator-less microbial fuel cell using artificial wastewater containing acetate and activated sludge collected from municipal sewage plant (Lee *et al.*, 2003). The genera *Acidovorax*, *Ochrobacterium*, *Dysgonomonas* and *Flavobacterium* related with clone sequences from the electrode biofilm were affiliated with clones retrieved from microbial fuel cell (Lee *et al.*, 2003). These results showed bacterial source and electron donor used in operating microbial fuel cell had an influence on the biodiversity in a microbial fuel cell biofilm.

4.3.2. DGGE

Amplicons of DNA extracted from four different samples, planktonic community in the anode compartment, the ion-exchange membrane biofilm, bacterial clumps and the electrode biofilm, were comparing using DGGE, with those of the activated sludge used as an inoculum (Figure 4.2; 4.8). As shown in Figure 4.8, DGGE patterns of the different samples in the fuel cell were different from that of the inoculum. This result suggests that the bacterial community has been altered during both operations of the fuel cell and also due to the different positions in the device. Some bands were present in all four different samples, though the total band patterns were different. The planktonic community in the anode compartment and the ion-exchange membrane biofilm had a low bacterial diversity that was dominated by four DGGE bands. Bands N1 and N2 were β-*Proteobacteria*, whilst band N3 was γ-*Proteobacteria* and band N4, associated with *Spirochaetes* phylum. In contrast, the bacterial clump and biofilm samples associated with electrode enriched with artificial wastewater for 18 months showed a high degree of sequence diversity but also contained three dominant DGGE bands (band N1, N2 and N3).

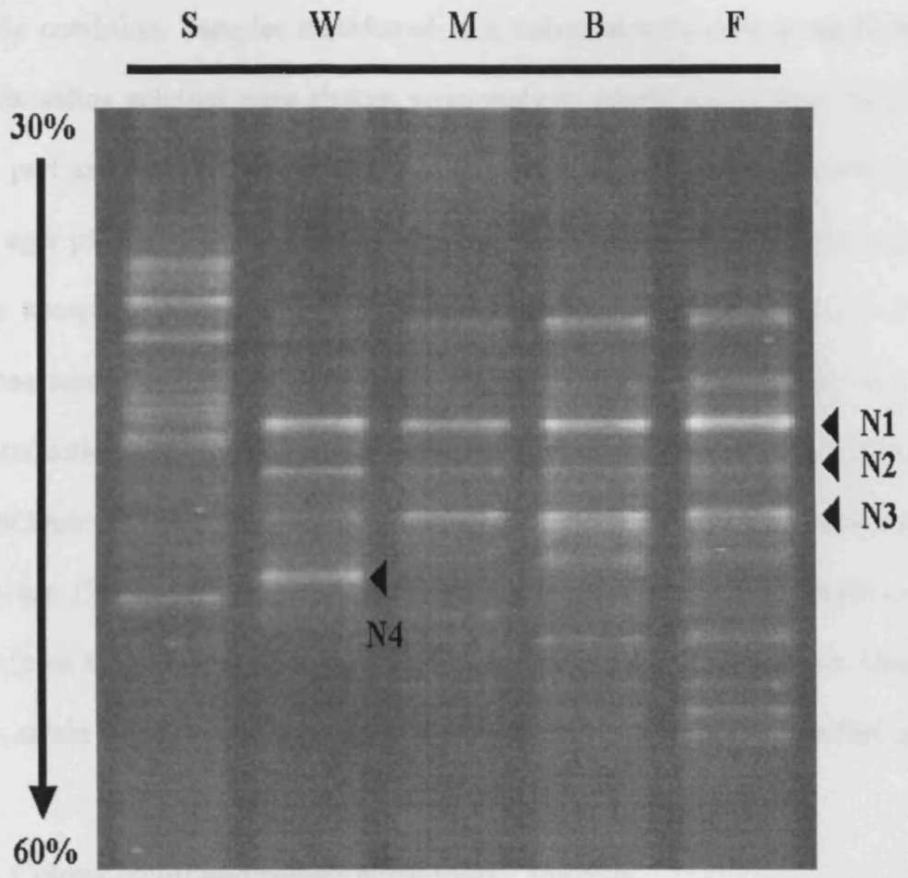

Figure 4.8 Comparison of bacterial communities in the fuel cell enriched with artificial wastewater by DGGE. The denaturing gradient used was from 30 to 60%. Lane S: sewage activated sludge (inoculum); lane W: planktonic community in the cell; lane M: the ion exchange membrane biofilm; lane B: the clump part of electrode; and lane F: the biofilm part of electrode. Arrows represent DGGE bands that were excised for sequencing.

4.3.3. Isolation of Fe(III)-reducing bacteria with electrochemical activity

4.3.3.1. Enrichment and isolation

A piece of electrode sample was collected from the anode compartment of the fuel cell in order to isolate a glucose oxidizing Fe(III)-reducing bacteria with electrochemical activity from biofilm part of the electrode. As described in the Materials and methods section, whole samples were aseptically handled under

anaerobic condition. Samples transferred in a universal tube containing 10 ml sterile anaerobic saline solution were shaken vigorously to separate microbial cells from the biofilm part and then serially diluted and cultivated in an anaerobic workstation on a PBBM agar plate containing 10 mM glucose with 20 mM ferric pyrophosphate as an electron acceptor. During cultivation under anaerobic condition, over 10^5 CFUs g^{-1} were measured for 7 days (Table 4.6). Colonies were isolated on the base of their Fe(III)-reduction and electrochemical activity. From over 120 isolates, 35 were selected based on their different appearance and tested for Fe(III)-reduction and electrochemical activity test (Table 4.7). 28.6% (10/35) of the isolates had a high Fe(III)-reduction activity (over 0.92 mM) and 65.7% (23/35) were electrochemically active. One of these isolates, strain WG2, was studied for its ability to generate current in the fuel cell.

4.3.3.2. Colony count and colony morphology analysis

The planktonic community, ion exchange membrane biofilm and bacterial clumps from electrode were also collected from the fuel cell anode compartment and these were compared with the number of colonies in biofilm. The suspended bacterial clumps and biofilm had more colonies than the planktonic community and the ion exchange membrane biofilm (Table 4.6). Similar numbers of colonies were observed on plates inoculated with clump and electrode biofilm. The number of colonies did not increase after adding acetate and lactate as alternative electron donors. Similar CFUs were formed on solid media with other electron acceptors including oxygen, nitrate and sulphate instead of Fe(III) in the medium (data not shown). These results showed that most of the colonies formed were fermentative bacteria. All the colonies appearing on the plates were examined microscopically and consisted of normal sized rod shaped bacteria (Table 4.7).

Fe(III) reducing colonies were easily recognized as their growth led to clearing zones around the colonies in the green-coloured ferric pyrophosphate medium and a change in medium colour from light to opaque green (Coates *et al.*, 1996). Colonies grown on 20 mM ferric pyrophosphate medium were typically less than 5 mm in diameter. Colonies showed various colours such as yellow, black, opaque green and white. They were domed and appeared to be coated with an Fe(II) mineral, similar to that observed for *Geobacter* species (Figure 4.9) Colony morphology analysis indicated that opaque green coloured and viscous colonies were the most abundant types in the sample, followed by white and yellow coloured strains.

Table 4.6 Colony forming units (CFUs) counts of biomass enriched with artificial wastewater in the fuel cell, plated on to various solid media.

Sample	Viable counts[a]		
	10 mM Glucose	20 mM Lactate	20 mM Acetate
Planktonic community[b]	$2.1\times10^{4}\pm0.24$	$1.4\times10^{4}\pm0.18$	$7.0\times10^{3}\pm0.28$
Membrane biofilm[c]	$5.0\times10^{5}\pm0.52$	$1.5\times10^{5}\pm0.43$	$7.5\times10^{4}\pm0.22$
Clumps from the electrode[c]	$7.8\times10^{5}\pm0.12$	$1.1\times10^{6}\pm1.42$	$4.9\times10^{5}\pm0.22$
Electrode biofilm[c]	$7.8\times10^{5}\pm0.22$	$3.1\times10^{6}\pm1.54$	$6.3\times10^{5}\pm0.35$

[a]Electron acceptor in media was 20 mM ferric pyrophosphate.

[b]CFUs ml^{-1} wastewater in the anode compartment.

[c]CFUs g^{-1} electrode or membrane biofilm.

*Data are presented as the mean ± S.D. (n=2)

Table 4.7 Characteristics of the 35 isolates from the electrode biofilm enriched with artificial wastewater and sewage activated sludge for 18 months. Fe(III) reduction was monitored spectrophotometrically by ferrozine assay of HCl-extractable Fe(II) (Phillips and Lovley, 1987).

Isolate name	Colour of colonies	Gram stain	Cell shape	Fe(III) reduction (mM)[a]	Cyclic voltammetry test[b]
WA3	dark green	-	rods	0.93 ± 0.04	+
BL2	white	+	rods	0.44 ± 0.08	-
WG2	dark green	-	rods	1.31 ± 0.04	+
MG4	dark green	-	rods	1.11 ± 0.05	+
FG3	cream	+	rods	0.64 ± 0.07	-
ML2	cream	+	rods	0.63 ± 0.08	+
BG3	transparent	-	rods	0.24 ± 0.11	-
ML1	light yellow	+	rods	0.87 ± 0.08	+
ML6-3	cream	+	rods	1.67 ± 0.07	+
ML6-2	transparent	-	rods	0.90 ± 0.08	-
ML6-1	light gray	-	rods	1.30 ± 0.08	+
MG6	cream	+	rods	0.79 ± 0.05	+
BG6	white	+	rods	0.61 ± 0.10	+
BG5	white	+	rods	0.73 ± 0.10	+
FG8	cream	+	rods	0.48 ± 0.11	+
FG7	white	+	rods	0.46 ± 0.12	+
FG6	cream	+	rods	0.26 ± 0.13	-
WG4	transparent	-	rods	0.72 ± 0.10	-
FA3	dark green	-	rods	0.55 ± 0.12	+
FG5	cream	-	rods	0.18 ± 0.15	-
MG2	cream	-	rods	0.31 ± 0.14	-

Table 4.7 continued.

Isolate	Colour of colonies	Gram stain	Cell shape	Fe(III) reduction (mM)[a]	Cyclic voltammetry test[b]
BL1	cream	+	rods	0.98 ± 0.12	+
FA4-2	cream	+	rods	0.61 ± 0.13	+
FA4-1	cream	+	rods	0.51 ± 0.14	+
FG4-2	cream	+	rods	0.17 ± 0.15	+
FG4-1	cream	-	rods	0.66 ± 0.13	-
ML3	light green	-	rods	0.40 ± 0.15	-
ML5-2	dark brown	-	rods	0.36 ± 0.15	-
WL4-2	cream	-	rods	1.30 ± 0.12	+
BA2-1	dark green	-	rods	0.94 ± 0.13	+
BA1-1	dark green	-	rods	1.16 ± 0.12	+
BA1-2	dark green	-	rods	0.85 ± 0.14	+
BA2-2	dark green	-	rods	1.18 ± 0.13	+
WL4-1	dark green	+	rods	0.75 ± 0.14	+
ML5-1	dark brown	-	rods	0.62 ± 0.14	-

[a]Data are presented as the mean ± S.D. of 2 tubes.

[b]See section 4.2.11.

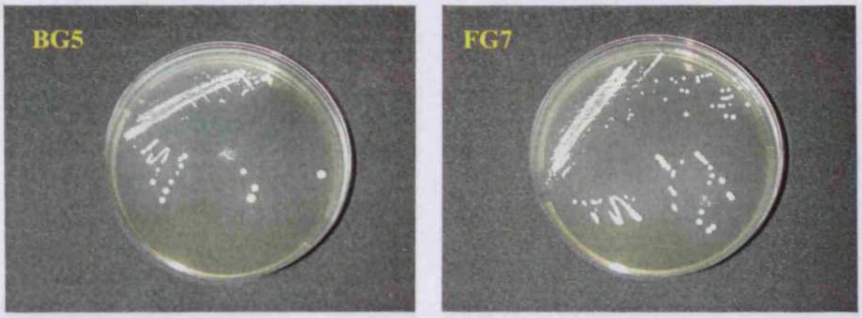

RDP *Firmicutes* phylum *Clostridiaceae* family

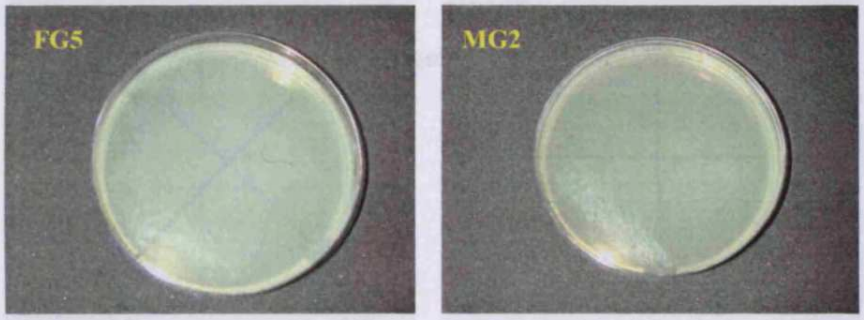

RDP β-*Proteobacteria* phylum *Rhodocyclaceae* family

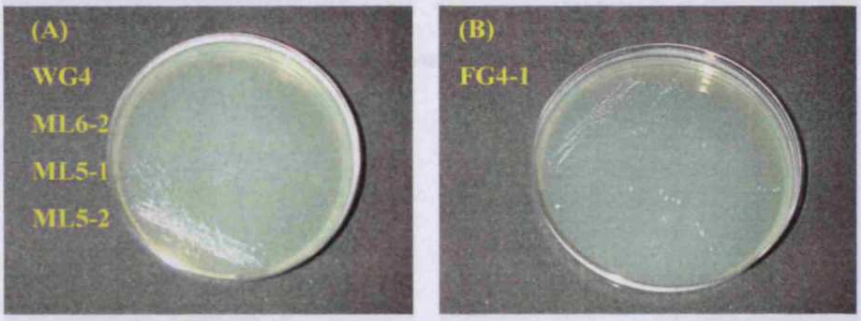

RDP β-*Proteobacteria* phylum *Desulfovibrionaceae* family (A) and *Bacteroidetes* phylum *Porphyromonadaceae* family (B)

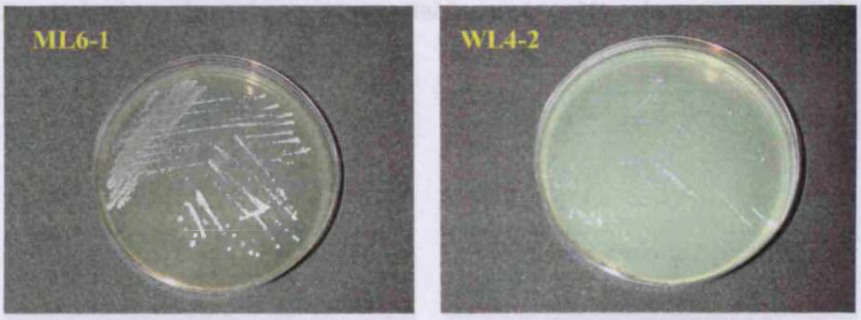

RDP *Bacteroidetes* phylum *Porphyromonadaceae* family

Figure 4.9 continued.

RDP γ-*Proteobacteria* phylum *Enterobacteriaceae* family

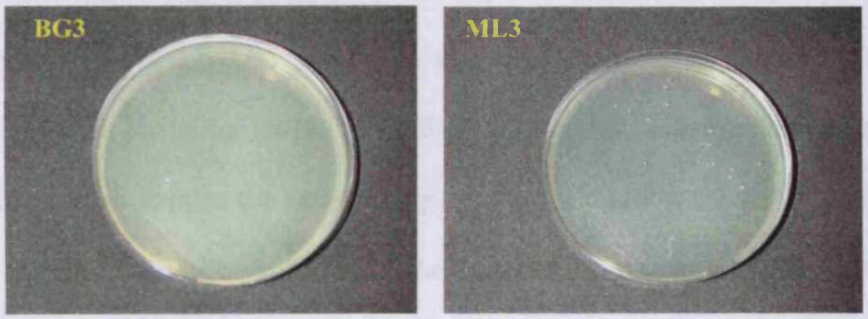

RDP γ-*Proteobacteria* phylum *Pseudomonadaceae* family

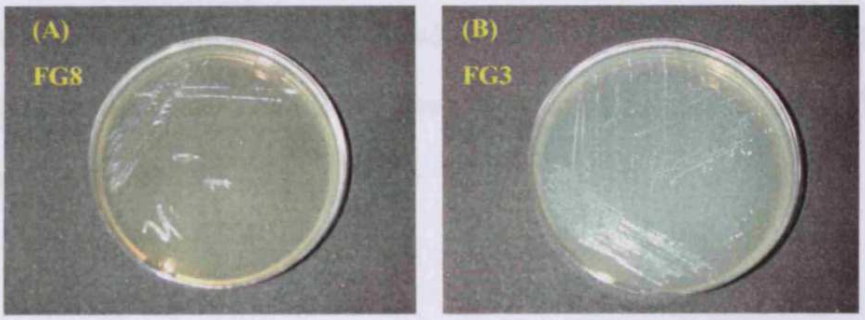

RDP *Actinobacteria* phylum *Norcardioidaceae* (A), *Microbacteriaceae* (B) family

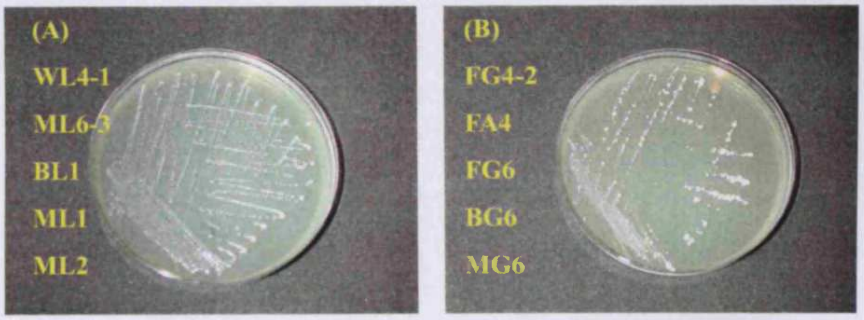

RDP *Actinobacteria* phylum *Propionibacteriaceae* (A), Unclassified (B) family

4.3.3.3. 16S rRNA gene sequencing and phylogenetic analysis

The 16S rRNA genes from the 35 isolates selected from colony morphology analysis were analysed phylogenetically (Table 4.8). All sequences were submitted to a RDP Sequence_Match query and a GenBank BLAST search to find their closest matches in the databases. Figure 4.10 shows that *Actinobacteria* (40.0%) was the most abundant phylum within total isolates, followed by γ-*Proteobacteria* (28.6%), δ-*Proteobacteria* (11.4%), *Bacteroidetes* (8.6%), *Firmicutes* (5.7%) and β-*Proteobacteria* (5.7%). Six of the 11 isolates with a high Fe(III) reduction activity (over 0.92 mM) belonged to the RDP γ-*Proteobacteria* phylum and were also electrochemically active. The isolate WG2 was selected based on its high Fe(III) reduction and electrochemical activity. A phylogenetic tree illustrates the relationship between isolate WG2 and Fe(III) reducers (Figure 4.11). The sequence similarity of the 16S rRNA gene was compared with those of reference organisms obtained from the GenBank database. The result revealed that the isolates WG2 is a member of the *Enterobacteriaceae* family of the γ-*Proteobacteria* phylum. *Klebsiella oxytoca* (AY150697) was the nearest neighbour with a 16S rRNA sequence similarity of 97%.

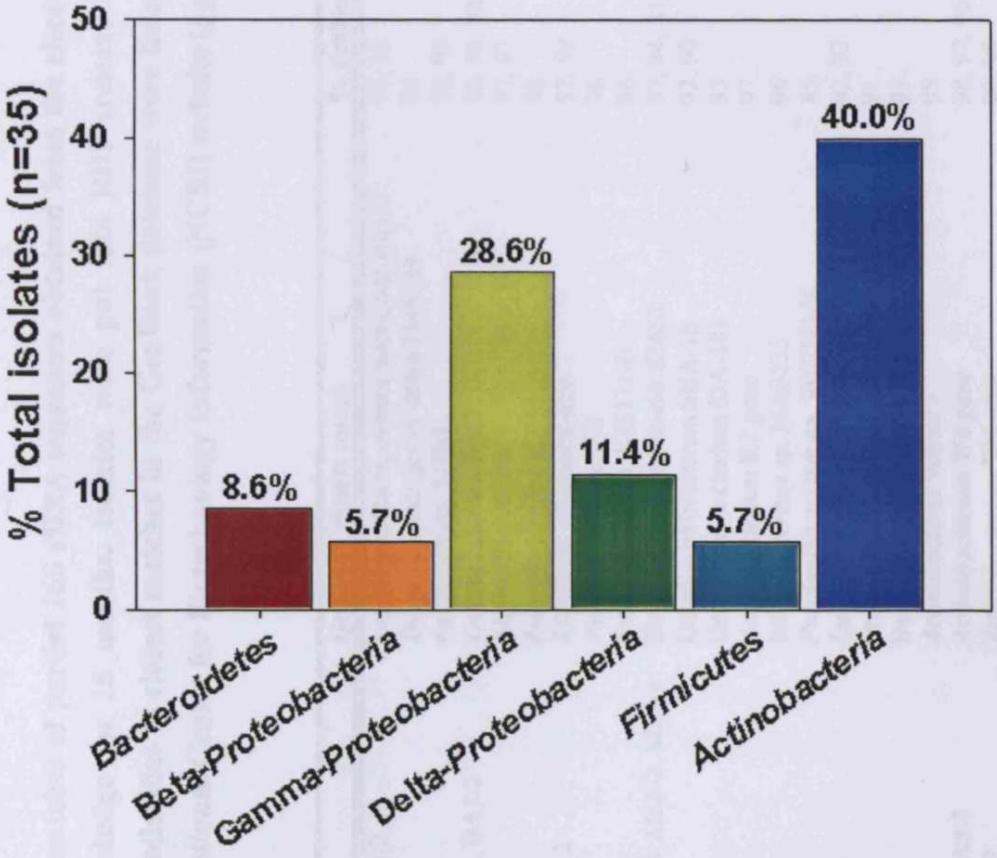

Figure 4.10 BLAST–based taxonomic distributions for 35 isolates from the fuel cell biofilm. The 16S rRNA genes from the 35 isolates selected colony morphology analysis were sequenced and phylogenetically analysed.

Table 4.8 Phylogenetic affiliation and closest matches of partial 16S rDNA sequences obtained from the electrode biofilm enriched with artificial wastewater and sewage activated sludge for 18 months. Isolates were put into RDP (release 8.1; Maidak *et al.*, 2000) Sequence_Match searches. The percentage similarities to closest matches in the GenBank database were listed according to the BLAST search program (Altschul *et al.*, 1997) in the national Centre for Biotechnology Information (NCBI) website (*http://www.ncbi.nlm.nih.gov*).

RDP phylum	RDP family	Isolate	GenBank closest match	% similarity	Sequence length (bp)
Bacteroidetes	*Porphyromonadaceae*	ML6-1, WL4-2	Uncultured Bacteroidetes bacterium Blci17	96, 98	697, 727
		FG4-1	*Dysgonomonas gadei* strain 1145589	94	1437
β-*Proteobacteria*	*Rhodocyclaceae*	FG5, MG2	*Bacterium* str. 51885	98, 96	658, 565
γ-*Proteobacteria*	*Enterobacteriaceae*	WA3, BA1-1, BA1-2	*Enterobacter* sp. B509	98, 98, 98	722, 680, 750
		WG2, MG4	*Klebsiella oxytoca*	97, 97	767, 726
		FA3	*Enterobacter kobei*	96	678
		BA2-1, BA2-2	*Klebsiella ornithinolytica*	97, 99	731, 716
	Pseudomonadaceae	BG3	*Pseudomonas* sp. 273	98	757
		ML3	*Pseudomonas* sp. KIE171-B	86	583
δ-*Proteobacteria*	*Desulfovibrionaceae*	ML6-2, WG4, ML5-2, ML5-1	*Desulfovibrio intestinalis* KMS2	97, 94, 81, 98	717, 636, 716, 772
Firmicutes	*Clostridiaceae*	BG5, FG7	Uncultured bacterium SHA-18	92, 90	706, 630
Actinobacteria	*Nocardioidaceae*	BL2	Uncultured bacterium SJA-181	95	1417
		FG8	*Actinobacterium* K2 gene	97	626
	Microbacteriaceae	FG3	*Microbacterium* sp. MAS133	96	694
	Propionibacteriaceae	ML2	*Propionibacterium* sp. V07/12348	85	698
		ML1, ML6-3	*Luteococcus* sp. CCUG38120	92, 92	1413, 1241
		BL1	*Propionibacterium* sp. LCDC-98A072	91	1225
		WL4-1	Bacterium 010.96.107	97	432
	Unclassified bacteria	MG6	*Actinobacteria* VeSm15	95	706
		BG6, FG6, FA4-2	*Actinobacterium* Wd gene	98, 97, 96	727, 738, 730
		FA4-1, FG4-2	*Actinobacterium* Wd gene	98, 95	740, 684

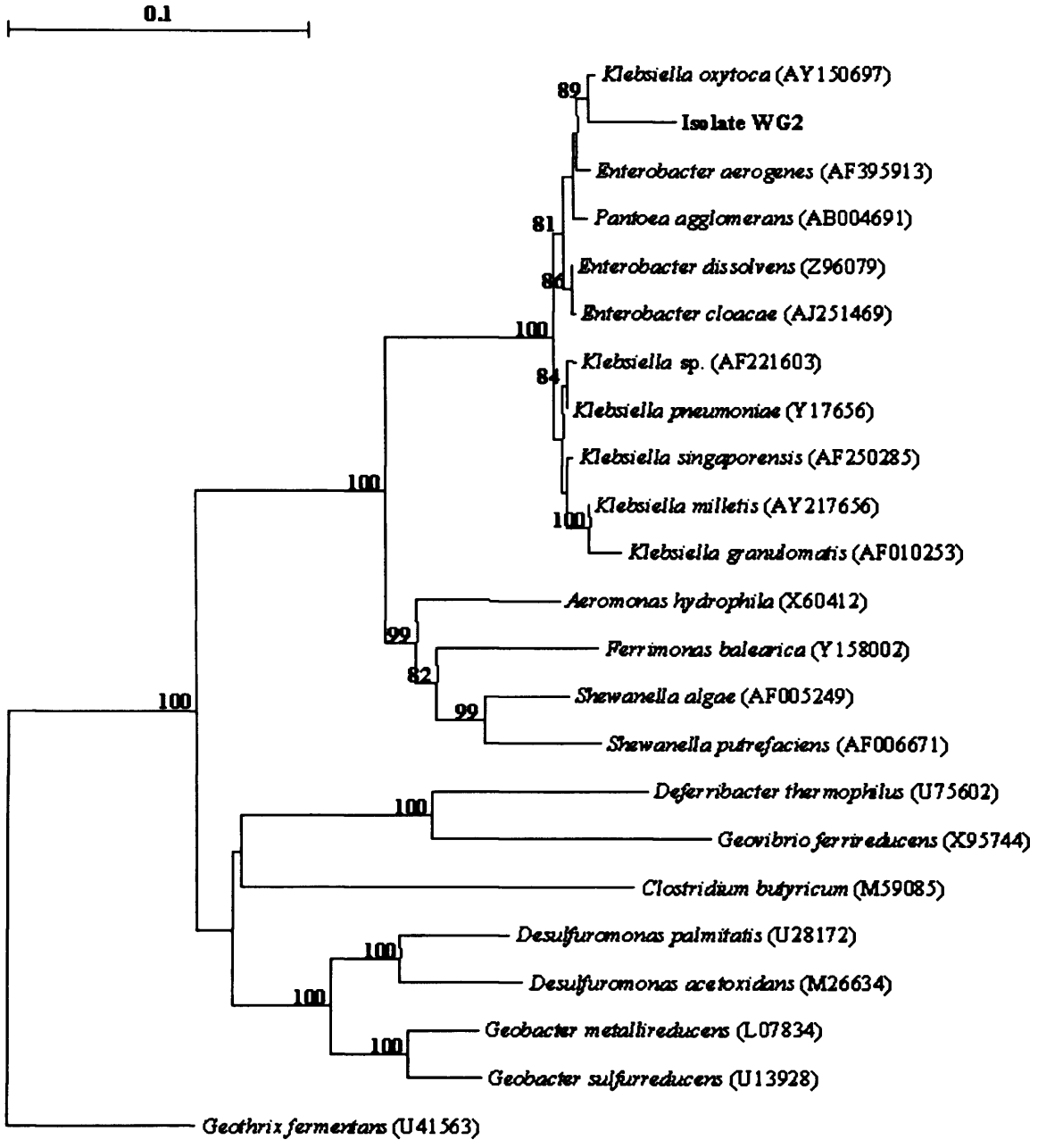

Figure 4.11 Phylogenetic position of the isolate WG2 with its related taxa and with Fe(III) reducers. 16S rRNA gene sequences were aligned using CLUSTAL W, and the tree was constructed by the neighbor-joining program from a similarity matrix of pair-wise comparisons made by the Jukes-Cantor algorithm in TREECON. The tree was rooted the *Acidobacteria Geothrix fermentans*. Bootstrap values over 70, from 100 replicate trees, are shown at the nodes. The scale bar represents 10% difference in nucleotide sequence.

4.3.3.4. Electrochemical activity of the bacterial isolates

Washed cell suspensions of the 35 isolates were used to determine the electrochemical activity using cyclic voltammetry. Over half of them were electrochemically active as mentioned above. Oxidation/reduction peaks were observed in the cyclic votammogram of cells grown under anaerobic conditions with ferric citrate, but cells grown under aerobic conditions or under anaerobic conditions without ferric citrate did not show electrochemical activity. The CV obtained from isolate WG2 showed different shapes of oxidation and reduction peaks with an apparent redox potential of around –200 mV against the Ag/AgCl reference electrode (Figure 4.12). This asymmetry shows that the redox reaction of the cell suspension is a quasi reversible reaction.

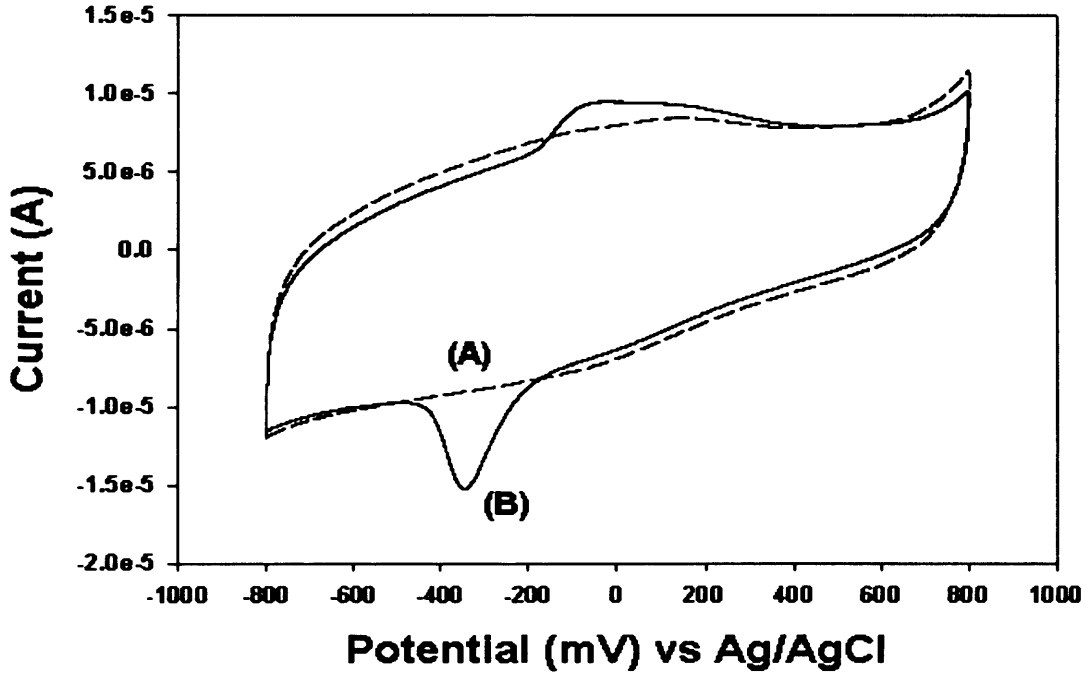

Figure 4.12 Cyclic voltammograms of an isolate WG2 cell suspension grown under anaerobic conditions with [solid line (B)] or without [dotted line (A)] ferric citrate as an electron acceptor.

The isolate WG2 was tested for its ability to generate current in a fuel cell-type electrochemical cell (Figure 4.13). The cell concentration increased about 7-fold, consuming glucose completely in about 25 h with concomitant current generation. The current generation was not proportional to the cell concentration. The highest current of 0.19 mA was observed at 36 h after inoculation, and dropped slowly to around 0.03 mA at the end of the stationary growth phase. The current did increase after the glucose was completely consumed.

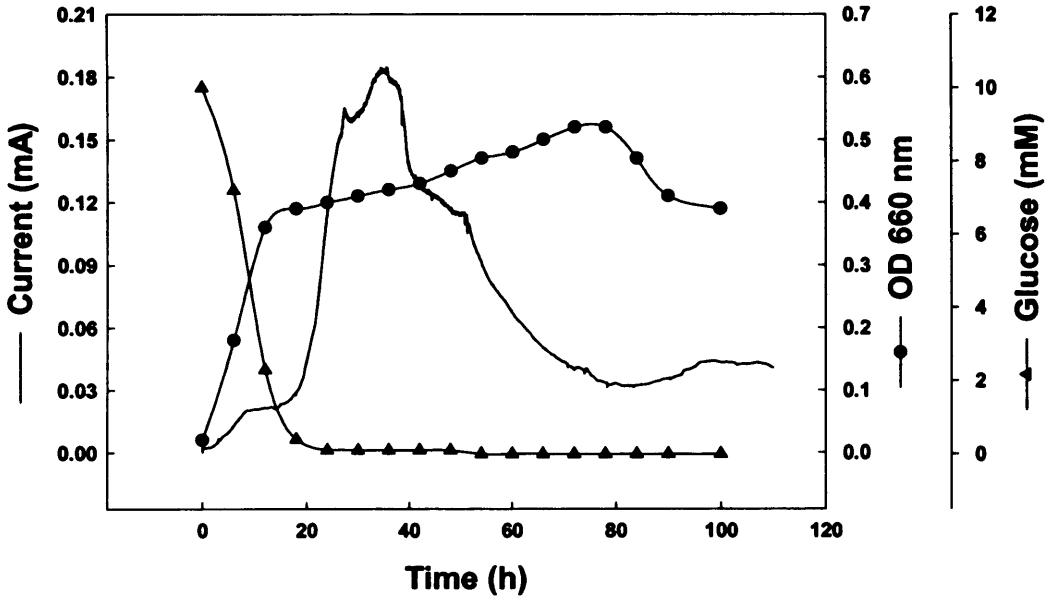

Figure 4.13 Growth and current generation by the isolate WG2 in a fuel cell-type electrochemical cell using glucose as the electron donor.

4.4. Discussion

In this study, fuel cell-type electrochemical cells which ran with activated sewage sludge for 18 months, successfully removed organic contaminants from artificial wastewater with concomitant electricity generation and in the absence of electron-transfer mediators. Certain microbes became enriched during this process. Microscopic observation showed an increase in the microbial population on the surface of electrode. The results of stable current generation suggest that a mediator-less microbial fuel cell is possible when the microbial community in the fuel cell metabolizes its fuel (electron donors) and transfers the resulting electrons to the electrode.

The study of the microbial community of samples from different parts of the anode compartment was started with 16S rRNA gene sequence analysis. These biodiversities varied in according to bacterial source and electron donors both of which could influence the genetic diversity of these communities. The sequences amplified from extracted DNA represented a wide range of bacterial phylogenetic groups, and sequences related to δ-*Proteobacteria* (1.3%) were only detected in the Library G (electrode biofilm). This result is different from Bond *et al.* (2002), who reported that δ-*Proteobacteria* were the major organism in the fuel cells enriched with acetate in seawater. This difference might be due to differences in the electron donors or in the salt concentration used as mentioned above. Phylogenetic analysis of the sequences provided clear evidence that there were differences in diversity according to position in the fuel cell system. In Library D (planktonic community), sequences of clones belonging to the *Bacteroidetes* were most abundant (49.3%), and these sequences were mainly related to the Gram-negative fermentative bacteria commonly found in activated sludge and freshwater. It seems that activated sewage sludge used as a source

of bacteria have an effect on the biodiversity of the planktonic community in the anode compartment. The majority of the *Firmicutes* in Library E (the ion exchange membrane biofilm) could be explained on the basis that these organisms firmly attached to the surface of the membrane and carried out glucose fermentation. A Gram-positive *Clostridium butyricum* was previously isolated from a microbial fuel cell using starch processing wastewater as fuel (Park *et al.*, 2001). In a comparison of the clone libraries directly related to power generation, the number of *Proteobacteria* was increased in Library F (bacterial clump) and G (electrode biofilm). Especially, 50% of the γ-*Proteobacteria* enriched were most closely related to Fe(III)-reducing microorganisms in the family *Enterobacteriaceae* (Baldi *et al.*, 2001). The increase of γ-*Proteobacteria* suggest that these microbes may involved in current generation. Based on these results, differences in each clone library might be due to the fact that the microbial community in the wastewater and the membrane biofilm ferments complex fuel into simple fermentation products. These products can then be used as substrates for electrochemically active bacteria within the biofilm to generate electricity (Figure 4.14). Recently, application of stable-isotope labeling of nucleic acids to determine the metabolic capabilities of active components of microbial communities has been developed for microbial ecological investigation (Radajewski *et al.*, 2000; Radajewski *et al.*, 2002). Stable-isotope probing (SIP) of nucleic acids could be successfully used to identify microorganisms potentially related to ^{13}C-enriched carbon sources e.g., glucose and acetate in the fuel cell. ^{13}C-enriched DNA, produced during the enrichment of metabolically distinct microbial groups in the fuel cell, can be purified by equilibrium centrifugation in CsCl-ethidium density gradients. PCR is used to amplify 16S rRNA genes from the ^{13}C-enriched DNA, and these are cloned and sequenced.

While several other rDNA or rRNA approaches are also available which could

provide more rapid analysis, e.g., DGGE, amplified ribosomal restriction analysis, terminal restriction fragment length polymorphism (T-RFLP) and fluorescence *in situ* hybridization, the great strength of sequence analysis is the generation of additive and retrievable data which can be used to generate phylogenetic probes and primers for use in further studies. DGGE analysis showed that the bacterial populations in the anode compartment were different from the activated sludge used to inoculate the fuel cell at the beginning of the enrichment. This shows that the microbial fuel cell allows the enrichment of a bacterial consortium that oxidizes organic contaminants with concomitant electron transfer to the electrode. The DGGE banding patterns observed in bacterial clump and electrode biofilm were very similar. It seems that the sampling method from the electrode is not efficient or that the microbial community is substantially same. A high degree of bacterial diversity in bacterial clumps and electrode biofilm samples suggest that more metabolically complex environments related to power generation might be present in the electrode. All samples were observed to have several brightly dominant bands which when excised and sequenced showed similar results in terms of 16S rRNA gene sequence analysis.

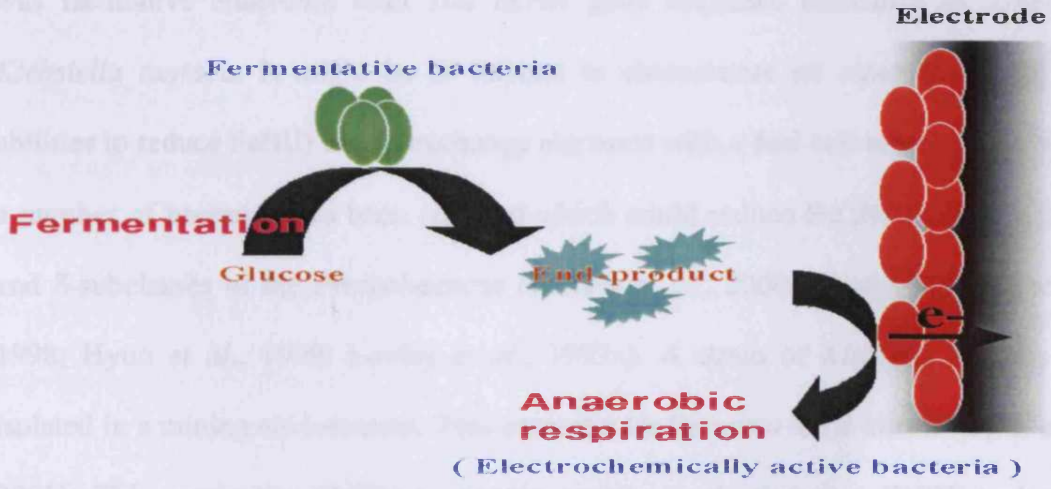

Figure 4.14 A proposed schematic diagram of microbial interactions in the microbial fuel fed with artificial wastewater for 18 months.

Various electron donor and acceptor combinations, including ferric iron as the electron acceptor were used to isolate bacteria from the enriched microbial fuel cell. However, the resulting number of colonies was smaller than expected. This suggests that most electrochemically active microbes cannot be cultivated under the conditions employed. It might also be true that not all electrochemically active bacteria can use Fe(III) as their electron acceptor. Cultivation based techniques showed the presence of *Klebsiella oxytoca*, *K. ornithinolytica*, *Dysgonomonas gadei* and *Desulfovibrio intestinalis*. All isolates of the family *Enterobacteriaceae* have Fe(III) reduction activity and are also electrochemically active. Species of the genus *Klebsiella* and *Enterobacter* fall into the γ-subclass of the *Proteobacteria*. These results correspond with data in 16S rRNA gene sequence analysis and also suggest that γ-*Proteobacteria* with Fe(III) reduction activity might be involved in direct electron transfer to the electrode. In addition, current generation from a microbial fuel cell has been reported to be related to Fe(III) reducing activity (Kim *et al.*, 1999b; Bond and Lovley, 2003). The isolate, WG2, was one of the colonies reducing Fe(III) on a solid medium with glucose as electron donor and ferric pyrophosphate as the electron acceptor. The isolate, WG2, was facultative anaerobic with 16S rRNA gene sequence similarity of 97% with *Klebsiella oxytoca*. It might be of interest to characterize an enterobacterium with abilities to reduce Fe(III) and to exchange electrons with a fuel cell electrode. Recently, a number of bacteria have been reported which could reduce Fe(III), mostly in the γ- and δ-subclasses of the *Proteobacteria* (Francis *et al.*, 2000; Knight and Blakemore, 1998; Hyun *et al.*, 1999; Lovley *et al.*, 1993a). A strain of *Klebsilla oxytoca* was isolated in a mining environment. This enterobacter ferments ferric citrate (Baldi *et al.*, 2001). This strain has ability to couple acetate production and Fe(III) reduction. Acetate has been suggested as the major extracellular intermediate in the oxidation of

fermentable organics in Fe(III) reducing sediments (Lovley *et al.*, 1992).

It was clearly shown that the isolate WG2 was electrochemically active using cyclic voltammetry as well as the fuel cell technique. The cyclic voltammogram of WG2 showed reduction and oxidation peaks at –350 mV and –60 mV, respectively. The cyclic voltammogram is very similar to that of other electrochemically active bacteria, e.g., *Shewanella putrifaciens* IR-1 (Kim *et al.*, 1999b) and *Aeromonas hydrophila* PA3 (Pham *et al.*, 2003). In addition, these two microorganisms classified in the γ-subclass of the *Proteobacteria* had *c*-type cytochromes on the cell surface, which were involved in dissimilatory reduction of diverse electron acceptor by this organism (Myers and Myers, 1992; Knight and Blakemore, 1998). It is plausible that the electrochemical activity observed in the isolate WG2 is due to the *c*-type cytochromes observed in dissimilatory Fe(III) reducers. It would be interesting to find cytochrome(s) and ferric reductase on the cell surface of the *Enterobacteriaceae*.

A cell suspension of the isolate, WG2, prepared from an anaerobic culture with Fe(III) showed quasi-reversible oxidation-reduction reaction in the cyclic voltammetry with a strong peak for reduction than for oxidation. These results showed that more electron flow was to the bacterial cells than in the reverse direction to the electrode. This might be that the bacterial cells were not loaded with enough electrons whilst the electrode was connected to a potentiostat. The cell suspension grown under anaerobic conditions without Fe(III) was not electrochemically active, while *Shewanella putrifaciens* was electrochemically active regardless of the presence of the Fe(III) (Park *et al.*, 1997). This results agrees with Pham *et al.* (2003) who reported that *Aeromonas hydrophila* was only electrochemically active in the anaerobic growth condition with Fe(III). Pham *et al.* (2003) suggested that these organisms might have different

regulatory mechanisms for the biosynthesis and translocation of *c*-type cytochromes.

The isolate, WG2, was also tested for its ability to generate current in the fuel cell. When the fuel cell was inoculated with the cell suspension containing glucose as electron donor, the low current was generated at a background level of less than 0.03 mA until the glucose was completely consumed with a rapid cell growth. However, current was increased rapidly to over 0.19 mA after that time, and then gradually decreased to the level of 0.3 mA. The reasons for slow current generation might be explained as follows. First, the isolate, WG2, needs time to adapt to the new environment in the fuel cell. Secondly, more electrons transfer to the electrode when fermentation products convert to a new reduced form with aid of various electron carrier enzymes.

In summary, conventional as well as molecular techniques did detect significant differences in bacterial diversity of four samples by position in the fuel cell and found that the family *Enterobacteriaceae* of the γ-*Proteobacteria* shows significant potential for the energy generation in the form of electricity. We have found that the isolate, WG2, is a strain of the genus *Klebsiella* with electrochemical and Fe(III) reducing activities. Our results suggested that this strain could be used as new biocatalyst to improve the performance of mediator-less microbial fuel cell.

CHAPTER V

General Discussion

5.1. A novel mediator-less microbial fuel cell as a wastewater treatment process

Microbial fuel cells seek to exploit the diversity of microbial catalytic abilities in highly efficient designs, which allow organic compounds, from simple carbohydrates to waste organic matter, to be converted into electricity (Bond and Lovley, 2003; Wingard *et al.*, 1982). In this thesis, a mediator-less microbial fuel cell was successfully used to enrich electrochemically-active bacteria from activated sludge using an artificial wastewater supplemented with glucose and glutamate as electron donors. Such fuel cells remove organic contaminants in an artificial wastewater with the concomitant generation of electricity.

Studies on the microbial conversion of organic matter to electricity revealed a number of problems. A major weak point is that microorganisms only partially oxidize organic substrates so that only a fraction of available electrons are transferred to electrodes. This means that the efficiency of the fuel cell is low. This might also be due to the leakage of electrons. For efficient electron transfer from a microbial electron carrier to an electrode to occur, soluble electron mediators are usually required (Fultz and Durst, 1982). Several researchers have previously shown that electrical current was effectively generated when soluble electron mediator compounds were added to these microbial cultures to facilitate electron transfer from bacteria to the electrodes. Examples of mediators include neutral red (Park and Zeikus, 2000), thionine (Kim *et al.*, 2000) and potassium ferricyanide (Emde *et al.*, 1989). However, the use of mediators also has problem, since many of these compounds are toxic to microorganisms if used at higher concentrations and cannot be used when electrical energy is harvested from organic matter in an open environment (Bond and Lovley,

2003).

Recently, mediator-less microbial fuel cells have been constructed using pure microbial cultures. Organisms used include *Geobacter sulfurreducens* (Bond and Lovley, 2003), *Shewanella putrefaciens* (Kim *et al.*, 2002), *Clostridium butyricum* (Park *et al.*, 2001) and *Aeromonas hydrophila* (Pham *et al.*, 2003). All these microorganisms are classified as Fe(III)-reducing bacteria. In Chapter IV 28.6% (10/35) of isolates from the fuel cell biofilm also have high Fe(III) reducing activity and are electrochemically active. It was clearly show that these bacteria, characterized as having membrane-bound Fe(III)-reduction with direct cell-oxide contact, can be used in microbial fuel cells as new bacterial biocatalysts. This suggested that membrane-bound proteins and cytochromes in Fe(III)-reducing bacteria could be directly involved in electron transfer to the electrode as terminal electron acceptor in the anode compartment.

In the fuel cell anode compartment organic compounds are oxidized to carbon dioxide, transferring electrons to the electrode and liberating protons into the aqueous phase. Dioxygen is reduced to water in the cathode compartment with electrons being transferred through the external circuit and protons through the membrane.

Current generation in a microbial fuel cell can be influenced by several factors. These include the rates of fuel oxidation and electron transfer to the electrode by microbes, the resistance of the circuit, proton transport to the cathode through the membrane and oxygen supply and its reduction in the cathode. Current output was affected by the different pH conditions in the anode compartment. A comparison of maximum current produced between pH 5.0 and 9.0 suggested that current generation in the fuel cell involved microorganisms since the final pH in the anode compartment

was around pH 7.0 characteristic of most biological processes. It is possible that this value could be due to reverse proton transfer from the cathode compartment. Previous studies on the effect of electrolytes on the performance of the microbial fuel cells showed that the microbial activity and electron transfer to the electrode in the anode compartment can be reduced due to the pH changes away from neutrality in addition to the slow cathode reaction due to limited supply of proton (Gil *et al.*, 2003). At low resistance value (100 Ω) the microbial fuel cell generated the highest current. These results suggest that the current flow using a low value resistance is facilitated by the electron driving force developed under low resistance value, and electrons are easily transferred to the cathode compartment. However, it is also possible to generate significant current with electron and proton captured under high load conditions. It was shown that current output also depends on aeration rate in the cathode and nitrogen-feeding rate in the anode compartment. These suggest that partially aerobic conditions interfere with electron transfer to the electrode in the anode compartment, and that sufficient aeration is required for complete oxidation of protons in the cathode compartment. In addition, air transfer from the cathode to the anode caused a drop in current since oxygen acts as an electron acceptor in the latter. These results demonstrate that several rate-limiting factors play an important part in fuel cell optimization for scale-up process.

Current generation was influenced by respiratory inhibitors. The uncoupler (DNP) and ATPase inhibitor (DCCD) inhibited current production. The uncoupler was expected to increase current generation as it increases oxygen consumption during aerobic respiration. The results suggest that electron transfer to the electrode requires a reverse electron-transport step. It is not clear how the uncoupler and ATPase inhibit the current generation, but it is assumed that these respiratory inhibitors interfered with

energetic fermentative metabolism, which plays a crucial role in the fuel cell. The use of inhibitors at high concentration was required for complete inhibition. *p*-CMPS (Fe-S cluster inhibitor), HQNO (cytochrome *b* site inhibitor), rotenone (NADH dehydrogenase inhibitor) and antimycin A (electron transport chain II inhibitor) also inhibited the current generation. The terminal oxidase inhibitors, cyanide and azide showed no inhibition. These results suggest that the electron transport system in electrochemically active microbes utilize NAD, iron/sulfur proteins, site 2 of the electron transport chain, and quinine as the electron carriers, but may not use classical terminal cytochrome oxidases.

5.2. Changes in the microbial population of the developing electrode biofilm

Several cultivation-independent techniques including PCR-DGGE, the 16S rRNA gene approach and FISH have been used to gain a better understanding of the microbial community and potential role of these bacteria in the microbial fuel cell. PCR-DGGE analysis showed that the bacterial population in the anode of the microbial fuel cell was different from that in the sludge used to inoculate it at the start of the enrichment. The banding patterns observed in the DGGE gels were more extensive and complex, indicating the development of a diverse bacterial community over the sampling time. It is believed that a number of fermentative bacteria with non-electrochemical activity, present at the surface of the electrode, were washed out during the enrichment process, replaced by electrochemically active microbes which became the major microbial community on the electrode biofilm. Some of the isolates from the microbial fuel cell were electrochemically active; and current generation was noted in a fuel cell using one of the isolates identified as a strain of *Klebsiella oxytoca*. These results clearly show

that electrochemically active microbes had been enriched in the fuel cell. The cell suspensions of isolates were electrochemically active when measured by cyclic voltammetry, suggesting that soluble electron carriers are not involved in electron transfer to the electrode, as reported by Bond *et al.* (2002). 16S rRNA gene sequence analyses of the 11 months enriched electrode revealed that γ-*Proteobacteria* was the most abundant division with 59.8% of the sequenced clones. In all clone libraries over the sampling time, a rise in γ-*Proteobacteria* and a concomitant fall in *Bacterioidetes* commonly found in activated sludge, suggested that the enriched population might be adapted to optimize energy generation. These results also showed that 80% of the γ-*Proteobacteria* isolated from the electrode biofilm had Fe(III) reducing and electrochemical activity. Several researchers have reported that δ-*Proteobacteria* was the major group in a microbial fuel cell enriched with acetate in seawater. This difference might be due to use of different electron donors or the presence of salt (Bond *et al.*, 2002; Tender *et al.*, 2002). As mentioned in Chapter III, results from the 16S rDNA clone library compared to that from *in situ* probing of the enriched electrode sample showed good agreement. However, these results might have several problems. It is not clear if FISH with 8 oligonucleotide probes covers all the microbial population in the electrode biofilm and also that small pieces of the enriched electrode may not represent the whole microbial diversity. To account for these it was necessary to use two or three oligonucleotide probes to investigate biodiversity at the same time, and also to find effective sampling procedures observing the enriched biofilm. Furthermore, it is necessary to construct oligonucleotide probes to detecting electrochemically active microbes associated with generating electricity on the electrode biofilm.

LVEM showed a biofilm which formed on the electrode surface as well as microbial clumps scattered around the electrode. SEM also revealed a thick film on the electrode

surface with particles of different sizes at its surface. It seems likely that the small particles and biofilm on the surface of electrode are involved in energy generation. CSLM showed Gram-negative and Gram-positive bacteria forming microcolonies over the whole electrode surface. The microbial clumps produced similar micrographs. The dense staining suggests that majority of the bacteria present in the biofilm and the bacterial clumps were alive.

5.3. Comparison of microbiological and molecular approaches

Microbiological techniques were used to determine the communities present in the electrode biofilm. From several previous studies (Park *et al.*, 2001; Pham *et al.*, 2003; Bond and Lovley, 2003), it was apparent that Fe(III)-reducing bacteria were associated with energy generation in the fuel cell biofilm. Cultivation based techniques using ferric pyrophosphate as electron acceptor showed that *Enterobacteriaceae* in the γ-*Proteobacteria* phylum had Fe(III) reducing activity and were electrochemically active. The work of Pham *et al.* (2003) showed that *Aeromonas hydrophila* isolated from a fuel cell fed with artificial wastewater containing acetate was electrochemically active and could use Fe(III) as electron acceptor. Furthermore, Kim *et al.* (2002) also showed evidence for direct electron flow from Fe(III)-reducing bacterium, *Shewanella putrefaciens*, to the electrode using the cyclic voltammetry techniques. One of the isolates obtained from the electrode biofilm in the present study, designated strain WG2, had a 16S rRNA gene sequence similarity of 97% with *Klebsiella oxytoca*. It was shown by cyclic voltammetry that strain WG2 was electrochemically active as well as its electrical output in the fuel cell. These results suggest that some members of the family *Enterobacteriaceae* play an important part in electricity generation in the fuel cell. On the other hand, if the conditions employed were not favorable for growth of

electrochemically active microbes, it is difficult to get reliable profile of the diversity of the microbial communities. Additionally, it was not clear whether the electrochemically active bacteria enriched in the fuel cell were Fe(III)-reducers. Some of the isolated bacteria showed electrochemical activities, but they did not reduce Fe(III), and it is possible that their electrochemical activities were not related to Fe(III)-reduction.

To get a better and more reliable profile of the microbial diversity in the anode compartment, molecular tools were used. Results with 16S rRNA gene sequence analysis of samples removed from different positions showed that the biodiversities were clearly altered and influenced by position in the fuel cell. As discussed in Chapter IV, differences in each clone library could be due to the different metabolic characteristics of microorganisms present in the anode compartment. It was considered that the microbial community in wastewater and in the membrane biofilm, fermented complex fuel into products, and that these products could be used as substrates for electrochemically-active bacteria within the electrode biofilm to generate electricity. The increase in the γ-*Proteobacteria* in the electrode biofilm suggested that these microbes were involved in current generation. These results correspond with data using the microbiological approach. A genetic fingerprint of diversity in the anode compartment was obtained using DGGE on the 16S rRNA gene fragments. The DGGE banding patterns of bacterial clumps and for this electrode biofilm showed considerable similarity and indicate that no major differences in bacterial species was present. However, bands of different intensity appeared, and more detailed analysis is necessary to get a complete image of the microbial communities that are present. For further characterization of bands observed, DNA fragments can be excised from the gel, reamplified and sequenced. There are some difficulties in analysing the sequence data,

because the band may not be a single fragment. In addition, if we used small PCR product size and universal primers instead of specific gene target primers to amplify 16S rRNA gene fragments, poor sequence data were obtained.

5.4. Future work

Recent studies in molecular microbial ecology have revealed that prokaryotes identified by standard cultivation methods represent only a small proportion of viable microorganisms in nature (Amann *et al.*, 2003; Hugenholtz *et al.*, 1998; Pace, 1997). To investigate the full extent of microbial diversity within the microbial fuel cell, it may be that metagenomics, a culture-independent genomic analysis of microbial communities, could be introduced in future work (Liles *et al.*, 2003; Rondon *et al.*, 2000). Function- and sequence-driven approaches have been used to obtain information from metagenomic libraries (Schloss and Handelsman, 2003). It is possible to understand the complex ecological roles and interactions of uncultured microorganisms affiliated with novel phylogenetic groups concerning electrochemical activity. One of the problems with alanysis of metagenomic libraries is the low frequency of clones of a desired nature. To increase the proportion of active clones in a library, bromodeoxyuridine (BrdU) labeling, stable-isotope probing (SIP) and metagenomic library enrichment using polychlorinated biphenyl (PCB) as a model substrate have been widely used to enrich for the genomes of interest before cloning (Urbach *et al.*, 1999; Radajewski *et al.*, 2002; Murrell and Radajewski, 2000; Abraham *et al.*, 2002).

It was observed that electricity generated from the microbial fuel cell was directly proportional to the concentration of the wastewater. This observation suggests that it may be possible to use this system as a biosensor. Previously, BOD sensors using a

membrane and an O_2 probe have many problems such as membrane fouling, short-term stability and calibration drift (Kang *et al.*, 2003). However, in the case of the fuel cell type BOD sensor which is simpler and more accurate system than those employing specific electrodes no such problem should exist (Kim *et al.*, 2003). Therefore, application of Fe(III)-reducing bacteria with electrochemical activity which can metabolize a range of organic contaminants will be required to construct more efficient BOD sensors.

For more general applications of the fuel cell, electrochemically active microbes which can use a wide range of electron donors are needed either in pure culture or as consortia. Pure cultures selected using the range of electrochemical, microbiological and molecular techniques described in this study and others will be required to develop and verify higher energy outputs. This will help to gain an insight into the complex processes involved in bacteria-electrode communication, both by identification of the bacteria present and by varying anode parameters. It is also necessary to investigate further, anode processes at two different levels: biological and electrochemical optimization. It is believed that more useful mediator-less microbial fuel cell systems would be obtained through modifying and improving the fuel cell format, the electrode and by selecting electrochemically active microbes with better ability to transfer energy-rich electrons to an external electrode instead of using them in a normal electron transport chain. In the long run, it is aim to provide large-scale microbial fuel cells for specific applications.

5.5. Concluding remarks

This project has shown that electrochemically active bacteria can be enriched using

an electrochemical fuel cell, and that this system can remove organic contaminants with concomitant electricity generation. Conventional as well as molecular techniques can be used to determine bacterial community diversity in the electrode biofilm. It has been shown that there can be good agreement between culture-dependent methods and culture-independent methods. Some members of the family *Enterobacteriaceae* such as *Klebsiella* sp. and *Enterobacter* sp. of the γ-*Proteobacteria* with Fe(III)-reduction and electrochemical activity showed significant potential for the energy generation in this system.

REFERENCES

Abraham, W.R., Nogales, B., Golyshin, P.N., Pieper, D.H. and Timmis, K.N. 2002. Polychlorinated biphenyl-degrading microbial communities in soils and sediments. *Curr Opin Microbiol* **5**, pp. 246-253.

Allen, R.M. and Bennetto, H.P. 1993. Microbial fuel cells: Electricity production from carbohydrates. *Appl Biochem Biotechnol* **39**, pp. 27-40.

Altschul, S.F., Hadden, T.L., Schaffer, A.A., Zhang, J., Zhang, Z., Miller, W. and Lipman, D.J. 1997. Gapped BLAST and PSI-BLAST: a new generation of protein database search programs. *Nucleic Acids Res* **25**, pp. 3389-3402.

Amann, R.I., Binder, B.J., Olson, R.J., Chisholm, S.W., Devereux, R. and Stahl D.A. 1990a. Combination of 16S rRNA-targeted oligonucleotide probes with flow cytometry for analyzing mixed microbial populations. *Appl Environ Microbiol* **56**, pp. 1919-1925.

Amann, R.I., Krumholz, L. and Stahl, D.A. 1990b. Fluorescent oligonucleotide probing of whole cells for determinative, phylogenetic and environmental studies in microbiology. *J Bacteriol* **172**, pp. 762-770.

Amann, R.I., Ludwig, W. and Schleifer, K.H. 1995. Phylogenetic identificaiton and *in situ* detection of individual microbial cells without cultivation. *Microbiol Rev* **59**, pp. 143-169.

Amann, R.I., Stromley, J., Devereux, R., Key, R. and Stahl, D.A. 1992. Molecular and microscopic identification of sulfate-reducing bacteria in multispecies biofilms. *Appl Environ Microbiol* **58**, pp. 614-623.

Anderson, R.T., Rooney-varga, J.N., Gaw, C.V. and Lovley, D.R. 1998. Anaerobic benzene oxidation in the Fe(III) reduction zone of petroleum contaminated aquifers. *Environ Sci Technol* **32**, pp. 1222-1229.

Archer, D.B. and Kirsop, B.H. 1991. The microbiology and control of anaerobic digestion, pp. 43-91, *In* A. Wheatly (ed.), Anaerobic digestion: A Waste Treatment Technology. Elsevier Applied Science, London.

Ardeleanu, I., Margineaunu, D.G and Vais, H. 1983. Electrochemical conversion in biofuel cells using *Clostridium butyricum* or *Staphylococcus aureus* oxford. *Bioelectrochem Bioenerg* **11**, pp. 273-277.

Ardern, E. and Lockett, W.T. 1914. Experiments on the oxidation of sewage without the aid of filters. *J Soc Chem Ind* **33**, p. 523.

Arnold, R.G., DiChristina, T.J. and Hoffmann, M.R. 1986. Inhibitor studies of dissimilative Fe(III) reduction by *Pseduomonas* sp. Strain 200 (*Psedomonas ferrireductans*). *Appl Environ Microbiol* **52**, pp. 281-289.

Arnold, R.G., DiChristina, T.J. and Hoffmann, M.R. 1988. Reductive dissolution of Fe(III) oxides by *Pseudomonas* sp. 200. *Biotechnol Bioeng* **32**, pp. 1081-1096.

Arnold, R.G., Hoffmann, M.R., DiChristina, T.J. and Picardal, F.W. 1990. Regulation of dissimilatory Fe(III) reduction activity in *Shewanella putrefaciens*. *Appl Environ Microbiol* **56**, pp. 2811-2817.

Ashelford, K.E., Weightman, A.J. and Fry, J.C. 2002. PRIMROSE: a computer program for generating and estimating the phylogenetic range of 16S rRNA oligonucleotide probes and primers in conjunction with the RDP-II database. *Nucleic Acids Res* **30**, pp. 3481-3489.

Aston, W.J. and Turner, A.P.F. 1984. Biosensors and biofuel cells. In *Biotechnol Genet Eng Rev* **1**, pp. 89-120.

Baldi, F., Minacci, A., Pepi, M. and Scozzafava, A. 2001. Gel sequestration of heavy metals by *Klebsiella oxytoca* isolated from iron mat. *FEMS Microbiol Ecol* **36**, pp. 169-174.

Beliaev, A.S. and Saffarini, D.A. 1998. *Shewanella putrefaciens mtrB* encodes an outer membrane protein required for Fe(III) and Mn(IV) reduction. *J Bacteriol* **180**, pp. 6292-6297.

Beliaev, A.S., Saffarini, D.A., McLaughlin, J.L. and Hunnicutt, D. 2001. MtrC, an outer membrane decahaem *c* cytochrome required for metal reduction in *Shewanella putrefaciens* MR-1. *Mol Microbiol* **39**, pp. 722-730.

Bennetto, H.P. 1984. Microbial fuel cells. In *Life Chemistry Reports*. **2**, pp. 363-453. Harwood Academic, London.

Bennetto, H.P. 1990. "Bugpower"- the generation of microbial electricity. In *Frontiers of Science,* Chapter. **6**, pp. 60-82. Blackwell, Oxford.

Bennetto, H.P., Box, J., Delaney, G.M., Mason, J.R., Roller, S.D., Stirling, J.L. and Thurston, C.F. 1987. Redox-mediated electrochemistry of whole micro-organisms: from fuel cell to biosensors, pp. 291-314. *In* Turner, A.F.T., Karube, I. and Wilson, G.S. (ed.). Biosensors: Fundamentals and applications. Oxford university press, Oxford.

Bond, D.R. and Lovley D.R. 2003. Electricity production by *Geobacter sulfurreducens* attached to electrodes. *Appl Environ Microbiol* **69**, pp. 1548-1555.

Bond, D.R., Holmes, D.E., Tender, L.M. and Lovley, D.R. 2002. Electrode-reducing microorganisms that harvest energy from marine sediments. *Science* **295**, pp. 483-485.

Bragg, P.D. 1974. Nonheme iron in respiratory chains. In Microbial Iron Metabolism ed. Netherlands, J.B. pp.303-348, New York, Academic Press.

Brock, T.D. 1987. The study of microorganisms *in situ*: progress and problems. *Symp Soc Gen Microbiol* **41**, pp. 1-17.

Brock, T.D. and Gustafson, J. 1976. Ferric iron reduction by sulfur- and iron-oxidizing bacteria. *Appl Environ Microbiol* **32**, pp. 567-571.

Brock, T.M., Madigan, M.T., Martinko, J.M. and Parker, J. 1994. *Biology of microorganisms*. New jersey. 7th ed. Prentice-Hall, Inc.

Buck, J.D. 1982. Nonstaining (KOH) method for determination of gram reactions of marine bacteria. *Appl Envion Microbiol* **44**, pp. 992-993.

Caccavo, F.Jr., Blackemore, R.P. and Lovley, D.R. 1992. A hydrogen-oxidizing, Fe(III)-reducing microorganism from the Great Bay estuary, New Hampshire. *Appl Environ Microbiol* **58**, pp. 3211-3216.

Caccavo, F.Jr., Coates, J.D., Rossello-Mora, R.A., Ludwig, W., Schleifer, K.H., Lovley, D.R. and McInerney, M.J. 1996a. *Geovibrio ferrireducens*, a phylogenetically distinct dissimilatory Fe(III)-reducing bacterium. *Arch Microbiol* **165**, pp. 370-376.

Caccavo, F.Jr., Frolund, B., Van O. Kloeke, F. and Nielsen, P.H. 1996b. Defloculation of activated sludge by the dissimilatory Fe(III)-reducing bacterium *Shewanella alga* BrY. *Appl Environ Microbiol* **62**, pp.1487-1490.

Caccavo, F.Jr., Lonergan, D.J., Lovley, D.R., Davis, M., Stolz, J.F. and Mcinerney, M.J. 1994. *Geobacter sulfurreducens* sp. nov., a hydrogen-, and acetate-oxidizing dissimilatory metal-reducing microorganism. *Appl Environ Microbiol* **60**, pp. 3752-3759.

Chang, R. 1981. *Physical chemistry with application to biological systems*, 2nd ed. Macmillan Publishing, New York, N.Y.

Characklis, W. and Marshall, K.C. 1990. *Biofilms*. New York: John Wiley & Sons, Inc.

Chaudhuri, S.K. and Lovley, D.R. 2003. Electricity generation by direct oxidation of glucose in mediatorless microbial fuel cells. *Nature Biotechnol* **21**, pp. 1229-1232.

Childers, S.E. and Lovley, D.R. 2001. Differences in Fe(III) reduction in the hyperthermophilic archaeon, *Pyrobaculum islandicum*, versus mesophilic Fe(III)-reducing bacteria. *FEMS Microbiol Lett* **195**, pp. 253-258.

Coates, J.D., Bhupathiraju, V.K., Achenbach, L.A., Mclnerney, M.J. and Lovley, D.R. 2001. *Geobacter hydrogenophilus*, *Geobacter chapellei* and *Geobacter grbiciae*, three new, strictly anaerobic, dissimilatory Fe(III)-reducers. *Int J Syst Evol Microbiol* **51**, pp. 581-588.

Coates, J.D., Ellis, D.J. and Lovley, D.R. 1999. *Geothrix fermentans* gen. nov. sp. nov., an acetate-oxidizing Fe(III) reducer capable of growth via fermentation. *Int J Syst Microbiol* **49**, pp. 1615-1622.

Coates, J.D., Phillips, E.J.P., Lonergan, D.J., Jenter, H. and Lovley, D.R. 1996. Isolation of *Geobacter* species from diverse sedimentary environments. *Appl Environ Microbiol* **64**, pp. 1531-1536.

Coleman, M.L., Hedrick, D.B., Lovley. D.R., White, D.C. and Pye, K. 1993. Reduction of Fe(III) in sediments by sulphate-reducing bacteria. *Nature* **361**, pp. 436-438.

Costerton, J.W. 1995. Overview of microbial biofilms. *J Ind Microbiol* **15**, pp.137-140.

Costerton, J.W. and Lappin-Scott, H.M. 1989. Behavior of bacteria in biofilms. *ASM News* **55**, pp. 650-654.

Cummings, D.E., March, A.W., Bostick, B., Spring, S., Caccavo, F. Jr., Fendorf. S. and

Rosenzweig, R.F. 2000. Evidence for microbial Fe(III) reduction in anoxic, mining-impacted lake sediments (Lake Coeur d'Alene, Idaho). *Appl Environ Microbiol* **66**, pp. 154-162.

Curtis, P., Nakatsu, C.H. and Konopka, A. 2002. Aciduric proteobacteria isolated from pH 2.9 soil. *Arch Microbiol* **178**, pp. 65-70.

Daims, H., Bruhl, A., Amann, R., Schleifer, K.H. and Wanger, M. 1999. The domain-specific probe EUB338 is insufficient for the detection of all *Bacteria*: development and evaluation of a more comprehensive probe set. *Syst Appl Microbiol* **22**, pp. 434-444.

Dalevi, D., Hugenholtz, P. and Blackall, L.L. 2001. A multiple-outgroup approach to resolving division-level phylogenetic relationships using 16S rDNA data. *Int J Syst Evol Microbiol* **51**, pp. 385-391.

Das, A. and Caccavo, F.Jr. 2000. Dissimilatory Fe(III) oxide reduction by *Shewanella alga* BrY requires adhesion. *Curr Microbiol* **40**, pp. 344-347.

Davies, D.G., Parsek, M,R., Pearson, J.P., Iglewski B.H., Costerton, J.W. and Greenberg, E.P. 1998. The involvement of cell-to-cell signals in the development of a bacterial biofilm. *Science* **280**, pp. 295-298.

Davis, G., Hill, H.A.O., Aston, W.J., Higgins I.J. and Turner, A.P.F. 1983. Bioelectrochemical fuel cell and sensor based on a quinoprotein, alcohol dehydrogenase. *Enzyme Microbiol Technol* **5**, pp.383-388.

De Lucas, A., Canizares, P., Rodriguez, L. and Villasenor, J. 2000. Respirometric determination of the readily biodegradable COD produced in the anaerobic stage of a biological phosphorus removal process. *J Environ Sci Heal* **35**, pp. 49-64.

Delaney, G.M., Bennetto, H.P., Mason, J.R., Roller, S.D., Stirling, J.L. and Thurston, C.F. 1984. Electron-transfer coupling in microbial fuel cells. 2. Performance of fuel cells containing selected microorganism-mediator substrate combinations. *J Chem Tech Biotechnol* **34**, pp. 13-27.

DeLong, E.F. 1992. Archaea in coastal marine environments. *Proc Natl Acad Sci U.S.A.* **89**, pp. 5685-5689.

DeLong, E.F., Wickham, G.S. and Pace, N.R. 1989. Phylogenetic stains: ribosomal RNA-based probes for the identification of single microbial cells. *Science* **243**, pp. 1360-1363.

Dias, F.F. and Bhat, J.V. 1964. Microbial ecology of activated sludge. *Appl Environ Microbiol* **12**, pp. 412-417.

DiChristina, T.J. 1992. Effects of nitrate and nitrite on dissimilatory iron reduction by *Shewanella putrefaciens* 200. *J Bacteriol* **174**, pp. 1891-1896.

DiChristina, T.J. and DeLong, E.F. 1994. Isolation of anaerobic respiratory mutants of *Shewanella putrefaciens* and genetic analysis of mutants deficient in anaerobic growth on Fe^{3+}. *J Bacteriol* **176**, pp. 1468-1474.

Dobbin, P.S., Warren, L.H., Cook, N.J., Mcewan, A.G, Powell, A.K. and Richardson, D.J. 1996. Dissimilatory iron(III) reduction by *Rhodobacter capsulatus*. *Microbiol* **142**, pp. 765-774.

Dolfing, J. 1996. Degradation of monochlorinated and nonchlorinated aromatic compounds under iron-reducing conditions. *Appl Environ Microbiol* **62**, pp. 3554-3554.

Dollhopf, M.E., Nealson, K.H., Simon, D.M. and Luther, G.W. 2000. Kinetics of Fe(III) and Mn(IV) reduction by the Black Sea strain of *Shewanella putrefaciens* using *in situ* solid state voltammetric Au/Hg electrodes. *Mar Chem* **70**, pp. 171-180.

Eaton, A.D., Clesceri, L.S. and Greenberg, A.E. 1995. Standard methods for the examination of water and wastewater, 19th ed. American Public Health Association. Washington. DC.

Emde, R., Swain, A. and Schink, B. 1989. Anaerobic oxidation of glycerol by *Escherichia coli* in an amperometric poised-potential culture system. *Appl Microbiol Biotechnol* **32**, pp. 170-175.

Farrelly, V., Rainey, F.A. and Stackebrandt, E. 1995. Effect of genome size and rrn gene copy number on PCR amplification of 16S rRNA genes from a mixture of bacterial species. *Appl Environ Microbiol* **61**, pp. 2798-2801.

Felsenstein, J. 1985. Confidence limits on phylogenies: an approach using the bootstrap. *Evolution* **39**, pp. 783-791.

Fenchel, T. and Blackburn, T.H. 1979. Bacteria and mineral cycling. New York. Academic press.

Ferris, M.J., Muyzer, G. and Ward, D.M. 1996. Denaturing gradient gel electrophoresis profiles of 16S rRNA-defined populations inhabiting a hot spring microbial community. *Appl Environ Microbiol* **62**, pp. 340-346.

Fischer, S.G. and Lerman, L.S. 1979. Length-independent separation of DNA restriction fragments in two-dimensional gel electrophoresis. *Cell* **16**, pp. 191-200.

Fischer, W.R. 1988. Microbiological reactions of iron in soils. In *Iron in Soils and Clay Minerals*, ed. Stucki, J.W., Goodman, B.A., Schwertmann, U. pp. 715-748. Boston. Reidel.

Francis, C.A., Obraztsova, A.Y. and Tebo, B.M. 2000. Dissimilatory metal reduction by the facultative anaerobe *Pantoea agglomerans* SP1. *Appl Environ Microbiol* **66**, pp. 543-548.

Fredrickson, J.K. and Gorby, Y.A. 1996. Environmental processes mediated by iron-reducing bacteria. *Curr Opin Microbiol* **7**, pp. 287-294.

Friedrich, M.W. 2002. Phylogenetic analysis reveals multiple lateral transfers of adenosine-5'-phosphosulfate reductase genes among sulfate-reducing microorganisms. *J Bacteriol* **184**, pp. 278-289.

Frohlich, J., Sass, H., Babenzien, H.D., Kuhnigk, T., Varma, A., Saxena, S., Nalepa, C., Pfeiffer, P. and Konig, H. 1999. Isolation of *Desulfovibrio intestinalis* sp. nov. from the hindgut' of the lower termite *Mastotermes darwiniensis*. *Can J Microbiol* **45**, pp. 145-152.

Fry, J.C. 1990. Direct methods and biomass estimation. pp. 41-85. *In* J.R. Norris & R. Grigorova (ed.), Methods in microbiology, Vol 22, Techniques in microbial ecology. Academic Press, London.

Fultz, M.L. and Durst, R.A. 1982. Mediator compounds for the electrochemical study of biological redox systems: a compilation. *Anal Chim Acta* **140**, pp. 1-18.

Fuqua, C., Winnans, S.C. and Greenberg, E.P. 1996. Census and consensus in bacterial

ecosystems: the LuxR-LuxI family of quorum-sensing transcriptional regulators. *Annu Rev Microbiol* **50**, pp. 727-751.

Gaspard, S., Vazquez, F. and Hollifer, C. 1998. Localization and solubilization of the iron(III) reductase of *Geobacter sulfurreducens*. *Appl Environ Microbiol* **64**, pp. 3188-3194.

Ghiorse, W.C. 1988. Microbial reduction of manganese and iron. In *Biology of Anaerobic Microorganisms*, ed. Zehnder, A.J.B. pp. 305-331. New York: Wiley.

Ghosh, S., Ombregt, J.P. and Pipyn, P. 1985. Methane production from industrial wastes by two phase anaerobic digestion. *Water Res* **19**, pp. 1083-1088.

Gil, G.C., Chang, I.S., Kim, B.H., Kim, M., Jang, J.K., Park, H.S. and Kim, H.J. 2003. Operational parameters affecting the performance of a mediator-less microbial fuel cell. *Biosen Bioelectron* **18**, pp. 327-334.

Giovannoni, S. and Rappé, M. 2000. Evolution, diversity, and molecular ecology of marine prokaryotes, pp. 47-84. *In* D.L. Kirchman (ed.), Microbial ecology of the oceans. Wiley-Liss, Inc., New York, N.Y.

Giovannoni, S.J., DeLong, E.F., Olsen, G.J. and Pace, N.R. 1988. Phylogentic group-specific oligodeoxynucleotide probes for identificaiton of single microbial cells. *J Bacteriol* **170**, pp. 3584-3592.

Gold, T. 1992. The deep, hot biosphere. *Proc Natl Acad Sci USA* **89**, pp. 6045-6049.

Gorby, Y. and Lovley, D.R. 1991. Electron transport in the dissimilatory iron-reducer, GS-15. *Appl Environ Microbiol* **57**, pp. 867-870.

Gutell, R.R., Larsen, N. and Woese, C.R. 1994. Lessons from anevolving rRNA: 16S and 23S rRNA structures from a comparative perspective. *Microbiol Rev* **58**, pp. 10-26.

Haberman, W. and Pommer, E.H. 1991. Biological fuel cells with sulphide storage capacity. *Appl Microbiol Biotechnol* **35**, pp. 128-133.

Hanson, R.S. 1994. Methods for general and molecular bacteriology. American Society for Microbiology, Washington, DC

Harold, J.B. 1994. Microbiological Applications. 6th ed. Brown Publishers.

Head, I.M., Saunders, J.R. and Pickup, R.W. 1998. Microbial evolution, Diversity and ecology: A decade of Ribosomal RNA analysis of uncultivated microorganisms. *Microbiol Ecol* **35**, pp. 1-21.

Heijnen, J.J., Vanloosdrecht, M.C.M., Mulder, A. and Tijhuis, L. 1992. Formation of biofilms in a biofilm airlift suspension reactor. *Water Sci Technol* **26**, pp. 647-654.

Hicks, R.E., Amann, R.I. and Stahl, D.A. 1992. Dual staining of natural bacterioplankton with 4',6-diamidino-2-phenylindole and fluorescent oligonucleotide probes targeting kingdom-level 16S rRNA sequences. *Appl Environ Microbiol* **58**, pp. 2158-2163.

Higgins, I.J. and Hill, H.A.O. 1985. Bioelectrochemistry. *Essays Biochem.* **21**, pp. 119-145.

Hill, A.O. and Hunt, N.I. 1993. Direct and indirect electrochemical investigations of metalloenzymes. *Methods Enzymol* **227**, pp. 501-526.

Hiraishi, A., Masamune, K. and Kitamura, H. 1989. Characterization of the bacterial population structure in an anaerobic-aerobic activated sludge system on the basis of respiratory quinone profiles. *Appl Environ Microbiol* **55**, pp. 897-901.

Hitchens, G.D. 1989. Electrodes surface microstrucures in studies of biological electron transfer. *Trends Biochem Sci* **14**, pp. 152-155.

Holmes, D.E., Bond, D.R. and Lovley, D.R. 2004. Electron transfer by *Desulfobulbus propionicus* to Fe(III) and Graphite electrodes. *Appl Environ Microbiol* **70**, pp. 1234-1237.

Hoover, S.R. and Porges, N. 1952. Assimilation of dairy wastes by activated sludge II: the equation of synthesis and oxygen utilization. *Sewage Ind Waste* **24**.

Hoyle, B.D., Jass, J. and Costerton, J.W. 1990. The biofilm glycocalyx as a resistance factor. *J Antimicrob Chemother* **26**, pp. 1-5.

Hugenholtz, P., Goebel, B.M. and Pace, N.R. 1998. Impact of culture-independent studies on the emerging phylogenetic view of bacterial diversity. *J Bacteriol* **180**, pp. 4765-4774.

Hugenholtz, P., Pitulle, C., Hershberger, K.L. and Pace, N.R. 1998. Novel division bacterial diversity in a Yellowstone hot spring. *J Bacteriol* **180**, pp. 366-376.

Hugenholtz, P., Tyson, G.W., Webb, R.I., Wagner, A.M. and Blackall, L.L. 2001. Investigation of candidate division TM7, a recently recognized major lineage of the domain bacteria with no known pure-culture representatives. *Appl Environ Microbiol* **67**, pp. 411-419.

Hungate, R.E. 1969. A roll tube method for cultivation of strict anaerobes. *Methods in Microbiol* **3B**, pp. 117-132.

Huser, B.A., Wuhrmann, K. and Zehnder, A.J.B. 1982. *Methanothrix soehngenii* gen. nov. sp. nov., a new acetotrophic non-hydrogen-oxidizing bacterium. *Arch Microbiol* **132**, pp. 1-9.

Hyun, M.S., Kim, B.H., Chang, I.S., Park, H.S., Kim, H.J., Kim, G.T., Kim, M.A. and Park, D.H. 1999. Isolation and identification of an anaerobic dissimilatory Fe(III)-reducing bacterium, *Shewanella putrefaciens* IR-1. *J Microbiol* **37**, pp. 206-212.

Iizuka, T. and Kotani, M. 1968. Analysis of a thermal equilibrium phenomenon between high-spin and low-spin states of ferrimyoglobin azide. *Biochim Biophys Acta* **154**, pp. 417-419.

Itamar, W., Arad, G. and Katz, E. 1998. A biofuel cell based on pyrroloquinoline quinoe and mciroperoxidase-11 monolayer-functionalized electrodes. *Biochelectrochem Bioenerget* **44**, pp. 209-214.

Jones, J.G. 1979. A guide to methods for estimating microbial numbers and biomass in fresh water. Freshwater Biological Association. Ambleside.

Jukes, T.H. and Cantor, C.R. 1969. Evolution of protein molecules, pp. 21-132. *In* H. N. Munro (ed.), Mammalian protein metabolism. Academic Press, New York, U.S.A.

Kang, K.H., Jang, J.K., Pham, T.H., Moon, H.S., Chang, I.S. and Kim, B.H. 2003. A microbial fuel cell with improved cathode reaction as a low biochemical oxygen

demand sensor. *Biotechnol Lett* **25**, pp. 1357-1361.

Kaprelyants, A.S., Gottschal, J.C. and Kell, D.B. 1993. Dormancy in non-sporulating Bacteria. *FEMS Microbiol Rev* **104**, pp. 271-286.

Kashefi, K., Holmes, D.E., Reysenbach, A.-L. and Lovley, D.R. 2002. Use of Fe(III) as an electron acceptor to recover previously uncultured hyperthermophiles: isolation and characterization of *Geothermobacterium ferrireducens* gen. nov., sp. nov. *Appl Environ Microbiol* **68**, pp. 1735-1742.

Kazlauskaite, J., Hill, H.A.O., Wilkins, P.C. and Dalton, H. 1996. Direct electrochemistry of the hydroxylase of soluble methane monooxygenase from *Methylococcus capsulatus* (Bath). *Eur J Biochem* **241**, pp. 552-556.

Kazumi, J., Haggblom, M.M. and Young, L.Y. 1995. Degradation of monochlorinated and nonchlorinated aromatic compounds under iron-reducing conditions. *Appl Environ Microbiol* **61**, pp. 4069-4073.

Kim B.H. 1995. Microbial physiology. Seoul. 2th ed Academy press.

Kim, B.H. 2002. A mediator-less microbial fuel cell, enrichment and optimization. In: Kim, B.H. *et al.* eds. Proceedings of the 9th international symposium on genetics of industrial microorganisms. pp. 7-14.

Kim, B.H., Chang, I.S., Gil, G.C., Park, H.S. and Kim, H.J. 2003. Novel BOD (biological oxygen demand) sensor using mediator-less microbial fuel cell. *Biotechnol Lett* **25**, pp. 541-545.

Kim, B.H., Ikeda, T., Park, H.S., Kim, H.J., Hyun, M.S., Kano, K., Takagi, K. and Tatsumi, H. 1999a. Electro-chemical activity of an Fe(III)-reducing bacterium, *Shewanella putrifaciens* IR-1, in the presence of alternative electron acceptors. *Biotechnol Tech* **13**, pp. 475-478.

Kim, B.H., Kim. H.J., Hyun, M.S. and Park, D.H. 1999b. Direct electrode reaction of Fe(III)-reducing bacterium, *Shewanella putrifaciens*. *J Microbiol Biotechnol* **9**, pp. 127-131.

Kim, G.T., Hyun, M.S., Chang, I.S., Kim, H.J., Park, H.S., Kim, B.H., Kim, S.D., Wimpenny, J.W.T. and Weightman, A.J. 2004. Dissimilatory Fe(III) reduction by

electrochemically active lactic acid bacterium phylogenetically related to *Enterococcus gallinarum* isolated from submerged soil. *J Appl Microbiol* (submitted).

Kim, H.J., Hyun, M.S., Chang, I.S. and Kim, B.H. 1999. A microbial fuel cell type lactate biosensor using a metal-reducing bacterium, *Shewanella putrefaciens*. *J Microbiol Biotechnol* **9**, pp. 365-367.

Kim, H.J., Park, H.S., Hyun, M.S., Chang, I.S., Kim, M. and Kim, B.H. 2002. A mediator-less microbial fuel cell using a metal reducing bacterium, *Shewanella putrefaciens*. *Enzyme Microb Technol* **30**, pp. 145-152.

Kim, N., Choi, Y., Jung, S., and Kim, S. 2000. Effect of initial carbon sources on the performance of microbial fuel cells containing *Proteus vulgaris*. *Biotechnol Bioeng* **70**, pp. 109-114.

Kim, T.S. and Kim, B.H. 1988. Modulation of *Clostridium acetobutylicum* fermentation by electrochemically supplied reducing equivalent. *Biotechnol Lett* **10**, pp. 123-128.

Knight, V. and Blakemore, R. 1998. Reduction of diverse electron acceptors by *Aeromonas hydrophila*. *Arch Microbiol* **169**, pp. 239-248.

Kopczynski, E.D., Bateson, M.M. and Ward, D.M. 1994. Recognition of chimeric small-subunit ribosomal DNAs composed of genes from uncultivated microorganisms. *Appl Environ Microbiol* **60**, pp. 746-748.

Lawrence, J.R., Korber, D.R., Hoyle, B.D., Costerton, J.W. and Caldwel, D.E. 1991. Optical sectioning of microbial fuel biofilms. *J Bacteriol* **173**, pp. 6558-6567.

Lee, J., Phung, N.T., Chang, I.S., Kim, B.H. and Sung, H.C. 2003. Use of acetate for enrichment of electrochemically active microorganisms and their 16S rDNA analyses. *FEMS Microbiol Lett* **223**, pp. 185-191.

Liles, M.R., Manske, B.F., Bintrim, S.B., Handelsman, J. and Goodman, R.M. 2003. A census of rRNA genes and linked genomic sequences within a soil metagenomic library. *Appl Environ Microbiol* **69**, pp. 2684-2691.

Lloyd, J.R., Blunt-Harris, E.L. and Lovley, D.R. 1999. The periplasmic 9.6-kilodalton *c*-type cytochrome of *Geobacter sulfurreducens* is not an electron shuttle to Fe(III). *J*

Bacterial **181**, pp. 7647-7649.

Lloyd, J.R., Sole, V.A., Van Praagh, C.V.G. and Lovley, D.R. 2000. Direct and Fe(II)-mediated reduction of technetium by Fe(III)-reducing bacteria. *Appl Environ Microbiol* **66**, pp. 3743-3749.

Lojou, E., Bianco, P. and Bruschi, M. 1998. Kinetic studies on the electron transfer between bacterial *c*-type cytochromes and metal oxides. *J Electroanal Chem* **452**, pp. 167-177.

Lonergan, D.J. and Lovley, D.R. 1991. Microbial oxidation of natural and anthropogenic aromatic compounds coupled to Fe(III) reduction. In *Organic Substances and Sediments in Water*, ed. Baker, R.A. pp. 327-338. Chelsea, MI: Lewis.

Lonergan, D.J., Jenter, H.L., Coates, J.D., Phillips, E.J.P., Schmidt, T.M. and Lovley, D.R. 1996. Phylogenetic analysis of dissimilatory Fe(III)-reducing bacteria. *J Bacteriol* **178**, pp. 2402-2408.

Lovley, D.R. 1987. Organic matter mineralization with the reduction of ferric iron: a review. *Geomicrobiol J* **5**, pp. 375-399.

Lovley, D.R. 1991. Dissimilatory Fe(III) and Mn(IV) reduction. *Microbiol Rev* **55**, pp. 259-287.

Lovley, D.R. 1992. Microbial oxidation of organic matter coupled to the reduction of Fe(III) and Mn(IV) oxides. *Catena* **21**, pp. 101-114.

Lovley, D.R. 1993. Dissimilatory metal reduction. *Annu Rev Microbiol.* **47**, pp. 263-290.

Lovley, D.R. 1995. Microbial reduction of iron, manganese and other metals. *Adv Agron* **54**, pp. 175-231.

Lovley, D.R. 1997. Microbial Fe(III) reduction in subsurface environments *FEMS Microbiol Rev* **20**, pp. 305-313.

Lovley, D.R. 2000. Fe(III) and Mn(IV) reduction. In *Environmental Microbe Metal Interactions*. Ed. Lovley, D.R. pp. 3-30. Washington. ASM.

Lovley, D.R. and Lonergan, D.J. 1990. Anaerobic oxidation of toluene, phenol, and *p*-cresol by the dissimilatory iron-reducing organism, GS-15. *Appl Environ Microbiol* **56**, pp.1858-1864.

Lovley, D.R. and Phillips, E.J.P. 1986. Organic matter mineralization with reduction of ferric iron in anaerobic sediments. *Appl Environ Microbiol* **51**, pp. 683-689.

Lovley, D.R. and Phillips, E.J.P. 1988. Novel mode of microbial energy metabolism: organic carbon oxidation coupled to dissimilatory reduction of iron or manganese. *Appl Environ Microbiol* **54**, pp. 1472-1480.

Lovley, D.R. and Phillips, E.J.P. 1989. Requirement for a microbial consortium to completely oxidize glucose in Fe(III)-reducing sediments. *Appl Environ Microbiol* **55**, pp. 3234-3236.

Lovley, D.R., Baedecker, M.J., Lonergan, D.J., Cozzarelli, I.M., Phillips, E.J.P. and Siegel, D.I. 1989a. Oxidation of aromatic contaminants coupled to microbial iron reduction. *Nature* **339**, pp. 297-299.

Lovley, D.R., Caccavo, F. and Phillips, E.J.P. 1992. Acetate oxidation by dissimilatory Fe(III) reducers. *Appl Environ Microbiol* **58**, pp. 3205-3206.

Lovley, D.R., Giovannoni, S.J., White, D.C., Champine, J.E., Phillips, E.J.P., Gorby, Y.A. and Goodwin, S. 1993a. *Geobacter metallireducens* gen. nov. sp. nov., a microorganism capable of coupling the complete oxidation of organic compounds to the reduction of iron and other metals. *Arch Microbiol* **159**, pp. 336-344.

Lovley, D.R., Kashefi, K., Vargas, M., Tor, J.M. and Blunt-Harris, E.L. 2000. Reduction of humic substances and Fe(III) by hyperthermophilic microorganisms. *Chem Geol* **169**, pp. 289-298.

Lovley, D.R., Phillips, E.J.P. and Lonergan, D.J. 1989b. Hydrogen and formate oxidation coupled to dissimilatory reduction of iron or manganese by *Alteromonas putrefaciens*. *Appl Environ Microbiol* **55**, pp. 700-706.

Lovley, D.R., Phillips, E.J.P. and Lonergan, D.J. 1991. Enzymatic versus nonenzymatic mechanisms for Fe(III) reduction in aquatic sediments. *Environ Sci Technol* **25**, pp. 1062-1267.

Lovley, D.R., Phillips, E.J.P., Lonergan, D.J. and Widman, P.K. 1995. Fe(III) and S^0 reduction by *Pelobacter carbinolicus*. *Appl Environ Microbiol* **61**, pp. 2132-2138.

Lovley, D.R., Roden, E.E., Phillips, E.J.P. and Woodwar, J.C. 1993b. Enzymatic iron and uranium reduction by sulfate-reducing bacteria. *Marine Geol* **113**, pp. 41-53.

Lovley, D.R., Stolz, J.F., Nord, G.L. and Phillips, E.J.P. 1987. Anaerobic production of magnetite by a dissimilatory iron-reducing microorganism. *Nature* **330**, pp. 252-254.

Lovley, D.R., Widman, P.K., Woodward, J.C. and Phillips, E.J.P. 1993c. Reduction of uranium by cytochrome c_3 of *Desulfovibrio vulgaris*. *Appl Environ Microbiol* **59**, pp. 3572-3576.

Mackie, R.I. and Bryant, M.P. 1981. Metabolic activity of fatty acid-oxidizing bacteria and the contribution of acetate, propionate, butyrate and CO_2 to methanogenesis in cattle waste at 40 and 60℃. *Appl Envrion Microbiol* **41**, pp. 1363-1373.

Magnuson, T.S., Hodges-Myerson, A.L. and Lovley, D.R. 2000. Characterization of a membrane-bound NADH-dependent Fe^{3+} reductase from the dissimilatory Fe^{3+}-reducing bacterium *Geobacter sulfurreducens*. *FEMS Microbiol Lett* **185**, pp. 205-211.

Maidak, B.L., Cole, J.R., Lilburn, T.G, Parker, C.T., Saxman, P.R., Stredwick, J.M., Garrity, G.M., Li, B., Olsen, G.J., Pramanik, S., Schmidt, T.M. and Tiedje, J.M. 2000. The RDP (Ribosomal Database Project) continues. *Nucleic Acids Res* **28**, pp. 173-174.

Manz, W., Amann, R., Ludwig, W., Vancanneyt, M. and Schleifer, K.H. 1996. Application of a suite of 16S rRNA-specific oligonuleotide probes designed to investigate bacteria of the phylum *Cytophaga-Flavobacter-Bacteroides* in the natural environment. *Microbiol* **142**, pp. 1097-1106.

Manz, W., Amann, R., Ludwig, W., Wanger, M. and Schleifer, K.H. 1992. Phylogenetic oligodeoxynucleotide probes for for the major subclasses of *Proteobacteria*: problems and solutions. *Syst Appl Microbiol* **15**, pp. 593-600.

Manz, W., Wagner, M., Amann, R. and Schleifer, K.H. 1994. *In situ* characterization of the microbial consortia active in two wastewater treatment plants. *Wat Res* **28**, pp. 1715-1723.

Marchesi, J.R., Sato, T., Weightman, A.J., Martin, T.A., Fry, J.C., Hiom, S.J. and Wade,

W.G. 1998. Design and evaluation of useful bacterium-specific PCR primers that amplify genes coding for bacterial 16S rRNA. *Appl Environ Microbiol* **64**, pp. 795-799.

Marsh, T.L. 1999. Terminal restriction fragment length polymorphism (T-RFLP): an emerging method for characterizing diversity among homologous populations of amplification products. *Curr Opin Microbiol* **2**, pp. 323-327.

Marshall, K.C. 1976. *Interfaces in Microbial Ecology.* Cambridge: Harvard University Press.

Marshall, K.C. 1988. Adhesion and growth of bacteria at surfaces in oligotrophic environments. *Can J Microbiol* **34**, pp. 503-506.

McCaig, A.E., Embley, T.M. and Prosser, J.I. 1994. Molecular analysis of enrichment cultures of marine ammonia oxidizers. *FEMS Microbiol Lett* **120**, pp. 363-368.

McCarty, P.L. and Smith D.P. 1986. Anaerobic wastewater treatment. *Environ Sci Tech* **20**, pp. 1200-1226.

McEldowney, S. and Fletcher, M. 1986. Effect of growth conditions and surface characteristics of aquatic bacteria on their attachment to soild surfaces. *J Gen Microbiol* **132**, pp. 513-523.

McInernay, M.J., Bryant, M.P., Hespell, R.B. and Costerton, J.W. 1981. *Syntrophomonas wolfei*, gen. Nov. sp. Nov., an aerobic syntrophic, fatty acid-oxidizing bacterium. *Appl Environ Microbiol* **41**, pp. 1029-1039.

McLaughlin, J.R., Ryden, J.C. and Syers, J.K. 1981. Sorption of inorganic phosphate by iron- and aluminum-containing components. *J Soil Sci* **32**, pp. 365-377.

Meier, H., Amann, R., Ludwig, W. and Schleifer, K.H. 1999. Specific oligonucleotide probes for *in situ* detection of a major group of gram-positive bacteria with low DNA G+C content. *Syst Appl Microbiol* **22**, pp. 186-196.

Metcalf and Eddy, Inc. 1991. *Wastewater Engineering: Treatment, Disposal and reuse* (3rd ed.). New York. McGraw Hill.

Mikkelsen, L.H., Gotfredsen, A.K., Agerbak, M.L., Nelsen, P.H. and Keiding, K. 1996. Effects of colloidal stability on clarification and dewatering of activated sludge. *Wat*

Sci Tech **34**, pp. 449-457.

Mittelman, M.W. 1998. Structure and functional characteristics of bacterial biofilms in fluid processing operations. *J Dairy Sci* **81**, pp. 2760-2764.

Mittelman, M.W. and Geesey, G.G. 1985. Copper-binding characteristics of exopolymers from a freshwater-sediment bacterium. *Appl Environ Microbiol* **49**, pp. 846-851.

Morita, R.Y. 1982. Starvation-survival of heterotrophs in the marine environment. *Adv Microb Ecol* **6**, pp. 171-198.

Morita, R.Y. 1985. Starvation and miniaturization of heterotrophs, with special emphasis on maintenance of the starved viable state. pp. 111-130 in Bacteria in the Natural Environments: The Effect of Nutrient Conditions. Fletcher, M and Floodgate, G. *Soc. Gen. Microbiol.* London.UK.

Mosteller, T. M. and Bishop, J.R. 1993. Sanitizer efficacy against attached bacteria in a milk biofilm. *J Food Prot* **56**, pp. 34-41.

Murrell, J.C. and Radajewski, S. 2000. Cultivation-independent techniques for studying methanotroph ecology. *Res Microbiol* **151**, pp. 807-814.

Muyzer, G., de Waal, E.C. and Uitterlinden, A.G. 1993. Profiling of complex microbial populations by denaturing gradient gel electrophoresis analysis of polymerase chain reaction-amplified genes coding for16S rRNA. *Appl Environ Microbiol* **59**, pp. 695-700.

Myers, C.R. and Myers, J.M. 1992. Localization of cytochromes to the outer membrane of anaerbically grown *Shewanella putrefaciens* MR-1. *J Bacteriol* **174**, pp. 3429-3438.

Myers, C.R. and Myers, J.M. 1993. Ferric reductase is associated with the membranes of anaerbically grown *Shewanella putrefaciens* MR-1. *FEMS Microbiol Lett* **108**, pp. 15-22.

Myers, C.R. and Myers, J.M. 1994. Ferric iron reduction-linked growth yields of *Shewanella putrefaciens* MR-1. *J Appl Bacterial* **76**, pp, 253-258.

Myers, C.R. and Myers, J.M. 1997. Outer membrane cytochromes of *Shewanella putrefaciens* MR-1: spectral analysis, and purification of the 83-kDA *c*-type cytochrome. *Biochim Biophys Acta.* **1326,** pp. 307-318.

Myers, C.R. and Nealson, K.H. 1988. Bacterial manganese reduction and growth with manganese oxide as the sole electron acceptor. *Science* **240,** pp. 1319-1321.

Myers, C.R. and Nealson, K.H. 1990. Respiration-linked proton translocation coupled to anaerobic reduction of manganese(IV) and iron(III) in *Shewanella putrefaciens* MR-1. *J Bacterial* **172,** pp. 6232-6238.

Nealson, K.H. and Krause, B. 1997. Physiology and enzymology involved in dinitrification by *Shewanella putrefaciens. Appl Environ Microbiol* **63,** pp. 2613-2618.

Nealson, K.H. and Saffarini, D. 1994. Iron and manganese in anaerobic respiration: Environmental significance, physiology, and regulation. *Annu Rev Microbiol* **48,** pp. 311-343.

Neef, A., Amann, R., Schlesner, H. and Schleifer, K.H. 1998. Monitoring a widespread bacterial group: in situ detection of *Planctomycetes* with 16S rRNA-targeted probes. *Microbiol* **144,** pp. 3257-3266.

Nevin, K.P. and Lovley, D.R. 2000. Lack of production of electron-shuttling compounds or solubilization of Fe(III) oxide by *Geobacter metallireducens. Appl Environ Microbiol* **66,** pp. 2248-2251.

Newman, D.K. and Kolter, R. 2000. A role for excreted quinines in extracellular electron transfer. *Nature* **405,** pp. 94-97.

Nielsen, J.L., Juretschko, S., Wagner, M. and Nielsen, P.H. 2002. Abundance and phylogenetic affiliation of iron reducers in activated sludge as assessed by fluorescence in situ hybridization and microautoradiography. *Appl Environ Microbiol* **68,** pp. 4629-4636.

Nielsen, P.H. 1996. The significance of microbial Fe(III) reduction in the activated sludge process. *Wat Sci Tech* **34,** pp. 129-136.

Nielsen, P.H., Frolund, B., Spring, S. and Caccavo, F. 1997. Microbial Fe(III) reduction in activated sludge. *Syst Appl Microbiol* **20,** pp. 645-651.

O'Toole, G.A. and Kolter, R. 1998. Initiation of biofilm formation in *Pseudomonas fluorescens* WCS356 proceeds via multiple, convergent signaling pathways: a genetic analysis. *Mol Microbiol* **28**, pp. 449-461.

Obuekwe, C.O., Westlake, D.W.S. and Cook, F.D. 1981. Effect of nitrate on reduction of ferric iron by a bacterium isolated form crude oil. *Can J Microbiol* **27**, pp. 692-697.

Olsen, G.J., Lane, D.J., Giovannoni, S.J., Pace, N.R. and Stahl, D.A. 1986. Microbial ecology and evolution: a ribosomal RNA approach. *Ann Rev Microbiol* **40**, pp. 337-365.

Olsen, G.J., Woese, C.R. and Overbeek, R. 1994. The winds of (evolutionary) change:breathing new life into microbiology. *J Bacteriol* **176**, pp. 1-6.

Pace, N.R. 1997. A molecular view of microbial diversity and the biosphere. *Science* **276**, pp. 734-740.

Park, D.H. and Zeikus, J.G. 2000. Electricity generation in microbial fuel cells using neutral red as an electronophore. *Appl Environ Microbiol* **66**, pp. 1292-1297.

Park, D.H., Kim, B.H., Moore, B., Hill, H.A.O., Song, M.K. and Rhee, H.W. 1997. Electrode reaction of *Desulfovibrio desulfuricans* modified with organic conductive compounds. *Biotechnol Tech* **11**, pp. 145-148.

Park, D.H., Laivenieks, M., Guettler, M.V., Jain, M.K. and Zeikus, J.G. 1999. Microbial utilization of electrically reduced neutral red as the sole electron donor for growth and metabolite production. *Appl Environ Microbiol* **65**, pp. 2912-2917.

Park, H.S., Kim, B.H., Kim, H.S., Kim, H.J., Kim, G.T., Kim, M., Chang, I.S., Park, Y.K. and Chang, H.I. 2001. A novel electrochemically active and Fe(III) reducing bacterium phylogenetically related to *Clostridium butyricum* isolated from a bacterial fuel cell. *Anaerobe* **7**, pp. 297-306.

Pham, C.A., Jung, S.J., Phung, N.T., Lee, J., Chang, I.S., Kim, B.H., Yi, H. and Chun, J. 2003. A novel electrochemically active and Fe(III)-reducing bacterium phylogenetically related to *Aeromonas hydrophila*, isolated from a microbial fuel cell. *FEMS Microbiol lett* **223**, pp. 129-134.

Phillips, E.J.P. and Lovley, D.R. 1987. Determination of Fe(III) and Fe(II) in oxalate

extract of sediment. *Soil Sci Soc Am J* **51**, pp. 938-941.

Plotkin, E.V., Higgins, I.J. and Hill, H.A.O. 1981. Methanol dehydrogenase bioelectrochemical cell and alcohol detector. *Biotechnol Lett* **3**, pp. 187-192.

Polprasert, C. 1989. *Organic Wastes Recycling*. Wiley, Chichester, U.K.

Pratt, L.A. and Kolter, R. 1998. Genetic analysis of *Escherichia coli* biofilm formation ; roles of flagella, motility, chemotaxis and type 1 pili. *Mol Microbiol* **30**, pp. 285-293.

Pronk, J.T., Liem, K., Bos, P. and Kuenen, J.G. 1991. Eenergy transduction by anaerobic ferric iron respiration in *Thiobacillus ferrooxidans*. *Appl Environ Microbiol* **57**, pp. 2063-2068.

Radajewski, S., Ineson, P., Parekh, N.R. and Murrell, J.C. 2000. Stable-isotope probing as a tool in microbial ecology. *Nature* **403**, pp. 646-649.

Radajewski, S., Webster, G., Reay, D.S., Morris, S.A., Ineson, P., Nedwell, J.I., Prosser, I. and Murrell, J.C. 2002. Identification of active methylotroph populations in an acidic forest soil by stable-isotope probing. *Microbiol* **148**, pp. 2331-2342.

Rainey, F.A., Ward, N., Sly, L.I. and Stackebrandt, E. 1994. Dependence on the taxon composition of clone libraries for PCR amplified, naturally occurring 16S rDNA, on the primer pair and the cloning system. *Experientia* **50**, pp. 796-797.

Rasmussen, H. and Nielsen, P.H. 1996. Iron reduction in activated sludge measured with different extraction techniques. *Wat Res* **30**, pp. 551-558.

Rasmussen, H., Bruus, J.H., keiding, K. and Nielsen, P.H. 1994. Observation on dewaterability and physical, chemical and microbiological changes in anaerobically stored activated sludge from a nutrient removal plant. *Wat Res* **28**, pp. 417-425.

Reysenbach, A.L., Giver, L.J., Wickman, G.S. and Pace, N.R. 1992. Differential amplification of rRNA genes by polymerase chain reaction. *Appl Environ Microbiol* **58**, pp. 3417-3418.

Rittmann, B.E., Jackson, D.E. and Storck, S.L. 1988. Potential for treatment of hazardous organic chemicals with biological processes. *Biotreatment Systems* **3**, pp. 15-

64, D.L. Wise, Ed. CRC Press, Boca Raton, FL.

Rochelle, P.A., Cragg, B.A., Fry, J.C., Parkes, R.J. and Weightman, A.J. 1994. Effect of sample handling on estimation of bacterial diversity in marine sediments by 16S rRNA gene sequence analysis. *FEMS Microbiol Ecol* **15**, pp. 215-226.

Roden, E.E. and Lovley, D.R. 1993. Dissimilatory Fe(III) reduction by the marine microorganism, *Desulfuromonas acetoxidans*. *Appl Environ Microbiol* **59**, pp. 734-742.

Rölleke, S., Muyzer, G., Wawer, C., Wanner, G. and Lubitz, W. 1996. Identification of bacteria in a biodegraded wall painting by denaturing gradient gel electrophoresis of PCR-amplified gene fragments coding for 16S rRNA. *Appl Environ Microbiol* **62**, pp. 2059-2065.

Roller, C., Wanger, M., Amann, R., Ludwig, W. and Schleifer, K.H. 1994. *In situ* probing of gram–positive bacteria with high DNA G+C content using 23S rRNA targeted oligonucleotide. *Microbiol* **140**, pp. 2849-2858.

Roller, S.B., Bennetto, H.P., Delaney, G.M., Mason, J.R., Striling, J.L. and Thurston, C.F. 1984. Electron-transfer coupling in microbial fuel cells. 1. Comparison of redox-mediator reduction rates and respiratory rates of bacteria. *J Chem Tech Biotechnol* **34B**, pp. 3-12.

Rondon, M.R., August, P.R., Bettermann, A.D., Brady, S.F., Grossman, T.H., Liles, M.R., Loiacono, K.A., Lynch, B.A., MacNeil, I.A., Minor, C., Tiong, C.L., Gilman, M., Osburne, M.S., Clardy, J., Handelsman, J. and Goodman, R.M. 2000. Cloning the soil metagenome: a strategy for accessing the genetic and functional diversity of uncultured microorganisms. *Appl Environ Microbiol* **66**, pp. 2541-2547.

Sambrook, J., Fritsch, E.F. and Maniatis, T. 1989. Molecular cloning: a laboratory manual, 2nd ed. Cold Spring Harbor Laboratory Press. Cold Spring Harbor. New York.

Schäfer, H. and Muyzer, G. 2000. Denaturing gradient gel electrophoresis in marine microbial ecology. In Paul, J.H., ed. Marine Microbiology. Methods in Microbiology, vol. **30**. Academic Press, London, pp. 425-468.

Schink, B. and Bomar, M. 1992. The genera *Acetobacterium*, *Acetogenium*, *Acetoanaerobium* and *Acetitomaculum*. In Balows A., Trüper, H.G., Dworkin, M., Harder, W. and Schleifer, K.-H., eds. The Prokaryotes, pp, 1923-1936. Springer-Verlag.

New York

Schmalenberger, A., Schwieger, F. and Tebbe, C.C. 2001. Effect of primers hybridizing to different evolutionarily conserved regions of the small-subunit rRNA gene in PCR-based microbial community analyses and genetic profiling. *Appl Environ Microbiol* **67**, pp. 3557-3563.

Schloss, P.D. and Handelsman, J. 2003. Biotechnological prospects from metagenomics. *Curr Opin Biotechnol* **14**, pp. 303-310.

Seeliger, S., Cord-Ruwisch, R. and Schink, B. 1998. A periplasmic and extracellular *c*-type cytochromes of *Geobacter sulfurreducens* acts as a ferric iron reductase and as an electron carrier to other acceptors or to partner bacteria. *J Bacterial* **180**, pp. 3686-3691.

Selenska-Pobell, S. 2002. Diversity and activity of bacteria in uranium mining waste piles, pp. 225-254. *In* Keith-Roach, M.J. and Lievens, F.R. (eds.), Radioactivity in the environment. Elsevier, New York, N.Y.

Semple, K.M. and Westlake, D.W.S. 1987. Characterization of iron-reducing *Alteromonas putrefaciens* strains from oil field fluids. *Can J Microbiol* **33**, pp. 366-371.

Seviour, R.J. and Blackall, L.L. 1999. The microbiology of activated sludge. Kluwer Academic Publishers. pp. 285-291. London, United Kingdom.

Sheffield, V.C., Cox, D.R., Lerman, L.S. and Myers, R.M. 1989. Attachment of a 40-base pair G+C rich sequence (GC-clamp) to genomic DNA fragments by the polymerase chain reaction results in improved detection of single-base changes. *Pros Natl Acad Sci* USA **86**, pp. 232-236.

Smith, M.R. and Mah, R.A. 1978. Growth and methanogenesis by *Methanosarcina* strain 227 on acetate and methanol. *Appl Environ Microbiol* **36**, pp 870-879.

Snaidr, J., Amann, R., Huber, I., Ludwig, W. and Schleifer, K.H. 1997. Phylogenetic analysis and in situ identification of bacteria in activated sludge. *Appl Environ Microbiol* **63**, pp. 2884-2896.

Sterritt, R.M. and Lester, J.N. 1988. *Microbiology for Environmental and Public Health Engineers*. Spon, London, UK.

Sugio, T., Katagiri, T., Inagaki, K. and Tano, T. 1989. Actual substrate for elemental sulfur oxidation by sulfur: ferric ion oxidoreductase purified from *Thiobacillus ferrooxidans*. *Biochim Biophys Acta* **973**, pp. 250-256.

Tayhas, G., Palmore, R. and Whitesides, M. 1994. Microbial and enzymatic biofuel cells, pp. 271-290. Enzymatic conversion of biomass for fuels production. *In* Himmel, M.E., Baker, J.O. and Overend, R.P. (ed.). American chemical society, Washington, D.C.

Tebo, B.M. and Obraztsova, A.Y. 1998. Sulfate-reducing bacterium grows with Cr(VI), U(VI), Mn(IV), and Fe(III) as electron acceptors. *FEMS Microbiol Lett* **162**, pp. 193-198.

Tender, L.M., Reimers, C.E., Stecher III, H.A., Holmes, D.E., Bond, D.R., Lowy, D.A., Pilobello, K., Fertig, S.J. and Lovley, D.R. 2002. Harnessing microbially generating power on the seafloor. *Nature Biotechnol* **20**, pp. 821-825.

Teske, A., Wawer, C., Muyzer, G. and Ramsing, N.B. 1996. Distribution of sulfate-reducing bacteria in a stratified fjord (Mariagerfjord. Denmark) as evaluated by most-probable-number counts and denaturing gradient gel electrophoresis of PCR-amplified ribosomal DNA fragments. *Appl Environ Microbiol* **62**, pp. 1405-1415.

Thauer, R.K., Jungermann, K. and Decker, K. 1977. Energy conservation in chemotrophic anaerobic bacteria. *Bacteriaol Rev* **41**, pp. 100-180.

Thompson, J.D., Higgins, D.G. and Gibson, T.J. 1994. CLUSTAL W: improving the sensitivity of progressive multiple sequence alignment through sequence weighting, position-specific gap penalties and weight matrix choice. *Nucleic Acid Res* **22**, pp. 4673-4680.

Tofield, B.C. 1981. Materials for energy-conservation and storage. *Appl Energ* **8**, pp. 89-142.

Tokutake, N., Miyoshi, H., Satoh, T., Hatano, T. and Iwamura, H. 1994. Structural factors of antimycin-A molecule required for inhibitory-action. *Biochim Biophys Acta - Bioenergetics* **1185**, pp. 271-278.

Tor, J.M. and Lovley D.R. 2001. Anaerobic degradation of aromatic compounds coupled to Fe(III) reduction by *Ferroglobus placidus*. *Environ Microbiol* **3**, pp. 281-287.

Turick, C.E., Tisa, L.S. and Caccavo, F.Jr. 2002. Melanin production and use as a soluble electron shuttle for Fe(III) oxide reduction and as a terminal electron acceptor by *Shewanella alga* BrY. *Appl Environ Microbiol* **68**, pp. 2436-2444.

Turner, A.P.F., Aston, W.J., Higgins, I.J., Davis, G. and Hill, H.A.O. 1982. Applied aspects of bioelectrochemistry: fuel cells, sensors, and bioorganic synthesis. *Biotechnol Bioeng* **12**, pp. 401-412.

Uosaki, K. and Hill, H.A.O. 1981. Adsorption behaviour of 4,4'-bipyridyl at a gold/ water interface and its role in the electron transfer reaction between cytochrome *c* and a gold electrode. *J Electroanal Chem* **122**, pp. 321-327.

Urbach, E., Vergin, K.L. and Giovannoni, S.J. 1999. Immunochemical detection and isolation of DNA from metabolically active bacteria. *Appl Environ Microbiol* **65**, pp. 1207-1213.

van de Peer, Y. and Wachter, R.De. 1994. TREECON for Windows: a software package for the construction and drawing of evolutionary trees for Microsoft Windows environment. *Comput Appl Biosci* **10**, pp. 569-570.

Vanhaecke, E., Remon, J.P., Raes, F., Moors, J., DeRudder, D. and Petghen, A.V. 1990. Kinetics of *Pseudomonas aeruginosa* adhesion to 304 and 316-L stainless steel: role of cell surface hydrophobicity. *Appl Envrion Microbiol* **56**, pp. 788-795.

Venosa, A.D. 1975. Lysis of *S. natans* swarm cells by *Bdellovibrio bacteriovorus*. *Appl Microbiol* **29**, pp. 702-705.

Von Wintzingerode, F., Gobel, U.B. and Stackebrandt, E. 1997. Determination of microbial diversity in environmental samples: pitfalls of PCR-based rRNA analysis. *FEMS Microbiol Rev* **21**, pp. 213-229.

Vonjagow, G. and Link, T.A. 1986. Use of specific inhibitors on the mitochondrial bc-1 complex. *Methods Enzymol* **126**, pp. 253-271.

Wagner, M., Amann, R., Lemmer, H. and Schleifer, K.H. 1993. Probeing activated

sludge with oligonucleotidees specific for proteobacteria: inadequacy of culture-dependent methods for describing microbial community structure. *Appl Environ Microbiol* **59**, pp. 1520-1525.

Wagner, M., Rath, G., Amann, R., Koops, H.P. and Schleifer, K.H. 1995. *In situ* identification of ammonia-oxidizing bacteria. *Syst Appl Microbiol* **18**, pp. 251-264.

Ward, D.M., Weller, R. and Bateson, M.M. 1990. 16S rRNA sequences reveal numerous uncultured microorganisms in a natural community. *Nature* **345**, pp. 63-65.

Wayne, L.G., Brenner, D.J. and Colwell, R.R. 1987. Report of the ad-hoc-committee on reconciliation of approaches to bacterial systematics. *Intl J Syst Bacteriol* **37**, pp. 463-464.

Webster, G., Embley, T.M. and Prosser, J.I. 2002. Grassland management regimens reduce small-scale heterogeneity and species diversity of Beta-Proteobacterial ammonia oxidizer populations. *Appl Environ Microbiol* **68**, pp. 20-30.

Wehnder, A.J.B. and Stumm, W. 1988. Geochemistry and biogeochemistry of anaerobic habitats, pp. 1-38. *In* A.J.B. Zehnder (ed.), Biology of anaerobic microorganisms. John Wiley & Sons. New York.

Willner, I., Arad. G. and Katz, E. 1998. A biofuel cell based on pyrroloquinoline quinone and microperoxidase-11 monolayer-functionalized electrodes. *Bioelectrodchem Bioenerg* **44**, pp. 209-214.

Wimpenny, J.W.T., Kinniment, S.L. and Scourfield, M.A. 1993. The physiology and biochemistry of biofilm. pp. 51-94. *In* S.P. Denyer (ed.), Microbial biofilms: formation and control. Blackwell Scientific Publications. Oxford.

Wingard, L.B., Jr., Shaw, C.E. and Castner, J.F. 1982. Bioelectrochemical fuel cells. *Enzyme Microb Technol* **4**, pp. 137-142.

Woese, C.R. 1987. Bacterial Evolution. *Microbiol Rev* **51**, pp. 221-271.

Woese, C.R., Kandler, O. and Wheelis, M.L. 1990. Towards a natural system of organisms : proposal for the domains Archaea, Bacteria, and Eucarya. *Proc Natl Acad Sci* USA **887**, pp. 4576-4579.

Yue, P.L. and Lowther, K. 1986. Enzymatic oxidation of C_1 compounds in a biochemical fuel cell. *Chem Eng J* **33B**, pp. 69-77.

Zhou, J., Bruns, M.A. and Tiedje, J.M. 1996. DNA recovery from soils of diverse composition. *Appl Environ Microbiol* **62**, pp. 316-322.

Zhou, J., Liu, S., Xia, B., Zhang, C., Palumbo, A.V. and Phelps, T.J. 2001. Molecular characterization and diversity of thermophilic iron-reducing enrichment cultures from deep subsurface environments. *J Appl Microbiol* **90**, pp. 96-105.

Zobell, C.E. 1943. The effect of solid surfaces upon bacterial activity. *J Bacteriol* **46**, pp. 39-56.